

# **Fire Development in Passenger Trains**

A thesis submitted in fulfilment of the requirements  
for the degree of  
Master of Engineering

by  
Nathan White

Centre for Environment Safety and Risk Engineering  
Victoria University, Australia

2010



## **ABSTRACT**

This thesis presents research consisting of experiments and analysis of fire development in a passenger train carriage. The aim of this research is to use experiments, particularly a full-scale passenger train fire experiment, to increase understanding of fire behaviour in passenger trains and evaluate existing design fire estimation methods applied to passenger trains.

A design fire represents a fire development scenario in terms of a heat release rate (HRR) vs time curve. The design fire is the most critical input affecting fire safety design of trains, tunnels and surrounding infrastructure. Large fires involving at least an entire carriage are rare but can result in severe consequences and require design consideration. Current understanding of fire development on passenger trains is limited. Very limited experimental research has been conducted, particularly full-scale HRR measurement of entire carriages. As a result, existing methods for design fire estimation applied to trains are based on crude assumptions and appropriate design fires for passenger trains are uncertain.

A series of fire experiments have been conducted on an Australian metropolitan passenger train, including one full-scale fully developed carriage fire, large-scale ignition experiments and cone calorimeter tests. The main focus of this thesis is the full-scale experiment. From these experiments it is concluded that an ignition source of 100-170 kW peak HRR is the minimum required to promote fire spread to the entire carriage. Ignition of upper wall and ceiling linings is critical for fire spread to the entire carriage. Significant fire spread to upper wall and ceiling linings at the ignition location lead to flashover conditions resulting in fire spread to the entire carriage interior. Flashover occurred starting from the ignition area at 140 s. The carriage interior became rapidly untenable at the onset of flashover. The occurrence of flashover severely limits time available for driver response and passenger evacuation. The fully developed HRR was affected by ventilation conditions with significant combustion occurring external to open doors. Window breakage significantly increased ventilation and HRR. For the full-scale experiment HRR was not measured and interior materials were only fitted over a 10 m section due to limited resources.

A conservation of energy model was used to estimate the HRR for the full-scale experiment based on experimental measurements and observation. Fully developed HRR was estimated to be 8 MW prior to window breakage, increasing to 11 MW after window breakage increased ventilation. It is expected the peak HRR and burn duration would be greater for a fully fitted carriage interior. This result does not represent an appropriate design fire due to the reduced fuel load but does provide a basis for understanding train fire development and evaluating design fire estimation methods by comparison to both experimental observations and the conservation of energy model. Existing design fire estimation methods were found to inappropriately represent real fire behaviour resulting in poor estimation of fire growth and burn duration. Although the methods provided a rough order of magnitude estimate of peak HRR for the full-scale experiment they do not realistically predict all aspects of design fires. These tools should only be used in conjunction with an experimental knowledge of train fire behaviour.

Application of the computational fluid dynamics (CFD) fire growth model Fire Dynamics Simulator (FDS) to predict design fires for trains has been reviewed. Work by other's applying FDS to estimate the HRR for the full-scale experiment is reviewed. An estimate of fire growth matching observations and measurements for the full-scale experiment was not achieved. It is concluded that FDS does not reliably predict realistic design fires for passenger trains due to simplifying assumptions in the FDS combustion and pyrolysis model and difficulty selecting appropriate input parameters for combustible material and glazing

It is demonstrated that no ideal method for estimating design fires for passenger trains exists. However in order to engineer fire safety designs for rail infrastructure, existing tools for design fire estimation must be applied. It is critical that these tools be applied by competent users giving proper consideration to both the limitation of the models and knowledge of real fire behaviour as demonstrated by this and previous research. Where possible, design fires should be supported by experiments. Clearly further research is needed to increase understanding of the range of fire scenario characteristics expected to influence fire behaviour.

## ACKNOWLEDGEMENTS

The author wishes to acknowledge:

- The vital support, patience and motivation from his family, especially his wife.
- The principle supervision of Professor Ian Thomas and Dr. Ian Bennetts, and also the assistance from all staff at the Centre for Environment Safety and Risk Engineering, Victoria University.
- CSIRO for providing both financial support and experimental resources.
- CSIRO fire researchers for their technical assistance in conducting experiments of a scale that required managed teamwork to succeed.
- Queensland Fire and Rescue Service for providing a location and fire service support required to conduct the large-scale passenger train fire experiment.
- WPI Fire engineering students and staff for undertaking CFD modelling of the full-scale experiment.

## DECLARATION

I, Nathan White, declare that the Master by Research thesis entitled “**Fire Development in Passenger Trains**” is no more than 60,000 words in length including quotes and exclusive of tables, figures, appendices, bibliography, references and footnotes. This thesis contains no material that has been submitted previously, in whole or in part, for the award of any other academic degree or diploma. Except where otherwise indicated, this thesis is my own work.

Signature:

Date: 10<sup>th</sup> June 2010

# TABLE OF CONTENTS

<b>ABSTRACT .....</b>	<b>I</b>
<b>ACKNOWLEDGEMENTS.....</b>	<b>III</b>
<b>DECLARATION.....</b>	<b>III</b>
<b>TABLE OF CONTENTS.....</b>	<b>IV</b>
<b>LIST OF ABBREVIATIONS.....</b>	<b>XII</b>
<b>CHAPTER 1 - INTRODUCTION.....</b>	<b>1</b>
1.1 BACKGROUND .....	1
1.2 RESEARCH AIMS .....	2
1.3 RESEARCH METHODOLOGY .....	2
1.4 LIMITATIONS OF RESEARCH.....	3
1.5 OVERVIEW OF THIS THESIS .....	3
<b>CHAPTER 2 - LITERATURE REVIEW.....</b>	<b>5</b>
<b>2.1 THE NEED FOR RESEARCH OF FIRE DEVELOPMENT IN PASSENGER TRAINS.....</b>	<b>5</b>
2.1.1 FIRE ENGINEERING DESIGN OF PASSENGER TRAINS.....	5
2.1.2 PASSENGER RAIL FIRE INCIDENTS .....	8
2.1.3 TUNNEL FIRE INCIDENTS.....	11
2.1.4 PASSENGER RAIL FIRE STATISTICS .....	12
2.1.5 THE NEED FOR RESEARCH ON FIRE DEVELOPMENT IN PASSENGER TRAINS .....	14
<b>2.2 EXPERIMENTAL RESEARCH ON PASSENGER TRAIN FIRES .....</b>	<b>15</b>
2.2.1 CATEGORIES OF EXPERIMENTAL WORK .....	15
2.2.2 JNR FIRE BEHAVIOUR ON A RUNNING TRAIN PROJECT (1974).....	16
2.2.3 NBS AMTRACK PROJECT (1984).....	18
2.2.4 SP FIRES IN BUSES AND TRAINS PROJECT (1990).....	20
2.2.5 EUREKA PROJECT (1995).....	21
2.2.6 FIRESTARR PROJECT (2001).....	24
2.2.7 CSIRO FIRE GROWTH ON PASSENGER RAIL INTERIORS (2000-2003).....	28
2.2.8 NIST- FIRE SAFETY OF PASSENGER TRAINS PROJECT (1999-2004).....	32
2.2.9 SP MODEL SCALE RAILCAR FIRE TESTS (2005) .....	36
2.2.10 OTHER EXPERIMENTAL PROJECTS .....	38
<b>2.3 DESIGN STANDARDS FOR PASSENGER TRAIN FIRE SAFETY.....</b>	<b>42</b>
2.3.1 AUSTRALIAN FIRE SAFETY REQUIREMENT .....	42
2.3.2 INTERNATIONAL STANDARDS .....	43
<b>2.4 DESIGN FIRE ESTIMATION METHODS.....</b>	<b>49</b>
2.4.1 “T <sup>2</sup> ” GROWTH RATES.....	50
2.4.2 PREDICTING FLASHOVER .....	52
2.4.3 AVERAGE HRR DESIGN FIRE ESTIMATION METHOD .....	57
2.4.4 DUGGAN’S METHOD .....	58
2.4.5 VENTILATION CONTROLLED BURNING.....	60

2.4.6	ZONE MODELLING.....	64
2.4.7	ONE-LAYER POST-FLASHOVER MODEL.....	66
2.4.8	ASSUMED DESIGN FIRES FOR LARGE TRAIN FIRES.....	68
<b>2.5</b>	<b>LITERATURE REVIEW CONCLUSIONS.....</b>	<b>71</b>

**CHAPTER 3 EXPERIMENTAL INVESTIGATION OF FIRE BEHAVIOUR ON A PASSENGER TRAIN CARRIAGE ..... 74**

<b>3.1</b>	<b>EXPERIMENTAL APPROACH.....</b>	<b>74</b>
3.1.1	IMPORTANT FIRE BEHAVIOUR FACTORS FOR PASSENGER LIFE SAFETY .....	74
3.1.2	OVERVIEW OF EXPERIMENTS CONDUCTED.....	76
3.1.3	LIMITATIONS AND CONDITIONS AFFECTING EXPERIMENTS .....	77
<b>3.2</b>	<b>CARRIAGE AND MATERIALS .....</b>	<b>78</b>
<b>3.3</b>	<b>CONE CALORIMETER EXPERIMENTS.....</b>	<b>81</b>
<b>3.4</b>	<b>LARGE-SCALE CORNER IGNITION EXPERIMENTS .....</b>	<b>85</b>
3.4.1	INSTALLATION OF MATERIALS IN CARRIAGE .....	85
3.4.2	INSTRUMENTATION AND APPARATUS.....	86
3.4.3	IGNITION SOURCES AND PROCEDURE .....	86
3.4.4	RESULTS .....	87
<b>3.5</b>	<b>FULL-SCALE EXPERIMENT .....</b>	<b>90</b>
3.5.1	INSTALLATION OF MATERIALS IN CARRIAGE .....	90
3.5.2	INSTRUMENTATION AND APPARATUS.....	92
3.5.3	IGNITION SOURCE .....	96
3.5.4	PROCEDURE.....	96
3.5.5	RESULTS .....	97
<b>3.6</b>	<b>EXPERIMENTAL CONCLUSIONS.....</b>	<b>117</b>

**CHAPTER 4 ANALYSIS OF FULL-SCALE EXPERIMENT ..... 119**

<b>4.1</b>	<b>ANALYTICAL APPROACH .....</b>	<b>119</b>
<b>4.2</b>	<b>APPLICATION OF EXISTING DESIGN FIRE ESTIMATION METHODS.....</b>	<b>119</b>
4.2.1	APPLICATION OF AVERAGE HRR METHOD .....	120
4.2.2	APPLICATION OF DUGGAN’S METHOD.....	123
4.2.3	APPLICATION OF METHODS TO PREDICT FLASHOVER .....	127
4.2.4	APPLICATION OF CORRELATION FOR VENTILATION CONTROLLED BURNING RATE.....	128
4.2.5	PRELIMINARY ESTIMATE OF FULL-SCALE EXPERIMENT PEAK HRR .....	132
<b>4.3</b>	<b>CONSERVATION OF ENERGY MODEL.....</b>	<b>133</b>
4.3.1	CONSERVATION OF ENERGY MODEL FRAMEWORK.....	133
4.3.2	ENERGY STORED .....	134
4.3.3	HEAT TRANSFER THROUGH BOUNDING SURFACES .....	136
4.3.4	VENT MASS FLOW ENERGY TRANSFER .....	145
4.3.5	EXTERIOR FIRE HEAT RELEASE RATE .....	156
4.3.6	TOTAL HEAT RELEASE RATE .....	165
<b>4.4</b>	<b>ANALYSIS CONCLUSIONS .....</b>	<b>170</b>

**CHAPTER 5 FDS MODELLING TO ESTIMATE TRAIN FIRE HRR ..... 172**

<b>5.1</b>	<b>INTRODUCTION TO CFD AND FDS .....</b>	<b>172</b>
<b>5.2</b>	<b>GOVERNING THEORY AND ASSUMPTIONS FOR FDS.....</b>	<b>174</b>
5.2.1	HYDRODYNAMIC MODEL.....	174
5.2.2	COMBUSTION MODEL.....	178
5.2.3	THERMAL RADIATION MODEL.....	182

5.2.4	THERMAL BOUNDARY CONDITIONS .....	182
5.2.5	PYROLYSIS MODEL .....	184
<b>5.3</b>	<b>VALIDITY/LIMITATIONS OF HRR PREDICTION BY FDS .....</b>	<b>187</b>
5.3.1	CAUSES OF ERROR FOR HRR PREDICTION .....	187
5.3.2	EXPERIMENTAL VALIDATION OF HRR PREDICTION .....	190
<b>5.4</b>	<b>MEASUREMENT OF MATERIAL PROPERTIES FOR INPUT TO FDS.....</b>	<b>193</b>
<b>5.5</b>	<b>APPLICATION OF FDS TO PASSENGER TRAIN FIRES .....</b>	<b>196</b>
5.5.1	SIMULATION OF A SINGAPORE METRO TRAIN FIRE .....	196
5.5.2	WPI SIMULATIONS OF FULL-SCALE TRAIN FIRE EXPERIMENT .....	200
<b>5.6</b>	<b>FDS CONCLUSIONS .....</b>	<b>211</b>

**CHAPTER 6 CONCLUSIONS AND FURTHER RESEARCH RECOMMENDATIONS .....** **212**

<b>6.1</b>	<b>CONCLUSIONS .....</b>	<b>212</b>
<b>6.2</b>	<b>FURTHER RESEARCH RECOMMENDATIONS .....</b>	<b>214</b>

**REFERENCES .....** **216**

**APPENDIX A - STANDARD TEST METHODS .....** **230**

<b>A.1</b>	<b>SMALL FLAME TESTS .....</b>	<b>230</b>
<b>A.2</b>	<b>SMOKE TESTS.....</b>	<b>231</b>
<b>A.3</b>	<b>TOXICITY TESTS .....</b>	<b>232</b>
<b>A.4</b>	<b>FLAME SPREAD TESTS.....</b>	<b>232</b>
<b>A.5</b>	<b>FIRE RESISTANCE TESTS.....</b>	<b>234</b>
<b>A.6</b>	<b>HEAT RELEASE RATE TESTS .....</b>	<b>234</b>
<b>A.7</b>	<b>OTHER TEST METHODS.....</b>	<b>236</b>

**APPENDIX B – FIRE SAFETY STANDARD MATERIAL REQUIREMENTS .....** **238**

**APPENDIX C – IGNITION SOURCES .....** **242**

**APPENDIX D – FULL-SCALE EXPERIMENTAL DRAWINGS .....** **246**

**APPENDIX E – FULL-SCALE EXPERIMENT PHOTOGRAPHS .....** **258**

**APPENDIX F – FULL-SCALE EXPERIMENT RESULT GRAPHS.....** **279**

**APPENDIX G – FULL-SCALE EXPERIMENT MEASUREMENTS SCALED FROM VIDEO FOOTAGE .....** **293**

**APPENDIX H – CONE CALORIMETER RESULT GRAPHS.....** **298**

**APPENDIX I – MEASUREMENT OF EFFECTIVE HEAT OF COMBUSTION.....** **303**

## NOMENCLATURE

Symbol	Description	Unit
$A$	Surface area	$m^2$
$A$	Arrhenius pre exponential factor (Section FDS)	m/s
$A_f$	Surface area of fuel	$m^2$
$A_O$	Area of opening	$m^2$
$A_T$	Total area of compartment enclosing surfaces excluding floor area or vent areas.	$m^2$
$c_p$	Specific heat	kJ/kg·K
$C$	Empirical constant	-
$C_d$	Flow coefficient	-
$D$	Diameter	M
$D_i$	Diffusion coefficient	$m^2/s$
$D_s$	Specific optical density	-
$E$	Arrhenius activation energy	kJ/kmol
$\mathbf{f}$	External force vector including gravity	(N)
$F_s$	Flame spread factor	-
$g$	Gravitational acceleration	$m/s^2$
$h$	Height	M
$h$	Enthalpy (section FDS)	(J)
$h_{conv-in}$	Convective heat transfer coefficient of inside surface	$W/m^2 \cdot K$
$h_{conv-out}$	Convective heat transfer coefficient of outside surface	$W/m^2 \cdot K$
$h_k$	Effective heat transfer coefficient	$kW/m^2 \cdot K$
$h_{rad-in}$	Radiant heat transfer coefficient of inside surface	$W/m^2 \cdot K$
$h_{rad-out}$	Radiant heat transfer coefficient of outside surface	$W/m^2 \cdot K$
$H$	Characteristic height	M
$H_N$	Neutral plane height	M
$H_O$	Height of opening	M
$i$	Small finite volume or time step number	-
$I_b$	Radiant heat intensity	$W/m^2 \cdot sr$

$I_s$	Radiant panel index	-
$k$	Thermal conductivity	W/m·K
$k_i$	Instantaneous smoke extinction coefficient	$m^{-1}$
$L$	Length	M
$m$	Mass	Kg
$m_{final}$	Final mass	Kg
$m_{initial}$	Initial mass	Kg
$\dot{m}'''$	Mass rate per unit volume	$kg/m^3 \cdot s$
$\dot{m}_a$	Mass flow rate of air into opening	kg/s
$\dot{m}_g$	Mass flow rate of gas out of opening	kg/s
$\dot{m}_f$	Mass rate of burning	kg/s
$M$	Molecular mass	kg/mol
$n$	Total number finite volumes or time steps	-
$P$	Pressure	Pa
$\mathbf{q}$	Radiant and convective heat flux vector	$W \cdot m^2$
$\dot{q}_{conv-in}$	Convective heat transfer rate to inside surface	kW
$\dot{q}_{conv-out}$	Convective heat transfer rate from outside surface	kW
$\dot{q}_{cond}$	Conductive heat transfer rate through a material	kW
$\dot{q}_{HeatTransfer}$	Rate of heat transferred out of the boundary of a control volume	kW
$\dot{q}_{MassFlowIn}$	Rate of heat transferred by mass flow into an enclosure	kW
$\dot{q}_{MassFlowOut}$	Rate of heat transferred by mass flow out of an enclosure	kW
$\dot{q}_{stored}$	Rate of heat stored within a control volume	kW
$\dot{q}_{rad-in}$	Radiant heat transfer rate to inside surface	kW
$\dot{q}_{rad-out}$	Radiant heat transfer rate from outside surface	kW
$\dot{q}''$	Heat Release rate per unit surface area	$kW/m^2$
$\dot{q}'''$	Heat Release rate per unit volume	$kW/m^3$
$Q$	Total Heat or Heat evolution factor	kJ or -

$\dot{Q}$	Heat release rate	kW
$\dot{Q}_{ave}$	Average heat release rate	kW
$\dot{Q}_{External}$	Heat release rate due to combustion external to a train carriage	kW
$\dot{Q}_{FO}$	Heat release rate required for the onset of flashover	kW
$\dot{Q}_{Internal}$	Heat release rate due to combustion internal to a train carriage	kW
$\dot{Q}_{loss}$	Net heat loss	kW
$\dot{Q}_{VentilationControlled}$	Ventilation controlled heat release rate	kW
$\dot{Q}^*$	Dimensionless energy release rate	-
$R$	Ideal gas constant (8.314)	J/kmol
$R_{cond}$	Conductive thermal resistance	K/W
$R_{conv-in}$	Convective thermal resistance at inside surface	K/W
$R_{conv-out}$	Convective thermal resistance at outside surface	K/W
$R_{rad-in}$	Radiant thermal resistance at inside surface	K/W
$R_{rad-out}$	Radiant thermal resistance at outside surface	K/W
$R_{tot}$	Total thermal resistance	K/W
$t$	Time	S
$t_{FO}$	Time to onset of flashover	S
$t_{ig}$	Time to ignition	S
$t_{VL}$	Time to loss of visibility	S
$T$	Temperature	K
$T_a$	Temperature of ambient air	K
$T_g$	Temperature of hot fire gas	K
$T_L$	Fraction of light transmission	-
$T_{s-in}$	Temperature of inside surface	K
$T_{s-out}$	Temperature of outside surface	K
$u$	Velocity	m/s
$\mathbf{u}$	Velocity vector	m/s
$v_i$	Instantaneous volume flow rate	m <sup>3</sup> /s
$v_i$	Stoichiometric coefficient	-

$V$	Volume	$m^3$
$y_{co}$	Carbon monoxide yield	kg/kg
$y_s$	Soot yield	kg/kg
$Y_i$	Mass fraction of individual species	kg/kg
$Z$	Mixture fraction	-
$\nabla$	$\left( \frac{\partial}{\partial x}, \frac{\partial}{\partial y}, \frac{\partial}{\partial z} \right)$	-

<b>Greek Symbol</b>	<b>Description</b>	<b>Unit</b>
$\alpha$	Fire intensity coefficient	-
$\delta$	Thickness	M
$\delta x$	Grid size	M
$\Delta H_c$	Gross Heat of combustion	MJ/kg
$\Delta H_{eff}$	Effective Heat of combustion	MJ/kg
$\Delta H_{net}$	Net Heat of combustion	MJ/kg
$\Delta H_O$	Energy released per unit mass oxygen consumed	MJ/kg
$\Delta H_v$	Heat of vaporization	MJ/kg
$\Delta P$	Pressure difference	Pa
$\Delta t$	Time difference	S
$\Delta T$	Temperature difference	K
$\varepsilon$	Emissivity	-
$\varepsilon_g$	Emissivity of gas	-
$\varepsilon_s$	Emissivity of surface	-
$\eta$	Correction factor for ventilation controlled HRR	-
$\Phi$	Kinetic energy dissipation vector	-
$\kappa$	Extinction coefficient	$m^{-1}$
$\kappa$	Absorption coefficient	-
$\rho$	Density	kg/m <sup>3</sup>
$\rho_a$	Ambient air density	kg/m <sup>3</sup>
$\rho_{char}$	Density of char	kg/m <sup>3</sup>
$\rho_g$	Density of hot fire gas	kg/m <sup>3</sup>
$\sigma$	Stefan-Boltzmann constant ( $5.67 \times 10^{11}$ )	kW/m <sup>2</sup> ·K

$\tau$	Transmissivity	-
$\tau_{ij}$	Viscous stress tensor	Pa
$\chi$	Combustion efficiency	-
$\chi_r$	Combustion efficiency	-

## LIST OF ABBREVIATIONS

<b>Acronym</b>	<b>Description</b>
AFAC	Australian Fire Authorities Council
ASET	Available safe egress time
ASTM	American Society for Testing and Materials
BRANZ	Building Research Association of New Zealand
CFAST	Consolidated Model of Fire and Smoke Transport
CFD	Computational fluid dynamics
CRF	Critical radiant heat flux
CSIRO	Commonwealth Science and Industry Research Organisation
DNS	Direct Numerical Simulation
ERRI	European Rail Research Institute
FAA	Federal Aviation Administration
FAR	Federal aviation regulation
FCRC	Fire Code Reform Centre
FDS	Fire Dynamics Simulator
FED	Fractional effective dose
FIRESTARR	Fire Standardisation Research in Railways
FR	Fire retarded
FRA	Federal Railroad Administration
FRP	Fibre reinforced polymer
GRP	Glass reinforced polymer
HRR	Heat release rate
HRRPUA	Heat release rate per unit area
ISO	International Organization for Standardization
JNR	Japan National Rail
KRRI	Korean Rail Research Institute
LES	Large eddy simulation
LS-PCP	Low smoke polychloroprene
NBS	National Bureau of Standards
NFPA	National Fire Protection Association
NIST	National Institute of Standards and Technology
PCP	Polychloroprene

PTC	Public Transport Corporation
PU	Polyurethane
PVC	Polyvinylchloride
RANS	Reynolds Averaged Navier-Stokes equations
RSET	Required safe egress time
ROA	Railways of Australia
SEA	Specific extinction area ( $\text{m}^2/\text{kg}$ )
SGS	Sub Grid Scale
SRA	State Rail Authority
THR	Total heat released
WMTA	Washington Metropolitan Transit Authority

## **CHAPTER 1 - INTRODUCTION**

### **1.1 Background**

Effective fire safety design of rail infrastructure is underpinned by application of realistic design fires representing credible train fire incidents. Effective fire safety design achieves an acceptable level of life safety with acceptable reliability for the least cost. A design fire represents a fire development scenario in terms of a heat release rate (HRR) vs time curve. This is the most critical input affecting design and prediction of performance for fire safety systems including, smoke management, detection and suppression, and stability of structures.<sup>[1]</sup> The design fire is also the most critical input affecting prediction of occupant tenability. This thesis focuses on passenger train interior fire scenarios.

One of many objectives for passenger train designers is to minimise both the probability of a large interior fire occurring and the maximum fire size and duration. Small arson fires that do not spread beyond the ignition area are common.<sup>[2]</sup> Fully developed fires involving at least an entire carriage interior are rare however the consequences of such a scenario can be severe and require design consideration.

Current understanding of fire development in passenger train interiors is limited. Previous experimental research in this field is limited and mostly focuses on the early stages of ignition and fire spread. Very little experimental research has involved large scale experiments to investigate fully developed train fire behaviour, particularly with measurement of HRR. Understanding of the affect of variables such as ignition source severity, material flammability properties, vehicle geometry and design, ventilation and window behaviour, and the environment external to the train on fire development in passenger trains is limited. As a result, existing methods for design fire estimation applied to trains are based on crude assumptions and therefore appropriate design fires for passenger trains are uncertain. A more detailed background is provided in the literature review.

## **1.2 Research Aims**

The aims of this research are to:

- Identify and develop an understanding of factors affecting ignition and fire growth on passenger trains.
- Experimentally investigate fully developed fire behaviour on a passenger train carriage and provide an estimate of HRR based on experimental measurements.
- Evaluate existing models used to estimate design fires for passenger trains.

## **1.3 Research Methodology**

The methods adopted in this research are:

- Literature review.
- Experiments including:
  - Cone calorimeter tests on interior materials.
  - A series of large-scale ignition experiments in a train carriage interior corner.
  - One full-scale fully developed train carriage experiment on a carriage with half the interior fitted.
- Analysis of HRR for the full-scale experiment based on experimental measurements and observations. Evaluation of existing design fire estimation methods against the full-scale experiment.
- Review of a CFD model Fire Dynamics Simulator (FDS) applied to estimate passenger train design fires. Particularly work by other fire engineering students using FDS to estimate HRR for the full-scale experiment is reviewed.

## **1.4 Limitations of Research**

The carriage and test facility used for the experimental work was only available for a limited period. This restricted the time available for both planning and conducting the experiments.

HRR was not directly measured for the full-scale or large scale experiments as no facility capable of HRR measurement on this scale exist in Australia and it is beyond the resources of this research to construct such a facility. Other instrumentation was used to enable HRR to be estimated.

A limited amount of train interior materials was available. Only a 10 m length of the carriage was fully fitted with interior materials. It is likely the fire size and burn duration would have increased had more materials been fitted, thus estimated HRR for the full-scale experiment is not representative of a fully fitted carriage.

Due to limited resources and time only one full-scale experiment, representing one fire scenario was conducted. Different fire scenarios involving different ventilation conditions, materials and the effects of a tunnel are not assessed.

Review of CFD modelling to estimate design fires only considers FDS V4. At the time of writing a new version (FDS V5) has been released but has not been significantly applied to train fires.

## **1.5 Overview of this Thesis**

This thesis has been arranged in the following manner:

Chapter 2 presents a review of literature on subjects related to the current research. These include: review of fire engineering design of passenger trains and train fire incidents and statistics to demonstrate the need for research, prior experimental research on passenger train fires, design standards for fire safety of passenger trains and design fire estimation methods.

Chapter 3 presents experimental research including the full-scale fully developed carriage fire experiment, the large-scale corner experiment and the cone calorimeter

tests. Details of the materials and carriage tested, instrumentation, ignition sources, procedure and results are presented. Conclusions are drawn regarding factors affecting ignition, fire growth and fully developed fire behaviour.

Chapter 4 presents the analysis. Existing design fire estimation methods are applied to, and evaluated against, the full-scale experiment. A conservation of energy model is used to estimate the actual HRR for the full-scale experiment based on measurements and observations.

Chapter 5 presents a review of FDS modelling applied to estimate design fires for passenger trains. This includes: governing theory and assumptions for FDS which affect HRR modelling, previous validation of the FDS HRR model and measurement of material properties for input to FDS. Two examples of application of FDS to predict passenger train design fire are reviewed. One application (carried out by others) was to estimate the HRR for the full-scale experiment.

Chapter 6 presents a final summary and conclusions.

Additional information regarding standard fire test methods for passenger trains, experimental results and analysis is provided in the appendices.

## **CHAPTER 2 - LITERATURE REVIEW**

### **2.1 THE NEED FOR RESEARCH OF FIRE DEVELOPMENT IN PASSENGER TRAINS**

In order to demonstrate the need for research of fire behaviour in passenger trains, the process of fire engineering design of passenger trains and its dependence on estimated design fires is reviewed. Severe fire incidents and fire incident statistics on passenger trains will then be reviewed to understand the consequences and likelihood of these incidents providing further motivation for this research.

#### **2.1.1 Fire Engineering Design of Passenger Trains**

Whenever a new rail system is designed or an existing system significantly modified, designers and operators are required, both by regulation and by duty of care, to ensure the fire safety of the resulting system is at a satisfactory level. Two approaches to ensure this are:

- Prescriptive approach applies specifications or standards to achieve life safety objectives through detailed requirements such as small-scale tests but does not quantify the life safety of the system.
- Performance based approach applies fire engineering analysis of systems to compare or quantify life safety ensuring that life safety objectives are met.

There are few prescriptive passenger rail fire safety standards (see Section 2.3). Prescriptive standards provide little design flexibility and do not clearly quantify the life safety of the system. Performance based fire engineering has been adopted for design of both passenger trains and rail infrastructure where:

- Prescriptive standards failed to enable design or assessment of materials, fire safety systems or operating procedures and their resulting affect on life safety.
- Prescriptive requirements prohibited other design objectives to be met and alternative designs requirements could be demonstrated to have equal or better efficacy.

England and Flower<sup>[3]</sup> present a framework adapting the Fire Engineering Guidelines<sup>[4]</sup> to passenger rail networks. The Fire Engineering Guidelines is intended

for application on buildings however the framework for applying fire engineering summarised in Figure 2.1 has been applied with some alteration to many passenger rail system designs in Australia.

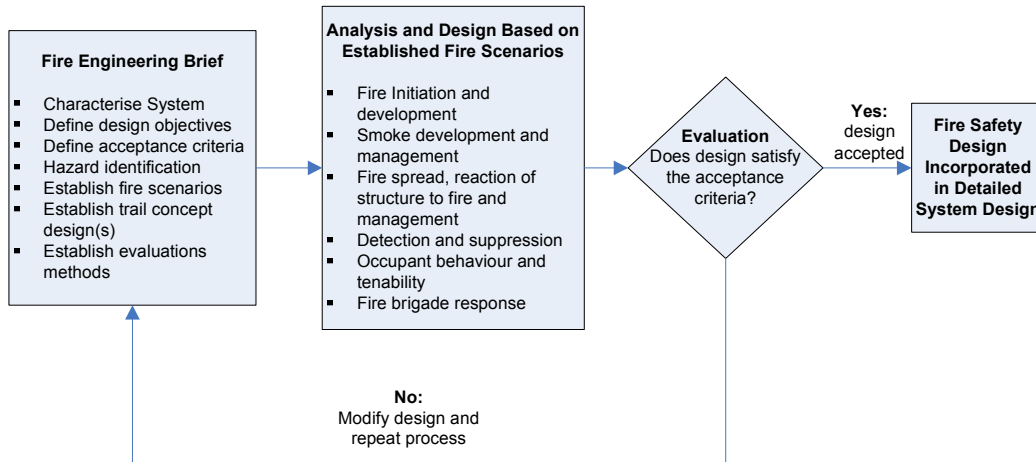


**Figure 2.1** Fire engineering design and analysis process

This framework identifies that the fire scenarios selected are a critical input to the design process.

Fire scenarios are characterised by design fires. Design fires are most easily and commonly expressed in terms of a HRR versus time curve for the course of the fire.<sup>[4]</sup> Throughout this thesis a HRR vs time curve is referred to as a HRR curve and instantaneous HRR is referred to as HRR. A HRR curve is a simple approximation of real fire behaviour and is normally considered to consist of three stages as shown in Figure 2.2.

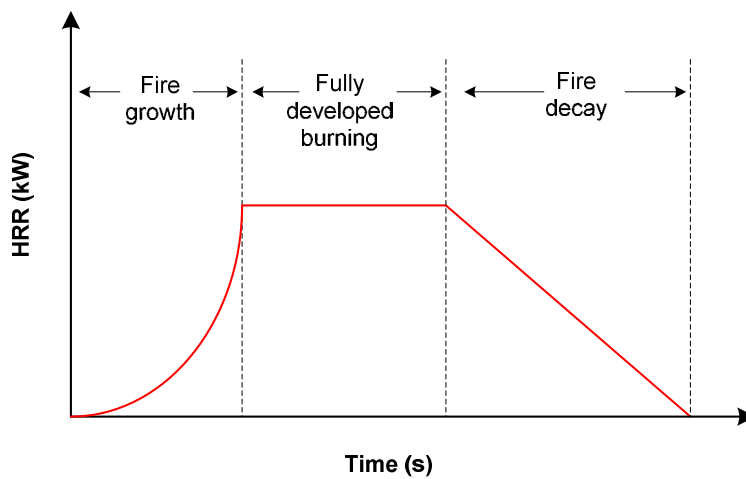


**Figure 2.2.** Design fire expressed as HRR vs. time curve

Fire growth is dependant on fuel and other conditions. For fires in enclosures an important fire growth concept is flashover. Flashover is the rapid transition from a localised fire to general conflagration involving all materials within an enclosed space. This concept is fully discussed in Section 2.4.2.

The importance of design fires for fire safety design is demonstrated by addressing each point of analysis described in Figure 2.1 as follows:

- **Fire initiation and development** – This involves the characterisation of key fire scenarios in terms of a HRR curve. Key factors affecting a HRR curve are the ignition source, material properties, material and enclosure arrangements and geometries, and ventilation conditions. Prediction of HRR curves based on these properties is extremely complex.<sup>[5]</sup>
- **Smoke development and management** -The rate of smoke production is related to HRR as well as material properties and ventilation conditions. All empirical correlations commonly used to predict smoke production rate are dependent on HRR.<sup>[6]</sup>
- **Fire spread, reaction of structure to fire and management** – The occurrence and rate of fire spread within a carriage, between carriages and to surrounding infrastructure is quantified by and dependent on the design fire HRR curve and vehicle design.<sup>[4]</sup> Surrounding infrastructure is also designed to maintain structural integrity when exposed to assumed design fires.<sup>[7]</sup>
- **Detection and suppression** – Detection and suppression systems are activated by hot gases or smoke which are related to HRR.<sup>[8]</sup> The effectiveness of suppression systems once activated is heavily dependent on HRR.
- **Occupant behaviour and tenability** – Tenability criteria are usually based on quantities such as hot layer height, radiant heat, convective heat, toxic gases and visibility/smoke obscuration. All of these quantities are strongly influenced by the HRR curve.<sup>[4]</sup>
- **Fire brigade response** –HRR directly affects the fire brigades actions and effectiveness.<sup>[9]</sup> For incidents such as the Mont Blanc Tunnel fire where extremely high HRR was coupled with limited access fire brigade response can be ineffective.<sup>[10]</sup>

Thus the fires chosen as a basis for design affect both cost and effectiveness of material selection, the fire safety system and the surrounding infrastructure. Where prescriptive regulations or standards are applied for passenger train fire safety the design and construction cost is primarily governed by the regulations or standards and the design fire and resulting level of life safety is either implicitly assumed or not addressed at all. Where performance based design is adopted then the design fire has a critical affect on the cost of fire protection systems (both active and passive), smoke management systems and facilities for occupant warning and egress. A significant cost may be associated with design and selection of train materials to achieve a required design fire. Significant cost of property and business continuity loss (as well as fatalities/injuries) may exist if a design fire is poorly chosen resulting in an ineffective fire safety design.

Insufficient understanding of fire behaviour within rail vehicles limits designers ability to predict realistic design fires.<sup>[11]</sup> The National Institute of Standards and Technology (NIST), in a review of fire safety of passenger trains,<sup>[12]</sup> have identified the ability to relate small scale test data to real scale burning behaviour through valid fire growth models as the major element lacking from fire safety design of passenger trains. They also recognize that real-scale tests of actual trains are required to develop and validate such models.

To produce a working design, current practise is to apply an assortment of non-validated assumptions to develop design fires. These assumptions, discussed in Section 2.4, reflect the limits of existing understanding of fire behaviour on passenger trains. If these assumptions are much more severe than reality then the resulting design may be excessively safe and unnecessarily costly. If the assumptions are much less severe than reality then the resulting design may not result in a suitable level of safety.

## **2.1.2 Passenger Rail Fire Incidents**

### **2.1.2.1 International Incidents**

Lists of major rail accidents, resulting in significant casualties, fatalities or property loss, around the world contain approximately 94 major rail accidents from 1990-

2005.<sup>[13]</sup> The majority of these involved derailments or collisions. Only five of these major accidents resulted from fire. There are some examples of passenger train fires resulting from collision such as the Ladbroke Grove incident <sup>[14]</sup> however such incidents usually involved liquid fuels and deaths and injuries may have resulted from the collision rather than the fire. Thus it is concluded that major passenger rail fires are not high frequency events. However review of the five incidents in Table 2-1 demonstrates they can have severe consequences. It is recognised that these incidents involve rail systems with significant cultural, design or operational differences to Australian railway systems.

**Table 2-1 Rail fire incidents resulting in large fatalities 1990-2005**

Location	Date	Description	Fatalities (Injuries)
Daegu, South Korea	18/02/2003	A arsonist ignited 4 l of petrol on train prior to stopping at Jungangno underground station. Approx. 4 min later a second train stopped opposite the burning train. At this time the fire had spread to other cars on the first train but most passengers had escaped. Electrical power to the second train was lost preventing it from moving. Doors failed to open trapping most of the passengers. The fire consumed all cars on both trains and spread to the platform, but did not spread to an adjoining shopping mall. <sup>[15-17]</sup>	192 (147)
Godhra, India	27/02/2002	Fire occurred on an intercity passenger train, the Sabarmati Express. The fire spread rapidly to multiple carriages. An investigation concluded that the fire started inside the train rather than externally. <sup>[18-20]</sup>	52 (-)
Al Ayatt, Egypt	19/02/2002	Fire on intercity commuter train. Fire started on the 4th carriage of an 11 carriage train. Source of the fire thought to be a gas stove used by a passenger. The train travelled for 7 km after ignition stopping at town of Al Ayatt. The fire spread rapidly to all carriages behind the carriage of fire origin. Seven carriages in total were consumed. Train was not air conditioned and most windows were open enabling rapid spread of the fire. The train was occupied beyond its designed capacity and bars were fitted to windows hampering evacuation. <sup>[21,22]</sup>	373 (-)
Kaprun, Austria	11/11/2000	Fire started at rear of underground cable drawn train travelling to Kaprun ski resort. The tunnel is 3200 m long with a maximum gradient of 50% connecting to an alpine centre at the top. The train came to a halt 530 m inside the tunnel. Twelve passengers escaped travelling down the tunnel past the fire at the rear. The fire grew rapidly, drawing air from the bottom of the tunnel and expelling combustion products out of the top of the tunnel. The remaining occupants were killed, the majority dying of asphyxiation attempting to travel up the tunnel. Smoke also affected people at alpine centre at the top of the tunnel. <sup>[23]</sup> The carriage was completely consumed. Ski equipment and clothes were thought to have fuelled the fire. The fire cause was a faulty heater and leakage of highly flammable hydraulic brake oil. <sup>[24]</sup>	155 (-)
Baku, Azerbaijan	28/10/1995	Fire occurred on an underground metro train. The metro system opened in 1967 and the carriages involved were nearly 30 years old. An investigation concluded that the fire was started accidentally by electrical sparks from wiring under one of the cars. <sup>[25]</sup>	292 (168)

### 2.1.2.2 Australian Incidents

A review of Australian railway disasters<sup>[26]</sup> and statistics reviewed in Section 2.1.4 indicate there have been no fires resulting in fatalities on modern Australian passenger trains however there are several cases of significant fire spread.

A large fire incident occurred on a NSW C-set double-deck train on the 22nd October 2006.<sup>[27]</sup> An arson fire was started in the corner of the upper deck of a carriage. Fire spread up to 4 m along upper wall and ceiling linings but did not reach flashover with no spread to seats, flooring or the lower deck. The carriage was filled with smoke. Approximately 30 passengers were evacuated with no injuries.

Two major fire incidents occurred on Melbourne trains during 2002. On April 9, 2002 an arson fire was lit using newspaper in the unoccupied end carriage of a three car set bound for the city. The train stopped at Merlynston station when the driver noticed the fire. The fire reached a flashover condition and consumed the entire carriage interior, valued at \$1.7 million. The fire did not spread to other cars and caused about \$10,000 damage to the station building. A similar event occurred on an 11:32 pm train from the city on August 30 2002 at Hampton station. The arson fire was lit in the unoccupied last car resulting in the entire car being consumed.

Two similar incidents also occurred in NSW in the 1970's.<sup>[28]</sup> These prompted some investigation by railway authorities into the performance of materials used in NSW trains at the time. In 1976 a fire was deliberately lit at the rear end of the lower deck on an unoccupied double deck carriage and rapidly spread to surrounding materials. It appears that flashover may have occurred when a passenger door was opened to allow fire fighting. Fire spread through the entire carriage. Another double deck carriage was completely destroyed in a similar event in 1973.

In Queensland in 2001 an arson fire was lit in the driver's cabin of a suburban train. The vehicle was stabled in the open at a rail yard. The fire brigade responded some 14 or 15 minutes after ignition and the fire was controlled around 11 minutes later. The driver's cabin had become fully involved and was extensively damaged by the fire. Only one of the driver's cabin windows remained intact. There was a small amount of

flame damage in the passenger saloon adjacent to the connecting door which had eventually burnt through.<sup>[29]</sup>

### **2.1.3 Tunnel Fire Incidents**

The use of tunnels and underground or covered stations also provides a motivation for research of fire development on passenger trains.<sup>[30]</sup> Tunnels contain heat and smoke from fires, restrict escape and rescue possibilities and can affect fire ventilation. Many underground stations are connected to shopping centres and public spaces. Also a fires growth rate and fully developed HRR can be significantly increased by both increased radiation effects due to tunnel geometry and forced ventilation. It is possible for these effects to increase the growth rate and fully developed HRR that would occur for an open fire load (such as an open hazardous good vehicle) in the open air by a factor ranging from 1-10 depending on the severity of the effects.<sup>[31]</sup> This increase of HRR due to tunnel effects may not be as severe for a passenger train as for an open fire load due to partial shielding of the trains body, however some limited increase in HRR could be expected.<sup>[32,33]</sup>

This containment of hazardous fire conditions and increase in fire growth and HRR leads to an increase in the consequences of a severe fire incident and requires cost effective fire safety design. The first European rail tunnels were built more than 150 years ago and since then the use of tunnels and underground stations has been increasing to meet transport needs. For example Germany has approximately 600 km of tunnel for underground, rapid transit and urban railways with a total of approximately 500 subterranean stops.<sup>[34]</sup> Increased application of fire safety engineering for rail tunnels requires suitable design fires for cost effective design.

Recent tunnel fires have demonstrated that the occurrence of a fire incident within a tunnel is likely to escalate the incident consequences. In 1996 a fire occurred in the Channel Tunnel which provides a rail link between Britain and France where road vehicles are carried on special rail cars. The fire started in a truck carrying combustible goods resulting in 34 people being injured and severe damage to the tunnel.<sup>[35]</sup> In 1999 a fire occurred on a truck carrying flour and margarine in the Mont Blanc tunnel in the Alps between France and Italy. This resulted in 42 fatalities. Also

in 1999 a fire in Austria's Tauern road tunnel resulted in 12 fatalities and 50 injuries.<sup>[10]</sup>

#### **2.1.4 Passenger Rail Fire Statistics**

The following review of passenger rail fire statistics demonstrates that small fire incidents, most often caused by arson, are common. However large fire incidents involving at least a large portion of a carriage are less common with six large fires reported in the literature in Australia over the past 30 years. Passenger train fire related fatalities are very rare.

##### **2.1.4.1 UK statistics**

The Railway Safety Organisation has reported fire statistics for all rail (passenger and freight) on Railtrack controlled infrastructure in the UK from 1992 to 2000.<sup>[2]</sup> Only train fires where there was the presence of flame were included in the data and 'smoke only' incidents were excluded. During this period and on this basis over 2900 fires occurred with 78% of these occurring on passenger trains. Arson was the major fire cause with 56% of passenger train fires being attributed to arson. Mechanical and electrical causes each accounted for approximately 14% of the passenger train fires. Of the arson fires, 90% occurred in metropolitan areas and 10% occurred in regional/intercity areas. Excluding 31 people who were killed in a major incident at Ladbroke Grove (1999) involving a collision and subsequent diesel fuel fire, only 1 fatality occurred due to fire during this period. Except for two arson fires which resulted in complete or severe damage to entire carriages and two fires involving collisions and/or fuel tanks rupturing, all other incidents did not result in severe damage to vehicles.

##### **2.1.4.2 Australian Statistics**

The rate of reported fire starts is very different for Melbourne (9-15 per year) compared to Sydney (80 per year). This significant difference is possibly due to differences in definition of a fire incident and thoroughness of reporting and record keeping.

##### **Melbourne**

Fire incident data for Melbourne passenger trains for the years 1993-1999 and 2002-2005<sup>[36]</sup> has been gathered by the Department of Infrastructure, Victoria. A total of 81

fires were reported during the 9 year period. Of these 52 fires were interior fires. Arson was the cause for 52% of total fires and 79% of internal fires. This is similar to UK statistics

A risk assessment study for railway lines at Federation Square<sup>[37]</sup> has tabled fire incidents recorded by the Public Transport Corporation (PTC) for the Melbourne suburban network from 1987 to 1997. Over this period there were 125 reported fires. Of these, 76 were deliberate and 49 were accidental. Another study<sup>[38]</sup> has tabled fire incidents recorded from 1998 to 2003 for about 60% of the Melbourne suburban network with 45 fires. Of these 20 are known to be arson fires including the 2 cases of arson resulting in spread to entire carriages discussed in section 2.1.2.2.

### **Sydney**

Railcorp safety statistics published since January 2006<sup>[39,40]</sup> indicate an average of one reported fire incident every three days on NSW City and outer suburban trains. Details of the size and source of the fires is not provided.

The State Rail Authority (SRA) have provided fire incident reports in NSW rolling stock for the period 1991 to 2000.<sup>[41]</sup> The database contains approximately 690 fire incidents. However a substantial number of these incidents involved smoke being emitted from over heating of traction motors, brakes, cables/batteries, A/C units and the like and have been excluded from consideration below. For internal car fires most fires involved construction materials and fittings with ignition sources commonly being newspapers, paper cups, lighter fluid etc. A limited statistical analysis conducted by Arup<sup>[41]</sup> of some 200 of the fires gives the following approximate figures:

- 41% started on seating.
- 2% started on walls.
- 11% started on floors.
- 12% started in light fittings.
- 20% were due to other electrical fittings.
- 14% occurred external to the car.

### **2.1.5 The Need for Research on Fire Development in Passenger Trains**

Barnett has conducted a review of events motivating improved fire safety for sea, road and rail.<sup>[42]</sup> Through review of some major transport fire incidents the potential for catastrophic life loss and consequences is recognised. The review also recognises that tunnels exacerbate the problem of rail fires. Barnett concludes that determination of appropriate design fires is critical to effective fire safety design leading to minimisation of such consequences.

Barnett's conclusions are in agreement with the findings of this review of fire engineering design, fire incidents and statistics which has demonstrated the following key points:

- Although large passenger train fires are infrequent they may have extreme consequences.
- Occurrence of such fires within tunnels or other underground infrastructure can escalate these consequences.
- Arson is the most frequent interior fire cause and the most likely to result in significant fire sizes.
- A suitable level of fire safety must be achieved via cost effective design. This requires increased understanding of fire behaviour to develop suitable design fires and to minimise fire incidents and fire size.

## 2.2 **EXPERIMENTAL RESEARCH ON PASSENGER TRAIN FIRES**

### 2.2.1 Categories of Experimental Work

Experimental work previously carried out on passenger train interiors falls into the following three categories:

- **Small-scale** - Experiments conducted on small, single or composite material specimens usually applying standard test methods. The actual conditions that occur in real fire scenarios are generally not well simulated. Small-scale experiments are the least costly and are useful for comparison or screening of materials.
- **Large-scale** - Experiments involving full sized specimens or which “mock-up” a small section of the interior of a train, usually involving a floor, seat, wall and/or ceiling combination. These experiments are designed to simulate the localised material and geometry combinations that occur in a real fire scenario without extending to include the full train carriage. Large-scale experiments simulate ignition and early fire growth in real scenarios. However such experiments do not simulate fire spread along a carriage or fully developed fire behaviour as the full carriage materials are not included and enclosure geometry and ventilation are usually different. Direct measurement of HRR is often applied.
- **Full-scale** - Experiments conducted on an actual or mocked up train carriage involving the complete, or a significant proportion of interior materials. These experiments are designed to provide data relating to fully developed fire behaviour and fire size. Full-scale experiments are generally extremely costly and direct measurement of HRR on such a scale is difficult and not normally attempted.

Due to cost and resource requirements most passenger train fire behaviour experimental programs have involved a combination of small and large-scale experiments. Very few full-scale experiments have been conducted. The main passenger train fire experimental research projects found in literature are summarised in Table 2-2.

**Table 2-2 Passenger train fire experimental research projects**

Project	Year	Experiments
JNR – Fire behaviour on a running train <sup>[43,44]</sup>	1974	<ul style="list-style-type: none"> <li>• Full-scale fire tests on moving trains</li> </ul>
NBS AMTRACK <sup>[45]</sup>	1984	<ul style="list-style-type: none"> <li>• Small-scale tests</li> <li>• Large-scale mock-up interior section tests</li> <li>• Large-scale calorimeter tests on seats</li> </ul>
SP-Fires on buses and trains <sup>[46]</sup>	1990	<ul style="list-style-type: none"> <li>• Large-scale mock-up interior section tests</li> <li>• Large-scale calorimeter tests on seats</li> </ul>
EUREKA <sup>[47-49]</sup>	1995	<ul style="list-style-type: none"> <li>• Full scale fully developed carriage fire tests conducted in tunnels with HRR measurement</li> </ul>
FIRESTARR <sup>[50,51]</sup>	2001	<ul style="list-style-type: none"> <li>• Small-scale tests</li> <li>• Large-scale mock-up interior section tests</li> <li>• Large-scale calorimeter tests on seats</li> </ul>
Previous CSIRO research <sup>[52]</sup>	2000-2003	<ul style="list-style-type: none"> <li>• Large-scale calorimeter tests on seats</li> <li>• Large-scale mock-up interior section test</li> <li>• ISO 9705 room fire test</li> </ul>
NIST-Fire safety of passenger trains <sup>[53-55]</sup>	1999-2004	<ul style="list-style-type: none"> <li>• Phase I Cone calorimeter compared with other standard small scale tests</li> <li>• Phase II Large-scale mock-up interior section tests to support <math>t^2</math> growth rates for zone fire models</li> <li>• Phase III Full scale tests on intercity coach</li> </ul>
SP – Model scale railcar fire tests <sup>[56,57]</sup>	2005	<ul style="list-style-type: none"> <li>• Small-scale tests on 1-10 scale model railcar investigating ventilation effects</li> </ul>

Descriptions of standard fire tests applied to rail vehicles are provided in Appendix A. These research projects are discussed as follows.

### 2.2.2 JNR Fire Behaviour on a Running Train Project (1974)

A train fire in the Hokuriku tunnel, Japan, 1972, resulted in destruction of one carriage, 30 fatalities and 700 injured. In response to this event Japan National Rail (JNR) refurbished its fleet with improved materials to increase fire safety and conducted full-scale experiments on moving multiple car trains to verify the improvement of fire safety and understand post-flashover fire behaviour on moving trains.<sup>[43,44]</sup>

Experiments were conducted both on an open air test track and in a 2.9 km tunnel. Ignition sources were placed on seats in the mid section of a middle carriage of a multiple car train. If the fire grew to flashover the train was set moving at 60 km/hr. Temperatures, smoke density, gas concentrations and toxicity were measured in the ignited carriage, adjoining carriages and in the test tunnel. Carriages were connected

via bellows but were separated by end doors. Experiments and results are summarised in Table 2-3.

**Table 2-3 JNR Full-scale train fire experiments and results**

Test	Location	Carriage details	Ignition source	Results
1	Open air	Refurbished car. Vents windows and doors closed,	20 pages of newspaper and 200 ml alcohol	No significant fire growth
2	Open air	Non-refurbished car. Vents windows and doors closed	20 pages of newspaper and 200 ml alcohol	Significant fire growth on seat, wall and ceiling linings. At 9 minutes flashover was imminent so train set in motion. However carriage filled with smoke and fire growth was choked. Due to lack of ventilation
3	Open air	Non-refurbished car. Vents and side doors open	40 pages of newspaper and 400 ml alcohol	Carriage flashed over after 3 minutes. Train was then set in motion. Ignited carriage was completely burned out with damage heavier to the rear. Only two windows were broken. No significant fire spread to adjoining carriages. Conditions remained tenable in the adjoining carriages.
4	Tunnel	Refurbished car. Vents open, windows partly open, doors closed	20 pages of newspaper and 300 ml alcohol	Carriage flashed over and the train was set in motion. Ignition carriage was completely burnt out. Fire spread to exterior of carriage behind. No spread of fire to interior of adjoining carriages Tenability was reduced in carriage behind ignition carriage. Average tunnel temperature increased 10°C and conditions remained tenable.
5	Tunnel	Refurbished car. Vents open, windows and doors closed	20 pages of newspaper and 300 ml alcohol	Carriage fire grew appeared to be growing to flashover and the train was set in motion. Fire was less severe due to restricted ventilation. Only the middle part and ceiling of the Ignition carriage were burned. No fire spread to adjoining carriages. Conditions remained tenable in carriage behind. Average tunnel temperature increased by 5°C and conditions remained tenable.

The JNR full-scale train fire experiments are unique as they appear to be the only full-scale experiments investigating fire growth on moving vehicles and observing multiple flashover train fires under different ventilation conditions. Other important points of these experiments are:

- Project literature states that “The fire initially develops on the ignition seat until sufficient heat is produced to ignite the adjacent wall lining and luggage in racks directly above. This increased fire size then ignites the ceiling. By this stage sufficient smoke has been produced to make visibility within the vehicle poor. Once ignited, flames will rapidly spread along the ceiling until a

flashover occurs. Up to the onset of flashover there is sufficient air within the vehicle to provide all the oxygen required for combustion. However after flashover a sudden consumption of oxygen takes place, temporarily affecting the rate of combustion causing a temporary drop in temperature. Subsequent spread of fire depends on the ventilation conditions of the vehicle”. This observation matches well with the experimental observations in Section 3.2 of this thesis.

- This project demonstrates fire will spread more aggressively in the opposite direction to the vehicle motion for a flashover carriage fire on a moving train.
- Improved fire performance of materials will reduce likelihood of flame spread beyond the ignition area.
- Fire spread from carriage to carriage is enhanced and more likely to occur in a tunnel. The effectiveness of carriage separation by use of end doors in preventing carriage to carriage fire spread is demonstrated.
- Only a moving train fire in a tunnel is investigated and it is concluded that the effects on the tunnel are not significant. However the effects both on tunnels and on vehicles are likely to be much greater if the fire is stationary.
- HRR was not measured for these experiments however the principal of oxygen consumption calorimetry was not in common use at this time.
- Vehicles used in these experiments were 1970’s intercity coaches. The fuel load and fire performance of materials for these vehicles compared with current metro passenger trains is unknown.

### 2.2.3 NBS AMTRACK Project (1984)

In 1984 the US National Bureau of Standards (NBS), was sponsored by the Federal Railroad Administration (FRA) to investigate fire behaviour of interior materials on an Amtrak intercity passenger coach.<sup>[45]</sup> The project investigated a range of alternative interior materials and was conducted in 3 parts:

- **Small-scale tests** – tests including smoke density chamber tests, flame spread tests, critical radiant flux tests and cone calorimeter tests were used to characterise the materials
- **Large-scale interior mock up experiments** - Eight experiments with mock-ups of a section the Amtrak passenger coach interior were conducted inside an

ISO 9705 enclosure. Different types of floor, wall and ceiling linings, two double seat assemblies and in some cases a luggage rack were fitted. For all tests either 50 double sheets (1.06 kg) or 100 sheets (2.12 kg) of newspaper were placed on the rear window seat and ignited. Temperatures, heat fluxes, gas concentrations and HRR were measured. Tenability criteria for temperatures and gas concentrations were applied to these experiments. Two of the tests applying 1.06 kg newspaper resulted in flashover. Both of these tests had carpet lined walls and ceilings. The larger ignition source was not applied to these linings.

- **Large scale seating calorimeter tests** – Four different full size, upholstered seat and squab cushions were mounted on a non-combustible seat frame directly under the calorimeter hood and ignited using 1.06 kg of newspaper to investigate fire behaviour of seating without interaction with other materials or surrounding geometry. Peak HRR for seating (with newspaper HRR subtracted) ranged from 30-140 kW.

The NBS Amtrack project assesses the viability of predicting large-scale behaviour from small scale tests. The research concludes that small-scale test results cannot be used to directly predict large scale behaviour; however they can be used to assess general improvement or deterioration in performance due to changes in materials within the same geometry. Other comments regarding the NBS AMTRACK project are:

- Occurrence of two flashover fires for tests with the most flammable combustible wall and ceiling linings demonstrates that material properties have a critical influence on fire spread beyond the area of ignition.
- Packing of newspaper ignition sources affects the severity of the ignition source. Packing density of ignition sources was not characterised. The 1.06 kg newspaper achieved a peak HRR of 55 kW at 100 s. This was sufficient to promote fire spread on some of the materials.
- Based on comparison with later research on newer vehicles the older NBS Amtrack intercity carriages typically have higher fire loads with more flammable interior materials than modern metropolitan passenger trains.

Decreased fuel load and material flammability decreases susceptibility to fire growth.

- The author's conclude “a suitable interior evaluation protocol would be to firstly conduct a small number of large-scale mock-up tests to determine a set of acceptable materials for a given vehicle geometry and then use comparative small-scale tests to assess alternative materials”<sup>[45]</sup>. This would be more adequate but costly compared to design according to current prescriptive rail design standards.

#### **2.2.4 SP Fires in Buses and Trains Project (1990)**

In 1990 the SP National Testing and Research Institute of Sweden conducted a project on fire performance and test methods for buses and trains.<sup>[46]</sup> This research involved a range of large-scale experiments to determine ignitability and HRR of a variety of interior materials from buses and trains. The research also reviewed suitable fire test methods and zone modelling for buses and trains. The SP fires in buses project is primarily focused on seating fire performance and only provides limited information on fire behaviour beyond the early stages of ignition relating to fully developed fire behaviour. Other comments regarding this experimental work are:

- BS 5852 small ignition sources were applied to a range of seats. When exposed to smouldering cigarettes, match flames and type 4 timber cribs the seats did not support fire growth. When slightly larger BS 5852 type 5 and 6 timber cribs were applied all seats ignited and produced peak HRR's ranging from 160-250 kW.
- Cone calorimeter tests were performed on seat materials but the results were not used for any purpose other than comparison of materials.
- Two large-scale experiments were conducted in a standard ISO 9705 enclosure. The enclosure was fitted with rows of seats, and floor, wall and ceiling linings from a bus. The exact details of the materials are not reported. A BS 5852 type 6 timber crib was applied to the middle seat. In both tests it was found that although the seat ignited and burnt with a peak HRR of 200kW there was no spread beyond the ignited seat.
- The ignition sources used for these experiments were very small with the largest timber crib used providing a peak HRR of approximately 10 kW.

Surveys of typical litter on trains<sup>[58]</sup> demonstrate that much larger ignition sources are credible. Given that very small ignition sources were used the performance of the seats tested appears to be poor.

- The ceiling height for the large-scale experiments was higher at 2.4 m than most typical trains or buses at approximately 2 m. This may have reduced flame impingement on ceiling linings. The project concluded that direct flame spread along wall and ceiling linings is unlikely and that fire is more likely to spread from seat to seat. This is contradictory to the findings of other research reviewed which highlight that wall and ceiling linings are critical for flame spread.

### **2.2.5 EUREKA Project (1995)**

Nine European nations cooperated in the EUREKA project EU 499 FIRETUN which primarily involved a series of full-scale fire experiments conducted in tunnels. The objective of this project was to investigate the effects of real transport fires on a tunnel environment and structure. Altogether 21 tests were conducted on a variety of transport vehicles and other materials such as timber between 1990 and 1992. Results of the experiments were evaluated from 1992 through 1995. Key results of the EUREKA project were summarised in the main project report<sup>[47]</sup> and in a tunnel fire safety paper<sup>[48]</sup> and the calculation of experimental HRR was reported by SP.<sup>[49]</sup>

The tunnel used was 2.3 km long. It had a horseshoe shaped cross section with a width varying between 5.3 and 7 m and height between 4.8 and 5.5 m. The tunnel had a steady slope of 1° however gas flows due to buoyancy were observed due to this small slope. Four rail cars were tested separately in these experiments including subway cars and intercity passenger cars. These had either steel or aluminium bodies. In addition to this two extra experiments, each involving half a passenger train with different wall and ceiling linings, were carried out to compare the fire performance of different linings. In these two experiments all other materials such as seats and carpeting were removed so two different types of wall and ceiling linings could be fitted. One half carriage was lined with polyester GRP, the other was lined with phenolic GRP. The absence of seats and other fittings for these two experiments significantly affects fire behaviour however the two experiments were intended as a

demonstration of the improve performance of phenolic GRP over polyester GRP. In all experiments trays of isopropanol were used as the ignition source. For most experiments 6 l isopropanol was used but if this did not induce significant fire growth then the quantity was increased to 12 l. Air velocities in the tunnel were varied for different experiments from 0 - 8 m/s.

The tunnel was instrumented to measure temperatures, air velocity, gas concentration and smoke density. The vehicles themselves were instrumented with a limited number of thermocouples. The vehicles could not easily be observed due to heat and smoke in the tunnel as the fire developed.

The method of estimating HRR by mass loss was rejected due to the heavy weight of the vehicles. Instead HRR measurement was attempted by two different methods. The first method was to measure the convective fraction of the HRR (typically 70%<sup>[5]</sup>) based on temperature and flow measurements alone. The second method of calculating HRR was the principle of Oxygen consumption calorimetry and/or CO<sub>2</sub> production calorimetry. A gas flow and concentration profile was estimated for the tunnel cross section from measurements. This was then used to estimate the total HRR. This method had a large error estimated to be of the order of  $\pm 25\%$ . The majority of this error may be due to instrumentation limitations. Gas velocity and O<sub>2</sub> concentration was usually measured at 3 points for a given tunnel cross section on either side of the fire source. Accuracy of laboratory fire calorimeters rely upon high Reynolds number flows producing well mixed, homogenous distribution of gas concentrations and temperature and a well defined velocity profile across an exhaust duct of much smaller diameter compared with the EUREKA test tunnel. For tunnels the ratio of velocity to cross sectional area is most likely lower, resulting in lower Reynolds number flows, poorer mixing, less homogenous distribution of gas concentration and temperature, and flow profiles across the tunnel that change significantly with fire size. For this reason 3 measurement points is likely to provide only a coarse measurement of HRR.

EUREKA experiments on passenger trains are summarised in Table 2-4.

**Table 2-4 EUREKA train fire experiment results**

Vehicle type	Fuel load (MJ)	Ignition source (kg isopropanol)	Result	HRR* $\pm 25\%$ (MW)
Subway car steel Body (F31)	32,670	0.7	Carriage burnt out Fire duration 20 min	-
Rail car steel body	62,480	6.2	Carriage burnt out Fire duration 70 min	20
Rail Car steel body	76,890	6.2	Carriage burnt out Fire duration 100 min	14
Subway car Aluminium body	41,360	6.2	Carriage burnt out and roof melted away Fire duration 20 min	35
Half railway car Polyester GRP	15,400	6.2	Carriage burnt out Fire peak at 8 minutes	-
Half railway car phenolic GRP	12,100	12.3	No fire spread	-

- = HRR not calculated or reported in EUREKA reports

\* Quoted HRR are estimates recommended by EUREKA report, there was significant variance in estimates

The EUREKA project full-scale measurement of HRR of complete train carriages in tunnels is unique. There is a large degree of variance of HRR calculated by different parties involved. This may be due to likely errors discussed above. Due to this inaccuracy and variance the resulting HRR quoted should not be taken as definitive. Rail carriages were calculated to have peak HRR ranging from 14-35 MW with maximum gas temperatures inside the vehicles of 800-1200 °C This research demonstrates the difficulties of full scale train fire HRR measurement. Other points regarding the EUREKA project are:

- The research was focused on tunnel fire performance and very little data was gathered on the internal fire growth within passenger trains.
- After initial localised fire growth at the ignition source location, all rail car fires exhibited a subsequent rapid fire development, during the first 10-15 minutes from ignition demonstrating that when an ignition source is large enough to promote fire spread beyond the ignition area then the fire is likely to rapidly grow to involve the entire carriage.
- Damage to the vehicle body integrity was observed to influence fire growth. Aluminium vehicle bodies (particularly the roof) were destroyed early into the fire tests significantly increasing ventilation and fire size when compared with steel bodied vehicles which maintained their integrity.

- The importance of wall and ceiling lining performance as a mechanism for flame spread beyond the ignition area is demonstrated by the comparative wall and ceiling lining tests. The polyester GRP supported significant fire spread throughout the carriage. The phenolic resin GRP did not support significant fire spread.

### 2.2.6 FIRESTARR Project (2001)

The Fire Standardisation Research in Railways (FIRESTARR) Project<sup>[50,51]</sup> was a 3 year project with the intention of assisting the development of a draft European Standard EN 45545 “Fire protection on railway vehicles”.<sup>[43]</sup> The project involved collaboration between 11 European research organisations. The objectives of the project were to select suitable test methods for assessment of the fire performance of materials and to propose a classification system for the materials. The project involved the following experiments on a broad range of interior materials:

**Small-scale tests** – Standard small-scale tests including small flame exposure tests, lateral flame spread tests, flooring radiant panel tests, cone calorimeter and smoke tests were conducted. The complete results of these small-scale tests were not provided in the final FIRESTARR report.

**Large-scale wall and ceiling lining tests** – Eleven different wall and ceiling linings were tested directly under an ISO 9705 hood, installed on a mock-up wall and ceiling corner section. The corner was open and well ventilated. A 75 kW gas burner was applied for 10 minutes. Heat release rate, smoke and toxic gas concentrations were measured in the exhaust duct. Six materials produced peak heat release rates in the range of 80-100 kW but one material, a polyester GRP, produced a peak HRR greater than 1000 kW.

Twelve different wall and ceiling linings (same materials as for corner test plus one extra carpet) were installed in a 10 m<sup>3</sup> enclosure, 2.3 m high by 1.9 m wide by 2.04 m long with a 1.9 m by 0.6 m open doorway. The compartment was located beneath an ISO 9705 fire calorimetry hood. A gas burner output of 75 kW for 2 minutes followed by 150 kW for 8 minutes was applied to one corner of the enclosure. Six materials,

including polyester GRP, melamine, plywood and decorative laminates went to flashover.

### **Large-scale furniture tests -**

Eight different seat types were tested using the NT FIRE 032 applying a square gas burner with a heat output of 7 kW to the top of the seat cushions. The seats were vandalised to different levels by slashing. The tests were firstly conducted in the open under an ISO 9705 hood and were then tested placed inside the same 10m<sup>3</sup> enclosure as used for lining experiments, against a corner wall. The enclosure door was closed for the first 3 minutes of each test then opened to simulate the ventilation conditions of a small seating compartment on a French intercity train. Once ignited the heat release rates of the seating ranged from approximately 100 kW to 350 kW.

Based on the small and large-scale test data, FIRESTARR recommended a set of test methods and criteria for classifying passenger rail materials. The material classifications were divided into 3 classes:

- Class A – materials to be used in underground or tunnel operations.
- Class B – materials for non-underground or non tunnel operations.
- Class C – for low risk limited use applications only.

The classification criteria for wall and ceiling linings, flooring and seating are summarized in Table 2-5 to Table 2-7. The fire growth and smoke visibility requirements are linked to the following empirical correlations based on cone calorimeter (ISO 5660-1<sup>[59]</sup>) and smoke density chamber (ISO 5659-2<sup>[60]</sup>) data test results:

- To predict the time when flashover will occur in a 10 m<sup>3</sup> compartment.

$$t_{FO} = 138.5 + 1.39(t_{max} - t_{ig}) \quad \text{Equation 2-1}$$

Where  $t_{ig}$  is time to ignition  $t_{max}$  is time to reach peak HRR in cone calorimeter at 50 kW/m<sup>2</sup>

- To predict time when visibility in a 40 m<sup>3</sup> corridor space will be reduced to 10 m visible distance due to smoke.

$$t_{VL} = 459 - 0.345(VOF4) \quad \text{Equation 2-2}$$

Where  $VOF4$  is a smoke rate index determined for the first 4 minutes from ISO 5659-2 at 50 kW/m<sup>2</sup>, no pilot. Visibility limit is a distance of 10 m.

**Table 2-5 Summary of FIRESTARR recommended requirements for wall and ceiling linings**

Parameter	Test Method	Test Conditions	Classification criteria		
			Class A	Class B	Class C
Ease of fire initiation	ISO 5658-2 <sup>[61]</sup>	Heat flux gradient 50 kW/m <sup>2</sup> to 1.5 kW/m <sup>2</sup>	CRF ≥ 37 kW/m <sup>2</sup>	CRF ≥ 30 kW/m <sup>2</sup>	CRF ≥ 10 kW/m <sup>2</sup>
	ISO 5660-1 <sup>[59]</sup>	Heat flux of 50 kW/m <sup>2</sup>	No ignition	Ignition	Ignition
Fire Growth	ISO 5660-1 <sup>[59]</sup>	Heat flux of 50 kW/m <sup>2</sup>	No Flashover or t <sub>FO</sub> ≥ 390 s	t <sub>FO</sub> ≥ 240 s	Not required
Loss of Visibility	ISO 5659-2 <sup>[60]</sup>	Heat flux of 50 kW/m <sup>2</sup> , without pilot flame	t <sub>VL</sub> ≥ 390 s	t <sub>VL</sub> ≥ 240 s	Not required
Toxic lethality	ISO 5660-1 <sup>[59]</sup>	Mass loss measurement at 35 kW/m <sup>2</sup>	FED < 1.0	FED < 10.0	Not required
	NFX-70-100 <sup>[62]</sup>	600 °C			

Note: - CRF = critical radiant flux to support flame propagation under test conditions.  
 - Flashover and t<sub>FO</sub> (time to flashover) is for a 10 m<sup>3</sup> enclosure predicted using Equation 2-1  
 - t<sub>VL</sub> is time to loss of visibility in 40 m<sup>3</sup> carriage/corridor is predicted using Equation 2-2.  
 - FED (Fractional effective dose) is predicted based on total mass loss from ISO 5660-1 and toxic gas concentrations from NFX 70-100.

**Table 2-6 Summary of FIRESTARR recommended requirements for floor linings**

Parameter	Test Method	Test Conditions	Classification criteria		
			Class A	Class B	Class C
Ease of fire initiation	Pr EN ISO 9239-1 <sup>[63]</sup>	Heat flux gradient 11 to 1.5 kW/m <sup>2</sup>	CRF ≥ 8.0 kW/m <sup>2</sup>	CRF ≥ 4.5 kW/m <sup>2</sup>	CRF ≥ 3.0 kW/m <sup>2</sup>
	ISO 5660-1 <sup>[59]</sup>	Heat flux of 25 kW/m <sup>2</sup>	No ignition	Ignition	Ignition
Fire Growth	ISO 5660-1 <sup>[59]</sup>	Heat flux of 25 kW/m <sup>2</sup>	THR ≤ 75 MJ/m <sup>2</sup>	THR ≤ 120 MJ/m <sup>2</sup>	Not required
Loss of Visibility	ISO 5659-2 <sup>[60]</sup>	Heat flux of 25 kW/m <sup>2</sup> , with pilot flame	VOF4 ≤ 100	VOF4 ≤ 1000	Not required
		Heat flux of 25 kW/m <sup>2</sup> , without pilot flame	VOF4 ≤ 100	VOF4 ≤ 200	Not required
Toxic lethality	ISO 5660-1 <sup>[59]</sup>	Mass loss measurement at 35 kW/m <sup>2</sup>	FED < 1.0	FED < 10.0	Not required
	NFX 70-100 <sup>[62]</sup>	600 °C			

Note: -THR = total heat released  
 - FED is predicted based on total mass loss from ISO 5660-1 and toxic gas concentrations from NFX 70-100

**Table 2-7 Summary of FIERSTARR recommended requirements for seating**

Parameter	Test Method	Test Conditions	Classification criteria		
			Class A	Class B	Class C
Ease of fire initiation	NT Fire 32 Furniture Calorimeter [64]	7 kW burner applied (representing 100g paper)  With and without vandalism  Gas analysis in the duct	v = 0, NI and v = 2, NI	v = 0, NI or $t_{ig} \geq 10$ min and v = 2, NI or $t_{ig} \geq 2$ min	Not required
Fire Growth			Time to peak HRR $\geq 10$ min and THR < 5 MJ	Time to peak HRR $\geq 6$ min and THR < 70 MJ	Time to peak HRR $\geq 6$ min and THR > 70 MJ
Loss of Visibility			Time to peak RSP $\geq 10$ min and TSP < 60 m <sup>2</sup>	Time to peak RSP $\geq 6$ min and TSP < 700 m <sup>2</sup>	Time to peak RSP < 6 min and TSP > 700 m <sup>2</sup>
Toxic lethality			FED < 1.0	FED < 5.0	Not required

Note: - NI = No Ignition, I = Ignition, THR = total heat released, RSP = rate of smoke production  
TSP = total smoke produced  
v = 0 : seat not vandalised  
v = 2 : a cross cut on the back and seat cushion cover and interliners and the fabrics pulled away from the foam

The FIRESTARR project focuses on development of prescriptive requirements, providing little increase in understanding of fire development in real scenarios on passenger trains. It would have been more innovative and useful if the project had focused on developing a framework and tools for a performance based regulation instead of a prescriptive one. Other comments regarding the FIRESTARR project are:

- Materials have only been tested in isolation. The interaction of different material types is not investigated. The enclosures used in experiments represent a small seating compartment arrangement for a French intercity coach and are not representative of typical metro passenger trains. The experiments do not simulate fire behaviour in a complete train carriage.
- The origins of the empirical correlations used to relate cone calorimeter and smoke test data to flashover and smoke production in large enclosures are not referenced and the correlations are not validated against the experimental data. The robustness of these correlations is dubious as the flashover correlation states that flashover cannot occur before 138 s. However given a very flammable lining a time to flashover of less than 138 s is quite possible.

- The relationship of criteria to a small 10 m<sup>3</sup> enclosure is not appropriate for typical passenger trains which have much larger enclosure volumes
- The appropriateness of the final recommended prescriptive criteria is not demonstrated by the experimental data in the final report.

### **2.2.7 CSIRO Fire Growth on Passenger Rail Interiors (2000-2003)**

Large-scale fire experiments have been conducted by the Commonwealth Scientific and Industrial Research Organisation (CSIRO) on current Australian passenger train interiors to understand factors affecting fire growth in trains.<sup>[52]</sup> Experiments resulted from numerous small client projects and were not designed as a comprehensive research project. Experiments include:

**Large-scale seat tests** – Experimental objectives were to assess fire growth and spread on seats in absence of adjacent combustible linings and investigate likelihood of direct seat to seat fire spread. Seats consisting of vinyl fabric lining and cushion materials ranging from fire retarded polyurethane to natural fibres were placed in rows in a plasterboard lined enclosure simulating the end of a carriage. Although the plasterboard was paper faced it was not expected to burn with sufficient intensity to influence combustion on the seating. Enclosure temperatures, heat fluxes, gas concentrations and HRR were measured. Ignition sources representing severe arson fires included 525 g cardboard box/newspaper cribs, 400 g and 600 g timber cribs, and 1 l and 2 l of kerosene. These were applied to the rear seat in the corner of the enclosure, see Figure 2.3. The majority of the measured HRR was due to combustion of ignition sources rather than seat material with a maximum HRR of 250 kW for 2 l kerosene. In all tests flames did not spread to adjacent seats and the ignition seat was not burnt to completion. The same tests on several different types of Australian passenger train seats yielded similar results.



**Figure 2.3** Large-scale room test on seating

**Large-scale seat and wall room fire tests** – Mock-ups involving a single seat unit and sections of polyester GRP wall and ceiling lining 1.5 m wide were tested inside an ISO 9705 enclosure. Two sets of material, one from an original un-refurbished train and one from a recently refurbished train were tested. Ignition sources including different amounts of crumpled newspaper and 1 l of kerosene were applied to the seat, see Figure 2.4. HRR was measured. It was found that 1 l kerosene caused fire spread for both material sets and that 600 g of crumpled newspaper caused fire spread on original materials but not on refurbished materials. Where fire spread occurred the wall lining became involved adding heat to the fire plume impinging on upper wall and ceiling. Once the ceiling became involved radiant heat increased burning of the seat and flames rolled across the ceiling. At this point flashover would have occurred if more materials were fitted.



**Figure 2.4** Original seat and wall lining exposed to 600 g crumpled newspaper

**ISO 9705 carriage end section room fire test** - The entire ceiling, rear wall and two side walls of an ISO 9705 room was lined with materials representing the end section of an Australian carriage.



**Figure 2.5.** Carriage end section materials installed in ISO 9705 burn room

Materials installed in the room included modified acrylic resin GRP wall panels and window surrounds, painted aluminium ceiling panels, polycarbonate light diffusers and nylon carpet covering the lower side wall panels. Seats and floor linings were not included. A corner gas burner was operated at 100 kW for 10 minutes followed by 300 kW for a further 10 minutes. During the 100 kW exposure, burner flames directly impinged on wall and ceiling linings however flames did not spread along the linings. However the fire rapidly grew to flashover when exposed to the 300 kW burner output. Several similar ISO 9705 room fire tests have been conducted by CSIRO on a range of Australian metropolitan train interiors, with gas burner output increased in 50 kW increments. All tests involved either polyester or modified acrylic resin GRP wall linings and painted aluminium or laminated ply wood ceilings.

For all such tests flashover occurred at a burner output of 250 kW.

Through this series of experiments CSIRO has focused on understanding interior fire growth on passenger trains from small localised fires to rapidly growing fires leading to flashover. Comments regarding the CSIRO research are:

- Research was limited and did not address fully developed fire behaviour on trains.
- Current passenger train seating typically has good fire performance. For the seats tested there is very little likelihood of direct fire spread from seat to seat.
- Upper wall and ceiling linings are critical to fire spread beyond the ignition location. Attention and improvements to geometry and materials used can greatly reduce the likelihood of fire growth beyond the ignition stage.
- For most wall and ceiling linings investigated, a critical ignition source peak HRR for fire growth beyond the ignition area to occur was found to be in the range 100-300 kW.
- If fire spread beyond the ignition area does occur then fire growth to the stage of flashover is likely. However these experiments have not simulated the interior geometry and ventilation conditions of an actual train.

### 2.2.8 NIST- Fire Safety of Passenger Trains Project (1999-2004)

In 1993 the Federal Railroad Administration (FRA) sponsored the National Institute of Standards and Testing (NIST) to conduct a comparative evaluation of existing US and European standard approaches to passenger train fire safety.<sup>[12]</sup> It was found that all approaches relied on dated prescriptive small-scale test methods that were poorly related to fire behaviour in real fire scenarios. A major conclusion of this study was that the use of fire engineering design techniques, supported by measurement methods using HRR, could potentially provide a more credible and cost effective means to achieve passenger train fire safety. However the understanding of passenger train fire behaviour required for this was lacking, limiting the credibility and cost effectiveness of this approach at that stage.

In response, from 1999 to 2004 FRA sponsored NIST to conduct a research project on the feasibility of applying HRR test methods and fire engineering design techniques to maintain and improve passenger train fire safety. A range of trains from the US Amtrak intercity coach fleet were the basis for experiments and fire engineering analysis. The project was conducted in 3 phases, addressed by three separate reports:

**Phase I**<sup>[53]</sup> – Cone calorimeter tests and small-scale tests required by FRA regulations at the time were conducted and compared. FRA required tests included:

- ASTM E 162<sup>[65]</sup> and ASTM D3675<sup>[66]</sup> flame spread tests.
- ASTM E 648<sup>[67]</sup> flooring critical radiant heat flux test
- FAR 25.853<sup>[68]</sup> bunsen burner test
- ASTM E 662<sup>[69]</sup> smoke box test

All cone calorimeter tests were conducted with a heat flux of 50 kW/m<sup>2</sup>. Empirical correlations linking cone calorimeter results to FRA test results were developed, however the accuracy of the correlations was too poor to be of practical value.

**Phase II**<sup>[54]</sup> - Fire engineering design techniques were applied to different passenger trains to assess impact on fire safety of changes to design and materials, detection and suppression systems, and emergency evacuation strategies. Zone fire modelling was applied using a range of assumed “t<sup>2</sup>” growth rates. “t<sup>2</sup>” growth rates are discussed in detail in Section 2.4.1. Large-scale experiments were conducted on interior furnishing

assemblies to obtain fire performance data and to match real fire scenario growth rates against the “ $t^2$ ” modelled growth rates. Large components including seats, bedding, wall linings, drapes and polycarbonate windows were tested individually directly under an oxygen consumption calorimeter hood. Ignition sources including trash bags and gas burners ranging in HRR from 17-480 kW were applied. The most significant fire growth was observed on sleeper cabin bedding and also on walls and ceilings lined with carpet. Seats performed well.

**Phase III**<sup>[55]</sup> - Full-scale fire experiments were conducted to verify the actual system performance against fire engineering predictions from phase II. Experiments were conducted on an Amtrak Amfleet I intercity passenger coach. Interior furnishings consisted of the materials considered in Phases I and II, with thick foam seating, carpets on floors, lower walls and luggage racks, polycarbonate window glazing and polyester resin GRP window shells lining the upper walls. All passenger doors and windows were sealed to contain combustion gases and an exhaust stack was mounted on the roof. Combustion gases were intended to flow out the exhaust stack to measure HRR by oxygen consumption calorimetry. Interior materials were removed from the end of the carriage which was lined with fire resistant calcium silicate board and fitted with a controllable gas burner. Test fires with “ $t^2$ ” growth rates up to 1 MW were conducted in the fire hardened end for comparison against zone model results. Fire tests applying various ignition sources to the interior furnishings were conducted to provide information on how actual fire scenarios fit within the assumed “ $t^2$ ” growth rates. The results are summarised in Table 2-8. Temperature, heat fluxes, gas concentration and optical density inside the carriage were measured, however the measurement of HRR failed. The NIST report does not discuss or provide a reason for the HRR measurement failure. The criterion for time to incapacitation was a hot layer height below 1.5 m and exceeding 150 °C. For “ $t^2$ ” growth rate tests the relative difference between experimental and calculated times to incapacitation averaged 13%.

**Table 2-8 Summary of Phase III full-scale experiment results**

Full-Scale Experiment	Ave. upper layer gas temp. (°C)	Time of peak upper layer gas temp. (s)	Peak heat flux at centre of floor (kW/m <sup>2</sup> )	Gas concentration (volume %)			Time to untenable conditions (s)
				Min O <sub>2</sub>	Max CO <sub>2</sub>	Max CO	
Slow t <sup>2</sup> gas burner	398	600	19	16	3.0	0.02	231
Medium t <sup>2</sup> gas burner	331	320	16	17	2.4	0.01	126
Fast t <sup>2</sup> gas burner	376	155	15	16	2.8	0.01	60
Ultra-Fast t <sup>2</sup> gas burner	372	80	14	17	2.3	0.03	40
Window drape – 25 kW burner ign source	53	510	0.3	20	0.3	0.01	-
Corner test, wall carpet and window surround – trash bag ign source	183	300	9	17	3.7	0.2	?
Seat – 17 kW gas burner ign source	47	600	0.2	21	0.2	0	-
Seat – 25 kW gas burner	53	565	0.5	21	0.3	0	-
Seat – trash bag ign source	363	270	27	12	6.6	1.4	50

Note : The average upper layer temperature is the average of thermocouple measurements in the upper layer at the peak of the fire size  
 - = untenable conditions did not occur  
 ? = time of untenable conditions not known

It is noted that the average upper layer gas temperatures given in Table 2-8 are low because they are an average of all temperatures in the upper layer (even at the opposite end of the carriage from the fire). The peak heat flux given in Table 2-8 are low because they are heat flux's measured at the centre of the floor rather than directly adjacent the fire.

For the fire tests on interior furnishings no significant fire spread resulted applying small ignition sources 17-25 kW. A trash bag (200 kW) applied to a corner without the seating resulted in significant spread 3 m along the underside of the luggage rack which decayed without suppression but appeared to be on the verge of a fire size that would result in continued fire spread. A trash bag applied to a seat against a window surround resulted in a large fire that would have continued to spread along the carriage and may have reached flashover had it not been suppressed.

The NIST Fire Safety of passenger trains project recognises the potential for fire safety engineering to be applied as a means of achieving cost effective passenger train fire safety. A series of experiments was applied investigating fire behaviour of interior

materials and investigating the suitability of using “ $t^2$ ” growth rates and zone modelling to modelling tenability conditions due to fire growth. The project only investigated the early stages of fire development up to the point of untenable conditions. The project did not investigate fully developed fire behaviour or how such scenarios should be considered in fire safety design. This part of the fire growth is also critical to life safety beyond the carriage. Unfortunately full-scale experiments did not measure fires sizes in terms of HRR. Other comments regarding the NIST project are:

- As the carriages and interior materials studied are from intercity passenger trains they are significantly different to current metropolitan passenger trains.
- Phase I recognises the need for a small scale test that can be used both for regulating materials and gathering HRR data required for fire engineering analysis. Existing small-scale tests cited by FRA do not serve this purpose. However the research failed to indicate criteria for regulating materials based on cone calorimeter data or methods of applying cone calorimeter data to fire engineering analysis.
- Correlations developed relating cone calorimeter results to FRA cited tests are too inaccurate for practical use. Difficulty achieving good correlations was mostly due to the significant differences in fire exposure conditions represented by the different test methods.
- Cone calorimeter and large scale test results indicate FRA prescriptive regulations and tests have resulted in better fire performance of seats than of wall and ceiling linings. This may also be the case in Australia as indicated by previous CSIRO research summarised in section 2.2.7.
- Phase II large-scale tests conducted on individual materials under free ventilation conditions does not simulate enclosure effects and material interactions in real fires. Fire scenarios for multiple components were characterised in terms of “ $t^2$ ” growth rates by summing the HRR curves for the separate large-scale tests on individual components. This assumption is incorrect as it does not consider interactions between materials or ventilation conditions within a train carriage.
- Phase III experiments using a gas burner controlled to “ $t^2$ ” growth rates attempt to provide validation of zone modelling for passenger trains. A very

good match between measured and modelled ASET was obtained with an average relative difference of 13% between experimental and calculated times to loss of tenability. The model assumptions and inputs are not explicitly stated and it is not clear if model inputs were iteratively modified to achieve a good match. As the volume and length of the carriage was effectively halved the affect of enclosure length to width ratio on validity of zone models applied to train carriages is not fully addressed.

- Phase III tests on interior seats and linings indicate a large ignition source up to 200 kW is required for significant spread beyond the ignition area and for untenable conditions to occur.

### 2.2.9 SP Model Scale Railcar Fire Tests (2005)

In 2005 the Swedish National Testing and Research Institute (SP) conducted a series of five tests on a 1:10 scale passenger train carriage.<sup>[56,57]</sup> The objective was to investigate the affect of ventilation on HRR for post flashover train fires. The model carriage was 2.44 m long x 0.30 m wide x 0.27 m high. It had one side door at one end of the carriage and nine windows on each side. The following two parameters were varied in the tests:

- The interior surface materials - either plywood or corrugated cardboard,
- Number of windows open – either all windows and the door were initially open or only the door was initially open and different numbers of windows were opened when the fire visually started to decelerate.

The ignition source for each test was a fibreboard cube soaked in 15 ml heptane, placed in the corner adjacent the open door. Mass loss of the model was measured via a load cell and HRR for each test was measured by oxygen consumption calorimetry. The measured HRR was compared against a correlation for ventilation controlled HRR (Equation 2-3). A correction factor ( $\eta$ ) was used for this comparison

$$\dot{Q}_{VentilationControlled} \approx 1500 A_0 \sqrt{H_0} \quad \text{Equation 2-3}$$

$$\eta = \frac{\dot{Q}_{Measured}}{\dot{Q}_{VentilationControlled}} \quad \text{Equation 2-4}$$

The concept of ventilation controlled HRR and the above equations are fully described in Section 2.4.5. SP acknowledge that an accurate scaling up of model HRR to predict full-scale HRR is impossible due to limitations including turbulence intensity, thermal inertia of materials and radiant heat effects. However SP did apply a Froude scaling technique to roughly estimate corresponding full-scale HRR. The experiments and results are summarised in

**Table 2-9. SP model scale rail car fire test results**

Test No	Surface material	Ventilation Condition	Maximum measured HRR (kW)	$\eta$	Full-scale HRR by Froude scaling (MW)
1	Plywood	Door plus all windows initially open	148	1.73	46.8
2	Plywood	Only door initially open	6	0.33	1.9
		Door plus first 4 windows open	70	1.45	22.1
		Door plus all windows open	136	1.59	43.2
3	Corrugated cardboard	All windows and doors initially open	143	1.68	45.2
4	Corrugated cardboard	All windows and doors initially open	148	1.73	46.7
5	Corrugated cardboard	Only door initially open	11	0.61	3.5
		Door plus first 4 windows open	60	1.25	19.0
		Door plus all windows open	113	-	35.8

A value of  $\eta$  is not calculated for test 5 where the door and all windows are open because the fire was observed to be fuel controlled due to burn out of fuel by this stage of the test.

For each ventilation condition the peak HRR was similar, independent of the interior surface materials used. This was particularly the case where all the windows and the door were open with HRR becoming more variable as ventilation was restricted. For The SP model rail car fire tests indicate that ventilation may be the most important

factor influencing post flashover HRR of a train carriage and that ventilation controlled HRR is likely to be independent of the type of material burning. Other conclusions are:

- The breakage and fall out of windows and the integrity of the carriage body will strongly affect ventilation and therefore HRR
- The correction factor  $\eta$  varied significantly with ventilation conditions. For the well ventilated case  $\eta$  was significantly greater than 1 but for the restricted ventilation case  $\eta$  was significantly less than 1. Therefore Equation 2-3 does not accurately describe ventilation controlled burning and should not be directly applied to estimate peak HRR.
- The surface interior material strongly influenced the initial rate of fire growth and the fire duration.
- A complete correspondence between model-scale and full-scale is not possible and full-scale HRR presented in Table 2-9 should not be relied upon.
- A scenario of two side doors open (one at each end) representing evacuation to a side platform is a likely scenario and may have a significant affect on fire spread from one end of a carriage to another and post flashover HRR however was not investigated.

### **2.2.10 Other Experimental Projects**

Other experimental projects that are not as significant or for which significant literature was not able to be obtained are discussed briefly.

#### **2.2.10.1 ERRI research**

The European Rail Research Institute (ERRI) has conducted a significant research project. Literature on ERRI research was not obtained however it is referred to by the NIST Fire Safety of Passenger Trains project reports. From 1992-1995 rail materials were tested in the cone calorimeter and in large scale tests. ERRI investigated the validity and use of zone models for trains. A zone model was used to simulate fire experiments in a 3 m x 3 m x 3m test enclosure. Based on this it was concluded that the use of a zone model to simulate fires in rail vehicle was feasible. This research appears to fail to address issues relating to the large, long slender volume of a train carriage and its impact on zone modelling validity

### 2.2.10.2 Japanese Railway Bureau experiments

In 1992 the Japanese Railway Bureau, Ministry of Transportation conducted a series of full-scale tests on a current electric metro passenger train carriage.<sup>[70]</sup> Research also reviewed Japan's rail fire safety requirements. Experiments were conducted on a complete carriage located inside a test tunnel. Large fans simulated train motion at 35 km/hr. Temperatures, smoke density and toxic gas concentrations were measured. HRR was not measured. Based on earlier experiments by JNR, ignition sources of 40 pages of newspaper with 300 ml alcohol and 80 pages newspaper with 600 ml alcohol were applied to seats in a series of five experiments with different ventilation conditions for windows and doors. For all experiments, flames from ignition sources impinged on the ceiling but failed to ignite the ceiling resulting in no significant fire spread. This indicated an increase of material fire performance since the JNR experiments. Unfortunately ignition source size was not increased to determine ignition source size required for significant spread. Other research projects have considered larger ignition sources to be credible.

### 2.2.10.3 KRRI Research

Several investigations were performed after the Daegu tunnel train fire but are poorly documented. One investigation performed by the Korean Rail Research Institute (KRRI) involved a large scale experiment attempting to replicate development of the actual fire incident.<sup>[17]</sup> The end section of a carriage was mocked up in an open ended enclosure fitted with seats, floor, and wall and ceiling linings. An unspecified quantity of petrol was applied as an ignition source. All materials in the enclosure became fully involved. Instrumentation and measured results are not documented. A CFD model was developed to extend the experimental result to a full train carriage. No comparison of experimental data and model is provided in the literature.

### 2.2.10.4 BHP Research experiments

In 1998 BHP Research performed a risk assessment of construction over railway lines at Federation Square, Melbourne.<sup>[37]</sup> Four large-scale experiments were conducted investigating fire development, given different ignition sources. Two opposing seat units were installed against a polyester GRP wall panel extending from floor level to include a curved transition to the ceiling. The materials were installed in an open space with no ceiling materials. Three experiments applied ignition sources ranging

from unspecified quantities of crumpled newspaper to 500 ml of methylated spirits on the seat cushion with no significant fire spread beyond the ignition area. The final test applied 1 l of methylated spirits in a tray at the base of the seat against the wall lining. This resulted in significant spread beyond the ignition area on the wall lining. It was assessed that if this fire occurred inside an actual carriage flashover could be expected after about 10 minutes. There were no instrumented measurements of these experiments with qualitative observation only. Lack of hot layer development due to the open test conditions and lack of ceiling material, a critical component for fire spread, means that time to flashover is most likely over estimated.

#### 2.2.10.5 WMTA project

In 1975 the US NBS conducted experiments on interior materials of Washington Metropolitan Area Transit Authority (WMTA) Metro rail cars.<sup>[71]</sup> A range of small-scale smoke and flammability tests were conducted. A smoke test was conducted on a complete carriage using pyrotechnic smoke generators placed beneath the carriage and a plastic skirt placed around the perimeter of the carriage to determine resistance to smoke penetration through the floor. Large-scale mock up experiments were conducted in a burn room enclosure fitted with floor, wall and ceiling linings (PVC), a window and 3 seat units. A range of different seat cushions were tested. Newspaper ignition sources ranging up to 0.9 kg of newspaper were applied to the seats. Gas temperatures, smoke density, gas concentrations and toxicity were measured. These large-scale experiments primarily investigated hazard from smoke and toxic gases. The following key conclusions were produced from this research:

- The floor resists rapid penetration of fire and smoke from beneath the car.
- Small-scale tests did not predict the fire performance of the complete system.
- Hazardous levels of smoke were found to occur for all tests.
- Seats and wall linings are potential sources of fire hazard.
- The carpet and ceiling linings do not contribute significantly to the initial fire hazard.

Although carriage floors have good fire resistance, known weak points in external fire resistance including flexible inter-car bellows sections, door seals, windows and vents were not assessed. Although large-scale experiments exhibited hazardous smoke concentrations prior to flame spread occurring, the tests neglected dilution which

occurs on real trains due to larger volumes of complete train carriages. Given this dilution, hazardous smoke levels may not occur until significant flame spread occurs. The conclusion that carpet does not contribute to fire hazard is reasonable only for the early stages of fire growth. The conclusion regarding ceiling linings is contradictory to the majority of other literature reviewed which indicate that ceiling linings are a critical factor for flame spread

## **2.3 DESIGN STANDARDS FOR PASSENGER TRAIN FIRE SAFETY**

Design standards for passenger train fire safety set minimum requirements for material fire performance and in some cases also address likely ignition sources, suppression, detection, communication and egress. Fire safety design standards are reviewed in this section because it is recognised that fire behaviour on passenger trains is influenced by the design of the vehicle.

### **2.3.1 Australian fire safety requirement**

There is no standard applied nationally in Australia which specifically addresses fire safety in passenger trains.<sup>[72]</sup>

AS 4292 Part 1<sup>[73]</sup> sets out a structure for managing general railway safety. AS 4292 Part 3<sup>[74]</sup> provides a structure for managing rolling stock safety. Both standards describe management structures, hazard identification and risk analysis, and identify some safety issues that a rail organisation should consider and address with their own standards and procedures. They do not quantify minimum levels of general safety and do not specifically address fire safety.

The Railways of Australia (ROA) manual of engineering standards<sup>[75]</sup> provides broad requirements for most aspects of rail design. Fire safety is briefly covered with prescriptive requirements for passenger car materials and configuration, smoke detection, alarms, fire extinguishers and egress. The manual recommends that materials be tested to AS 1530.3 to determine fire performance. However, AS 1530.3 is a poor small scale test for this use as it was only designed for use on wall linings and is a test method unique to Australia.<sup>[14]</sup> The ROA fire safety requirements have rarely been applied in recent practice.

The lack of a suitable Australian national standard has resulted in different specifications being created by rail organisations for each new train. This variation of fire safety requirements creates a costly and inefficient environment for manufacturers without increasing fire safety<sup>[72]</sup>. Dowling recommends<sup>[72]</sup> a strong performance based national code is needed, possibly having a similar structure to that of the Building

Code of Australia<sup>[76]</sup> with deemed-to-satisfy and alternative performance based requirements.

Recent Australian projects involving manufacture, refurbishment or purchase from overseas of metro rail vehicles are listed in Table 2-10. Most of these projects have involved individual specifications for the fire safety design of vehicles.

**Table 2-10 Major Australian metropolitan rail projects since 2000**

<b>Metro rail projects</b>	<b>State</b>
PPP- outer suburban cars	NSW
4GT/Millennium Train	NSW
Hunter Rail Car	NSW
Outer Suburban Car	NSW
Perth Urban Rail Development	WA
Brisbane airport train	QLD
Brisbane EMU SM Series 220	QLD
Tilt Train	QLD
Connex Xtrapolis	VIC
Connex Siemens	VIC
Comeng refurbishments	VIC

The Perth Urban Rail Development (PURD) is an example involving construction of rail tunnels and a new metro passenger train for Perth. The PURD fire safety specification<sup>[77]</sup> was performance based requiring risk assessment to demonstrate hazards were as low as reasonably practicable (ALARP). In support of this risk assessment small and large-scale fire tests were required as well as estimation of design fires and fire and egress modelling. The PPP – outer suburban car project is another recent project applying similar fire engineering principles.

### **2.3.2 International Standards**

Fire safety standards of other countries are more comprehensive and often applied in Australia. All standards provide prescriptive design and testing requirements with some also allowing for alternative solutions demonstrated by fire engineering. NIST have compared a number of international standards.<sup>[12]</sup> This thesis reviews current US and British standards as they are commonly referenced or applied in part in Australia. French, German and European standards are also considered as these countries are the predominant international manufacturers of rail vehicles, some of which are used in Australia. Prescriptive requirements of these standards are detailed in Appendix B.

### 2.3.2.1 U.S.A. standards

In the U.S.A. the Federal Railroad Administration (FRA) is the federal body responsible for administering railroad operations and the National Railroad Passenger Corporation is a provider of passenger rail services. The three main fire safety standards in the U.S.A. are:

- NFPA 130.<sup>[78]</sup>
- Federal Railroad Administration (FRA) regulations.<sup>[79]</sup>
- National Railroad Passenger Corporation AMTRAK specification 352.<sup>[80]</sup>

Considerable overlap exists between these standards. Material flammability requirements for the three standards are almost identical.

NFPA 130 is most commonly referenced and adopted. It sets out fire safety requirements for passenger rail as a complete system including stations, trainways (underground, surface and elevated), ventilation systems, vehicles, vehicle storage and maintenance areas, emergency procedures and communications.

NFPA 130 prescriptive requirements for passenger train interiors include:

- Standard small-scale tests (see Appendix B).
- Large-scale seat tests using pass/fail criteria of California Technical Bulletin 133<sup>[81]</sup> in lieu of small-scale tests.
- Fire resistance furnace tests on components separating major ignition energy or fuel loading sources from the passenger compartment such as floors and penetrations. Integrity must be maintained for periods at least twice the expected evacuation time and a minimum of 15 minutes.
- Ventilation systems to be deactivated manually or automatically in the event of a fire.
- Minimum of two paths of emergency egress from a carriage, typically side doors.
- Requirements for electrical safety, lighting, signage, communications and fire extinguishers.

NFPA 130 prescriptive requirements do not increase in severity for more hazardous operating environments such as tunnels. There are no requirements for material fire toxicity.

NFPA 130 allows alternative solutions supported by fire engineering in place of prescriptive requirements. The performance criterion is that occupants not intimate with the ignition, are not exposed to untenable conditions. NFPA 130 recommends fire scenarios set out in ASTM E 2061<sup>[82]</sup> be adopted as a minimum. No method to quantify design fires to represent the fire scenarios is provided.

NFPA 130 Annex D presents a “hazard load” calculation. Small-scale test data for total heat released (MJ) per unit area over a 3 minute period is multiplied by total exposed surface area for each material installed in a carriage. The total heat for all materials is summed and divided by internal carriage volume. This produces an energy density called a “hazard load” in terms of MJ/m<sup>3</sup>. The purpose of the “hazard load” calculation is not clearly stated. It may be useful for comparing fuel loading of materials however it not a method of characterising fire size.

ASTM E 2061 guide for fire hazard assessment of rail vehicles<sup>[82]</sup> provides guidance for hazard assessment and alternative solutions applying fire engineering to passenger trains. It does not provide regulatory requirements or acceptance criteria. ASTM E 2061 states the primary safety objective is to ensure safe evacuation without exposure to untenable conditions. The secondary objective is to prevent flashover. A range of interior and exterior fire scenarios are suggested including arson. HRR test methods including cone calorimeter tests and large-scale mock up tests are recommended to support fire engineering design. Ignition sources for large-scale seat tests up to 50 kW are recommended. Burn room experiments such as ISO 9705 are recommended for interior linings however it is stated most interior linings for trains are likely to support fire growth to flashover when tested according to ISO 9705. ASTM E 2061 suggests zone fire models, requiring input of assumed design fire HRR curves, for modelling tenability and conditions that may lead to flashover. Correlations relating enclosure geometry and ventilation to the minimum HRR required for flashover are discussed. ASTM E 2061 provides no design fires representing fire scenarios or methods of estimating design fires based on tests. This

is the critical input that is required for assessing the timing of untenable conditions and occurrence of flashover

### 2.3.2.2 British standard

BS 6853<sup>[83]</sup> sets requirements for fire safety of passenger train vehicles only. Stated objectives of BS 6853 are:

- To control power, duration and frequency of ignition sources.
- To control reaction of materials to ignition sources.
- For small ignition sources, order of 1 kW, ensure conditions within affected vehicles remain tenable.
- For larger ignition sources, order of 10 kW, ensure conditions remain tenable for the required evacuation time.
- For largest ignition sources, of order 100 kW, ensure probability of flashover is minimized.
- To limit HRR from the vehicle on flashover.
- To limit the impact fire on areas remote from the seat of the fire.

BS 6853 separates vehicles into 3 classes dependent on operating environment:

- Category Ia – Substantial operating periods in a single track tunnel with no side exits to a walkway and escape shafts, or sleeper vehicles which operate underground for significant periods, or trains that operate without staff.
- Category Ib – Substantial operating periods in multi-track tunnel, or a tunnel with side exits to a walkway and escape shafts, or sleeper vehicles which do not operate under ground for significant periods.
- Category II – Surface stock with no substantial operating periods in tunnels.

BS 6853 prescriptive requirements for passenger train interiors include:

- Standard small scale tests for flammability and fire toxicity (see appendix B).
- Fire resistance tests on floors (20 min integrity and insulation), vehicle body end (30 min integrity) and passenger/drivers cab partition (30 in integrity and insulation).
- Requirements for fire detection and suppression systems, communications and egress.

The prescriptive requirements of BS 6853 increase in severity for hazardous environments such as tunnels.

The stated objectives of BS 6853, listed above, relate to fire scenarios on real vehicles. The prescriptive requirements fail to directly predict if these objectives would be met. BS 6853 does not provide an option to develop an alternative solution based on fire engineering design methods.

BS 6853 Annex C recommends cone calorimeter tests to provide HRR data for use to determine realistic design fires for design of systems such as ventilation. However no pass fail criteria or method for using the data to calculate design fires is specified.

### 2.3.2.3 Other International standards

NF F 16-101 specifies French material flammability requirements for passenger trains.<sup>[12]</sup> NF F 16-101 separates vehicles into categories of rolling stock which travel frequently through tunnels and metropolitan or intercity rolling stock not travelling frequently through tunnels. NF F 16-101 prescribes a complex set small-scale tests and acceptance criteria based on indexes for fire performance and smoke. NF F 16-101 does not provide an option to develop an alternative solution based on fire engineering design methods.

Compared to British and US standards, NF F 16-101 is an excessively complex set of prescriptive requirements. It is expected this will cause confusion and difficulty in interpreting and meeting the criteria. The complexity does not increase fire safety but may in fact reduce it due to various caveats to the standard allowing acceptance of materials to alternative tests and criteria where they have performed poorly under other tests.

The DIN 5510 series of standards<sup>[84]</sup> specifies fire safety of passenger trains in Germany. DIN 5510 part 2 specifies requirements for material flammability and smoke production based on small-scale tests. HRR test methods are not used. A mock up seat test is cited applying a 100g newspaper ignition source. DIN 5510 part 4 sets requirements for structural design of vehicles requiring that trains are divided into fire

sections capable of containing fires for at least 30 min. Floors must have a fire resistance of 30 min.

UIC Code 564-2<sup>[85]</sup> is a European standard produced by the International Union of Railways (UIC). This prescribes requirements for material flammability and smoke production based on small scale test methods. There is no requirement for fire toxicity of interior materials.

prEN 45545<sup>[43]</sup> is a draft for public comment European standard for fire safety of passenger trains developed based on the FIRESTARR research project, see Section 2.2.6. This prescribes requirements for material flammability based on small-scale tests with the exception of furniture calorimeter tests for seats. The standard utilises HRR test methods such as the cone calorimeter. Pass/fail criteria are based on correlations relating test results to flashover and untenable conditions in enclosures. The doubtful validity of these correlations is discussed in Section 2.2.6. The standard does not allow for performance based solutions or provide a method for predicting design fires. This standard has not yet been adopted.

## **2.4 DESIGN FIRE ESTIMATION METHODS**

Passenger train interior fire scenarios can be grouped into two broad categories:

- Small localised fires.
- Larger fires involving either a significant section or an entire carriage.

Small localised fires represent those involving single items, a seat for example, with limited or no spread to adjacent materials. Usually design fires for similar burning items from literature are assumed or large-scale mock-up HRR tests are used. Feedback between the small fire and its environment is usually neglected. Methods for estimating small design fires are not included in the scope of this thesis. However representation of such scenarios applying “ $t^2$ ” growth rates is reviewed.

Larger design fires must consider the ability for small localised fires to spread to involve an entire carriage. Experimental research (see Section 2.2) indicates flashover is normally the mechanism for fire spread to involve an entire carriage. This section reviews flashover prediction methods.

The experimental research reviewed in Section 2.2 indicates that fire behaviour for scenarios involving entire carriage interiors are affected by the following key factors:

- Ignition source HRR curve.
- Material properties.
- Physical configuration of vehicle and materials.
- Available ventilation.

Influence of these factors on fire behaviour is complex and full scale experiments on passenger trains incorporating HRR measurement are very limited. As a result fire engineers either assume design fires or estimate design fires based on simplified methods. This section reviews methods currently applied to estimate designs fire for large fires in passenger train interiors.

### 2.4.1 “t<sup>2</sup>” Growth Rates

Not all phases of a design fire are important depending on the design criteria of concern. If the criterion is only to maintain occupant life safety within a carriage or limit/prevent flashover then the growth phase of the design fire is most important. If criteria consider effects on infrastructure or life safety beyond the carriage of fire origin then the fully developed design fire phase also becomes important.

Fire growth in terms of HRR is commonly fitted to a “t<sup>2</sup>” growth rate, expressed as;

$$\dot{Q} = \alpha t^2 \quad \text{Equation 2-5}$$

Where  $\alpha$  is the fire intensity coefficient. NFPA standard 72<sup>[86]</sup> specifies specific “t<sup>2</sup>” growth rates, shown in Figure 2.6, to represent the possible range of growths from different fuels. These are commonly assumed by engineers to represent building fires, particularly in design of fire detection and suppression systems.

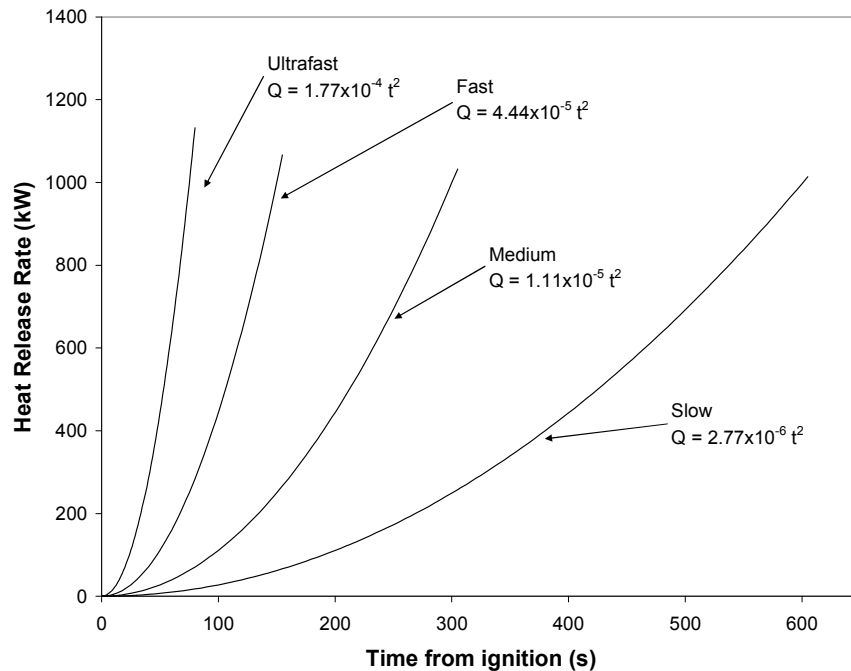


Figure 2.6. “t<sup>2</sup>” fire growth rates

Phase II of the NIST fire safety of passenger trains project<sup>[54]</sup> involved fire engineering analysis for an intercity passenger train applying “t<sup>2</sup>” growth rates.

Passenger tenability was the primary criteria. Conservative tenability criteria applied were:

- Hot layer height  $\leq 1.5\text{m}$  and hot layer temperature  $>65\text{ }^\circ\text{C}$ , or
- Hot layer height  $< 1\text{ m}$  and hot layer optical density  $\geq 0.5\text{ m}^{-1}$ .

Hot layer development and time to untenable conditions was modelled using the zone fire model CFAST (described in Section 2.4.6) assuming each of the four growth rates shown in Figure 2.6. The predicted available safe egress times (ASET) are presented in Figure 2.7. The required safe egress time (RSET) for a fully occupied carriage was calculated to be  $88 \pm 8\text{ s}$  applying 3 alternative egress models. To provide a context for the assumed growth rates they were compared against large-scale experiments described in Section 2.2.8.

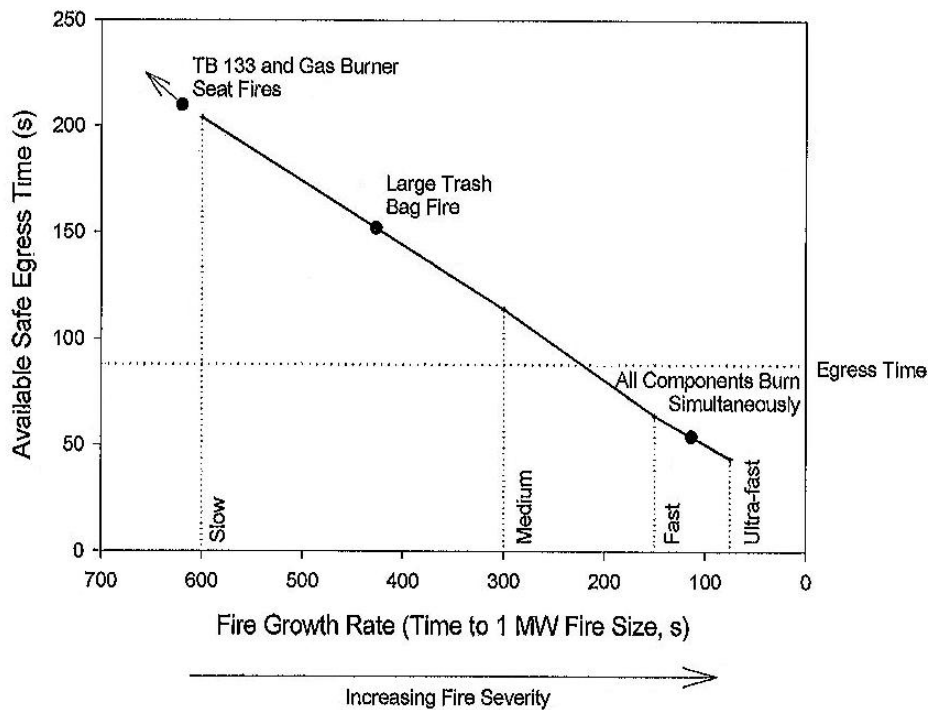


Figure 2.7. Fire performance assuming different “t squared” growth rates.<sup>[54]</sup>

The analyses NIST applying “t<sup>2</sup>” growth rates assumed that all fires continued to grow until untenable conditions was achieved. The analyses did not identify that, in reality, many small localised fires considered as slower growing often reach a peak HRR and then burn out and do not grow to a sufficient size to cause untenable

conditions. Fires that grow large enough to produce untenable conditions on a train will most likely be fast growing fires approaching flashover, as is indicated by experimental research reviewed in Section 2.2. The calculated RSET of 88 s fails to consider if a train stops at or between stations, time required to stop the train, and the presence of mobility disabled passengers. The analysis by NIST demonstrates that it is possible that Fast or Ultrafast fires could result in fatalities.

Use of “ $t^2$ ” growth rates may be appropriate for representing various train fire scenarios in the growth phase. However NIST only provides comparison to actual train fire growth rates for a limited set of materials and scenarios. Beyond this there appears to be no published validation or guidance on appropriate  $t^2$  growth rates to represent train fire scenarios.

#### **2.4.2 Predicting Flashover**

Flashover is most commonly defined as the transition from a localised fire to the general conflagration within an enclosed space when all fuel surfaces are burning.<sup>[87]</sup> Flashover is not a discrete event such as ignition, but rather it is a rapid fire growth which occurs over time. A localised or spreading fire in a compartment produces hot combustion products and unburnt gas which rise due to buoyancy and form a hot layer of gas at the ceiling with a cool layer of air below. As the HRR increases, the depth and temperature of the hot layer increases. Hot layer development is also affected by flow out of the enclosure which may be restricted by the available ventilation. If sufficient air/fuel mixture and temperatures exist, the hot layer surface interfacing with the lower cool air layer may ignite significantly increasing radiant heat emitted by the hot layer. Heat from the hot layer and localised flame body radiates to combustible surfaces in the cool lower layer. When the radiant heat received by a combustible surface exceeds its critical heat flux for ignition it may ignite. A feedback loop is established in that additional heat from combustion of the newly ignited surface increases the heat flux to other combustibles. This results in the rapid fire spread termed flashover<sup>[5]</sup>.

Many experimental studies have focused on predicting the onset of flashover. These are well discussed by Drysdale<sup>[87]</sup> and Walton and Thomas.<sup>[88]</sup> Most research and resulting correlations are based on ISO 9705 size or smaller enclosures.

Different criteria applied for estimating the time of onset of flashover in ISO 9705 enclosures include any of the following:

- 20 kW/m<sup>2</sup> radiant heat flux at floor level.
- Hot layer temperatures of approximately 600 °C.
- Flames emerging from the open door.

The typical critical radiant heat flux for interior fittings is 20 kW/m<sup>2</sup>. Considering the above discussion of flashover, radiant heat transfer is the most significant mode of heat transfer affecting flashover, as identified in Section 4.3.3, and is the most appropriate criterion

The studies presented by Drysdale<sup>[87]</sup> and Walton and Thomas<sup>[88]</sup> consider that onset of flashover is mainly affected by the following characteristics :

- HRR of the fire (which affects temperature of hot layer and radiant heat to other combustibles)
- Available ventilation (which affects hot layer out flow and fire size).
- Room geometry (ceiling height affects hot layer distance to combustibles and internal surface area affects hot layer geometry, volume to be filled and cooling of hot layer).

Therefore, the minimum HRR required to induce the onset of flashover ( $\dot{Q}_{FO}$ ) may be expressed as a function of available ventilation and room geometry. The correlations for  $\dot{Q}_{FO}$  summarized in Table 2-11 are commonly applied by fire engineers.

**Table 2-11 Correlations for minimum HRR required to induce flashover**

Author	Correlation	Equation No.
Babrauskas <sup>[89]</sup>	$\dot{Q}_{FO} (kW) = 750 A_0 \sqrt{H_0}$	Equation 2-6
Thomas <sup>[90]</sup>	$\dot{Q}_{FO} (kW) = 7.8 A_T + 378 A_0 \sqrt{H_0}$	Equation 2-7
McCaffrey, Quintiere and Harkleroad <sup>[91]</sup>	$\dot{Q}_{FO} (kW) = 610 (h_k A_T A_0 \sqrt{H_0})^{1/2}$	Equation 2-8

These correlations apply a term defined as the ventilation factor ( $A_0\sqrt{H_0}$ ) for an enclosure where  $A_0$  is the area of openings ( $\text{m}^2$ ) and  $H_0$  is the height of openings (m).  $A_T$  is the total area of compartment enclosing surfaces not including floor area or vent areas ( $\text{m}^2$ ).  $h_k$  is the thermal conductivity of the room walls and ceiling.

The ventilation factor is important in defining air flow into a compartment for fires nearing flashover or post flashover fires. Kawagoe empirically developed the concept of ventilation factor from analysis of post flashover fire experiments. This is discussed more in Section 2.4.5. The concept of ventilation factor and correlations for  $\dot{Q}_{FO}$  are based on a limited data set of flashover experiments in small near cubical enclosures limited to a low range of  $A_T/A_0\sqrt{H_0}$  (small enclosures with large openings). These correlations are not validated for and neglect affects for large, elongated enclosure geometry. Train carriages are elongated compartments with a volumes typically an order of 10 greater than the volumes of enclosures that flashover correlations are based on. Validity of these correlations for large enclosures is not well understood in the literature but is expected to be poor. There is no large-scale data available in literature to assess the validity of the flashover correlations applied to trains although they have been applied by fire engineers to trains and buses.<sup>[92]</sup>

Affect of room wall area on  $\dot{Q}_{FO}$  predicted by flashover correlations has been compared to experimental room flashover data.<sup>[88]</sup> Figure 2.8 shows  $\dot{Q}_{FO}$  as a function of compartment wall area ( $A_w$ ) divided by ventilation factor. This demonstrates that all correlations are conservative in their predictions of  $\dot{Q}_{FO}$  for small enclosures; however no comparison has been made to large enclosures similar to train carriages.

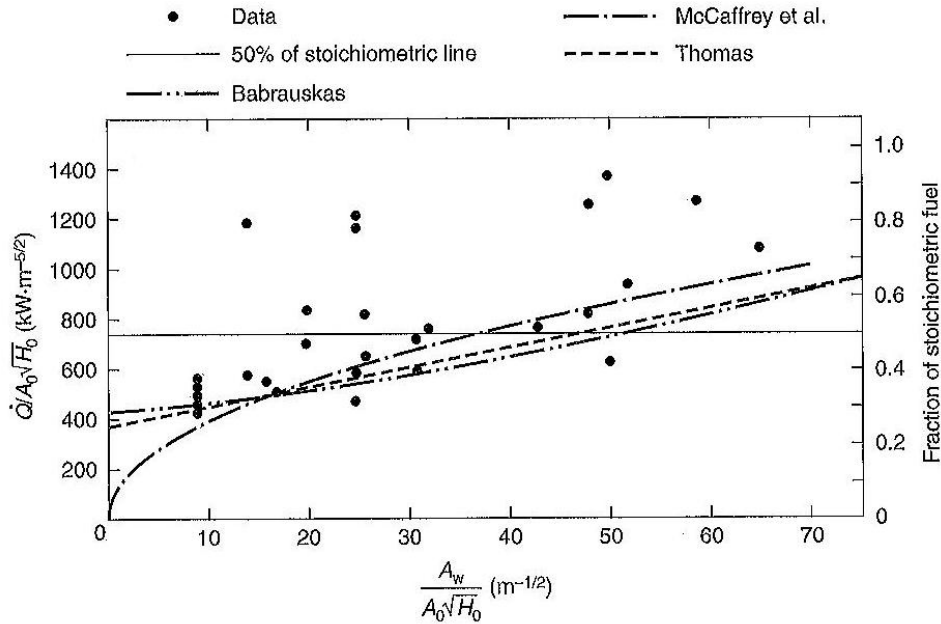


**Figure 2.8** Comparison of flashover correlations against experimental data.

All of these correlations assume flashover occurs once the homogenous hot layer temperature exceeds 500-600 °C. For elongated train carriages these assumptions are likely to break down as the hot layer will take longer to develop for a given fire size, is less likely to have a uniform temperature and will have a different aspect ratio for radiant heat transfer to combustible surfaces compared to fires in small rooms.

These flashover correlations have been compared assuming a typical train enclosure area ( $A_T$ ) of 175 m<sup>2</sup>, an opening height ( $H_O$ ) of 2 m and  $h_k = 0.03$  kW/m·K (typical of 16 mm plasterboard). The opening area ( $A_O$ ) is varied from 0 m<sup>2</sup> to 8 m<sup>2</sup> typical of all passenger doors open, see Figure 2.9.

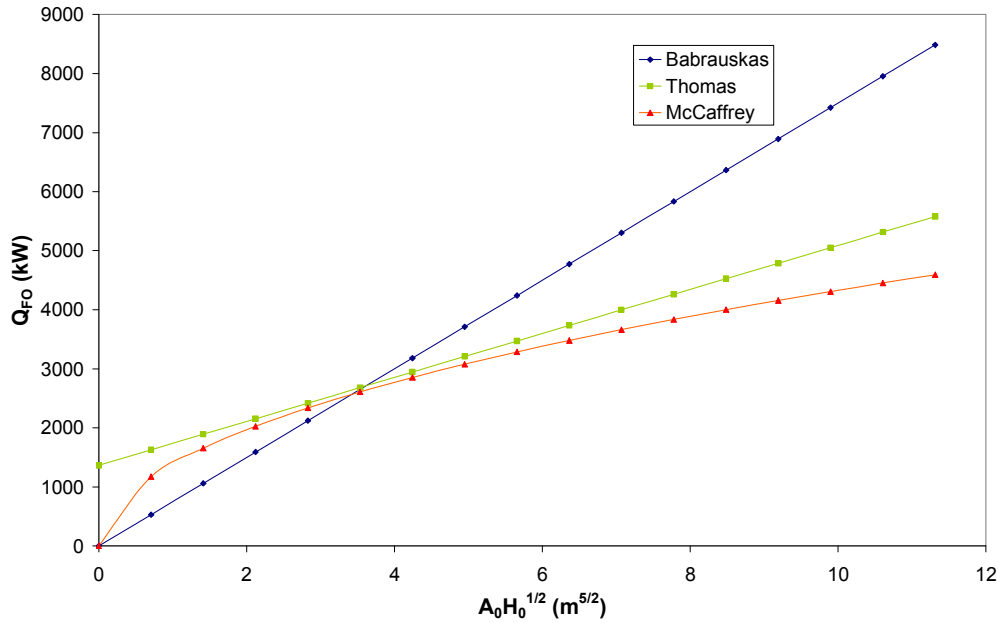


**Figure 2.9.** Comparison of flashover correlations applied to typical train carriage

Figure 2.9 shows the strong dependence of  $\dot{Q}_{FO}$  on ventilation. There is significant variation in results between the correlations. Figure 2.9 shows that for train carriages with very little ventilation the correlations (Babrauskas and McCaffrey in particular) are not valid because in real fires there will be a minimum value for  $\dot{Q}_{FO} > 0$ . These correlations predict that  $\dot{Q}_{FO}$  for a train carriage with two doors open may be as high as 4-6 MW (see Section 4.2.3). Large-scale experiments reviewed indicate that much smaller fires of the order of 100-300kW are likely to promote localised flame spread to a point where flashover can occur. This critical ignition fire size is the more important quantity affecting fire behaviour and life safety than  $\dot{Q}_{FO}$ .

The flashover correlations do not provide a prediction of time to onset of flashover. This is dependent on the pre flashover fire growth. To estimate time to flashover designers will sometimes assume a pre-flashover growth rate, use flashover correlations to estimate  $\dot{Q}_{FO}$  and determine the time that  $\dot{Q}_{FO}$  is achieved for the assumed growth rate.

Zone and CFD modelling, discussed in Sections 2.4.6 and 5, may be used to model hot layer temperatures and radiant heat flux at floor level inputting an assumed design

fire HRR curve. Fire engineers may assume a design fire for a localised fuel controlled fire and use such models to indicate if flashover conditions are achieved. If so the assumed design fire may be modified to account for the rapid fire growth characterised by flashover. This is an alternative method of flashover prediction to the use of flashover correlations

### 2.4.3 Average HRR Design Fire Estimation Method

The average HRR method<sup>[93]</sup> is one of the earliest and simplest methods applied to estimate design fires for large fire scenarios involving fire spread to an entire vehicle interior. This method sums the total interior fuel load for the vehicle and divides it by assumed burn time:

$$\dot{Q}_{ave} (MW) = \frac{\text{Total Fuel Load (MJ)}}{\text{Burn Duration (s)}} \quad \text{Equation 2-9}$$

The design fire is assumed a constant average HRR over the burn duration. Fuel load is often calculated from heat of combustion (MJ/kg) values taken from literature or determined by tests such as the cone calorimeter.

This method was first applied in 1975 for design of rail tunnel ventilation systems in Atlanta, Baltimore, Hong Kong and Pittsburgh. Burn times of approximately 1 hour were initially assumed based on observations of two Montreal subway system fires in 1971 and 1974. Later, shorter burn durations of 20 minutes were applied to design for Los Angeles, Philadelphia and Atlanta systems based on a more severe fire incident with shorter burn time on the Bay Area Rapid Transit (BART) subway system in 1979. Following the introduction of NFPA 130 in 1983 it was expected that fire performance for train interior materials would generally improve, resulting in fires of reduced peak HRR but possibly increased burn duration due to reduced fire intensity. Although the affect of NFPA 130 on burn time could not be quantified the assumed burn time was increased from 20 minutes to about 30 minutes and was applied to Seattle, Shanghai, Singapore and Taipei transit systems.

The average HRR method is an extreme simplification of complex fire behaviour and does not produce realistic design fires for the following reasons:

- The growth and decay phase of fire behaviour are neglected.
- Average HRR is completely dependent on arbitrarily assumed burn time.
- It is assumed that all materials burn to completion.
- Dependence of fire behaviour, such as the burn duration and HRR, on material properties, physical configuration and available ventilation is neglected.
- The actual peak HRR must be greater than the estimated average HRR over the actual burn duration. If systems such as ventilation are designed using average HRR they are likely to be overwhelmed by a larger peak HRR.

#### 2.4.4 Duggan's Method

A method for estimating design fires for flashover scenarios with fire spread to an entire carriage interior is presented by Duggan.<sup>[94]</sup> Time dependent HRR per unit area (HRRPUA) data from cone calorimeter tests at the following irradiances is applied:

- Horizontal prone (ceiling like)      50 kW/m<sup>2</sup>.
- Vertical (wall like)                      35 kW/m<sup>2</sup>.
- Horizontal supine (floor like)        25 kW/m<sup>2</sup>.

Where cone calorimeter tests for a material are performed in triplicate the median HRRPUA curve is applied. For each material, the HRRPUA curve ( $\dot{q}_i''(t)$ ) is multiplied by exposed material surface area in the vehicle to produce a time dependent HRR curve for each individual material in MW. The HRR curve for each individual material is summed giving a total HRR curve for the entire train interior. This calculation is summarised as follows:

$$\dot{Q}_{(t)} = \sum \left( \frac{A_i \dot{q}_i''(t)}{1000} \right) \quad \text{Equation 2-10}$$

The total HRR curve is often smoothed using a 20-30 s running average to remove peaks which are resolved but close together. The basis for this is that a combination of materials is unlikely to combust in such a resolved manner in a real incident however these resolved peaks result from the summation of small-scale test HRR curves for each material.

Implicit assumptions of this method are:

- Fire behaviour of combinations of installed materials is assumed to be predicted by summation of cone calorimeter data for combustion of single specimens. This neglects complex interaction of heat transfer and fire spread between different materials in interiors which strongly influence fire behaviour. This assumption results in resolved peaks that must be smoothed. The peak HRR predicted by Duggan's method is heavily affected by this assumption. If a number of materials have cone calorimeter derived HRR curves with coincident peaks at the same time then the total HRR peak will be very high. If the cone calorimeter determined HRR for materials have peaks well spread in time then the total HRR peak will be relatively low.
- It is assumed all materials are instantaneously exposed to the constant heat fluxes listed above. This is not valid. The incident heat flux received by materials will vary as the fire grows. Therefore fire growth and spread inside the carriage is effectively neglected. During pre flashover fire growth most materials will be exposed to gradually increasing heat fluxes significantly less than those assumed by Duggan. This results in a failure to predict pre-flashover fire growth and means that the time to untenable conditions in the vehicle cannot be estimated using Duggan's method. For a post-flashover fire heat fluxes are likely to be significantly higher, of the order of  $100 \text{ kW/m}^2$ <sup>[5]</sup>.
- Well ventilated fuel controlled burning is assumed. This assumption is most likely not valid as ventilation conditions are likely to affect fire behaviour. If ventilation conditions do reduce HRR then Duggan's method is likely to over estimate peak HRR.

Duggan acknowledges these simplifications but states that this method is superior to the previously used “average HRR” method. However, consideration of the above assumptions indicates that Duggan's method does not predict a realistic or valid design fire and at best is only useful for comparing alternative materials with different HRRPUA and exposed surface areas against one another. It is concluded that Duggan's method is not a useful improvement on the “average HRR” method.

Dowling supports this conclusion through comparison of Duggan's method applied to ISO 9705 room HRR tests.<sup>[11]</sup> Poor predictions of HRR for ISO room fires resulted,

with the prediction achieving a higher peak HRR in a much shorter time than for the actual ISO 9705 tests.

A modification of Duggan's method which attempts to consider fire spread along the train interior has been proposed.<sup>[95]</sup> This assumes that as ignition cannot commence on all surfaces at once a rolling ignition occurs at an arbitrary rate of 10% of interior materials per minute. The calculation described above is modified with the summation of total HRR staggered so the HRR curve for 10% of all interior materials is added every minute. All other assumptions are as listed above. Full-scale experiments reviewed in Section 2.2 indicate that pre flashover fire growth is dependant on the ignition fire size and interior material fire performance and that, whilst pre flashover fire growth may take some time, fire spread along the interior after the onset of flashover is likely to be much more rapid than 10% per minute. It is concluded that this modified method does not produce a realistic or valid estimate of design fire.

Despite this lack of validity, both Duggan's method and the modified version of Duggan's method have been applied to the design of several rail vehicles and systems both in Australia and internationally. These methods have been applied due to a lack of any other validated methods.

#### **2.4.5 Ventilation Controlled Burning**

Experiments reviewed in Section 2.2 indicate that large interior train fires are affected by ventilation conditions and post flashover HRR may be mostly dictated by ventilation conditions until fuel burnout begins to occur. A fire engineering concept commonly applied to fully developed building enclosure fires is that rate of burning is controlled either by available ventilation or available fuel.<sup>[4]</sup> For compartment fires with relatively small HRR and/or large ventilation openings combustible surfaces burn as they would in the open except for some enhancement from hot layer radiation. Such a fire is said to be fuel controlled. As HRR increases and/or ventilation openings decrease there will be insufficient oxygen available in the compartment to fully combust all volatiles being evolved from the combustible surfaces. Thus the rate of burning becomes affected by rate of air into the compartment. Such a fire is said to be ventilation controlled.

This effect was first studied by Kawagoe<sup>[96]</sup> who conducted fire experiments burning timber cribs in small compartments with different sized openings. For fires nearing flashover and post flashover the mass flow rate of air into an enclosure through an opening  $m_a$  has been found to be approximately proportional to ventilation factor ( $A_0\sqrt{H_0}$ ).<sup>[97]</sup> The proportionality constant is estimated to be 0.52 or 0.5 by Thomas and Heselden.<sup>[98]</sup>

$$m_a = 0.5A_0\sqrt{H_0} \quad \text{Equation 2-11}$$

As demonstrated by Huggett the heat release per unit mass of oxygen consumed for complete combustion is approximately  $13.1 \times 10^3$  kJ/kg for a wide range of combustible materials. Therefore a correlation for ventilation controlled HRR may be expressed as:

$$\dot{Q}_{\text{VentilationControlled}} = 13.1 \times 10^3 \times 0.231 \times 0.5A_0\sqrt{H_0} \approx 1500A_0\sqrt{H_0} \quad \text{Equation 2-12}$$

Fire engineers typically predict the ventilation controlled HRR applying Equation 2-12 and predict the fuel controlled HRR based on experimental data for open burning or assumptions of pyrolysis rate (for trains engineers have used the average HRR method and Duggan's method). The lesser of the two is taken as the peak

Equation 2-11 and Equation 2-12 are based on data from small room enclosure tests with ventilation openings only a small fraction of the compartment surface area and involving timber crib combustion. The correlations have not been validated for large elongated enclosures such as trains. Despite this fire engineers have applied it to trains and buses. <sup>[4,92,93][92,92,93]</sup>

Equation 2-12 assumes stoichiometric burning with only air entering the compartment available for combustion. This reduces to the intrinsic assumption that all combustion occurs within the enclosure. This is at odds with common observations for fully developed ventilation controlled fires with unburnt volatiles flowing out of the compartment, mixing with the available outside air and burning in a fire plume outside of the ventilation opening. Drysdale<sup>[87]</sup> suggests burning rate for ventilation

controlled burning is primarily controlled by radiant heat received by combustible surfaces which controls rate of fuel volatilisation. Ventilation affects radiant heat by affecting hot layer properties and combustion within the compartment. Drysdale suggests ventilation controlled fires involving fuels with larger surface areas like wall linings or pool fires, that are more open to radiant heat than timber cribs, will produce a greater HRR than predicted by Equation 2-12. Bullen and Thomas<sup>[99]</sup> conducted experiments applying liquid pool fires to small compartments measuring burning rate and rates of air inflow. Combustion was observed in fire plumes outside of ventilation openings. The measured rate of burning was greater than both that predicted by Equation 2-12 and burning rates for the same pool fires in the open. This divergence from the HRR predicted by Equation 2-12 is illustrated in Figure 2.10.

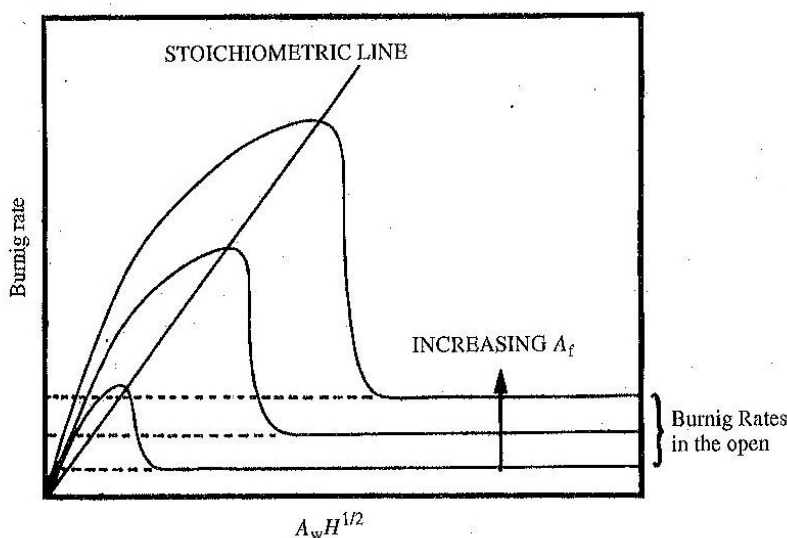


**Figure 2.10.** Schematic showing variation of mass burning rate with ventilation factor and fuel surface area.<sup>[99]</sup>

Figure 2.10 illustrates how burning outside the enclosure and volatilisation driven by increased radiant heat for intermediate ventilation factors can result in greater HRR than predicted for stoichiometric or open fires. Figure 2.10 also illustrates how very restricted ventilation factors cause almost no combustion inside the enclosure and very little feedback of radiant heat from external combustion to the interior surfaces resulting in less HRR than predicted for stoichiometric or open fires. Bullen and Thomas proposed a correction factor ( $\eta$ ) may be used to compensate for deviations from Equation 2-12 as follows:

$$\dot{Q}_{\text{VentilationControlled}} = \eta 1500 A_0 \sqrt{H_0} \quad \text{Equation 2-13}$$

However model-scale experiments by Ingason<sup>[56,57]</sup> indicate that correction factor  $\eta$  varies significantly with ventilation conditions. For well ventilated conditions  $\eta$  is significantly greater than 1 but for the restricted ventilation conditions  $\eta$  is significantly less than 1. No appropriate values of  $\eta$  for various ventilation conditions have been validated for full-scale carriages.

For trains, the elongated enclosure and arrangement of multiple openings may also induce particular air flows which result in divergence from Kawagoe's correlation. Inspection of burnt out Comeng carriages in Melbourne (see Section 2.1.2.2) revealed that steel bodies above windows were more heat affected on one side of the carriage than the other. This indicates that if windows break on both sides of a train then a cross flow can be achieved where air predominantly flows in one side and combustion products and flame predominantly flow out the opposing side. This flow may be started or enhanced by wind blowing perpendicular to the carriage. The affect of such a flow on HRR is unknown.

It is concluded that Kawagoe's correlation is unlikely to produce a realistic estimate of ventilation controlled HRR for train fires and an appropriate, ventilation dependant, correction factor  $\eta$  has not been determined. Except for computational fluid dynamics (CFD) modelling, no other significant methods for quantifying affect of ventilation on train fires have been identified in the literature reviewed.

Breakage and fall-out of glazed windows and doors has a critical affect on ventilation and HRR for large train fires. Prediction of glazing failure in fires has been the subject of many studies.<sup>[100-104]</sup> These studies indicate that glazing failure is dependant on a number of factors including:

- Glazing material (including different types of glass and polymer materials and different construction or treatments such as lamination and tempering/toughening)
- Glazing thickness and surface area.
- Glass defects, particularly micro cracks that are influenced by edge treatment
- Edge frame material.

General criteria for glazing failure and fall out suggested by the these studies include

- Surface temperature criteria (temperatures are averages with significant experimental deviations) –
  - 300°C surface temperature as a lower bound for failure.
  - 3 mm window glass may break around 340°C.
  - 4-6 mm glass may break around 450°C,
  - Double-glazed windows using 6 mm glass may break out around 600°C.
  - Tempered-glass is not likely to break out until after room flashover.
- Heat flux criteria –
  - At a heat flux of 9 kW/m<sup>2</sup> some ordinary glass may possibility of fallout, but the probability of fallout increases with heat flux until about 35 kW/m<sup>2</sup> is reached.
  - Double-glazed windows can resist approximately 25 kW/m<sup>2</sup> without falling out.
  - Tempered glass is able to resist fluxes of 43 kW/m<sup>2</sup>,

These studies indicate that it is very difficult to predict when glass will break enough to fall out in a real fire. Ultimately designers must rely on very simplified assumptions for window performance.

#### **2.4.6 Zone Modelling**

Zone modelling is not a method of predicting design fire HRR but rather a method of predicting the conditions within an enclosure for a given assumed design fire HRR curve. Zone modelling is briefly reviewed because it is applied to trains by fire engineers to predict available safe egress time. Quintiere provides a more complete summary of zone fire modelling.<sup>[5]</sup>

Zone fire models represent the fire enclosure as a small number of zones having homogeneous properties such as temperature and pressure. Most zone models apply two zones, an upper volume referred to as the hot layer and a lower volume referred to as the cold layer. This is based on thermal stratification due to buoyancy in pre-flashover enclosure fires.

Zone models apply conservation of energy and conservation of mass equations to the hot and cold layers assuming a predefined HRR curve to predict hot layer temperature, cold layer temperature, layer interface height and flow through vents. If fire species yields are input to the zone model then gas concentrations and smoke optical density may also be modelled. Zone models apply empirical plume correlations to predict mass rate of entrainment of the fire plume. These correlations have been developed for simple fire plumes such as pool fires in the centre of a room. Plume correlations specific for walls or corners are less well developed and are not usually applied. Fire induced flows through openings (doors and windows) are predicted based on gas temperature differences on either side of the opening, assuming hydrostatic pressure and applying Bernoulli's equation. Gas mixing at the interface between hot and cold layers is predicted applying empirical correlations. Heat transfer between layers and from the enclosure is usually predicted assuming simple steady state heat transfer equations.

Zone models are usually developed as computer programs to solve the above equations. There are many different zone models in existence. Walton provides a summary of the most common zone models.<sup>[105]</sup> Common examples of zone models are CFAST<sup>[106]</sup> and BRANZFIRE.<sup>[107]</sup>

Several limitations result from the assumption of two homogeneous zones. A small fire in a large space may not result in the formation of two well defined layers. Instead, due to cooling of the fire plume, combustion products may stratify at the mid height of very tall enclosures or cool and mix below the predicted hot layer further away from the fire in very long enclosures. A very large fire in a small enclosure may not result in the formation of two well defined layers. Instead powerful turbulence may cause gases in the enclosure to be well mixed. For this reason two zone models are not applicable to post flashover fires. COMPF2<sup>[108]</sup> is a single zone model developed specifically for post flashover fires which assumes a single well mixed volume and relies on the ventilation controlled correlations described in Section 2.4.5. Quintiere<sup>[5]</sup> states that zone models may not be suitable for application to enclosures with very large length to width ratios. This is both because asymmetrical flows may be established and cooling may result in a breakdown of the two zone assumption.

Due to the large length to width ratio of a train interior, multiple car trains connected by open walkways, application of zone models may not be valid.

As described in Section 2.4.1, NIST have conducted a series of controlled “t<sup>2</sup>” gas burner experiments in an intercity passenger train.<sup>[55]</sup> A very good match between these experimental results and CFAST models of the experiments was achieved. However the effective length of the carriage was halved for the experiments, as discussed in Section 2.2.8. Therefore the validity of zone models applied to trains particularly multiple car trains connected by open walkways has not been fully demonstrated.

Computational fluid dynamics (CFD) or field modelling is increasingly being applied to trains to either:

- Model temperature, smoke and other conditions internal to a carriage to enable assessment of tenability given an assumed design fire, or
- Model interior fire growth to predict design fire HRR curves.

CFD modelling applied to trains is discussed in detail in Chapter 5.

#### **2.4.7 One-Layer Post-Flashover Model**

Lattimer and Bayler have developed and presented a one-layer post flashover model to predict the HRR of fully developed passenger train fires.<sup>[109]</sup> The model applies an energy balance to a control volume around the compartment as shown below and is used to predict temperature inside the compartment.

The HRR of the fire was calculated to be the minimum of the HRR of the pyrolyzed fuel and the HRR that the air into the compartment could support. A combustion efficiency factor is included to account for incomplete mixing and reaction of air with fuel. Lattimer and Beylers paper does not fully present all correlations used in the model, particularly the correlation for mass rate of air flow into the enclosure is not given. Therefore there is insufficient information given in the paper to replicate this model.

$$\dot{m}_o = \dot{m}_i + \dot{m}_f$$

$$Q = q_{bound} + q_{vent} + q_{pyrol} - \dot{m}_i h_i - \dot{m}_f h_f + \dot{m}_o h_o$$

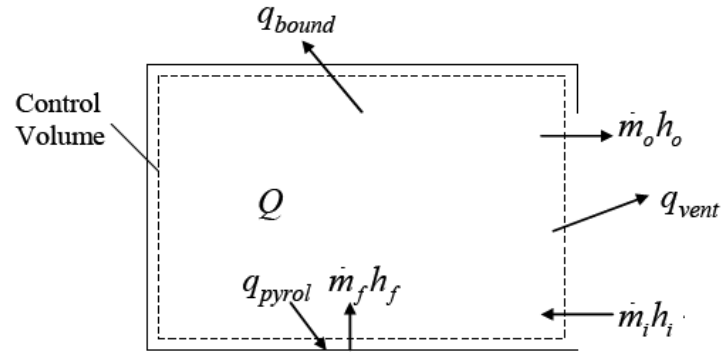


Figure 2.11. Energy Balance on one-layer-post flashover model

The model was validated against gas temperatures and mass loss rate data of post-flashover fires in a compartment 2m wide, 1 m high, 1 m deep. The model was then applied to predict HRR for both an intercity and a subway rail car. The intercity rail car was significantly longer and had more windows. Interior material properties were based on cone calorimeter data from the NIST Fire Safety of Passenger trains project. The windows were assumed to be glazed with polycarbonate and were simply assumed to fall out at pre defined times based on previous research.<sup>[104]</sup> For each train a variety of scenarios were modelled including :

- 1 or 2 doors open
- Window failure starting at 0 min, 6 min or 12 min

Predicted Peak HRR for these scenarios for the Intercity car ranged from 19-41 MW and for the subway car ranged from 14-22 MW.

This modelling indicates that HRR of fully developed train fires is dependant on fire properties of interior materials, surface area and combustible mass of fuel inside the train and ventilation conditions into the railcar. Window fallout was predicted to

result in large increases (3-27 MW) in HRR, if sufficient fuel was available and had not already burnt out at the time of fall out.

Limitations of this model include

- assumed times of window failure (which strongly affects HRR). In large scale experiments window failure has been affected by both the glazing properties and the fire exposure
- one-layer model assumption of uniform heat flux and temperature conditions. Large scale experiments have demonstrated that post flashover combustion may become located at open windows and doors resulting in non-uniform conditions within the compartment. This may affect pyrolysis
- The model has not been validated against large-scale train fires therefore the accuracy of the HRR predictions is not quantified.

Lattimer and Beylor's model appears to be an improvement on the basic fuel controlled or ventilation controlled models. As there is insufficient information given in the paper to replicate this model it has not been applied to the full scale passenger train experiment presented in Chapter 3 of this thesis.

#### **2.4.8 Assumed Design Fires for Large Train Fires**

Fire engineers will sometimes simply assume a design fire to represent a large train fire based on either review of experimental data, review of past design fires applied, specification by a regulating authority or "Expert Judgment". A brief review of assumed design fires has been conducted however the information found was limited because in most cases assumed design fires are not made available in general literature due to commercial security.

The "RailCorp Infrastructure Engineering Standard – Structures – Tunnels ESC 340" and the Australian Rail Track Corporation standard "Design and Installation – Tunnel Fire Safety – New Passenger Railway Tunnels" both specify a maximum design fire for the design of a passenger rail tunnel fire safety strategy as a 20 MW steady state HRR and a minimum design fire as 1 MW steady state HRR. The 20 MW steady

state design fire is stated to be based on assessment of older rolling stock operating on the network but no details of such assessments are referenced.

In some cases the EUREKA Project measured fire curves ranging from 14-35 MW peak HRR have been directly applied to other passenger trains. <sup>[47-49]</sup>

In 1997 Duggan used his calculation method to assess cars to be used for the Heathrow Express and found a maximum “fire power output” of 5 MW per car. <sup>[94]</sup> Following this the Hong Kong Mass Transit Rail Corporation adopted the requirement that the peak HRR of a rail carriage saloon should not exceed 5 MW as determined by Duggan’s method. <sup>[95]</sup> Since then some Australian rail authorities have adopted specifications setting limits of 20 MW per carriage as determined by Duggan’s method.

Barber et al provide estimates of peak HRR for British Rail and Thai Railways passenger vehicles. Estimates of between 7MW and 16.3MW are quoted for relatively old vehicles. That reference concludes that 16MW lasting for up to 30 minutes is a conservative design fire for one passenger carriage on fire.

The German Railway Authority (Deutsche Bahn AG) have assumed a design fire HRR curve for their passenger carriages that reaches a peak of 25MW after 20 minutes from ignition, sustains this peak up to 55 minutes from ignition and decays to 10 MW by 60 minutes after ignition. <sup>[110]</sup>

Assumed design fires are commonly selected for road tunnels by choosing a maximum HRR from a standard design table. Examples of such design tables are summarized in Table 2-12. These standards also propose appropriate time vs. temperature for assessment of structural fire resistance. Fire engineers have in some cases applied the design fire peak HRR recommended for buses to represent a single passenger carriage. Design fires recommended by NFPA have recently been increased due to road tunnel fire experiments demonstrating larger fire sizes than previously expected.

**Table 2-12.**  
**Standard design HRR for road tunnels**

Vehicle	Maximum HRR (MW)		
	PIARC <sup>[111]</sup>	NFPA (2001) <sup>[112]</sup>	NFPA (2008) <sup>[113]</sup>
1 small car	2.5	-	-
1 large car	5	5	5-10
2-3 cars	8	-	10-20
Van	15	-	-
Bus	20	20	20-30
HGV	20-30	-	70-200
Tanker	100	100	200-300

The UPTUN project on design fires in tunnels proposes a design fire for passenger carriages in tunnels with a peak HRR of 30 MW and a growth rate of 10 MW/min. [114]

Ingason has proposed design fires based on review of experimental data.<sup>[115]</sup> The following peak HRR and  $t^2$  growth rates were proposed:

**Table 2-13. Train peak HRR and growth rate proposed by Ingason<sup>[115]</sup>**

Type of vehicle	Peak HRR (MW)	$t^2$ growth rate (kW/s <sup>2</sup> )
Train (steel body construction)	15	0.01
Subway car (aluminium body construction)	35	0.3

In summary a range of assumed design fires with peak HRR varying from 5-35 MW have been found in literature. Generally there is little detail provided regarding most assumed design fires and in most cases only peak HRR is provided and fire growth rate and decay or fire duration are not considered. Generally only a fully developed fire on a single carriage is considered and fire spread to multiple carriages is not considered. Experiments reviewed in Section 2.2 indicate that fire behaviour is very dependant on characteristics such as flammability and quantity of interior materials, performance of windows, barriers to fire spread to adjacent carriages etc. As these characteristics change for different train designs the use of assumed design fires for a broad range of designs is not likely to result in cost effective fire safety design.

## 2.5 LITERATURE REVIEW CONCLUSIONS

This literature review has identified that there is a need for further research on to develop better understanding of large fire behaviour on passenger trains develop valid design fire estimation methods. Other conclusions drawn from this literature review are:

- The design fire is an extremely critical input affecting cost-effective fire safety design of trains, tunnels and surrounding infrastructure.
- Although large passenger train fire events are infrequent they potentially have extreme consequences. Therefore large train fires must be considered or made extremely unlikely through fire safety design.
- Fire records reviewed indicate that deliberate arson fires are the most frequent occurring interior ignition source and are the most likely ignition source to result in significant fire spread beyond the ignition area.
- There are currently no robust relationships between small-scale test methods and real train fire behaviour enabling direct prediction of realistic design fires.
- The majority of relevant large-scale and full-scale experimental research has investigated the pre-flashover stage of fire development. No research with the exception of the EUREKA and JNR projects has focused on the occurrence of flashover and post-flashover fire size and behaviour.
- Full-scale train fire HRR measurement has only been attempted in the NIST and EUREKA projects. These HRR measurements have significant limitations and estimated errors of the order of  $\pm 25\%$ . This highlights the difficulty of full-scale HRR measurement. Not all likely variations of key factors affecting fire behaviour, such as ventilation and fuel conditions, have been investigated. Therefore these full-scale HRR measurements can not be applied for design of other vehicles. However these experiments are valuable as they are the only available HRR measurements of fully equipped passenger train and they have been useful in roughly quantifying possible train fire sizes and improving the level of understanding of fire behaviour.
- Experiments involving HRR measurement on scale model trains ( $1/10^{\text{th}}$  scale) have provided a less expensive method of qualitatively investigating the effect of ventilation on HRR. It was found that for well ventilated fires

$HRR \gg 1500A_0\sqrt{H_0}$  and for restricted ventilation fires  $HRR \ll 1500A_0\sqrt{H_0}$ . Experiments on scale models may be very useful for developing qualitative understanding of fire behaviour and bridging gaps between limited full-scale experiments however complete correspondence between model-scale and full-scale is not possible due to limitations including turbulence intensity, thermal inertial of materials and radiant heat effects.

- Experimental research leads to the hypothesis that ceiling and upper wall lining flammability properties are critical for fire spread beyond the ignition area due to their interior location as vertical and inverted horizontal surfaces high within a carriage. If ceiling and upper wall linings are not ignited then flame spread beyond the ignition area is extremely unlikely. Seating and lower wall lining flammability properties are less critical because direct seat to seat spread or lateral spread along lower wall linings is very unlikely for modern materials due to their lower height within the carriage and their location with separations. Involvement of seats or lower wall linings by an ignition source is only likely to affect the fire severity impinging on upper wall and ceiling linings. The flammability properties of modern floor linings are less critical than those of seats or lower wall linings to fire spread until the onset of flashover.
- Experimental research demonstrates that for a wide range of metro passenger trains the ignition source peak HRR required to promote significant flame spread is in the range 100-300 kW.
- There is no standard applied nationally in Australia which specifically addresses passenger vehicle fire safety design. Instead individual specifications are set by state based rail authorities for each new set of trains.
- There has been a recent move towards performance based fire safety specifications for new trains in Australia. These specifications usually require design fire estimates.
- International standards are generally prescriptive and prescribe small-scale test methods which do not directly indicate actual fire scenario behaviour. Some international standards do provide a framework for alternative, performance based fire safety design, however no standards or specifications reviewed

detail appropriate, valid methods of modelling fire behaviour on passenger trains to obtain design fires.

- Existing design fire estimation methods are based on overly simplifying assumptions, have not been validated and are unlikely to yield reasonably accurate predictions for HRR. However these methods are applied by fire engineers to predict rough design fires as there is no better method available. CFD fire growth modelling is a developing science and its use in this application is reviewed in Chapter 5.

# CHAPTER 3 EXPERIMENTAL INVESTIGATION OF FIRE BEHAVIOUR ON A PASSENGER TRAIN CARRIAGE

## 3.1 EXPERIMENTAL APPROACH

### 3.1.1 Important fire behaviour factors for passenger life safety

Factors relating to fire that affect passenger life safety have been identified and considered based on the findings of the literature review. Consideration of factors that affect life safety is intended to clarify the relevance of the experimental work undertaken in this research and give it context. Figure 3.1 summarises the important factors affecting passenger life safety.

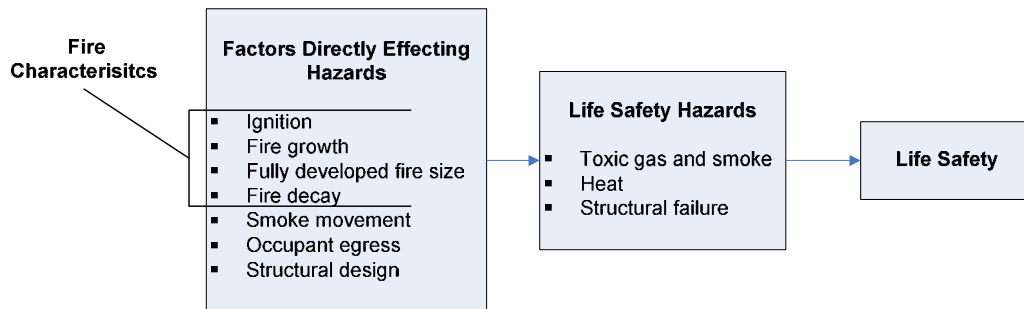
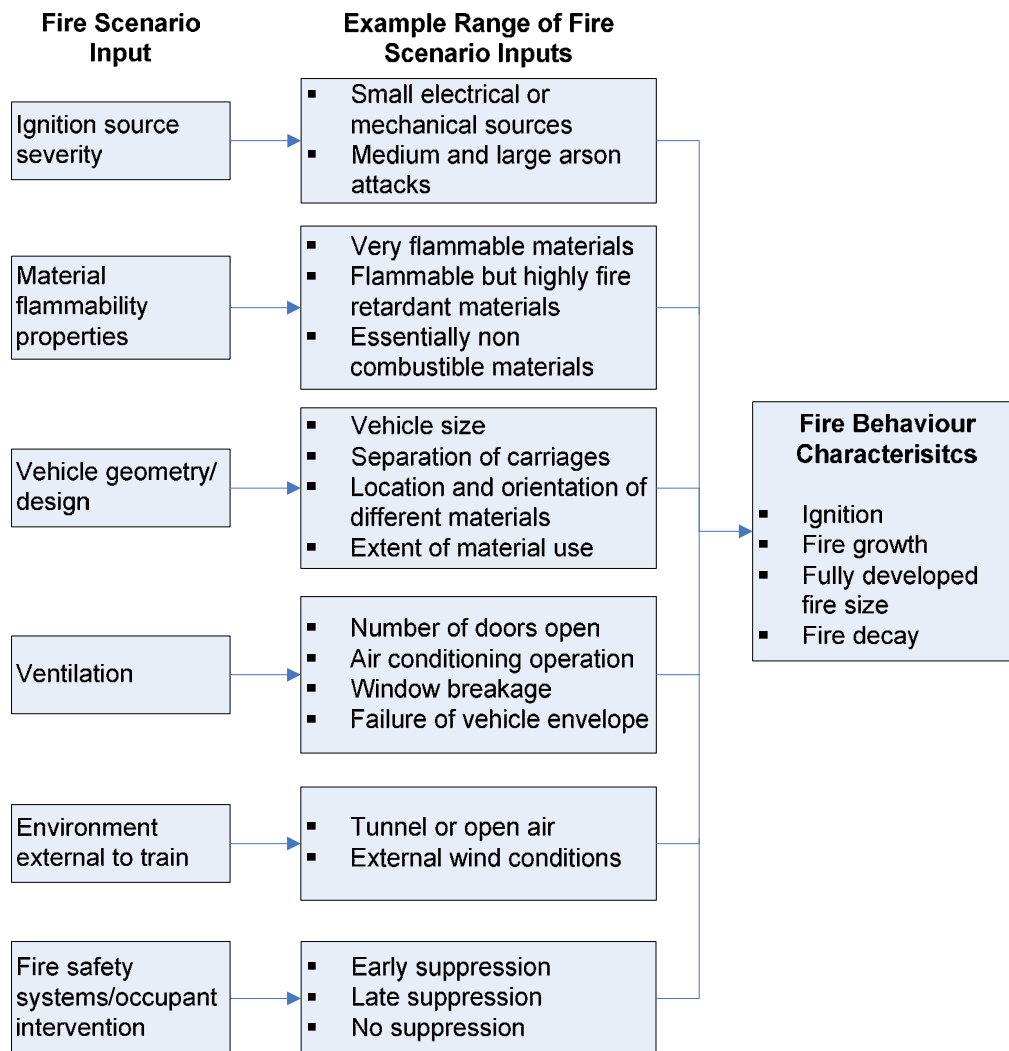


Figure 3.1. Factors affecting life safety in an interior train fire incident

Ignition, fire growth, fully developed fire size and fire decay are identified as the key characteristics of a fire that affect hazards to passenger life safety. These fire characteristics are represented by design fires. Therefore experimental research on passenger train fire behaviour should be focussed on developing an understanding and ability to predict these fire characteristics leading to better design fires.

From the literature review it is possible to identify the fire scenario inputs that are likely to have a significant affect on these fire characteristics as summarised in Figure 3.2.



**Figure 3.2. Fire scenario inputs that affect fire behaviour for an interior fire.**

Our ability to predict fire behaviour in passenger trains for a given set of fire scenario inputs is currently very limited. Ideally, research to develop understanding of fire behaviour and improve prediction methods should consist of a series of experiments where each of the fire scenario inputs is varied independently and systematically. Due to the number of fire scenario inputs and the broad range of possible states for each input a very large number of experiments would be required to generate a sufficient data set. Due to the effects of scale, discussed in the literature review, large or full-scale experiments would be required to properly determine the effects of each fire scenario input on the resulting fire behaviour. The state of each fire scenario input except material flammability can be determined by simple measurement or observation. Small-scale flammability tests such as the cone calorimeter are required

to measure the state of material flammability terms of measurable quantities such as ignition time and HRR.

It is beyond the resources of this research to conduct the number of experiments required to generate a sufficient data set representing all credible variations of the 6 fire scenario inputs identified in Figure 3.2. Instead a limited but focused set of experiments has been conducted as described in this chapter.

### **3.1.2 Overview of experiments conducted**

Experiments have been conducted on an Australian metro passenger train carriage. The following experiments have been conducted.

#### **3.1.2.1 Cone calorimeter experiments overview.**

Cone calorimeter tests were performed on the major interior materials, including GRP wall and ceiling linings, seat cushions and carpet. The objectives of these tests were to measure material flammability quantities such as ignitability and HRR and other data required for design fire models.

The results are summarised briefly as it is a standard test method required for input in further analysis.

#### **3.1.2.2 Large-scale corner ignition experiments overview**

Prior to the full-scale experiment, a series of large-scale corner ignition experiments was conducted in the carriage. Interior materials were installed in one corner of the carriage. A range of ignition sources were applied. The objectives of these experiments were to:

- Characterise ignition source severity necessary to initiate fire spread.
- Investigate mechanisms of early fire spread from the ignition source to adjacent interior materials.

The results of these experiments are reported in less detail because as they are not the main focus of this thesis and are not applied in any further analysis.

### 3.1.2.3 Full-scale experiment overview

A single, full-scale fire experiment was conducted in the carriage. Interior materials were installed in approximately half the carriage. A scenario involving a stationary carriage with both passenger doors open only on one side of the carriage was represented. This scenario would likely result if passengers evacuated to a platform at one side of the carriage. A fire was allowed to fully develop, involving all combustible materials within the carriage. The objective of this experiment was to obtain observations and measurements to increase understanding of large fire growth on trains and enable an analysis of design fire estimation methods. The results of this experiment are reported in detail so that they can be applied in the analyses in Chapter 4.

### 3.1.3 Limitations and conditions affecting experiments

The experimental component of this research was made possible due to collaboration with a rail operator. This collaborator and the model of passenger train carriage on which the experiments were based is not identified for reasons of commercial security. Experiments were designed and conducted based on existing knowledge of fire behaviour in passenger trains demonstrated by the literature review and previous experimental work. The experiments were subject to the following limitations:

- A limited variety and amount of train interior materials were available. This limited both the variety of experiments and ability to conduct further tests.
- HRR was not measured due to a lack of resources. A facility capable of measuring full-scale train fire HRR does not exist in Australia and it is well beyond the resources of this research to construct such a facility.
- The facility available for the full-scale experiment was an open air pad at a fire brigade training centre. The carriage and facility were only available for a limited period which restricted time available for both planning and conducting the experiments.
- Total smoke production and smoke density within the carriage were not measured due to a lack of resources.
- For the full-scale experiment the ability to observe fire growth on the inside of the carriage was very limited due to smoke obscuration.

- For the full-scale experiment, from approximately 400 s, some internal thermocouple, heat flux meter and flow probe measurements were adversely affected by the collapse of materials or the fusing of materials to the sensors. Where identified affected measurements have been removed for analysis.
- Measurement of glass surface temperature is subject to errors as identified in Section 3.5.2. There may also have been temperature variations across the glass surface not captured by the application of a single thermocouple.
- Gas concentrations could only be measured at one location due to lack of resources.
- Flow probe measurements were affected by wind. Wind speeds appear to have been of the same order of magnitude as buoyancy driven fire flows. Therefore the flow measurements may significant errors and are disregarded.
- The wind speed at the time of the full-scale test was not measured. It was observed to be moderate and easterly, blowing into the open doorways. This produced minor affects on smoke movement inside the carriage prior to flashover and a moderate tilt on exterior flames and smoke plumes post flashover.

## **3.2 CARRIAGE AND MATERIALS**

The experiments were conducted on an Australian metro passenger train carriage that was approximately 20 years old and still in operation until, due to collision, it was made available for the experiments. Interior materials tested were selected from scrap and spares stock specific to the carriage selected. Many interior materials used had minor damage. It was not determined if any of the materials had been tested to any flammability standards during there design or use on passenger trains.

### **3.2.1.1 Carriage**

The carriage had been involved in a collision that did not involve a fire. The bare carriage consisted of a stainless steel frame and shell. It was fitted with plywood flooring and sheet aluminium over internal walls and ceiling. Glass fibre insulation and insulated wiring was fitted behind the aluminium and plywood surfaces in the floor, walls and ceiling. All other materials and fittings had been removed for salvage, including the under-carriage, GRP wall and ceiling panels, carpet, seats, windows, roof mounted air-conditioner units and doors. The carriage was approximately 23 m

long and had a total of six doors with two passenger doors on each side and an inter-car door at either end. There were nine windows on each side of the carriage. For identification the doors and windows were labelled alphanumerically as shown in the drawings in Appendix D. Basic dimensions and details of the train carriage are given in Table 3-1. Dimensioned drawings of the carriage are also given in Appendix D. The carriage prior to instrumentation and fitting of materials is shown in Figure 3.3. The carriage was mounted on top of six jack stands 1 m above ground level.

**Table 3-1 Key carriage dimensions**

<b>Geometry</b>	<b>Dimension (mm)</b>
Carriage length	23,050
Carriage width	2720
Ply floor to GRP ceiling	2010
Ply floor to stainless steel roof	2509
Window width	1601
Window height	1019
Window sill height	860
Door height	1995
Door width	1460



**Figure 3.3 Empty carriage viewed from south-east and interior**

The carriage had penetrations through the floor and walls caused by the accident. The penetration through the floor was approximately 1 m<sup>2</sup> in area and was patched using 18 mm thick plywood covered with 10 mm thick plasterboard. The floor penetration was not observed to fail until after the fully developed fire had begun to decay and is not thought to have affected the full-scale experiment. Penetrations through the lower

wall of the carriage did not influence the experiment as they were only in the exterior stainless steel and did not penetrate through the internal aluminium panels.

### 3.2.1.2 Materials

Interior materials summarised in Table 3-2 were available for use in the full-scale experiment. All materials were selected from salvaged or spare parts stock and were in used condition.

**Table 3-2 Installed materials**

<b>Carriage component</b>	<b>Material description</b>
Floor and lower wall coverings	5mm thick nylon loop pile carpet with a 3mm thick jute backing
Window surround, end wall and vestibule wall linings	Gel-coated polyester GRP panels 3-5 mm thick.
Ceiling linings	Gel-coated polyester GRP panels 3-5 mm thick
Seating	Fabric covered polyurethane foam. Mainly on steel frames. A limited number of polyester GRP frames.
Windows	Aluminium-framed. The top openable panels were constructed of single layers of toughened 5 mm Armourfloat glass. The fixed bottom panels were double glazed. The outer layer was 6.5 mm Neutrex laminated glass with a medium neutral brown tint. The inner layer was a single layer of hardened 6 mm Armourfloat glass. See Appendix D for a drawing of the window construction

### Seats

A mixture of seat cushions was available and had to be used due to the limited total number of seat cushions available. The different cushions represented the different types of original or refurbished cushions likely to have been used on the model of carriage during its service. These varied in their materials; however all had similar dimensions and construction. All seat cushions can basically be described as lined, flexible polyurethane seat foam.

Some seat cushions consisted of polyurethane foam with a black fire-retarded foam layer on top. Other cushions consisted of “Dunlop NL” fire-retarded polyurethane foam fitted with a fire-retardant inter-liner (lining material placed between foam and outer fabric lining). The majority of the seat cushions consisted of “Plaskona” fire-retarded polyurethane foam without any inter-liner. Two different types of seat outer lining fabric were used on the above cushions. The older type was a green coloured 100% wool “Dobbie” weave fabric. The newer type was maroon coloured, 95% wool 5% nylon, flat “Jacquard” weave fabric. All cushions had a plywood backing. All seat base cushions were approximately 400 mm deep, 440 mm wide and 130 mm thick.

All seat back cushions were approximately 500 mm high, 400 mm wide and 100 mm thick. More base cushions were available than backs.

Four seat frames were available, each consisting of two seats. The frames were designed to cantilever from the lower wall rather than mount to the floor. Two of the frames were constructed of metal with sheet metal on the back and base, and an exterior gel-coated polyester GRP panel on the back. The other two were moulded polyester GRP seat frames with gel coated GRP panels on the back and base.

#### GRP wall and ceiling lining panels

Wall and ceiling lining panels available from stock were constructed of 3–5 mm polyester GRP a bone coloured gel coat. The thickness of the panels varied over their area due to their manufacture by hand lay-up methods. Panels included window shells (which lined the area around each window and up to the ceiling), ceiling panels, vestibule wall panels and end wall panels. Many of the panels had penetrations for lights, air-conditioning and other services. These panels are designated as “old” GRP in this thesis.

The availability of these panels was limited, so additional polyester GRP panels were manufactured and used for vestibule wall and end wall panels. The panels were constructed to 3-5 mm thick. The resin was FGI 61628 with minimal fire retardant. The panels were gel coated white. These panels are designated as “new” GRP in this thesis.

### **3.3 CONE CALORIMETER EXPERIMENTS**

#### **3.3.1.1 Cone Calorimeter Specimens**

Major interior materials, including carpet, seat cushions, and old and new GRP, have been tested in the cone calorimeter. The materials were prepared as 100 × 100 mm specimens. In the case of seat cushions, the maroon 95% wool 5% nylon flat “Jacquard” weave fabric and “Plaskona” polyurethane foam were tested in composite, and were cut to a thickness of 45 mm. The prepared specimens were conditioned at a temperature of  $23 \pm 2^\circ\text{C}$  and a relative humidity of  $50 \pm 5\%$  for seven days immediately prior to being tested.

### 3.3.1.2 Cone Calorimeter procedure

Cone calorimeter tests were carried out in accordance with AS/NZS 3837. All specimens were tested in the horizontal orientation with the standard pilot operating. Some specimens were tested with the use of an edge frame to retain the specimen and reduce burning at the side surfaces of the specimen, as allowed in the standard. The edge frame reduced the test surface area from 0.01 to 0.0088 m<sup>2</sup>, and this was the area used in the calculations. Specimens were packed to the correct test height using ceramic fibre blanket.

Three specimens of each material were tested at each irradiance level. Flooring carpet was tested at an irradiance level of 25 kW/m<sup>2</sup>. Seat material was tested at irradiance levels of 25 and 35 kW/m<sup>2</sup>. Wall and ceiling linings were tested at irradiance levels of 25, 35 and 50 kW/m<sup>2</sup>. These irradiance levels are commonly applied in calculations such as Duggan's method.

The nominal exhaust flow rate of the cone calorimeter for all tests was 0.024 m<sup>3</sup>/s. A measured quantity of methanol was burnt on the day of testing to calibrate the HRR measurement of the apparatus. Prior to testing, a poly methylmethacrylate reference specimen was tested to ensure that all systems were working correctly.

### 3.3.1.3 Results

Cone calorimeter results are summarised in Table 3-3. Plotted HRRPUA for all cone calorimeter tests are presented in Appendix H.

The carpet HRR per unit area vs. time curves exhibited a double peak with the first peak being the highest resulting from ignition of the surface of the carpet pile. The second peak was due to ignition of the jute backing. The seat cushion demonstrated a similar double peak with the first peak being due to ignition and charring of the fabric lining and the second peak due to ignition of the polyurethane foam behind the lining. The old and new GRP exhibited similar times to ignition however the old GRP achieved higher a peak HRR than for the new GRP.

**Table 3-3 Cone calorimeter results for interior materials used in full-scale train fire experiment**

Material	Specimen	Heat flux (kW/m <sup>2</sup> )	Time to ignition (s)	End of test (s)	Specimen mass (g)	Final mass (g)	Ave. mass loss rate (g/m <sup>2</sup> s) <sup>a</sup>	Specimen area (m <sup>2</sup> )	Total heat released (MJ/m <sup>2</sup> )	Peak HRR (kW/m <sup>2</sup> )	Time of peak HRR (s)	Average HRR <sup>a</sup> (kW/m <sup>2</sup> )			Average EHC (MJ/kg) <sup>b</sup>	Average SEA (m <sup>2</sup> /kg) <sup>b</sup>	Average CO (kg/kg) <sup>b</sup>	Average CO <sub>2</sub> (kg/kg) <sup>b</sup>
												60 s	180 s	300 s				
Carpet – 5 mm thick nylon loop pile with 3 mm thick jute backing	576bB25	25	36	145	41.9	35.3	6	0.01	9.2	211.5	45	139.8	55.5	49	8.7	40.6	0.002	0.53
	576C25	25	37	150	41.7	34.4	5.9	0.01	10.2	230.9	45	148.5	65.6	49.5	10.3	57.5	0.003	0.52
	576D25	25	38	135	41.1	34.7	6.3	0.01	9	210	45	139.2	59.8	50.6	9.1	47.1	0.002	0.53
		Mean	37.00	143.33	41.57	34.80	6.07	0.01	9.47	217.47	45.00	142.50	60.30	49.70	9.37	48.40	0.00	0.53
		SD	1.00	7.64	0.42	0.46	0.21	0.00	0.64	11.66	0.00	5.20	5.07	0.82	0.83	8.52	0.00	0.01
	576B35	35	19	495	40.1	11.3	6	0.01	47.8	273.4	30	189	124.6	121.9	16	227.3	0.015	1.05
	576C35	35	18	515	42	12.8	5.9	0.01	50.1	271.6	35	182	120.9	121.5	16.8	234.2	0.015	1.14
	576D35	35	16	485	38.9	10.1	6.1	0.01	45.1	249.5	30	174.6	130.1	119.4	14.8	221.7	0.021	1.09
		Mean	17.67	498.33	40.33	11.40	6.00	0.01	47.67	264.83	31.67	181.87	125.20	120.93	15.87	227.73	0.02	1.09
		SD	1.53	15.28	1.56	1.35	0.10	0.00	2.50	13.31	2.89	7.20	4.63	1.34	1.01	6.26	0.00	0.05
Seat cushion – Plaskona polyurethane foam with maroon wool/nylon fabric, 45 mm	577A25	25	29	100	57.4	54.5	4.7	0.0088	3.2	97.7	35	52.3	34.5	28.5	6.2	54.1	0.006	0.43
	577D25	25	28	200	61.6	56.2	10.2	0.0088	6.8	85.1	35	52.1	41.2	32.9	5.2	39.6	0.011	0.18
	577E25	25	30	275	62.8	44.3	11.5	0.0088	6.8	103.1	35	55	30.4	27.9	3.2	25.1	0.006	0.06
		Mean	29.00	191.67	60.60	51.67	8.80	0.01	5.60	95.30	35.00	53.13	35.37	29.77	4.87	39.60	0.01	0.22
		SD	1.00	87.80	2.84	6.44	3.61	0.00	2.08	9.24	0.00	1.62	5.45	2.73	1.53	14.50	0.00	0.19
	577A35	35	17	100	53.2	43	17.1	0.0088	4	146.4	25	65.2	32	21.1	2.3	109.5	0.006	0.25
	577B35	35	19	155	54.6	48.3	11.9	0.0088	8.2	166.2	25	84.7	47	32.8	6.3	46	0.017	0.44
	577C35	35	20	850	55.3	16.5	5.4	0.0088	71.7	160.9	25	80.6	85.8	93.6	16.5	169.9	0.065	0.94
		Mean	18.67	368.33	54.37	35.93	11.47	0.0088	27.97	157.83	25.00	76.83	54.93	49.17	8.37	108.47	0.03	0.54
		SD	1.53	418.04	1.07	17.04	5.86	0.00	37.93	10.25	0.00	10.28	27.76	38.92	7.32	61.96	0.03	0.36
GRP – old with bone coloured gel coat	578A25	25	109	520	58.2	29.5	8	0.0088	50.1	240.7	130	200.8	182.7	146.4	12.1	484.5	0.061	0.94
	578B25	25	107	510	59.3	26	9.4	0.0088	59.4	246.7	135	186.1	192	170.2	13	620.5	0.052	0.99
	578C25	25	118	580	64.5	30.7	8.4	0.0088	62.4	256.8	145	217.9	187.2	167.5	13	523.1	0.06	0.92
		Mean	111.33	536.67	60.67	28.73	8.60	0.0088	57.30	248.07	136.67	201.60	187.30	161.37	12.70	542.70	0.06	0.95
		SD	5.86	37.86	3.37	2.44	0.72	0.00	6.41	8.14	7.64	15.92	4.65	13.03	0.52	70.09	0.00	0.04
	578A35	35	58	300	42.3	18.3	11.6	0.0088	47.4	307.2	115	265.4	242.6	166	14.2	638.3	0.063	1.14
	578B35	35	57	275	39.3	18.7	10.7	0.0088	40	306.6	100	251.8	211.9	144.3	13.9	732.7	0.067	1.09
	578C35	35	60	285	41.3	17.6	12	0.0088	46.3	334.1	110	277	243	164.9	13.9	741.8	0.062	1.1
		Mean	58.33	286.67	40.97	18.20	11.43	0.0088	44.57	315.97	108.33	264.73	232.50	158.40	14.00	704.27	0.06	1.11
		SD	1.53	12.58	1.53	0.56	0.67	0.00	3.99	15.71	7.64	12.61	17.84	12.22	0.17	57.31	0.00	0.03
	578A50	50	32	260	43.6	18.1	12.8	0.0088	47.1	322.2	70	263.3	245.5	165	14.6	930	0.064	1.05
	578B50	50	31	255	43.1	19.5	12.2	0.0088	45.7	386.6	75	309.4	240.3	161.8	15.2	883.4	0.065	1.09
	578C50	50	30	250	41.9	18.7	12.2	0.0088	43.7	332.5	50	274.8	231.5	154.8	14.9	828	0.066	1.08
		Mean	31.00	255.00	42.87	18.77	12.40	0.0088	45.50	347.10	65.00	282.50	239.10	160.53	14.90	880.47	0.07	1.07
		SD	1.00	5.00	0.87	0.70	0.35	0.00	1.71	34.59	13.23	24.00	7.08	5.22	0.30	51.06	0.00	0.02

<sup>a</sup> Calculated from ignition.<sup>b</sup> Calculated from start of test.

**Table 3-6** *Continued*

Material	Specimen	Heat flux (kW/m <sup>2</sup> )	Time to ignition (s)	End of test (s)	Specimen mass (g)	Final mass (g)	Ave. mass loss rate (g/m <sup>2</sup> s) <sup>a</sup>	Specimen area (m <sup>2</sup> )	Total heat released (MJ/m <sup>2</sup> )	Peak HRR (kW/m <sup>2</sup> )	Time of peak HRR (s)	Average HRR <sup>a</sup> (kW/m <sup>2</sup> )			Average EHC (MJ/kg) <sup>b</sup>	Average SEA (m <sup>2</sup> /kg) <sup>b</sup>	Average CO (kg/kg) <sup>b</sup>	Average CO <sub>2</sub> (kg/kg)
												60 s	180 s	300 s				
GRP – new with white coloured gel coat	578bA25	25	125	330	44.6	17.8	12.7	0.01	33.7	231.4	185	182.7	184.3	#N/A	8.7	724.1	0.064	0.51
	578bB25	25	251	380	43.4	19.5	7.3	0.0088	16.4	186.4	270	178.4	103.8	71.9	10.9	836.9	0.056	0.67
	578bC25	25	110	375	42.5	19.9	9.7	0.0088	36.9	207.9	145	159.3	163.1	128.2	10.9	876.5	0.058	0.67
		Mean	162.00	361.67	43.50	19.07	9.90	0.0092	29.00	208.57	200.00	173.47	150.40	#N/A	10.17	812.50	0.06	0.62
		SD	77.44	27.54	1.05	1.12	2.71	0.00	11.03	22.51	63.84	12.46	41.73	#N/A	1.27	79.08	0.00	0.09
	578bA35	35	73	370	53.5	25.5	10.7	0.0088	44.5	216.6	105	169.7	176.7	149.8	11.9	1054.9	0.064	0.78
	578bB35	35	71	310	43.6	19.2	11.6	0.0088	40.7	243.1	100	195.1	200.1	145.2	12.5	984.2	0.068	0.71
	578bC35	35	71	380	52.3	22.6	10.9	0.0088	47.7	213.2	110	154.5	178.2	158.1	12.2	1022.5	0.066	0.77
		Mean	71.67	353.33	49.80	22.43	11.07	0.0088	44.30	224.30	105.00	173.10	185.00	151.03	12.20	1020.53	0.07	0.75
		SD	1.15	37.86	5.40	3.15	0.47	0.00	3.50	16.37	5.00	20.51	13.10	6.54	0.30	35.39	0.00	0.04
	578bA50	50	29	240	42.1	19.8	12.5	0.0088	37.6	271.2	55	205.4	200.9	136.8	13.6	1113.5	0.07	0.86
	578bB50	50	29	245	44.4	20.6	12.8	0.0088	37.8	257.1	60	196.6	201.2	134.4	12.8	1065.8	0.072	0.85
	578bC50	50	27	245	43.2	20.1	12.2	0.0088	37.5	263.5	65	187.3	197.7	133.5	13.3	1045.5	0.071	0.88
		Mean	28.33	243.33	43.23	20.17	12.50	0.0088	37.63	263.93	60.00	196.43	199.93	134.90	13.23	1074.93	0.07	0.86
		SD	1.15	2.89	1.15	0.40	0.30	0.00	0.15	7.06	5.00	9.05	1.94	1.71	0.40	34.91	0.00	0.02

<sup>a</sup> Calculated from ignition.<sup>b</sup> Calculated from start of test.

### 3.4 LARGE-SCALE CORNER IGNITION EXPERIMENTS

#### 3.4.1 Installation of Materials in Carriage

These experiments were conducted prior to the full-scale experiment. The same carriage and materials were used. All ignition experiments were conducted on a section of interior materials including flooring, wall linings, ceiling linings and one two-seat unit installed in one end corner of the carriage. The arrangement of materials for ignition experiments is shown in Figure 3.4.

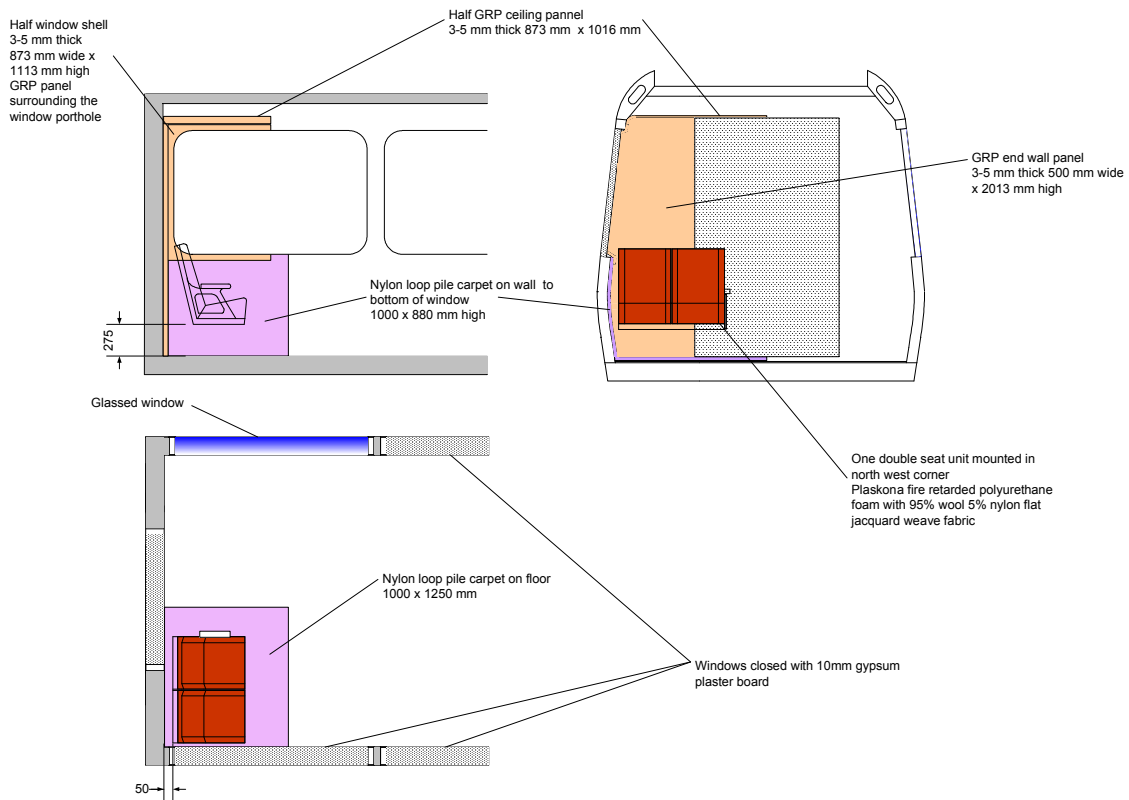


**Figure 3.4 Materials installed for train carriage corner ignition experiments**

Carpet extended from the centre of the carriage floor to the west wall, and lined the wall up to the bottom of the window shell. The carpet extended 1 m from the end-wall. Half of one window shell was mounted in the corner around the window, extending 870 mm from the end wall. One end wall panel extending from floor to ceiling and from the west wall to the edge of the carriage end door was installed. In some experiments, the original old GRP end wall panel was replaced by new GRP due to a lack of available material. Half of one ceiling panel was mounted in the corner

extending from the west wall to the carriage centre and 870 mm from the end wall. One two-seat unit was installed transversely in the corner. For most experiments the steel seat frames were used. The GRP seat frames were used in some experiments to investigate their fire behaviour.

The ventilation conditions were the same as for the full-scale experiment, with only two side doors open on the west side of the carriage and all other doors and windows closed. One glazed window unit was fitted to the window on the east wall, opposite the furnished corner, to investigate glass performance. All other windows, the inter-car end doors and side doors on the east side were closed with plasterboard.

### **3.4.2 Instrumentation and Apparatus**

The same instrumentation layout applying temperature measurement, gas flow measurement and gas analysis, as described in Section 3.5.2 for the full-scale fire experiment was applied for all instruments except the heat flux meters. Because fires would be suppressed prior to flashover for the large-scale experiments, heat flux meters were less likely to be damaged by heat and were positioned closer to the ignition corner to measure heat flux at floor level, at an adjacent seat position and at the centre of the glazed window opposite the ignition corner. HRR was not measured.

### **3.4.3 Ignition sources and procedure**

A range of ignition sources consisting of crumpled newspaper, timber cribs and kerosene were applied to a variety of locations in the test corner as detailed in Table 3-4. The ignition sources are characterised in Appendix C. Tests were conducted burning the various ignition sources on a non-combustible corner and seat under an ISO 9705 hood to measure the ignition source HRR provided in Appendix C and Table 3-4.

The experimental procedure was essentially the same as for the full-scale experiment. The ignition source was placed in the desired location and ignited by applying a gas blow torch. Video and still photographs were taken and instruments were logged throughout the test. If a fire grew to involve the entire ceiling panel, it was concluded that the fire would continue to spread to involve other materials in the vehicle if installed. At this point, the fire was suppressed to prevent unnecessary damage to the

glazed window and carriage. Based on the results of preceding experiments, new experiments were conducted using refined ignition sources and locations. Damaged materials were replaced after each experiment.

### 3.4.4 Results

Results of the large-scale corner ignition experiments are summarised in Table 3-4.

**Table 3-4 Summary of results from ignition experiments**

Experiment number	Ignition source	Ignition source quantities measured with non-combustible corner and seat			Sufficient fire growth for continued spread to entire vehicle
		Average peak HRR (kW)	Average time to peak HRR (s)	Burn duration (s)	
1	300 g crumpled newspaper piled on seat against wall	90	30	165	No
2	600 g crumpled newspaper piled on seat against wall	167	25	160	Yes
3	150 g timber crib on seat against wall	38	50	145	No
4	400 g timber crib on seat against wall	26	135	377	No
5	500 ml kerosene poured onto slashed seat adjacent wall	Not measured	Not measured	Not measured	Yes
6	450 g crumpled newspaper piled on seat against wall	105	22	155	No
7	450 g crumpled newspaper piled on floor in corner behind steel seat shell	74	33	192	Yes
8	300 g crumpled newspaper piled on floor in corner behind GRP seat shell	62	33	172	Yes
9	600 g timber crib on seat against wall.	50	155	387	No

As for large-scale experiments reviewed from literature, these experiments demonstrated that for typical passenger rail vehicles, the behaviour of ceiling and wall linings is critical for fire spread beyond the ignition area, with seating being less critical.

It was observed that seat cushions initially only became involved where directly in contact with the ignition source. The majority of the heat was released from the ignition source rather than the cushions. Flames from the ignition source impinged on the GRP wall linings in the corner. The gel coat was initially effective in preventing the involvement of the GRP. However, once the gel coat was charred, cracked and delaminated the polyester resin beneath became readily involved on the wall linings in

the corner. However, at this stage flames did not spread laterally across the wall linings. If the combined flames from the ignition source and corner wall linings then impinged on the ceiling GRP for a sufficient duration, the gel coat broke down and the polyester resin on the ceiling became involved. At this stage flames spread laterally across to involve the whole ceiling panel, and would have continued to spread to the entire vehicle if fully fitted with materials, see Figure 3.5. There was no lateral flame spread across the seats or lower wall linings. Thus, in these experiments ceiling and upper wall lining fire performance was critical to fire spread beyond an ignition area. An ignition source of 450–600 g (100–170 kW) of crumpled newspaper located on the seat was required for fire spread to the entire vehicle. Less severe ignition sources resulted in limited involvement of the seat and wall linings without sufficient impingement on the ceiling panel for spread.



**Figure 3.5. Test 2 at 40 s and 170 s demonstrating fire spread to ceiling linings.**

Applying 500 ml of kerosene to slashed seating also resulted in the involvement of the entire ceiling panel. Timber cribs located on the seat did not cause significant fire spread. The cribs burn for a longer duration and provide more severe ember attack to the seat than newspaper, however they produce a lower peak HRR, which is critical for the involvement of the ceiling.

The most severe ignition location was found to be on the floor behind the seat in the corner. The seat back was covered in a GRP panel and was located approximately 50 mm from the end wall GRP panel. Flames from the ignition source spread out and

rose between these combustible vertical panels and, once involved, the panels re-radiated upon each other. The much lower quantity of 300 g (60 kW) of crumpled newspaper ignited these panels and resulted in strong flame impingement on the ceiling, causing the involvement of the entire ceiling panel.

Experiment 6 demonstrated the largest ignition source (100 kW peak HRR) that did not result in fire spread beyond the ignition location. The measured gas temperatures near the ignition location for Experiments 6 are shown in Figure 3.6, and the measured gas concentrations are shown in Figure 3.7. These results show that conditions did not become untenable for the majority of the carriage interior if the fire failed to spread beyond the ignition location.

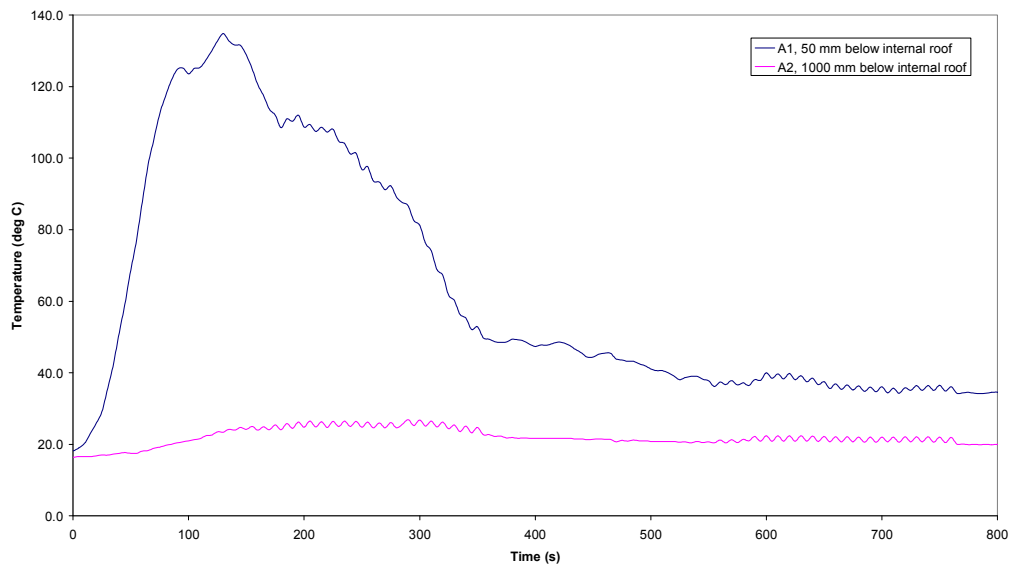


**Figure 3.6** Experiment 6 – temperatures at centre of carriage 2 m from ignition point

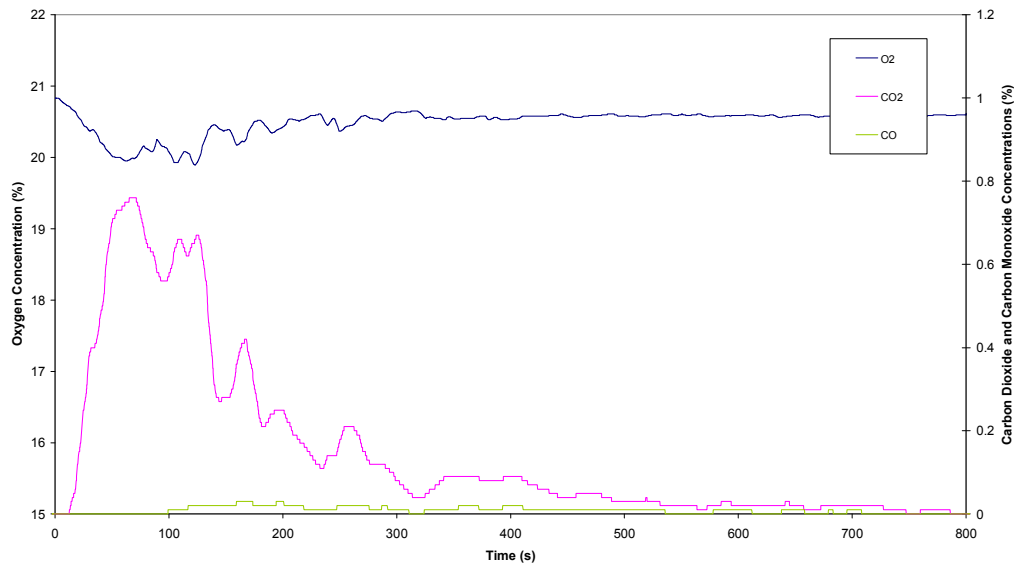


**Figure 3.7 Experiment 6 – gas concentrations at head height**

### 3.5 FULL-SCALE EXPERIMENT

#### 3.5.1 Installation of Materials in Carriage

Insufficient materials were available to fit out the entire carriage. Instead, a 10 m long section of the north end of the carriage was fitted with all materials available. Drawings detailing the size and location of fitted materials are provided in Appendix D. The interior materials in the fitted section were complete except for the following components:

- Metal skinned doors.
- Light diffusers.
- Metal air conditioning diffusers.

These omitted components would not be expected to contribute appreciably to the total fuel load or fire behaviour due to non-combustible materials of construction or limited quantities of combustible materials. However penetrations in GRP ceiling panels where diffusers were omitted resulted in flames penetrating to the rear surface of GRP ceiling panels at an earlier stage during the full-scale test.

The installed materials are shown in Figure 3.8.



**Figure 3.8** Carriage interior and exterior prior to full-scale experiment

To simulate the ventilation scenario of a stationary carriage with only two passenger doors open on one side, both carriage end doors and passenger doors on the east wall were sealed with 10 mm thick gypsum plasterboard. Actual doors were unavailable. This plaster board was originally expected to maintain integrity for the duration of the experiment however loss of integrity did occur mostly during the fire decay (see Section 3.5.5). Both passenger doors on the west side were left open. The open side doors are labelled Door A and Door B as shown in Appendix D

Eleven glazed window units were available and were fitted at the north end of the carriage. All other windows were sealed with 10 mm thick gypsum plasterboard. The fitted glazed windows were labelled alphabetically from WA to WL as shown in Appendix D.

Carpet extended 10 m along the floor from the north end wall. Carpet also extended 0.85 m from floor to window sill on each side wall, except in the vestibule area.

An “old” GRP end wall panel extended from floor to ceiling on the east side of the north end wall. The other end wall panel extending from floor to ceiling on the west side of the north end wall was constructed of “new” GRP sheet. “Old” GRP window shells extended 9.6 m from the north end wall on both side walls, except in the vestibule area adjacent the side doors. In the vestibule area, GRP wall panels

extending from floor to ceiling were installed on both sides of the door on both side walls. These were constructed from a mixture of “old” and “new” GRP. “Old” GRP ceiling panels covering the entire ceiling width, 2 m above the floor, also extended 9.6 m from the north end wall.

A total of sixteen sets of two-seat units were installed in the fitted out area. Two GRP seat frames were installed against the end wall in the east corner where the ignition source was to be applied. The next two-seat frames on the west side were steel frames with GRP backs. The GRP on all 4 of these seats had been partially consumed during prior ignition experiments, see Section 3.4. The rest of the seat frames were mock-ups constructed with steel frames and sheet metal behind the seat base and back. The six seat back cushions closest to the north-east corner were lined with green coloured 100% wool “Dobbie” weave fabric. All other seat base and back cushions were lined with maroon coloured, 95% wool 5% nylon, flat “Jacquard” weave fabric. Seat base cushions were used in place of back cushions for the majority of the seats due to limited availability of back cushions.

### **3.5.2 Instrumentation and Apparatus**

As HRR could not be directly measured, other instruments were applied to measure quantities that may be used to estimate fire growth rate and tenability. The location and labelling of all instrumentation is provided in Appendix D.

#### **3.5.2.1 Temperature measurement**

Temperature provides a reasonable indication of fire growth and decay because enclosure temperature is largely dependent upon fire HRR. Temperatures at different locations provide a good indication of flame location (fire spread). For these reasons and also because thermocouples are less expensive than other types of instruments a far greater number of thermocouples was used compared with heat flux meters, gas flow probe and gas analysis. The measured temperatures are an important input to the model developed to estimate the HRR for this experiment.

All temperatures were measured using 1.5 mm Type K mineral-insulated metal-sheathed (MIMS) thermocouples. These thermocouples were selected because they are sufficiently durable to withstand flashover fires and also have an appropriate

thermal response. Type K thermocouples are commonly used for fire testing due to cheaper materials of construction and appropriate temperature range.<sup>[116]</sup> Type K extension grade compensating cable was used to connect the thermocouples to the data acquisition devices.

Gas temperatures within the carriage were monitored using 11 thermocouple trees at 2 m spacing's along the centre of the carriage. One thermocouple tree at the centre of each end section of the carriage and the centre of the mid-section of the carriage was fitted with 9 thermocouples evenly spaced from 50 mm to 1650 mm below the ceiling. All other centre thermocouple trees consisted of 2 thermocouples with one thermocouple 50 mm below the ceiling and the other at mid floor to ceiling height. These thermocouples were intended to monitor both flame spread and development of a hot gas layer within the carriage.

Thermocouple trees were placed at the centre of both open side doors consisting of 12 thermocouples at regular vertical spacing from 50 mm below the top of the door to 1450 mm below the top of the door. These were intended to monitor out flowing gas and flame and neutral plane height.

Two thermocouples were mounted on the outside of each glazed window unit to monitor the time of window glazing failure and out flowing gas temperatures. Two windows near the ignition area were more fully instrumented with six thermocouples on the internal and external glass surfaces of each window unit to provide information relating to the conditions for failure of the glazing and out flowing gas temperatures once the glazing failed. For surface measurement, a 30 mm length at the end of each thermocouple was lightly coated with a silicon based heat transfer paste and pressed parallel to the glass surface to maximise thermal contact. Radiant and conductive heat transfer as well as poor thermal contact can produce significant errors for temperature measurement of glazed surfaces.<sup>[116]</sup> This error cannot easily be quantified or eliminated.

### 3.5.2.2 Heat flux measurement

Heat flux is rate of heat energy flow per unit area. Total heat flux transported through air from fire consists of radiant heat and convective heat. Gardon-type water-cooled heat flux meters<sup>[117]</sup> with a range of 0-100 kW/m<sup>2</sup> were used to measure the total heat flux from the fire at different points. Three heat flux meters were placed at floor level facing the ceiling. One was located at each end between the carriage end and vestibule, and in the centre between both vestibules. These were to provide measurement of heat flux at floor level, important for determining the development of the hot layer and flashover conditions along the carriage. A fourth heat flux meter was placed outside the carriage at a distance of 6 m from the side door closest to the ignition seat. This was to measure the heat flux that people and infrastructure outside the carriage would be exposed to. For the fully developed fire, no heat flux meters were placed above floor level within the carriage as they would be expected to become damaged by excessive heat early in the experiment.

### 3.5.2.3 Gas flow measurement

Temperature and flow rate of gas or flame through an opening is also related to HRR. Bi-directional pressure probes<sup>[118]</sup> connected to differential pressure transducers were used to measure the flow of gases at the openings. These are used for fire flow measurements in preference to pitot tubes which foul or hot wire anemometers which are affected by temperature. Setra Model 264 differential pressure transducers with ranges from 0–24 to  $\pm 240$  Pa were used. Due to cost there were insufficient pressure probes and transducers to instrument all openings. Instead, one door and one window were instrumented, to provide data that could then be related to the observed behaviour at other openings.

Three pressure probes were mounted at 250 mm, 1050 mm and 1450 mm below the top of the door in the centre of the north-west side doorway. Three pressure probes were mounted at 260 mm, 530 mm and 920 mm above the window sill outside the window opposite the ignition point, in order to measure gas flows through the window if the glass broke.

#### 3.5.2.4 Gas analysis

Gases were continuously sampled from one point within the carriage using a stainless steel sample tube and diaphragm sample pump. The gas concentrations of O<sub>2</sub>, CO and CO<sub>2</sub> within the sample were measured using a portable Coda electrochemical gas analyser. Gas was continuously sampled from a point located 1.9 m above floor level, between the ignition end of the carriage and the vestibule. The 1.9 m sample height was selected because it was slightly above typical head height but below the 2.0 m ceiling height, to provide data relating to tenability and fire behaviour.

#### 3.5.2.5 Data Acquisition

All instrumentation, except the gas analyser, was logged at 5 s intervals using two series 505 DataTakers with 30 single-ended analogue channels each. One DataTaker was connected to 2 expansion modules; the other was connected to one expansion module. Each expansion module provided an additional 30 single-ended analogue channels. Each DataTaker and its expansion modules were housed inside protective 5 mm thick steel boxes placed at elevated positions underneath the carriage, at one-third and two-thirds distances along the length of the carriage. Data was stored both in the internal DataTaker memory cards and transmitted in real time to laptop PCs located 30 m away at the experimental control centre. The Coda gas analyser had a self-contained data acquisition system.

#### 3.5.2.6 Video equipment

One video camera and one infra-red camera were mounted to view through the plasterboard blocking the south end door. One hand-held video camera was used to film the inside of the carriage during the first 30 s. Video cameras were mounted outside the carriage at the north-west, south-west and south-east corners. Still cameras were also used to photograph significant events.

### 3.5.3 Ignition source

Crumpled newspaper was used to represent an arson fire using typical ignition fuel found on passenger trains. One kilogram of crumpled newspaper was placed on the floor, underneath and behind the end seat in the north east interior corner of the carriage. Individual tabloid size newspaper sheets were loosely crumpled into approximately 70 mm diameter balls and stacked against the bounding surfaces until the required total mass was achieved. The resulting pile size beneath the end seat was approximately 260 mm high × 600 mm × 400 mm. A gas blow torch was used to ignite the newspaper. Additional calorimetry experiments have determined that this ignition source isolated by non combustible bounding surfaces representing the under seat geometry produces a peak HRR of 140 kW with a burn duration of 260 s (see Appendix C). It is important to note that HRR of crumpled newspaper may significantly vary dependent on packing density.

Although prior experiments indicate that 300 g of crumpled newspaper applied to the same location is sufficient to lead to flashover (see Section 3.4) 1 kg was applied to ensure development of a large fire involving all combustibles.

### 3.5.4 Procedure

The newspaper balls were placed in position. A camera operator and suppression team wearing full breathing apparatus and protective kits were located inside the carriage near door A. Logging of all instruments commenced at least one minute prior to ignition. Prior to ignition, a member of the suppression team breathed into the gas sample point as an event marker to synchronise the Coda gas analyser time with the DataTaker times. The newspaper was then ignited. Due to the expected size of the fire, the ignition and camera operators exited the vehicle 34 s after ignition. Data logging and observation was maintained throughout the growth of the fire and continued until the fire had decayed significantly, at which point the vehicle was suppressed by the fire brigade to avoid prolonged flaming and smouldering.

### 3.5.5 Results

A complete sequence of photographs showing the carriage prior to and throughout the experiment is given in Appendix E. All instrument measurements are graphed and presented in Appendix F.

#### 3.5.5.1 Observation

##### Test Observation

On the day of the experiment a moderate easterly wind was observed. The ambient air temperature at the start of the test was 18 °C.

The 1 kg newspaper ignition fire grew rapidly on the floor behind the end seat, with flames impinging on the ceiling at 20 s. The flames rose up between the end wall GRP panel and the rear seat shell GRP panel, which were spaced 50 mm apart. Both these panels ignited shortly after ignition of the newspaper. Re-radiation between these panels enhanced the fire growth.



**Figure 3.9** Full-scale experiment – interior at approximately 34 s

The fire continued to grow on the corner seat, wall and particularly ceiling linings, with increased smoke production. Flames on the floor carpet were observed through Door A at 119 s. At 140 s the fire size rapidly increased and flames began to flow out of Door A. Temperature and heat flux measurements confirm this to be the onset of flashover. At this point materials such as carpets and seats below the already burning ceiling ignited, and the fire proceeded to rapidly spread along the vehicle to involve all fitted materials. At 152 s the flames out of Door A were observed to intensify,

reaching a height of 2.5 m above the top of the carriage with a maximum flame plume diameter of 2 m. The flame plume flowing out of Door A maintained this size for approximately 300 s and exhibited cyclic pulsing.



**Figure 3.10 Full-scale fire experiment fire size and smoke production at 3 minutes**

Window glazing in the top window quarter panels began to fail at 190 s. This did not result in a large change in ventilation conditions, as the top window quarter panels represent a small vent surface area. At 190 s observations from both the video camera and the thermal imaging camera mounted through the plasterboard at the south end passenger door were totally obscured by hot smoke, and were therefore removed to prevent damage. At 240 s small flames were observed to be issuing from holes for air-conditioning units in the roof near Door A that had been patched with plasterboard. Small intermittent flames began issuing from Door B at 255 s. A loud crashing noise was heard at 269 s and the flames out of Door B became much larger. The noise is thought to be ceiling panels falling from the ceiling, exposing an increased fuel surface area.

At 279 s the flames issuing from Door B extended 2 m above the top of the carriage. At this point flaming of the plywood floor was observed through Door B. The flames out of Door B began to gradually decrease from 310 s, and at 369 s the flames out of Door B ceased. Flames began to penetrate through the plasterboard covering the north-east side door at 350 s, and by 400 s the plasterboard had completely fallen away, fully opening the door.

The glazing in the bottom window quarter panels began to fail progressively from 380 s, gradually increasing the ventilation to the carriage as each window broke. At the same time, flames exterior to the carriage began to significantly decrease. At 460 s the flames exiting Door A had reduced in height to 1 m above the top of the train.

Prior to significant window breakage, much of the observed combustion was in the fire plumes exiting the doors and towards the south end of the fitted area where ventilation was available. As the windows progressively broke, combustion gradually re-establish itself at the northern end of the carriage where, after the onset of flashover, there had not been sufficient ventilation to fully burn all available material. Thus, the windows at the north end were the last to fail.

At 790 s the plywood patching a large hole in the floor at the centre of the carriage burnt through. Small flames were observed to lick out of the bottom of the carriage. By 850 s only small intermittent flames continued to flow out of Door A and by 970 s they had ceased. After this time, materials inside the carriage continued to flame and smoulder at a decreasing rate.

The experiment was continued with full data logging for 1600 s after ignition. After this time, the fire brigade suppressed the remaining flaming and smouldering materials using water.



**Figure 3.11.** Internal damage viewed from south of door B and damage to external west side

### Post test observations

The following observations were made from inspection of the damaged carriage. Photographs of the damage resulting from the full-scale experiment are given in Appendix E.

All plaster used to seal doors and windows, beyond the area fitted with materials, was still intact. The plaster blocking the north-east side door opposite Door A had failed. The plaster blocking the north end door had remained mostly intact for the experiment, but had been removed by fire fighters during suppression. All window glazing had failed except for the bottom quarter panels of Window WL, the window furthest from the ignition location. For Window WL, the inner layer of hardened non-laminated glass had cracked, become brittle and failed, however the laminated outboard glass had cracked but remained in place. For all other windows, a similar failure mechanism was observed, except the lamination film had softened allowing the broken glass to fall out of place. The aluminium window frames of Windows WL, WG, WB, WF, WJ and WK were still intact. The aluminium window frames of Windows WE, WD and WH were only partially damaged, with sections of the frame melting. The aluminium window frames of Windows WA and WC were mostly destroyed, with the majority of the window frame melted away. Glass had melted onto some window thermocouples and pressure probes. This would have caused faulty measurements for the instruments affected. The stainless steel carriage shell was only slightly damaged by buckling at the tops of doors and windows.

All insulation on wires running along the ceiling and walls was consumed along the full length of the carriage. In most cases, the insulation was glass fibre and the binding material had been consumed, leaving the glass fibre behind.

Soot markings on the walls indicated that the smoke layer dropped down to less than 500 mm above floor level at the south end of the carriage past Door B. The plywood floor in this area did not show signs of charring or ignition. Exposed aluminium at ceiling level in this area and the fibreglass insulation behind it were still in place and had not melted.

The plywood floor at Door B had ignited and charred only at the surface. The depth of charring increased with distance north along the carriage. At the edge of the area fitted with materials, 10 m from the ignition point, the char penetrated all the way through the plywood. After the experiment, the charred plywood was still in place; however it was mostly ripped up or crushed by fire fighters during suppression. The fibreglass insulation batts in the floor beneath the plywood had been protected and the yellow phenolic binder was not consumed. The plywood used to patch the pre-existing penetration through the floor at the centre of the carriage had burnt through. The sheet aluminium lower wall panels were still intact beyond the area fitted with materials, 10 m from the ignition point. Within the fitted area, the lower wall panels had melted away and the phenolic binder had been consumed from the fibreglass insulation batts.

All carpet fitted to the floor and lower walls had been consumed. Where molten aluminium had pooled on top of the carpet, this provided some protection during later stages of fire development. Under the aluminium, small amounts of natural fibre carpet backing were present and charring of the plywood was less severe. All seat cushions had been completely consumed. The steel seat shells had softened and buckled. The polyester resin in the GRP seat shells installed at the north end was completely consumed.

The polyester resin from all GRP window shells, and wall and ceiling panels was completely consumed. Remaining glass fibre matting from the GRP panels generally fell to the floor, however in some locations the matting remained in place. For the new GRP panels with white gel coat, the gel coat was completely consumed, however for the old GRP panels with bone coloured gel coat, the gel coat formed a flaked, powdered char. The fibreglass matting was still in place in the north-west corner near Window B. This was the final location of significant burning during the fire's decay.

Exposed sheet aluminium panels at ceiling height in the area between the edge of the fitted area (10 m from north end) and Door B had mostly melted away, however some softened aluminium remained in place in corners. All binder had been consumed in the insulation batts behind these ceiling panels, leaving the glass fibre sagging from the ceiling. Within the fitted area, all aluminium panels behind the GRP ceiling panels had completely melted away. The binder had been completely consumed from the

insulation bats in the walls and ceilings in this area, with most of the fibreglass falling to the floor. Fibreglass insulation that remained in the ceiling was observed to have melted and fused together.

All observations during the full-scale fire experiment are summarised in Table 3-5, including window and plasterboard failure times.

**Table 3-5 Observations during full-scale fire experiment**

<b>Time from ignition (s)</b>	<b>Location</b>	<b>Observation</b>
00	Ignition	Ignition
21	Inside	Flames from ignition source lick ceiling
29	Door A	Light smoke from Door A
32	Inside	Inside camera turned off, moved to south-east exterior and turned back on
34	Door A	Ignition and camera operators exit Door A
59	Door B	Light smoke out of Door B (more smoke out Door B than Door A)
80	Door A	Smoke out of Door A increases
101	North-east door	Smoke leakage around edge of north-west door plaster
106	South-east door	Smoke leakage around edge of south-west door plaster
119	Inside ignition area	Flames visible on carpet through Door A
121	Window WA	Smoke leaking from tops of Windows WA, WC, WE and WG
	Window WC	Smoke leaking from tops of Windows WA, WC, WE and WG
	Window WE	Smoke leaking from tops of Windows WA, WC, WE and WG
	Window WG	Smoke leaking from tops of Windows WA, WC, WE and WG
144	Door A	First flames out of Door A
152	Door A	Flames out of Door A intensify
156	North-east door	Small flames around edge of north-west door plaster
189	Window WH	Flames out top of Window WH
190	South end door	Cameras at south end door removed
193	Window WH	Flames out top left of Window WH
241	Roof	Appears to be flames coming from air-conditioning holes in roof (plastered)
251	Window WH	Flames out top right of Window WH
	Window WF	Flames out top left of Window WF
253	Window WF	Flames out top left of Window WF
266	Window WC	Flames from top of Window WC
267	Door B	Flames out of Door B
	Window WF	Flames out top right of Window WF
268	Window WF	Flames out top right of Window WF
275	Inside	Flames visible on floor at Door B
284	Window WD	Glass falls out top left of Window WD, with intense smoke out but no flames
289	South end door	Camera moved to reveal smoke leaking out south end door
306	Window WD	Glass falls out top right of Window WD, with intense smoke out but no flames
311	Window WD	Flames out top of Window WD
	Window WJ	Flames out top of Window WJ
331	Window WA	Flames at top of Window WA
350	North-east door	Flames begin to penetrate through plaster covering north-east side door
353	Window WE	Flames out top of Window WE
369	Door B	Flames out of Door B cease
371	Window WB	Smoke out top left of Window WB but no flames
373	Window WI	Flames out top of Window WI
381	Window WH	Small flames out bottom of Window WH
	Window WF	Small flames out bottom of Window WF
394	Window WF	Flames out bottom of Window WF
396	Window WE	Glass at the bottom of Window WE breaks, issuing large flames
	North-east door	Plaster covering north-east door fails
	Window WG	Small flames at bottom of Window WG
399	Window WJ	Flames out top of Window WJ
	Door B	Small flames begin issuing from Door B again
401	Window WF	More glass falls out bottom left of Window WF
404	Window WF	Flames out of Window WF intensify
	Window WG	Flames out bottom of Window WG
416	South-east door	Small flames around edge of south-east door plaster

Table 3-3. *Continued*

Time from ignition (s)	Location	Observation
429	Window WD	Flames out bottom of Window WD
430	Window WH	More glass falls out bottom left of Window WH
	Window WJ	Small flames out bottom of Window WJ
431	Window WD	Small flames out bottom of Window WD
450	Window WG	Glass falls out bottom of Window WG, issuing larger flames
451	Window WG	Remaining glass falls out bottom left of Window WG
481	Window WG	Remaining glass falls out bottom right of Window WG
484	Window WL	Flames out top of Window WL
495	Window WI	Glass falls out bottom of Window WI, issuing larger flames
499	East side	Flames visible either from roof or east side openings (viewed from west side)
579	Window WD	More glass falls out bottom of Window WD and flames intensify
591	Window WA	Small flames at bottom of Window WA
599	East Side	More intense flames from either roof or east side (viewed from west side)
631	Window WB	Flames out top right of Window WB
639	Window WD	Remaining glass falls out bottom of Window WD
676	Window WB	Small flames out bottom right of Window WB
686	Window WA	Glass falls out bottom of Window WA, issuing larger flames
694	South-east side door	Flames out of plaster opposite Door B (or maybe roof) (viewed from west side)
726	Window WB	Flames out top left of Window WB
801	Window WB	Small flames out bottom left of Window WB
828	Window WB	Remaining glass falls out bottom right of Window WB
849	Window WB	Flames out bottom of Window WB
851	Window WB	Remaining glass falls out bottom left of Window WB
	Door A	Only small intermittent flames out of Door A
969	Door A	Flames out of Door A cease

### 3.5.5.2 Discussion of results

#### Ease of ignition

This experiment demonstrated that 1 kg of crumpled piled newspaper applied to the passenger train tested is easily capable of igniting adjacent materials and developing into a large fire involving the entire carriage. The HRR for 1 kg of crumpled piled newspaper burnt, both in isolation on the floor and beneath a non combustible mock up of a seat and corner arrangement, is shown in Figure 3.12. This ignition source burns for a short duration with a peak HRR of 140 kW.

A typical Melbourne Saturday newspaper represents approximately 1 kg of paper and this quantity of paper is considered a credible arson ignition source, as discussed in Section 2.1.2. The ease of ignition and fire growth from such an ignition source demonstrates that Fire Engineers should consider fire scenarios of complete carriage involvement.

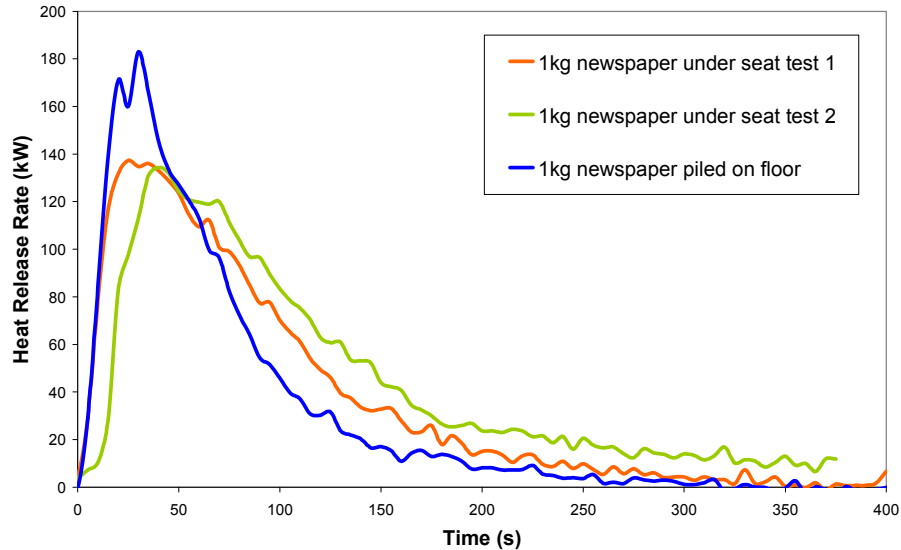


**Figure 3.12. HRR for 1 kg of crumpled piled newspaper**

The ignition location for the full-scale experiment was selected to be the most severe location based on large-scale ignition experiments presented in Section 3.4 . The GRP end wall panel and the GRP rear seat panel formed two opposed vertical sheets of combustible material. This material arrangement was very susceptible to ignition and fire growth.

#### Fire Growth

The fire initially grew on the wall and ceiling linings located in the ignition corner. As the fire grew the ceiling linings and upper wall linings became more involved with limited flame spread away from the ignition area. At this point it was observed that the radiant heat emitted by the fire was sufficient to initiate flashover. It was at this time that seats, lower wall and floor linings adjacent to the ignition location became involved.

From visual observations including involvement of interior materials and flames out doors, and a review of the measured data, the onset of flashover was determined to have occurred at 140 s. At this time the fire size was observed to rapidly increase, with flames starting to flow out of Door A. At 140 s gas temperatures near the ignition area at mid-height rapidly increased to well above the ignition temperature for common combustibles, indicating the occurrence of flashover, see Figure 3.13.

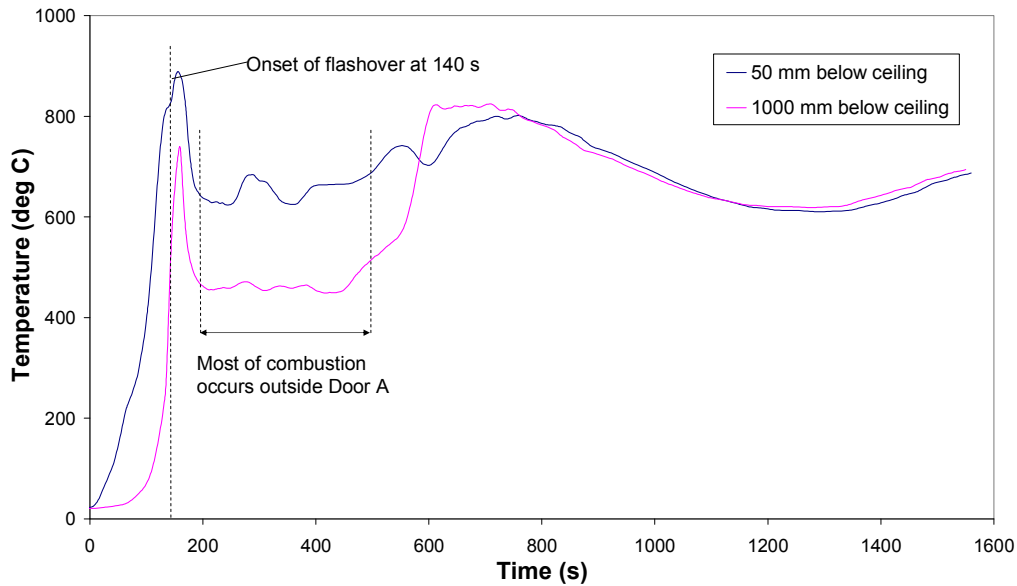


**Figure 3.13. Full-scale experiment – temperatures at centre of carriage 2 m from ignition point (Tree B)**

Total heat flux measurements for the fully developed experiment are illustrated in Figure 3.14. At 140 s the measured heat flux at floor level 3 m away from the ignition point was approximately  $20 \text{ kW/m}^2$  and rapidly increasing. As discussed in Section 2.4.2, the critical radiant heat flux of  $20 \text{ kW/m}^2$  at floor level is an appropriate criterion for the onset of flashover.<sup>[87]</sup>

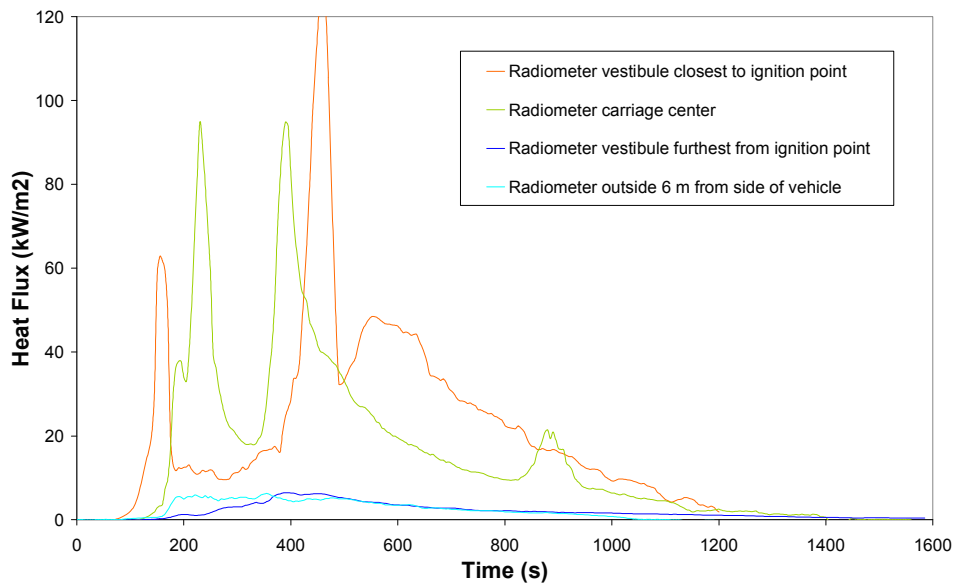


**Figure 3.14. Full-scale experiment – total heat flux measurement**

At 140 s flashover was initiated at the ignition end of the carriage involving all materials in that area. However flashover was not instantaneously achieved for all locations in the carriage. It took time for burning and radiant heat conditions at distances further along the carriage to increase sufficiently for a flashover condition to be achieved in these areas. Figure 3.15 shows the time to involvement of materials at thermocouple tree positions along the carriage, as determined by temperatures measured at 1 m below ceiling level exceeding 400°C, which is greater than the piloted ignition temperature for most combustibles. Figure 3.15 demonstrates that, following the onset of flashover at the ignition end at 140 s, the fire spread to fully involve materials at the end of the fitted area 10 m from the ignition point at 175 s. This corresponded to a measured heat flux of 20 kW/m<sup>2</sup> at floor level at the end of the fitted area of the carriage at 175 s, as shown in Figure 3.14.

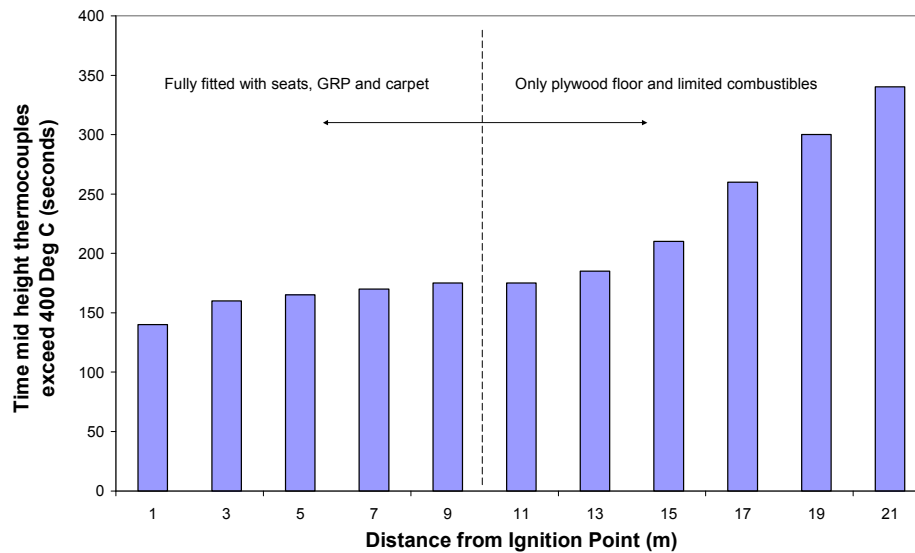


**Figure 3.15. Full-scale experiment – time to involvement of materials at discrete distances along the carriage**

In summary, this experiment demonstrates the following relating to fire growth:

- Fire growth on upper wall and ceiling linings has a critical affect on the initiation of flashover. Careful consideration should be given to fire performance of these materials to reduce the likelihood of flashover.
- Significant fire spread on seats, lower wall and floor linings did not occur until the onset of flashover.
- Flashover can occur on a train carriage. Without the onset of flashover a fire is not likely to spread to consume the entire carriage.

- Once flashover is initiated in one area of the carriage, fire growth to involve the rest of the carriage is very rapid but not instantaneous.
- This rapid fire growth will have a significant impact on tenability, available response time for drivers, damage to surrounding infrastructure and fire fighting activity.

#### Fully Developed Fire Size

The spread of fire extending beyond 15 m from the ignition point was slower than the fire spread within the fitted area due to the limited combustibles available in the south half of the carriage. However, aluminium panels eventually melted, exposing fibreglass insulation and insulated wires which ignited. The exposed plywood floor ignited, with burning of the surface extending to the side door B (18 m from ignition point). Beyond this the plywood did not ignite.

Figure 3.16 shows that temperatures at the ceiling at the end of the carriage opposite the ignition point exceeded 600°C. This is above the ignition temperature of many materials. Also flames were observed to roll along the ceiling and out Door B, however windows at this end of the carriage did not fail as they were sealed with plasterboard. From these observations it is evident that the fire may not have spread on the exposed plywood beyond door B because of poor ventilation in this area resulting in low oxygen content. If the vehicle had been fitted with complete interior materials and glazed windows for the entire carriage length, then it is likely that after the onset of flashover, the fire would have rapidly spread on the materials up to door B due to the availability of ventilation and fuel at this location and that fire spread beyond door B would have been dependant on breakage of glazing in this area

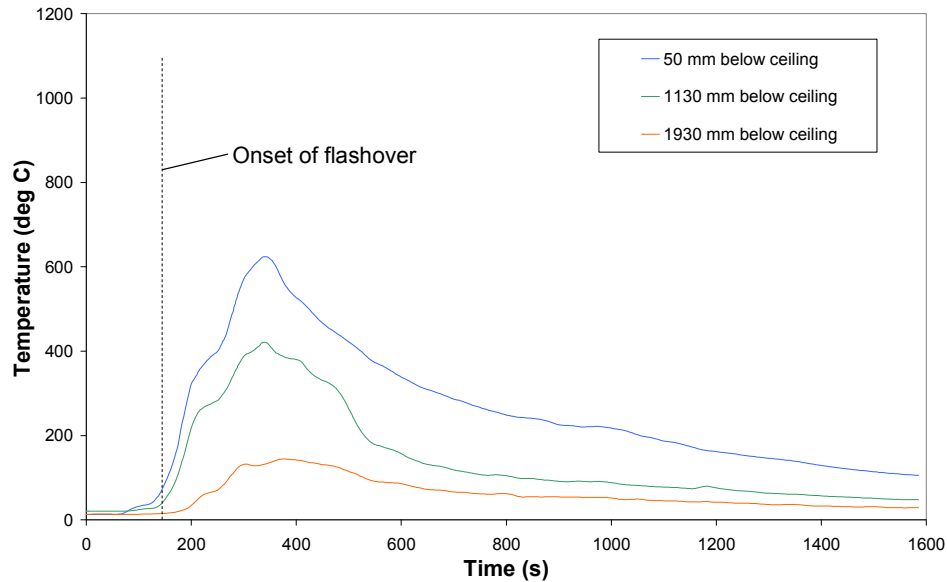


**Figure 3.16. Full-scale experiment – gas temperatures at carriage end opposite ignition point**

Large flames were observed to extend from door A and, to a lesser extent door B from 150s to 400s. During this period significantly more exterior flame was visible than interior flame, partially due to obscuration by smoke and the carriage body. Based only on observations, it was initially concluded that this period represented the peak HRR and that most of the total HRR during the peak was due to exterior combustion. However, based on analysis of experimental measurements presented in Section 4.3, it was subsequently estimated that exterior combustion during this period accounted for 40% of the total HRR and the peak HRR occurred for a short duration after this period between 400-500 s, when increased ventilation enabled more combustion to occur inside the carriage.

During the period 150 s to 400 s, the burning rate for materials inside the carriage was affected by the ventilation to the interior. A significant portion of the combustion occurred in the fire plumes outside each open door where oxygen was available rather than inside the carriage. This is demonstrated by the temperatures at both passenger doors shown in Figure 3.17 and Figure 3.18, which are higher than the interior gas temperatures in the same areas, shown in Figure 3.13 and Figure 3.16, during this period. In fact Figure 3.13 demonstrates that gas temperatures inside the fitted area of the carriage decreased during this period indicating that combustion inside the carriage was partially choked. As windows broke, increasing ventilation, combustion inside the fitted area of the carriage was observed to increase as demonstrated by

second peaks in measured internal temperatures and heat flux's. This effect was similarly observed by Ingason in his model scale tests.<sup>[56]</sup> Ingason observed that if windows were incrementally opened the fire would burn in the location of ventilation and become choked in other areas until the fire would start to decelerate. If more windows were opened a second peak was observed.

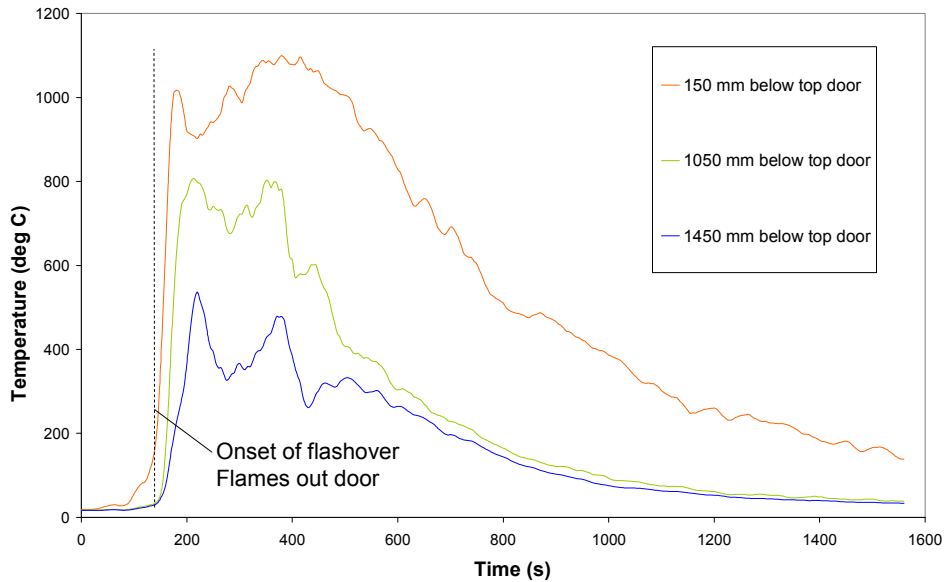


Figure 3.17. Full-scale experiment – gas temperatures at open passenger Door A

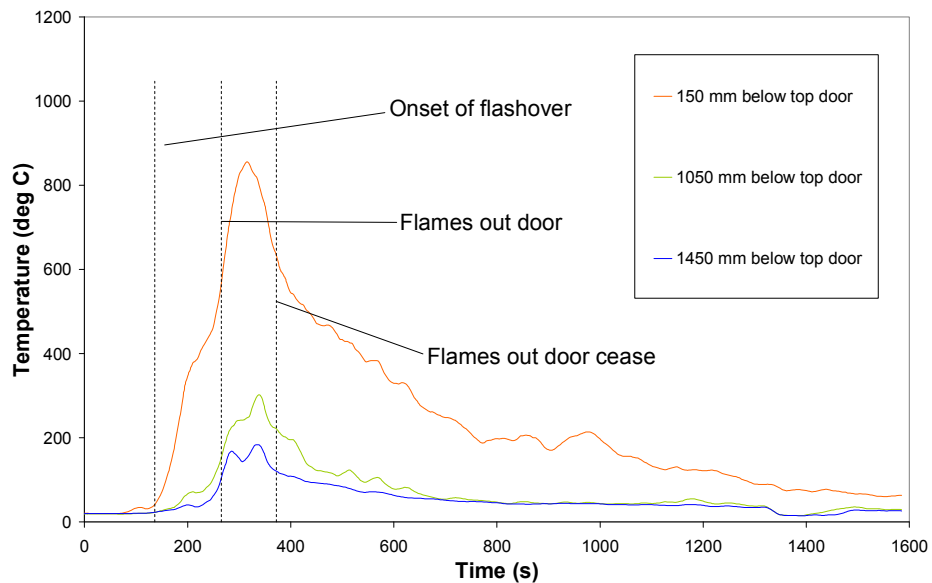


Figure 3.18. Full-scale experiment – gas temperatures at open passenger Door B

After 500 s the fuel load began to burn out and flaming both interior and exterior to the carriage was observed to gradually decrease. This is reflected by decrease in measured temperatures.

The observation of ventilation affects on burning is significant and indicates that HRR estimation methods that assume rapid involvement of all materials, relating HRR to fuel loading without considering ventilation, are flawed.

This experiment also demonstrates that carriage openings such as doors and windows will have a critical affect on fully developed fire size. The majority of the glass window area was not open due to failure until after 400 s.

The fully developed fire size for this experiment is estimated in terms of HRR in Chapter 4.

#### Window Performance

Window failure will have a significant affect on the burning rate for a ventilation affected fire as identified by Ingason. <sup>[56]</sup> For this experiment window glazing maintained integrity and prevented significant increases in fire ventilation throughout most of the fire peak. The upper window quarter panels constructed of single layers of toughened glass began to fail at approximately 200 s, however upper window quarter panels only represented approximately 15% of the total window area. The lower quarter panels constructed of double glazed laminated toughened glass began to fail at 380 s. Typical temperature data for Window D (located near door A) is given in Figure 3.19. This supports the observation that the windows did not break instantaneously. Instead the windows progressively cracked, initially issuing small flames with the ventilation increasing as more pieces of glass fell out.

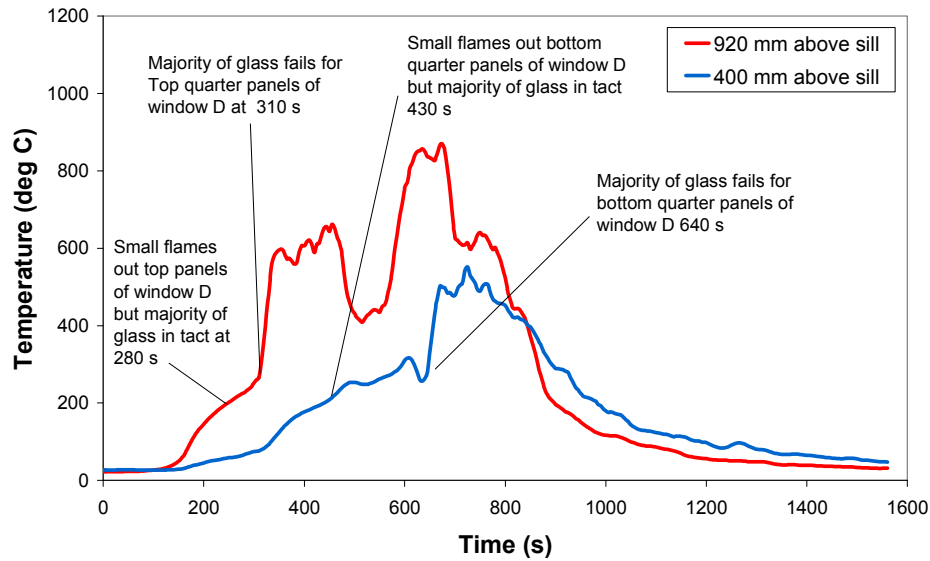


Figure 3.19. Full-scale experiment – temperatures outside Window D

The initial observed failure times and measured surface temperatures for different window panels are given in Table 3-6. Initial observed failure times are taken to be the time that flames or smoke were first observed to pass through the glazing. This shows that there is significant variation in external surface temperatures at the time of initial failure and that accurate prediction of window failure time based on temperature may be difficult. Some of this variation may be due to errors in temperature measurement discussed in Section 3.5.2.1. However for the majority of windows, failure occurred when the measured external surface temperature was in the range 200-240 °C. Internal surface temperatures were only measured for two windows. Internal surface temperatures were much higher at approximately 500 °C. Obviously interior panes for double glazed windows would have failed earlier than exterior panes.

**Table 3-6. Initial window failure times and temperatures**

Window	Panel	Initial failure time (s)	Measured temperature at initial failure time (°C)	
			Outside surface	Inside surface
H	Top	190	40	-
F	Top	250	225	-
C	Top	250	117	500
D	Top	280	225	550
A	Top	330	195	-
E	Top	350	320	-
B	Top	370	220	-
H	Bottom	430	225	-
F	Bottom	380	270	-
E	Bottom	395	230	-
G	Bottom	400	80	-
D	Bottom	430	200	480
A	Bottom	590	210	-
B	Bottom	680	240	-

- = window not fitted with interior surface thermocouples

The windows were observed to maintain their integrity for a substantial period. A range of different glazing materials are used for different train designs that will have different levels of fire performance. If windows had broken earlier during this fire experiment it would most likely have resulted in an increased HRR being achieved earlier due to ventilation enabling increased combustion inside the carriage as discussed in Chapter 4..

### Tenability

Conservative tenability criteria as adopted by the “NIST Fire Safety of Passenger Trains Project”<sup>[55]</sup> have been applied for measured temperatures. Carriage interior conditions are untenable if the hot layer height  $\leq 1.5\text{m}$  and hot layer temperature  $>65\text{ }^{\circ}\text{C}$ . The height requirement for these criteria is different to those typically applied to buildings. This is due to the reduced ceiling height and confined space of a train carriage.

The affect on tenability conditions due to toxic gases and low oxygen is most appropriately assessed applying a more complex fractional effective dose over time

method. For this simple comparison the following general criteria for untenable conditions within the carriage due to gas concentrations are applied<sup>[119]</sup>:

- $\text{CO} > 3\%$  results in rapid incapacitation in less than 2 minutes.
- $\text{O}_2 < 10\%$  results in critical hypoxia.

As smoke density was not measured it cannot be used as an indicator for tenability.

Figure 3.20 shows gas concentrations measured inside the carriage near door A rapidly exceeded tenability criteria immediately after flashover.

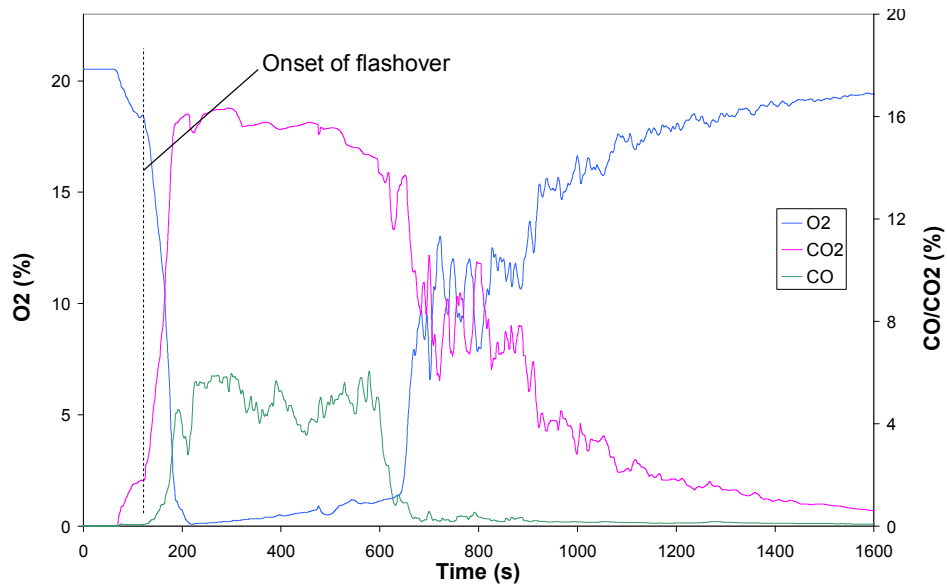


**Figure 3.20. Full-scale experiment – gas concentrations at head height**

The temperatures adjacent to the ignition location shown in Figure 3.13 exceeded tenability criteria prior to the onset of flashover at 100s. However all other thermocouple trees indicate that temperatures became rapidly exceeded the tenability criteria at the onset of flashover at times ranging from 140-150s along the carriage. Heat flux shown in Figure 3.14 also indicates that conditions rapidly became untenable within the carriage at the onset of flashover.

Time to untenable conditions for the ventilation conditions and fire growth rate tested was very rapid and coincided with the onset of flashover at 140 s. This is significant as it indicates the time which is available for a fire to be detected, the driver to respond and stop the train and the passengers (if aboard) to evacuate safely. It is

credible that the time for this response may exceed 140 s for cases where the fire is not immediately identified or the train is a significant distance away from a station.

This experiment demonstrates that it may be reasonable for engineers to consider large flashover fire scenarios that may result in fatalities. However available incident data (Section 2.1.4) suggests that large fires are most likely to occur on unoccupied carriages and are unlikely to occur on carriages with passengers. This may be strongly influenced by the opportunity for unhindered arson.<sup>[38]</sup> Due to this large consequence but low probability a risk analysis may be the best means for evaluating such scenarios.

It is noted that ventilation of the carriage will have a significant affect on tenability conditions within the carriage. Only one condition of two doors open was tested. If all doors were closed it is likely that smoke and hot toxic gases would be contained within the carriage resulting in untenable conditions occurring earlier even though there may not be sufficient ventilation for flashover to occur. However if there are passenger on board it is highly likely that doors will be opened to enable escape.

A very large quantity of smoke was observed to be produced from this fire. This demonstrated that for underground large train fires smoke production will have a critical affect on tenability of infrastructure such as underground stations and connected shopping complexes.

#### Affect on Adjacent Infrastructure

This experiment was conducted in the open air without adjacent infrastructure such as stations, underpasses and tunnels. However the following can be determined from measurements and observation.

The heat flux external to the vehicle measured at a point 6 m horizontally from Door A maintained a steady 5–6 kW/m<sup>2</sup> from 190 s to 350 s and then steadily decayed. A heat flux of 2.5 kW/m<sup>2</sup> is commonly used as the tenability limit for evacuation in a fire.<sup>[120]</sup> Exposure to a heat flux of 6 kW/m<sup>2</sup> causes pain in 8 s and blistering of the skin in 20 s but is unlikely to cause damage to surrounding

infrastructure. However as heat flux increases with proximity to fire plume some damage may be expected.

Fire plumes were observed to extend out of the open side doors rising 2.5 m above the carriage with a maximum plume diameter of 2 m for a period of 300 s. Smaller flames and convected heat rose from the broken windows and open doors for more than 1000 s. This heat was sufficient to buckle the stainless steel carriage shell above the doors. It is considered that this heat would have limited effect on open air infrastructure however it may have serious effects on covered or underground infrastructure that it would impinge upon.

As stated above, the amount of smoke produced would most likely have serious effects on tenability if contained within underground infrastructure.

It is concluded that this fire would have a much more severe effect on covered or underground infrastructure than for open air infrastructure. It is beyond the scope of this thesis to consider effects on infrastructure any further.

#### Influence of Door Openings

This experiment did not investigate the influence that the number of doors open has on the fire behaviour. The following points are identified from the literature review.

- If all doors and windows remained closed it is likely that insufficient ventilation would be available for flashover to occur
- As the number of door open increases the ventilation increases enabling flashover to occur however the radiant heat due to hot layer development may decrease resulting in a increased time to onset of flashover.
- As the number of doors open increases the fully developed HRR is expected to increase due to increased ventilation. A point may be reached where further increases in ventilation would not significantly increase HRR, the fire would become fuel controlled.

### **3.6 EXPERIMENTAL CONCLUSIONS**

The experimental observations and measurements described in this chapter have provided a basis for estimation of HRR for the full-scale fire experiment and evaluation of existing methods for estimating large train interior design fires. This analysis is presented in chapters 4 and 5 HRR.

Based on these experiments the following conclusions have been drawn:

- For the vehicle studied a crumpled newspaper ignition source of 170 kW peak HRR and 160 s burn duration located on a corner seat was required for fire spread to the entire vehicle. This is within the range of 100-300 kW found to be required to promote fire spread on a range of other metropolitan passenger trains as concluded in Section 2.5.
- Combustible panels in a closely spaced vertical arrangement are very susceptible to ignition and should be avoided in design, see Section 3.4.4. For the vehicle studied ignition sources less than 60 kW peak HRR placed between the combustible seat back and end wall panel could result in spread to the entire vehicle.
- Ignition of upper wall and ceiling linings is a critical mechanism for fire spread beyond the ignition area leading to flashover. Therefore, improved fire performance of these materials is desirable to reduce the likelihood of flashover.
- Flashover occurred in the vehicle studied. Without the onset of flashover a fire is not likely to spread to consume the entire carriage. Flashover conditions were not instantaneously achieved for all locations in the carriage; rather it took approximately 35 s to progress 10 m from the ignition point to the end of the fitted area. The onset of flashover occurred at 140 s.
- The fully developed fire duration was approximately 400 s from the onset of flashover to significant fire decay. The entire fire duration including the fire growth phase and a long fire decay phase was in excess of 1500 s. However if the carriage had been fitted with more interior materials and glazed windows for the entire length of the carriage the fire duration would have been longer, dependant upon window failure.

- The fully developed fire size was affected by ventilation with a significant portion of combustion occurring in exterior flames extending from open doors. Once a significant area of windows began to break the fully developed fire behaviour changed with more combustion occurring inside the carriage. This demonstrates the important influence of ventilation conditions on fire behaviour and HRR.
- Windows for the vehicle studied exhibited significant fire resistance typically failing when the exterior glass surface reached temperatures of 200-240 °C. Window breakage significantly affects fully developed fire behaviour by increasing ventilation to the enclosure.
- For the scenario considered, conditions in the carriage rapidly became untenable after the onset of flashover resulting in 140-150 s available safe egress time. This severely limits the time available for detection, driver response and occupant egress. Conditions may become untenable prior to flashover if all doors are closed.
- The consequence of this fully developed carriage fire occurring in covered or underground infrastructure was not investigated. Significant quantities of exterior flames and smoke were observed in the open air test and would likely result in increased consequences if contained within covered or underground infrastructure.

## **CHAPTER 4 ANALYSIS OF FULL-SCALE EXPERIMENT**

### **4.1 ANALYTICAL APPROACH**

The purpose of the following analysis is to estimate HRR for the full-scale experiment. Through this analysis an increased understanding of fire behaviour and its effect on HRR during the experiment is gained. The suitability of existing design fire estimation methods is also assessed. This analysis has been applied to the full-scale experiment described in Chapter 3.

The analysis is in two parts; application of existing design fire estimation methods and estimation of HRR applying experimental measurements and a conservation of energy model.

### **4.2 APPLICATION OF EXISTING DESIGN FIRE ESTIMATION METHODS**

Design fire estimation methods commonly applied to estimate large fully developed design fires for passenger trains have been applied to the full-scale experiment. These methods include the average HRR method, Duggan's method, and the ventilation controlled burn rate correlation. Prediction methods for the HRR required for the onset of flashover to occur have also been applied.

These estimation methods have been applied to the full-scale experiment for the following purposes:

- To obtain a first approximation of a credible fire size for the full-scale experiment.
- To investigate issues relating to input data required and assumptions implicit in the estimation methods through practical application to a real fire.
- To investigate the validity of these methods the results have been compared to an estimate of HRR for the full-scale experiment based on measurements from the experiment in Section 4.3.

### 4.2.1 Application of Average HRR method

The average HRR method is described in Section 1.4.2 of the literature review. This is represented by the following equation.

$$\dot{Q}_{ave} (MW) = \frac{\text{Burnt Fuel Load (MJ)}}{\text{Burn Duration (s)}} \quad \text{Equation 4-1}$$

#### 4.2.1.1 Burnt fuel load

Fuel load or fire load is commonly define in terms of MJ per m<sup>2</sup> of floor area and is used by fire engineers to estimate fuel controlled HRR and time temperature curves for compartments in different building types.<sup>[4,120]</sup>

In this case burnt fuel load is defined to be the total heat energy stored in the interior materials (in MJ) that was burnt. Burnt fuel load is estimated as follows.

$$\text{Burnt fuel load} = \sum_{\text{all materials}} \Delta H_{eff} \times \text{total mass} \quad \text{Equation 4-2}$$

Heat of combustion is defined as the total amount of heat released when a unit quantity of fuel is burnt.<sup>[121]</sup> Due to the various definitions of heat of combustion, different methods for measuring heat of combustion and the significant variation in quoted heats of combustion in literature the values assumed for this quantity are a potential source of error for the average HRR method. The definition and calculation of effective heat of combustion for the interior materials is presented in Appendix I. Effective heat of combustion has been calculated from cone calorimeter test data.

The total mass of materials installed in the full-scale experiment has been estimated based on the measured density or mass per unit area of cone calorimeter specimens and the measured volume or surface area of the materials installed in the full scale experiment. The combustible mass of GRP has been reduced considering that approximately 30% of the mass of GRP panels is non-combustible glass fibre (based on cone calorimeter tests).

As discussed in Section 4.2.1.3, the total mass burnt is assumed to equal the mass of fitted interior materials. The total fuel load has been calculated applying Equation 4-2 as summarized in Table 4-1.

**Table 4-1**      **Burnt fuel load for full-scale experiment**

Material	Mass (kg)	$\Delta H_{\text{eff}}$ (MJ/kg)	Fuel Load (MJ)
Carpet	146	16.7	2443
Old GRP	132	16.7	2197
New GRP	31	14.4	452
seats	184	15.6	2870
<b>Total Fuel Load (MJ)</b>			<b>7,961</b>

Kennedy, et al. estimate the fuel load for a typical subway car interior as 24,400 MJ. A metro car tested in the EUREKA project had a total internal and external fuel load of 41,300 MJ.

The calculated burnt fuel load for the full-scale experiment is significantly less than typical values from literature for two reasons:

- Total fuel load including external and non exposed combustibles is given in the literature rather than the burnt fuel load as calculated. The tested carriage had other combustibles including plywood flooring, fibre glass insulation and electrical cables. Contribution of these materials to fuel load is only considered as a sensitivity analysis.
- The carriage for the full-scale experiment was only partially (approximately 40%) fitted with lining materials and seats.

#### 4.2.1.2 Burn Duration

As discussed in Section 3.2, the flames external to the carriage for the full scale experiment reached a peak at approximately 280-320 s. Flames exterior to the carriage then reduced and combustion in the interior increased as windows and the north east door began to fail. The fire size then decayed and at 970 s flames had ceased to issue from both doors. After this point the most significant flaming combustion continued at the northern end of the carriage, between door A and the car end, on a small fraction of the originally fitted material that had not been completely burnt until this stage due to lack of ventilation. After approximately 1200 s the fire

had decayed and mainly consisted of smouldering debris on the floor of the carriage. The remaining smouldering debris was extinguished after 1600 s. From the inspection of the carriage interior after the test, it is reasonable to consider that all lining materials and seat cushions were completely consumed. Significant quantities of ply flooring and lesser quantities, in terms of mass, of binder from glass fibre insulation and cable insulation were also consumed.

For calculation of average HRR, a burn duration of 970 s has been applied to represent the duration of significant burning as indicated by elevated temperatures within the carriage and by flames out of doors. It is assumed that the fitted mass of carpet, GRP and seats was completely consumed during this period because they were directly exposed to the fire. The effect of combustion of plywood and alternative burn durations shall be considered as a sensitivity analysis.

#### 4.2.1.3 Average HRR

Dividing the calculated burnt fuel load for the test by the observed duration gives the following average HRR:

$$\text{Average HRR} = \frac{7961}{970} = 8.2 \text{ MW}$$

The contribution of plywood, glass fibre insulation and cables to the average HRR has been neglected based on the following considerations:

- The total fuel load represented by insulation (of which the binder is the only combustible) and cables is very low compared to that of GRP, carpet and seats. It is likely that some of this material, particularly in the ceiling space, burnt during the first 970 s. However the mass burnt is relatively small.
- The plywood not covered by carpet was observed to ignite and burn at door B by 270 s however most of the exposed ply was only burnt on the upper surface and not consumed to a substantial thickness due to charring. The ply covered by the carpet would have been shielded from much of the heat during the peak of the fire both by carpet and by falling debris. Some of the combustion of the ply would have occurred as smouldering between 970s and 1600 s due both to the charring/smouldering behaviour of timber<sup>[87]</sup> and the collapsed smouldering debris of other combustibles on top of the flooring during this period

As a sensitivity analysis the average HRR is estimated assuming all observed plywood was consumed over the 970 s period. From measurements and post experiment inspection the total mass of plywood observed to be consumed is estimated as 250 kg. The  $\Delta H_{eff}$  of wood is taken from literature<sup>[122]</sup> as 15 MJ/kg. Therefore the contribution of the ply to the total fuel load would be 3,750 MJ increasing the average HRR over 970 s to 12.0 MW. Thus the estimate for the quantity of ply burnt may have a significant effect on average HRR.

From 970 s to 1200 s the flaming combustion at the northern end of the carriage had decayed and the fire was reduced to smouldering and low level flaming of debris on the floors. If a burn duration of 1200 s is applied with a fuel load of 7960 MJ then the average HRR is reduced to 6.6 MW.

It is noted that the combustion efficiency in the full-scale experiment is not likely to be as high as for the cone calorimeter tests used to measure  $\Delta H_{eff}$ . This is because combustion in the cone calorimeter is on a small surface area that is well-ventilated compared to the full-scale experiment. The estimate of fuel load and therefore average HRR is directly proportional to  $\Delta H_{eff}$ .

The calculated average HRR of 8.2 MW is considered to be a lowest credible limit for a first approximation of the actual peak HRR of the full-scale experiment. This is because it is an average which is based on experimentally observed burn duration and quantities of fuel burnt.

#### 4.2.2 Application of Duggan's Method

Duggan's method<sup>[94]</sup> is described in Section 1.4.3. This method attempts to estimate the total HRR for flashover fires where the entire train interior is involved. The method consists of a summation of time dependent HRRPUA determined from the cone calorimeter multiplied by the exposed surface area for all the significant interior materials, summarised as follows:

$$\dot{Q}_{(t)} = \sum_{i=1}^n (A_i \dot{q}_{i(t)}'' ) \quad \text{Equation 4-3}$$

The time dependent HRRPUA ( $\dot{q}''_{i(t)}$ ) is measured in cone calorimeter tests conducted at irradiances of 25, 35 and 50 kW/m<sup>2</sup> that are dependent on the materials location/orientation within the train interior as detailed in Section 1.4.3.

For each material at each irradiance level, cone calorimeter tests were conducted in triplicate. Rather than average the three HRRPUA curves, which can lead to artificially low peak HRRPUA if the time to peak heat release varies, the median curve was chosen. The median curve was taken as the curve which has the median value for the peak HRRPUA, or if two or more curves have the same peak value of HRRPUA the median curve is the curve which has the median value of time to peak.

The total areas of the installed interior materials for the full-scale experiment were estimated based on measured dimensions. These material surface areas and median cone calorimeter results are summarised in Table 4-2.

**Table 4-2 Input data used for application of Duggan’s method to full-scale experiment**

Material and location	Exposed surface area (m)	Cone Calorimeter Test Irradiance (kW/m <sup>2</sup> )	Median Cone Calorimeter test	Peak HRRPUA (kW/m <sup>2</sup> )	Time of Peak HRRPUA (s)
Carpet on floor	24.2	25	576B25	212	50
Carpet on walls	11.5	35	576C35	272	35
Old GRP on walls	9.8	35	578A35	307	115
Old GRP on ceiling	17.6	50	578C50	333	60
New GRP on walls	6.9	35	578bA35	217	110
Seat cushion bases (horizontal)	10.8	25	577A25	98	40
Seat cushion backs (vertical)	10.8	35	577C35	161	30

A total HRR vs. time curve was calculated applying the above surface areas and HRRPUA curves to Equation 4-3. The total HRR curve was smoothed applying a 30 s running average to remove peaks which are resolved but close together, as recommended by Duggan.<sup>[94]</sup> The resulting total HRR curve is shown in Figure 4.1.

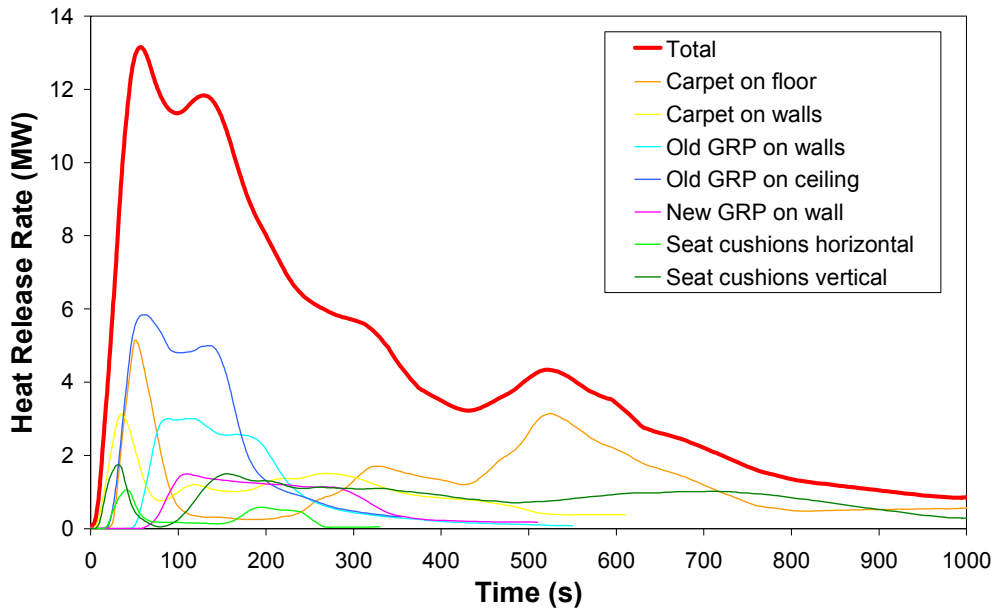


**Figure 4.1 Total HRR curve for full-scale experiment estimated applying Duggan's method**

Compared with measured temperatures and observed fire behaviour, Figure 4.1 does not represent the fire development for the full-scale experiment very well at all. Duggan's method estimates a peak HRR of 13 MW at 60 s for the full scale experiment. This demonstrates how Duggan's method neglects the pre-flashover growth phase of the full-scale fire experiment. For the experiment the onset of flashover was observed at 140 s and the peak external fire size was observed at 280-320 s. However Duggan's method assumes that the onset of flashover begins instantaneously and predicts a peak fire size at 60-140 s. Also, the HRR curve in Figure 4.1 begins to decay at 150-200 s. This is much earlier than full-scale experiment where combustion at door A starts to decay at about 400-450 s based on measured temperatures and observation. Even if Duggan's method was applied with an assumed delay of 140 s (to account for pre flashover time) the duration of peak burning predicted by Duggan's method is still significantly shorter than observed for the real fire.

Time to peak HRRPUA of the median cone calorimeter data for each material has a critical affect on the Duggan's method estimate. For this application of Duggan's method the peak HRRPUA determined from cone calorimeter tests occurs at fairly consistent times for all materials resulting in the summed HRR having a single high peak. However, if there was a more significant spread of times to peak HRRPUA of

individual materials then the resulting summed HRR would have a lower peak and may consist of several smaller peaks. This demonstrates how Duggan's method neglects the complex interaction between materials in an enclosure fire. This interaction is primarily driven by the feedback of heat to materials from all burning materials in the enclosure.

Measured heat flux at floor level in the large-scale fire experiment exhibited peaks of the order of 100-140 kW/m<sup>2</sup> demonstrating heat flux received by interior materials was significantly higher than those applied by Duggan. For free burning, ignition time decreases and peak HRRPUA increases with heat flux exposure. If Duggan's method was applied to cone calorimeter data at irradiance levels of the order of 100 kW/m<sup>2</sup> then the higher peak HRRPUA and higher consistency in timing of these peaks would result in a higher total HRR. It is also noted that Duggan's method applied cone calorimeter data for seat cushions tested at an irradiance of 25 kW/m<sup>2</sup>. At this irradiance the seat foam was not completely burnt due to shielding by the charred wool liner. In the full scale experiment all seats were fully consumed indicating that the heat fluxes applied in Duggan's method are low.

It is evident from observation of the flames out of the doors and choked internal combustion for a period prior to significant window failure in the experiment that ventilation conditions had an effect in reducing the peak HRR during this period. Duggan's method assumes well ventilated combustion. Therefore the Duggan's method estimate of peak HRR is likely to be an overestimate for this ventilation affected period.

Although Duggan's method neglects several significant fire dynamics effects observed in the experiment and does not produce a HRR curve that represents actual fire development, the estimated peak HRR of 13 MW may be considered a credible upper limit for a first approximation of peak HRR for the experiment. This estimate is considered conservative for the following reasons:

- Time of peak HRRPUA for individual materials are similar.
- Duggan's method neglects pre flashover fire growth and post flashover ventilation effects.

### 4.2.3 Application of Methods to Predict Flashover

Empirical correlations relating ventilation factor and the size of an enclosure to the HRR required for the onset of flashover ( $\dot{Q}_{FO}$ ) to occur were discussed in Section 2.4.2. The Babrauskas, Thomas, and McCaffrey correlations for predicting flashover<sup>[88]</sup> have been applied to the carriage used in the full-scale experiment for a range of ventilation factors, shown in Figure 4.2. These correlations have been developed based on enclosure tests lined with materials such as gypsum plasterboard. The walls roof and floor of the train carriage tested was insulated with glass fibre insulation, 100 mm thick with a typical effective heat transfer coefficient of  $h_k = 8 \times 10^{-4}$  kW/m $\cdot$ K.<sup>[123]</sup> Gypsum plasterboard 16 mm thick has an effective heat transfer coefficient of  $h_k = 0.03$  kW/m $\cdot$ K. These two heat transfer coefficients have been applied to the McCaffrey correlation.

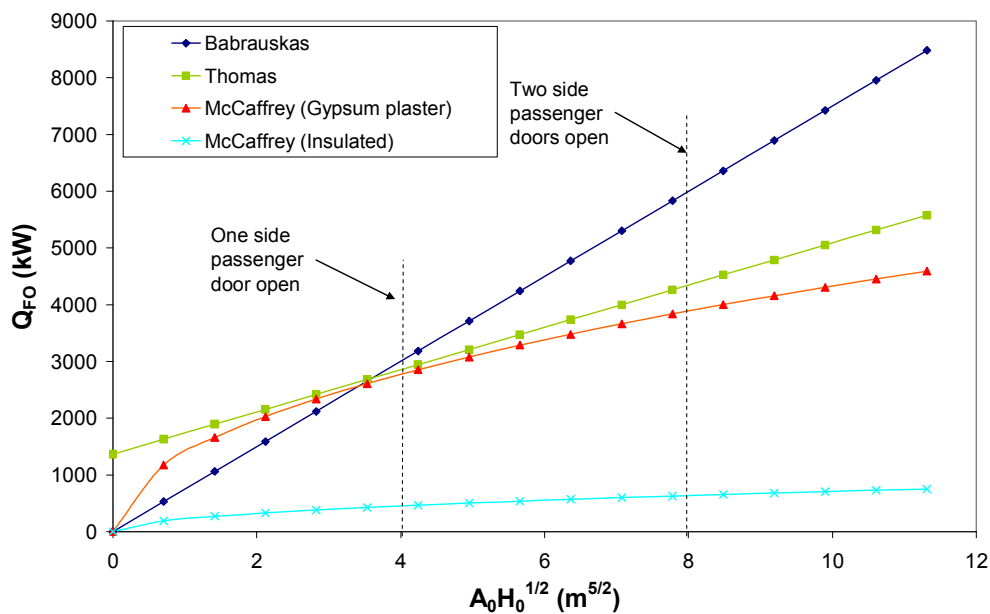


**Figure 4.2. Predicted HRR required for flashover of full scale experiment**

Figure 4.2 demonstrates that the McCaffrey correlation is very sensitive to the heat transfer coefficient assumed reducing the estimate of  $\dot{Q}_{FO}$  with 2 doors open from 4-6MW to less than 1 MW.

As discussed in the literature review, these correlations have been empirically developed from tests in small room enclosures with non-combustible linings using isolated fuels such as timber cribs and determining onset of flashover by ignition of

combustible newspaper targets on the floor. In these experiments flashover was the result of elevated hot layer temperatures caused by a confined (non-spreading) fire.

For a train carriage with combustible wall and ceiling linings, fire spread on these linings is a critical step to flashover.<sup>[52,124]</sup> The ignition source HRR required to promote fire spread on the wall and ceiling linings beyond the ignition area and continued growth to flashover is the critical quantity leading to flashover, not  $Q_{FO}$  as determined with the inherent assumptions of these correlations.

#### 4.2.4 Application of Correlation for Ventilation Controlled Burning Rate.

A correlation for ventilation controlled HRR<sup>[87,96]</sup> was discussed in Section 2.4.5 and may be expressed as:

$$\dot{Q}_{VentilationControlled} \approx 1500 A_0 \sqrt{H_0} \quad \text{Equation 4-4}$$

The ventilation controlled HRR vs. ventilation factor has been plotted applying this correlation for the carriage tested, see Figure 4.3.

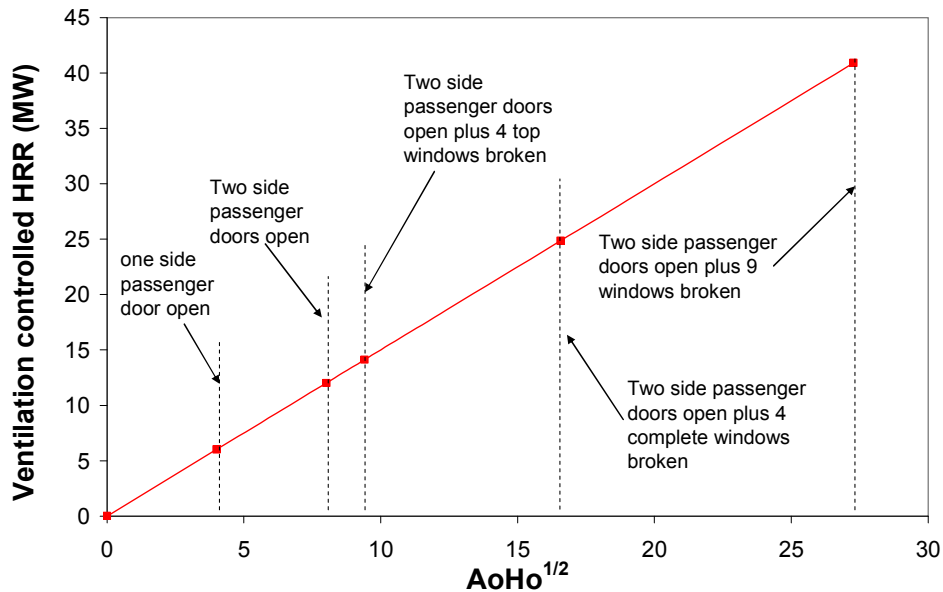


Figure 4.3 Ventilation controlled HRR vs. ventilation factor

During the period of observed peak flames external to the carriage and choked combustion inside the carriage (270–380 s) two side doors were open and the top sections of 4 windows had broken giving a total opening area of 6.7m<sup>2</sup> and a

ventilation factor of  $9.4 \text{ m}^{3/2}$ . Equation 4-4 predicts a ventilation controlled HRR of 12.0 MW for this ventilation factor. From 400-500s 4 windows were observed to be completely broken resulting in observed reduced external flames and increased combustion inside the carriage. During this period the ventilation factor was  $16.6 \text{ m}^{3/2}$  and Equation 4-4 predicts a ventilation controlled HRR of 24.9 MW. From 500 s onwards decay in fire size was observed due to burn out of the fuel.

Equation 4-4 assumes that burning is stoichiometric and only the air entering the compartment is available for combustion which reduces to the intrinsic assumption that all combustion is occurring within the enclosure.

This is at odds with the ventilation effects observed in the full-scale experiment. During the period 280-320 s a large portion of the combustion was occurring in fire plumes outside both doors A and B. Measurements of heat flux at floor level and temperatures inside the carriage are given in Figure 4.4, Figure 4.5 and Figure 4.6. These figures demonstrate the heat flux and temperature inside the carriage peaked at the time of flashover in the different areas of the carriage and that shortly after flashover, heat flux and temperature inside the carriage reduced and did not peak again until flaming out of the doors reduced at about 400 s. This is the time when ventilation of the carriage was increased by the increased failure of window glazing and the partial failure of plasterboard blocking the passenger door on the north east side.

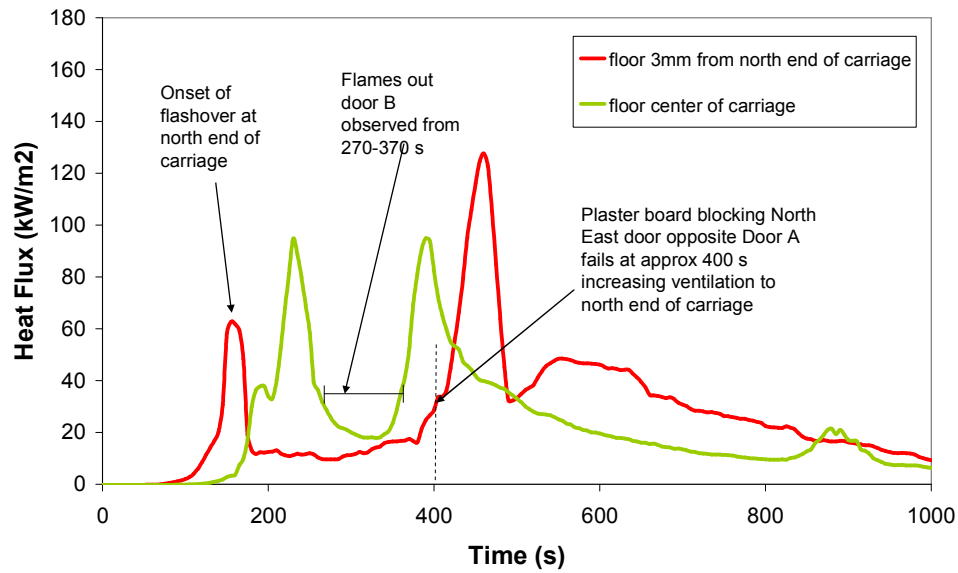


Figure 4.4 Heat flux measurements showing reduction of heat flux inside carriage during periods of flames occurring out doors

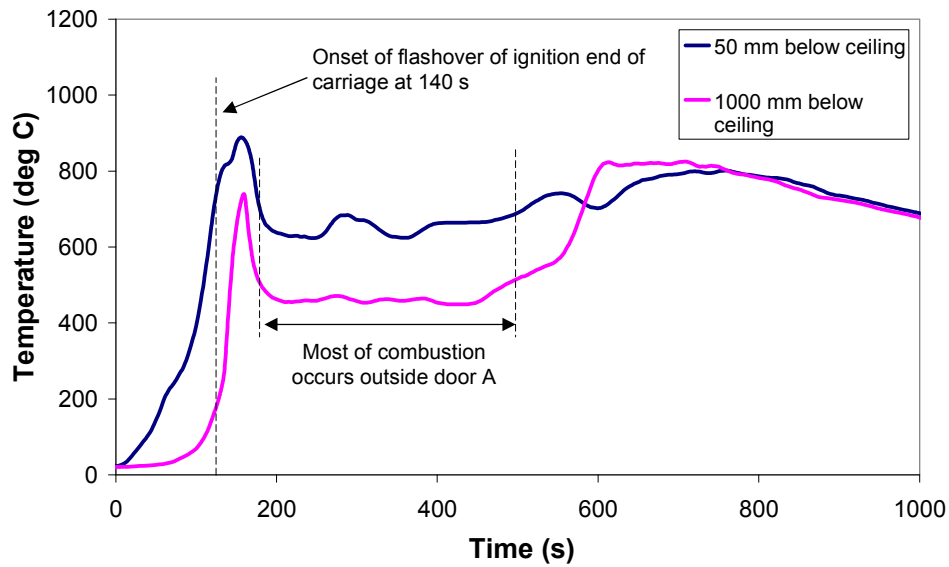
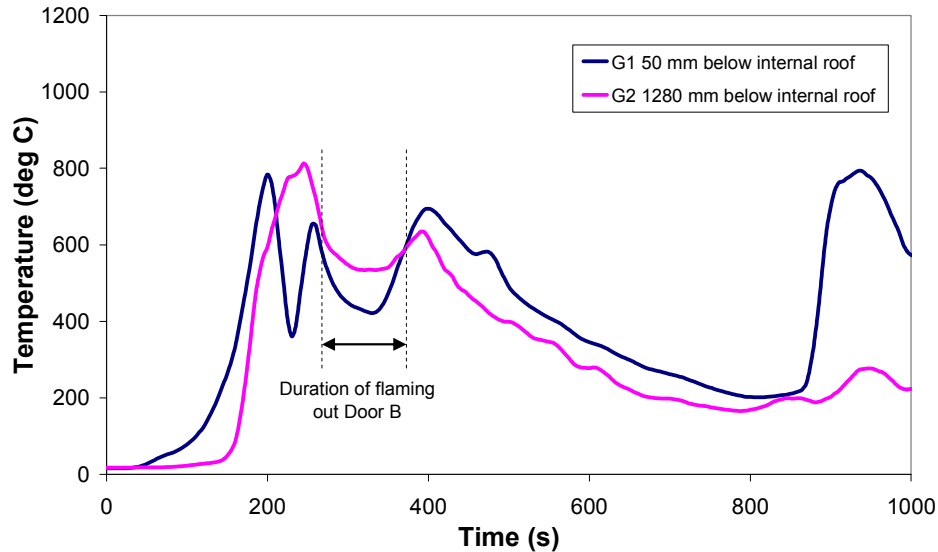


Figure 4.5 Interior gas temperatures at TC Tree A (north end) showing reduction in interior temperatures during period of large flames occurring out door A



**Figure 4.6 Interior gas temperatures at TC Tree G (middle of carriage) showing reduction in interior temperatures during period of flaming out door B**

This suggests that post flashover there was not sufficient ventilation inside the carriage to support complete combustion of all pyrolysed fuel and that combustion inside the carriage was partially choked and reduced. Much of the pyrolysed fuel burnt outside the doors where there was sufficient oxygen. This choking of combustion inside the carriage resulted in the reduction in interior heat flux and temperatures and would have had a controlling effect on the rate of pyrolysis for materials inside the carriage. Observations indicate that when the ventilation was significantly increased by failure of windows and plasterboard, flaming out of the doors reduced but increased inside the carriage. This resulted in a second peak of interior heat flux and temperature. It is not clear from observations and experimental results if the maximum burning rate during the period from 400-500 s was limited by ventilation conditions. The observations of reduced external flames and the short period of 400-500 prior to obvious observations of fire decay suggest insufficient fuel may have existed at this time to achieve a fully ventilation controlled burning condition. Similar ventilation effects have been observed by Thomas for experiments on long slender enclosures with limited ventilation.<sup>[125]</sup>

### 4.2.5 Preliminary Estimate of Full-Scale Experiment Peak HRR

The results from application of existing design fire estimation methods are summarised in Table 4-3.

**Table 4-3 Design fire estimation methods applied to full-scale experiment**

<b>Design fire estimation method</b>	<b>Result</b>
Average HRR method	Average HRR = 8.2 MW over 970 burn duration
Duggan's method	Peak HRR of 13 MW
Ventilation controlled correlation	Peak HRR of 12 MW (prior to significant window breakage)
	Peak HRR of 25 MW (after significant window breakage)

Based on the application of existing design fire estimation methods a preliminary estimate of peak HRR for the full-scale experiment is 8-13 MW. The estimate for ventilation controlled HRR of 25 kW is discarded as it is unlikely that sufficient fuel was available to support this HRR at the time increased ventilation conditions occurred. The estimation methods used have been demonstrated to be based on simplified assumptions which neglect significant fire dynamics observed in the full-scale experiment. None of these methods successfully estimate the duration of the fully developed fire.

### 4.3 CONSERVATION OF ENERGY MODEL

A model has been developed to estimate HRR for the full-scale experiment based on experimental measurements and observations. This model is based on the principles of conservation of energy and conservation of mass. The model presented applies fire dynamics concepts and models that are well described in key fire science texts such as Karlsson and Quintierre,<sup>[5]</sup> Drysdale,<sup>[87]</sup> Milke and Klote<sup>[6]</sup> and the SFPE handbook.<sup>[126]</sup>

#### 4.3.1 Conservation of Energy Model Framework

Flow of energy and mass for the carriage fire is summarised in a simplified diagram considering a control volume defined by the carriage boundary, see Figure 4.7.

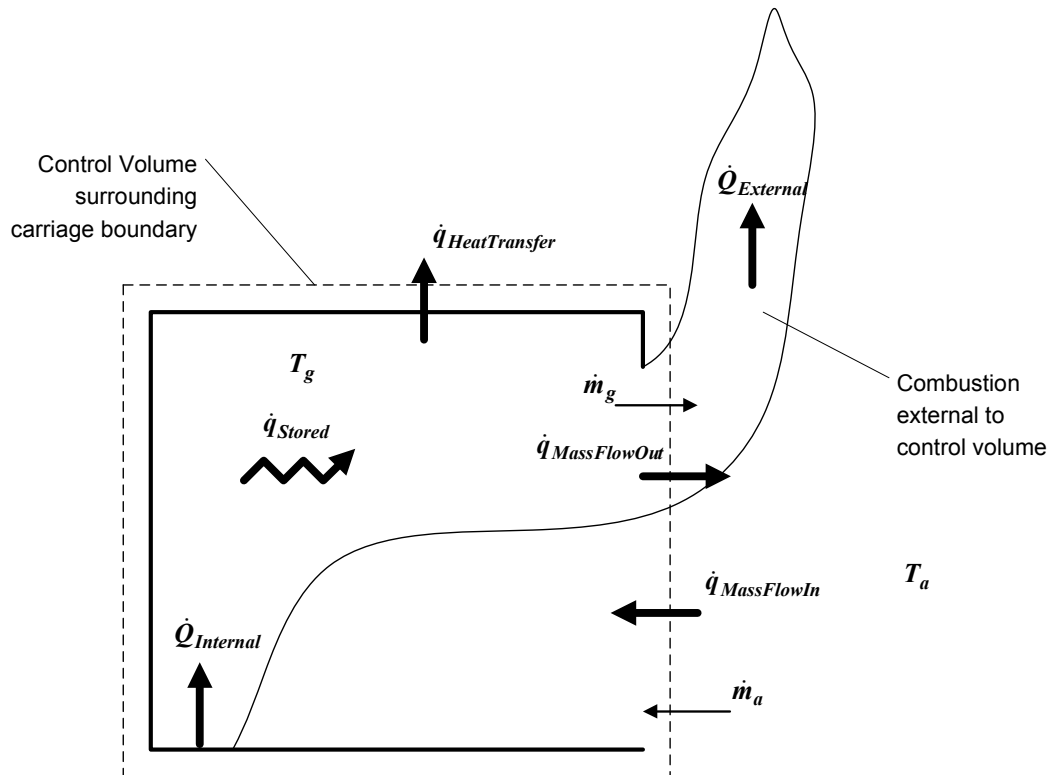


Figure 4.7. Model of energy and mass flow for full-scale experiment

Applying conservation of energy, the heat flows identified within the control volume and between the control volume and its surroundings in Figure 4.7 are related to the HRR of combustion occurring inside the control volume ( $\dot{Q}_{Internal}$ ) as follows:

$$\dot{Q}_{Internal} = \dot{q}_{Stored} + \dot{q}_{HeatTransfer} + \dot{q}_{MassFlowOut} - \dot{q}_{MassFlowIn} \quad \text{Equation 4-5}$$

Considering conservation of mass, mass flow out of the control volume is assumed to equal the total mass flow in:

$$\dot{m}_g = \dot{m}_a \quad \text{Equation 4-6}$$

A significant amount of heat release also occurred exterior to the control volume due to combustion in external flames. The total HRR is the sum of the interior and exterior HRR:

$$\dot{Q} = \dot{Q}_{Internal} + \dot{Q}_{External} \quad \text{Equation 4-7}$$

Transfer of energy from the exterior combustion to the interior of the control volume is neglected. The two zone or well mixed assumptions for gas temperatures are not applied. Instead, the distribution of temperatures measured within the carriage is applied. Each component of heat flow identified above is detailed in the following sections.

### 4.3.2 Energy Stored

The rate of heat energy storage within a given control volume of gas, CV, may be expressed as the following integral bounded by the control volume:<sup>[127]</sup>

$$\dot{q}_{stored} = \frac{d}{dt} \int_{cv} mc_p dT \quad \text{Equation 4-8}$$

Equation 4-8 may be numerically integrated by dividing the control volume into a finite number ( $n$ ) of smaller volumes and applying the following summation:

$$\dot{q}_{stored} = \sum_{i=1}^n V_i \rho_i c_p \frac{\Delta T_i}{\Delta t} \quad \text{Equation 4-9}$$

The interior volume of the carriage was divided into a grid of 45 smaller volumes, one for each internal thermocouple located on trees along the centre line of the carriage. Each thermocouple was located approximately at the centre of each volume. Specific heat capacity ( $c_p$ ) for both combustion gas and air is taken be 1.0 kJ/kg.K<sup>[123]</sup> as combustion gas will mostly consist of entrained air.<sup>[6]</sup> Although  $c_p$  increases slightly with gas temperature, the error in assuming constant  $c_p$  is negligible compared with temperature measurement errors and the assumption of uniform temperatures within

finite volumes. Density can be calculated from temperature and pressure applying the ideal gas law, defined as:

$$PM = \rho RT \quad \text{Equation 4-10}$$

Where  $P$  is pressure,  $M$  is molecular weight of gas,  $R$  is ideal gas constant  $\approx 8.314 \text{ J/(K mol)}$  and  $T$  is temperature in degrees Kelvin. As changes in pressure due to thermal expansion are small for a fire enclosure with openings, the value of standard atmospheric pressure,  $101.3 \times 10^3 \text{ Pa}$  is applied. The molecular weight of air,  $0.0289 \text{ kg/mol}$  is applied for both air and combustion gases. For these values the ideal gas law may be expressed as:

$$\rho = \frac{353}{T} \quad \text{Equation 4-11}$$

Equation 4-9 was applied for each 5s time step of temperature measurement data to produce an estimate of the rate of heat energy stored in gas within the carriage, as shown in Figure 4.8.

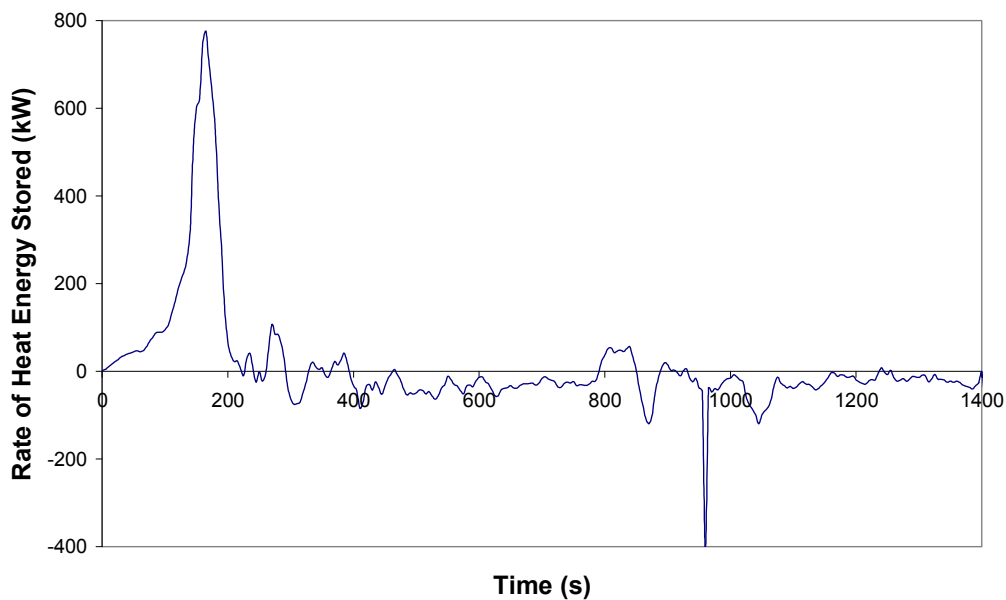


**Figure 4.8.** Rate of heat energy stored in gas within the carriage.

It is noted that energy storage is only significant during the period of rapid fire growth up to 200 s. Sources of uncertainty for this estimate are discussed in Section 4.3.6.

### 4.3.3 Heat Transfer through Bounding Surfaces

#### 4.3.3.1 Heat transfer through walls and roof

Heat transfer through the solid area of walls and the roof is considered. Heat transfer through the floor is neglected. The floor consisted of a sheet stainless steel exterior body, 100 mm thick glass fibre insulation bats and 16 mm thick plywood floor covered with carpet. The floor was well insulated and this insulation was observed to be maintained throughout the test therefore only a negligible amount of heat is expected to be transferred through the floor.

The heat transfer into the bounding surface from the interior flame and hot gas is by convection and radiation. Heat transfer from the inside surface to the outside surface is by conduction. Heat transfer from the outside surface to the ambient environment is by convection and radiation. For simplicity the heat transfer is assumed to be one dimensional and steady state. In reality the heat transfer would not be steady state due to thermal storage in the boundary materials. The significance of the steady state assumption is investigated in the discussion of conduction.

This heat transfer system is represented by a thermal circuit consisting of series and parallel thermal resistances shown in Figure 4.9.<sup>[123]</sup>

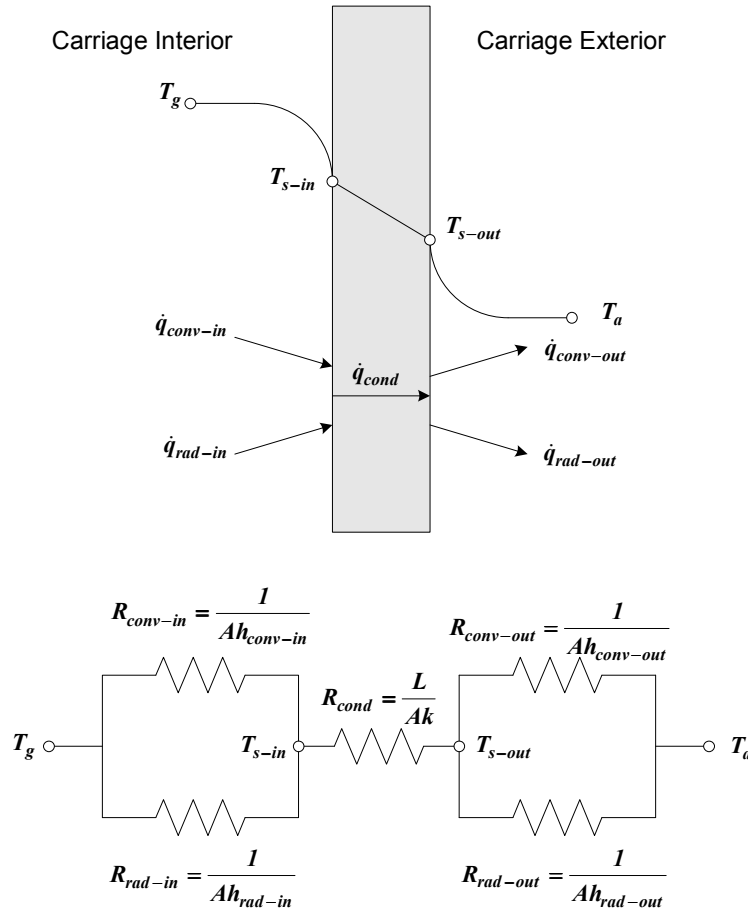


**Figure 4.9. Thermal circuit for one dimensional, steady state heat transfer through walls and roof**

Applying conservation of energy the total heat transfer rate can be expressed as:

$$\dot{q}_{HeatTransfer} = \dot{q}_{conv-in} + \dot{q}_{rad-in} = \dot{q}_{cond} = \dot{q}_{conv-out} + \dot{q}_{rad-out} \quad \text{Equation 4-12}$$

Where:

$$\begin{aligned} \dot{q}_{conv-in} + \dot{q}_{rad-in} &= A(h_{conv-in} + h_{rad-in})(T_g - T_{s-in}) \\ \dot{q}_{cond} &= \frac{Ak}{L}(T_{s-in} - T_{s-out}) \end{aligned} \quad \text{Equation 4-13}$$

$$\dot{q}_{conv-out} + \dot{q}_{rad-out} = A(h_{conv-out} + h_{rad-out})(T_{s-out} - T_a)$$

Alternatively, applying an electrical circuit analogy, the total heat transfer rate may be expressed as a function of the overall temperature difference as follows:

$$\dot{q}_{HeatTransfer} = \frac{T_g - T_a}{R_{tot}} \quad \text{Equation 4-14}$$

$$R_{tot} = \frac{1}{A} \left( \frac{1}{h_{conv-in} + h_{rad-in}} + \frac{L}{k} + \frac{1}{h_{conv-out} + h_{rad-out}} \right) \quad \text{Equation 4-15}$$

## Convection

The rate equation for convection is:

$$\dot{q}_{conv} = Ah_{conv}(T_s - T_a) \quad \text{Equation 4-16}$$

Most natural fire and flows associated with fire are in the domain of free convection.<sup>[5]</sup> For free convection of gases the heat transfer coefficient is typically in the range 2-25 W/m<sup>2</sup>K.<sup>[123]</sup> Heat transfer coefficients for free convection may be estimated using empirical correlations that relate Nusselt number as a function of Rayleigh number. Heat transfer coefficient for convection ( $h_{conv}$ ) is dependent on surface orientation, characteristic length of the surface and the temperature difference between the surface and the gas. Applying such correlations for fire enclosure temperatures of 800-1000 °C demonstrates that  $h_{conv-in}$  is typically of the order of 10 W/m<sup>2</sup>K for fire enclosures. The heat transfer coefficient for convection in a fire enclosure is typically an order of magnitude less than that for radiation. Therefore accurate estimation of  $h_{conv-in}$  is not critical and 10 W/m<sup>2</sup>K is assumed.

The exterior of the carriage was exposed to a moderate wind. Given that the wind speed was not measured it is not possible to accurately estimate  $h_{conv-out}$  and it is simply assumed as 5 W/m<sup>2</sup>K which is typical for a 5-10 m/s turbulent parallel flow on a 2 m long plate.

## Radiation

The net rate of radiant heat exchange between a surface and its surroundings is:

$$\dot{q}_{rad} = A\varepsilon\sigma(T_s^4 - T_a^4) \quad \text{Equation 4-17}$$

Equation 4-17 is used to represent radiant heat transfer from the outside surface of the carriage to the surrounding atmosphere. It is convenient to express the above equation in the following linearized form:

$$\dot{q}_{rad-out} = Ah_{rad-out}(T_{s-out} - T_a) \quad \text{Equation 4-18}$$

Where the radiant heat transfer coefficient,  $h_{rad}$  is:

$$h_{rad-out} = \varepsilon\sigma(T_{s-out} + T_a)(T_{s-out}^2 + T_a^2) \quad \text{Equation 4-19}$$

The emissivity of polished stainless steel can be less than 0.20. However emissivity for lightly to highly oxidized stainless steel is typically in the range 0.3-0.7.<sup>[123]</sup> Considering the carriage exterior was oxidised and dirty an emissivity of 0.7 is assumed for the external surface.

Radiant heat transfer between the carriage interior surface and the hot gas and smoke it contains is represented by the following simplified equation.<sup>[128]</sup>

$$\dot{q}_{rad-in} = \frac{A\sigma(T_g^4 - T_{s-in}^4)}{\frac{1}{\varepsilon_g} + \frac{1}{\varepsilon_s} - 1} \quad \text{Equation 4-20}$$

Where  $\varepsilon_g$  is the emissivity of the enclosure gas (flames and smoke) and  $\varepsilon_s$  is the emissivity of the interior surface of the carriage. The post experiment inspection revealed the majority of the interior of the carriage became soot covered. It is therefore reasonable to assume  $\varepsilon_s \approx 1$ . For convenience Equation 4-20 is expressed as:

$$\dot{q}_{rad-in} = Ah_{rad-in}(T_g - T_{s-in}) \quad \text{Equation 4-21}$$

Where:

$$h_{rad-in} = \varepsilon_g\sigma(T_g + T_{s-in})(T_g^2 + T_{s-in}^2) \quad \text{Equation 4-22}$$

Emissivity of the enclosure gas can be estimated from the following correlation:

$$\varepsilon_g = 1 - e^{-\kappa H} \quad \text{Equation 4-23}$$

Where H is a characteristic dimension of the enclosure, typically height, and the absorption coefficient  $\kappa$ , can range from 0.4 to 1.2 m<sup>-1</sup> for typical flames. Typically,  $\varepsilon_g$  ranges from 0.6 for small experimental enclosures up to 1 for realistic fires greater than a critical path length nominally 1 to 2 m.<sup>[5]</sup> For these calculations an emissivity of 1 shall be assumed.

Assuming  $T_g = 1000$  K and  $T_s = 500$  K, then  $h_{rad-in} = 106$  W/m<sup>2</sup>K. This demonstrates that the heat transfer by radiation was an order of magnitude greater than by convection ( $h_{conv} = 10$  W/m<sup>2</sup>K) to the interior surfaces. Because of the strong dependence on temperature, values for radiant heat transfer coefficients have been calculated for each time step of the experiment applying calculated surface temperatures.

### Conduction

The rate equation for heat transfer by one dimensional, steady state conduction is:

$$\dot{q}_{cond} = A \frac{k}{L} (T_{s-in} - T_{s-out}) \quad \text{Equation 4-24}$$

The walls and roof of the carriage were a composite of materials consisting of 3 mm thick GRP, 100 mm thick glass fibre insulation and stainless steel body approximately 1-2 mm thick. The insulating properties of the glass fibre insulation will dominate the conductive heat transfer for in-tact sections of wall and roof and it is reasonable to simply assume the wall has the conductive properties of 100 mm thick glass fibre insulation for areas where the insulation remained in-tact. Glass fibre insulation has a typical thermal conductivity of 0.04 W/mK at 310 K and 0.08 W/mK at 530 K.<sup>[123]</sup> For these calculations a constant thermal conductivity of 0.08 is assumed.

Examination of the carriage revealed that for some sections of the interior, particularly the ceiling, GRP and glass fibre insulation had been consumed and fallen away exposing the stainless steel body. The thermal conductivity of stainless steel is typically 15 W/mK at 300K, 20 W/mK at 600 K and 25 W/mK at 1000K.<sup>[123]</sup> In these areas a constant thermal conductivity of 20 W/mK and 2 mm thickness has been assumed. This significantly increases the rate of conduction by many orders of magnitude in these areas.

In reality conduction would have been transient due to the changing boundary conditions resulting from the fire growth and decay. Solving for transient conduction is difficult and requires application of a finite difference solution. The specific heat capacity and density of glass fibre insulation is very low and therefore the affects of

thermal storage on conduction are small. The specific heat and density of stainless steel are high however its thermal conductivity is high and its thickness is small, reducing the affects of thermal storage. Considering errors relating to estimation of material thermal properties and the exact coverage of insulation during the test, the assumption of steady state heat transfer is considered reasonable for the purpose of simplicity and Equation 4-24 is applied.

Based on the observed remaining coverage of insulation at the end of the experiment the walls and ceilings up to 10 m from the north end of the carriage were assumed to have thermal conductivity equivalent to 2 mm stainless steel. Walls and roof beyond 10 m were assumed to have thermal conductivity equivalent to 100mm glass fibre insulation. The sensitivity of estimated total heat transfer to the assumed insulation coverage is discussed in Section 4.3.3.3; however it was not possible to reasonably estimate the progressive destruction of insulation during the experiment.

#### 4.3.3.2 Heat transfer through glazed and open doors and windows

Other than energy transfer by mass flow (described in Section 4.3.4) another mode of heat transfer through glazed and open doors and windows is radiant heat transfer. For the double glazed windows radiant heat transfer would be much more significant than conduction, which has been neglected. Radiant heat transfer through these openings has been calculated applying the following equation:

$$\dot{q}_{rad} = A \tau \sigma (T_g^4 - T_a^4) \quad \text{Equation 4-25}$$

Where  $\tau$  is the transmissivity through the opening. Float glass has a transmissivity of 0.79.<sup>[123]</sup> In the experiment the majority of the window area was double glazed, reducing the transmissivity. The inside surface of the glass also became coated with soot which would further reduce transmissivity. In the case of doors and windows with broken glass the presence of out flowing combustion gas, soot and flame would block transmission of some radiant heat. As it is not possible to accurately calculate the transmissivity for each of these cases, an estimate of 0.7 is assumed for both glass and open windows and doors. The estimate of heat transfer through glazed and open doors and windows is directly proportional to the  $\tau$  value assumed.

#### 4.3.3.3 Procedure for calculation of total heat transfer through bounding surfaces.

As for the calculation of energy stored, the interior of the carriage was divided into 45 smaller volumes, one volume for each internal thermocouple located on trees along the centre line of the carriage. Each thermocouple was located approximately at the centre of each volume. Each volume contained a portion of the total carriage boundary area. For each volume the following calculation procedure was applied:

- The boundary surface area consisting of walls and ceiling, and boundary surface area consisting of windows and doors was calculated.
- $T_a$  was assumed to be constant at 20 °C. For  $t = 0$  it was assumed  $T_{s-in} = T_{s-out} = T_g = 20$  °C.
- For each time step  $h_{rad-in}$  and  $h_{rad-out}$  was calculated applying Equation 4-19 and Equation 4-22.
- To calculate  $h_{rad-in}$  and  $h_{rad-out}$  for each time step  $T_{s-in}$  and  $T_{s-out}$  must be estimated. The total heat transfer rate and the radiant heat transfer coefficients for the previous time step are applied to estimate the surface temperatures for the next time step applying the following:

$$T_{s-in}(t=i) = T_g(t=i) - \frac{\dot{q}_{HeatTransfer}(t=i-1)}{A(h_{rad-in}(t=i-1) + h_{conv-in})} \quad \text{Equation 4-26}$$

$$T_{s-out}(t=i) = \frac{\frac{k}{L}T_{s-in}(t=i) + T_a(h_{conv-out} + h_{rad-out}(t=i-1))}{h_{conv-out} + h_{rad-out}(t=i-1) + \frac{k}{L}} \quad \text{Equation 4-27}$$

- The heat transfer rate through the body (solid walls and roof) and the heat transfer rate for the openings (windows and doors) for each time step is calculated applying Equation 4-14 and Equation 4-25.

The heat transfer rates for each volume are summed to give the total heat transfer rate curve shown in Figure 4.10.

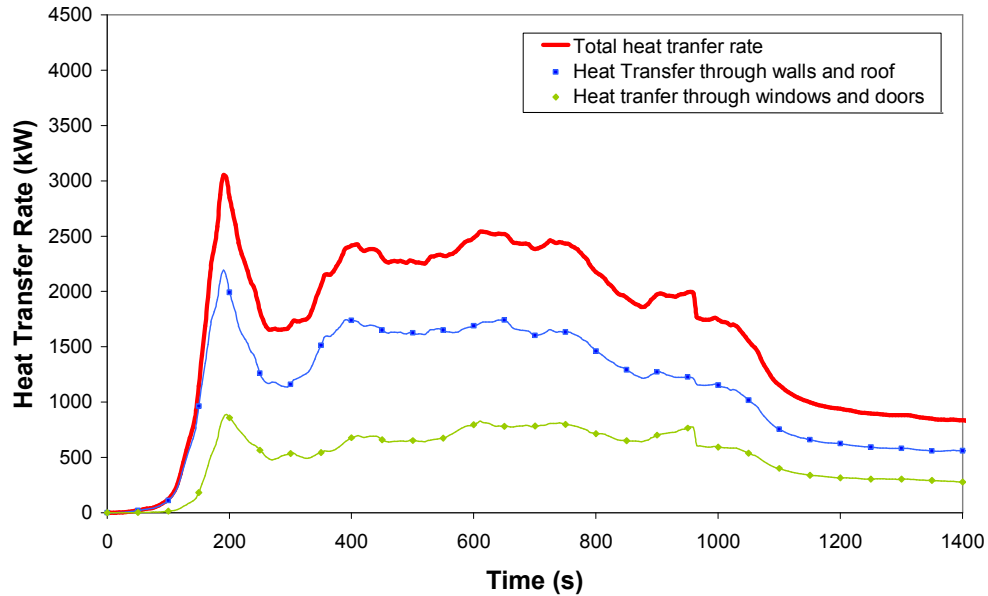


**Figure 4.10. Total heat transfer assuming partial destruction of wall and ceiling insulation**

An initial peak heat transfer rate of 3.0 MW with a second peak heat transfer rate of 2.5 MW is estimated. The decrease in heat transfer rate between the two peaks corresponds to the period where large flames extended outside the doors and combustion inside the carriage was partially choked.

The estimate of heat transfer rate through windows and doors is directly proportional to the transmissivity assumed and the estimate of heat transfer rate through walls and roof is very sensitive to the thermal conductivity assumed. Figure 4.11 demonstrates the case assuming thermal conductivity of 2 mm stainless steel for all walls and roof. Figure 4.12 demonstrates the case assuming thermal conductivity of 100 mm glass fibre insulation for all walls and roof. Destruction of the wall and roof insulation was not instantaneous but was the result of fire exposure over duration. It is possible that much of the insulation may have still been in place during the early part of the experiment, reducing the initial heat transfer significantly from the above estimate. However, as the time of destruction of insulation cannot be determined the above estimate is used.

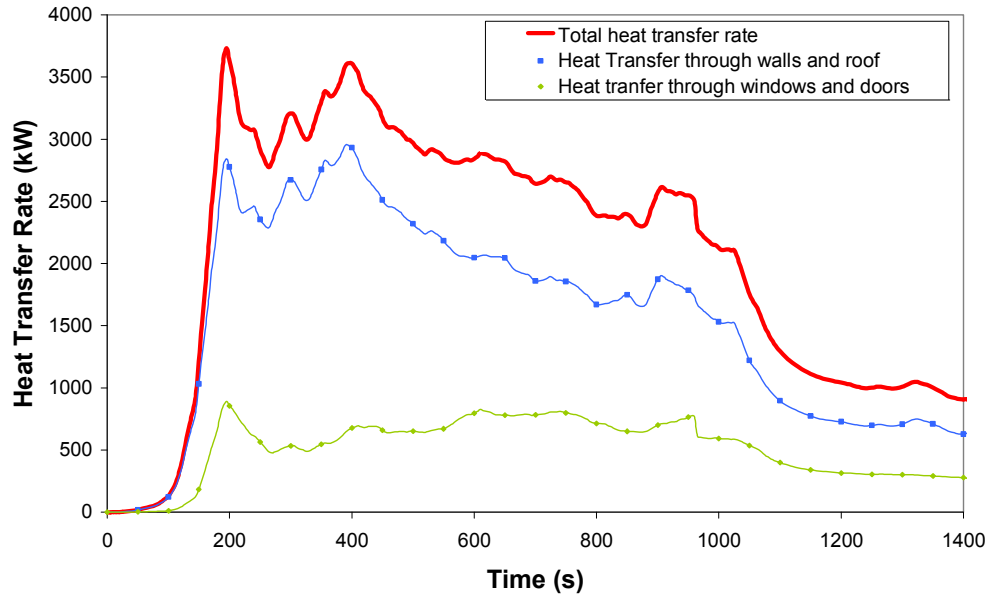


Figure 4.11. Total heat transfer assuming thermal conductivity of 2mm stainless steel for all walls and roof.

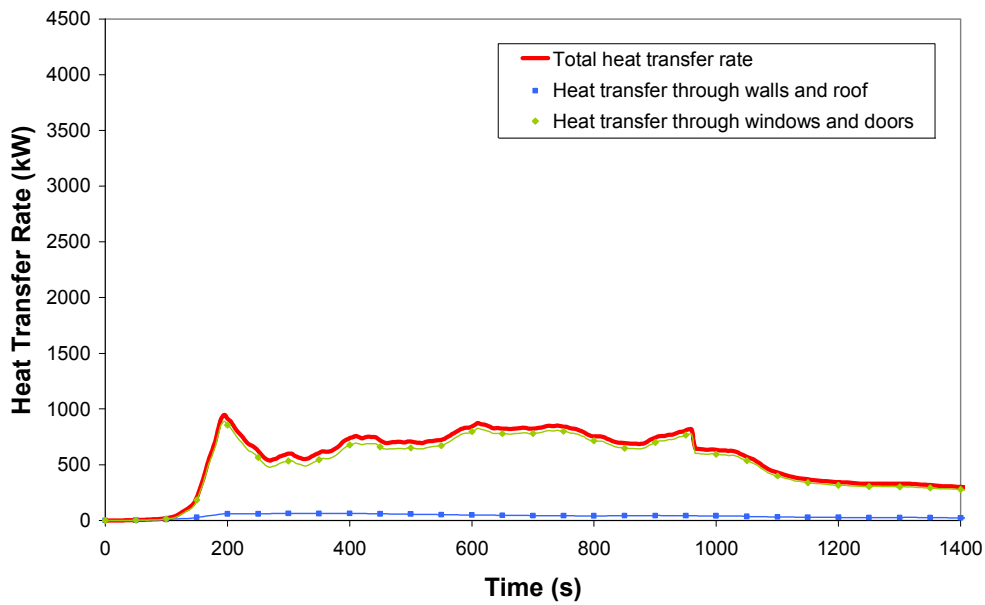


Figure 4.12. Total heat transfer assuming thermal conductivity of 100 mm glass fibre insulation for all walls and roof

### 4.3.4 Vent Mass Flow Energy Transfer

#### 4.3.4.1 General equations for vent mass flow energy transfer.

In fire enclosures it is usually the difference in temperature, and therefore densities, between inside and outside air that causes air flow in and out of a vent in the enclosure. This flow phenomenon is known as buoyancy or stack effect.

Hydrostatic pressure is defined as gravitational pressure due to a column of fluid of a given height and density, as follows:

$$\Delta P = h\rho g \qquad \text{Equation 4-28}$$

Buoyancy induced flow is due to a difference in hydrostatic pressure. The hydrostatic pressure profiles for hot air inside an enclosure and cold air outside an enclosure can be represented diagrammatically as shown in Figure 4.13 and Figure 4.14. A positive pressure difference at the top of the vent causes air to flow out and a negative pressure difference at the bottom of the vent causes air to flow in.

The pressure profiles of the air inside the enclosure and the air outside the enclosure will be equal at a certain height called the neutral plane height. At this height the pressure differences are zero and there is no net flow into or out of the enclosure. The neutral plane can lie anywhere between the top and bottom of the vent and is dependent on both the internal and external pressure profiles and gas flow at any other vents in the enclosure.

Fire enclosure gas conditions and hydrostatic pressure profiles at vents are commonly represented as either a simplified two-zone case or well mixed case as shown in Figure 4.13 and Figure 4.14.

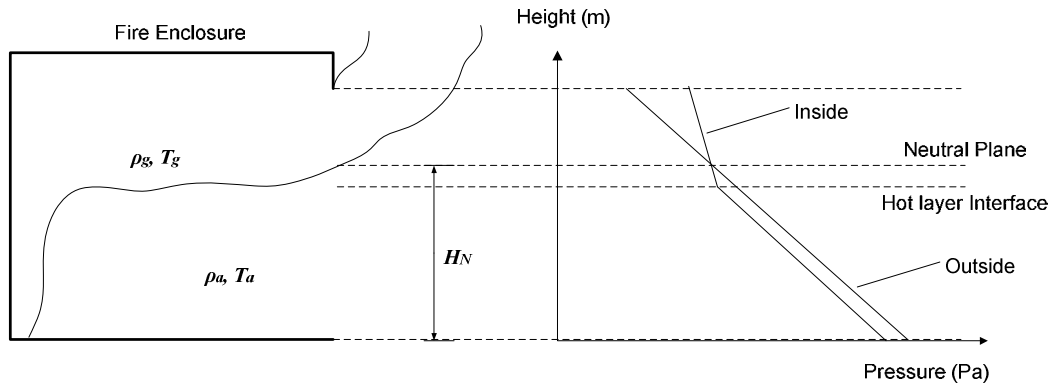


Figure 4.13 Enclosure fire two zone case

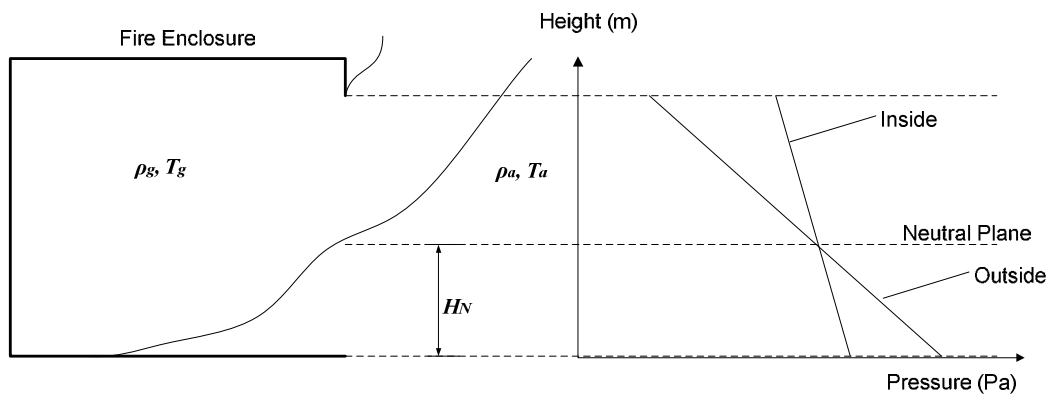


Figure 4.14 Enclosure fire well mixed case

The two zone case represents an enclosure consisting of two gas zones, an upper volume of hot gas of a uniformly distributed temperature and density and a lower volume of gas of an ambient temperature and density equal to the gas properties outside the enclosure. This case reasonably approximates a pre-flashover fire enclosure.

The well mixed case represents an enclosure consisting of hot gas of a uniform temperature and density over the entire volume of the enclosure. This is often used to approximate a post flashover enclosure.

Equations for vent mass flows are well described by Karlson & Quintierre<sup>[5]</sup> and Emmons.<sup>[129]</sup> The following equations have been derived from first principles to facilitate understanding and application to the train fire experiment. For either of the above cases, or any other vertical vent case where temperatures are not homogenous within zones, consider the region of out flowing gas above the neutral plane.

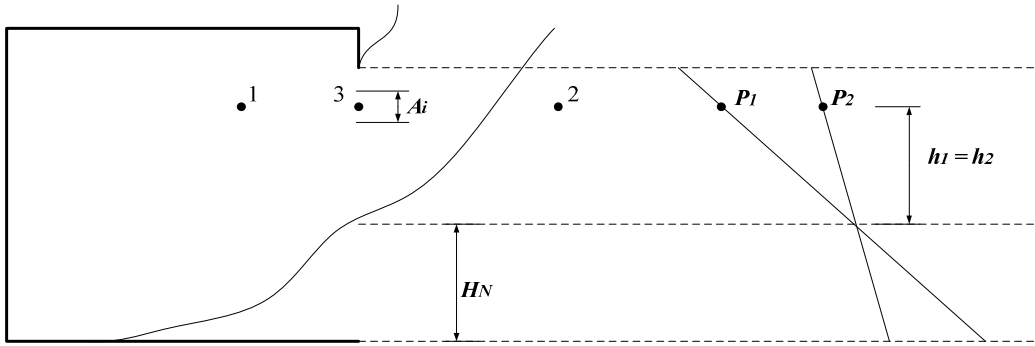


Figure 4.15. Flow between points of an equal height

Consider points 1 and 2 at equal height,  $h$ , above the neutral plane. Consider the gas flowing from point 1, through an infinitesimally small stream line area ( $A_i$ ) at point 3, to point 2. Bernoulli's equation may be applied to points 1 and 2. Bernoulli's equation is derived applying conservation of energy to the flow of an incompressible fluid and is stated as:

$$P_1 + \frac{1}{2}u_1^2 \rho_1 + h_1 \rho_1 g = P_2 + \frac{1}{2}u_2^2 \rho_2 + h_2 \rho_2 g \quad \text{Equation 4-29}$$

The terms  $P_1$  and  $P_2$  are the static pressure head. The velocity terms represent the hydrodynamic pressure. The gravity terms represent the hydrostatic pressure. As gas flows through the vent at point 3 hydrostatic pressure is converted to hydrodynamic pressure. It is reasonably assumed that  $T_3 = T_1$ ,  $\rho_3 = \rho_1$  and  $P_3 = P_2$ . Since the velocities at points 1 and 2 are zero Equation 4-29 is rewritten as:

$$\begin{aligned} P_1 - P_2 &= h_2 \rho_2 g - h_1 \rho_1 g \\ &= h(\rho_2 - \rho_3)g \end{aligned} \quad \text{Equation 4-30}$$

Bernoulli's equation applied between points 1 and 3 is rewritten as:

$$P_1 + \frac{1}{2}u_1^2 \rho_1 + h_1 \rho_1 g = P_3 + \frac{1}{2}u_3^2 \rho_3 + h_3 \rho_3 g \quad \text{Equation 4-31}$$

As  $u_1 = 0$  and  $h_1 \rho_1 g = h_3 \rho_3 g$ , Equation 4-31 may be expressed as:

$$P_1 - P_3 = \frac{1}{2}u_3^2 \rho_3 \quad \text{Equation 4-32}$$

Rearranging Equation 4-32 provides the following expression for gas velocity exiting the vent at point 3:

$$u_3 = \sqrt{\frac{2(P_1 - P_3)}{\rho_3}} \quad \text{Equation 4-33}$$

As  $P_3 = P_2$  Equation 4-30 is substituted into Equation 4-33 to give:

$$u_3 = \sqrt{\frac{2h(\rho_2 - \rho_3)g}{\rho_3}} \quad \text{Equation 4-34}$$

If the total height of  $A_i$  is small then  $u_3$  may be assumed to be the average gas velocity through  $A_i$ . Densities  $\rho_2$  and  $\rho_3$  may be calculated from temperatures applying the ideal gas law. As both the hydrodynamic pressure and hydrostatic pressure differences for a typical fire enclosure are only a very small fraction of atmospheric pressure, the value of standard atmospheric pressure,  $101.3 \times 10^3$  Pa is applied and Equation 4-11 may be applied.

For vents of constant pressure difference the mass flow can be expressed as:

$$\dot{m} = C_d A u \rho \quad \text{Equation 4-35}$$

$C_d$  is a flow coefficient that is used to account for losses due to deviation from ideal flow, i.e. incompressible, isothermal, friction-free and adiabatic flow.  $C_d$  is a function of Reynolds number and for most fire vents is typically 0.6-0.7. For large openings such as doors and windows  $C_d$  is closer to 0.6.<sup>[5]</sup> For these calculations  $C_d = 0.6$  has been applied. Substituting Equation 4-34 into Equation 4-35 gives the following expression for mass flow through the considered area  $A_i$ :

$$\dot{m}_i = C_d A_i \rho_3 \sqrt{\frac{2h(\rho_2 - \rho_3)g}{\rho_3}} \quad \text{Equation 4-36}$$

The total mass flow out of a vent ( $\dot{m}_g$ ) may be calculated by integrating Equation 4-36 from the neutral plane to the top of the vent. Numerical integration has been applied using the experimental data. Neglecting thermal expansion of gas within the enclosure and applying conservation of mass it is reasonably assumed that the mass flow out is matched by an equivalent mass flow in. In the case of multiple vents more

mass will flow out of vents located higher in the enclosure and more mass will flow into vents located lower in the enclosure.

The rate of heat energy transferred out of the enclosure via vent mass flow can be calculated as:

$$\dot{q}_{MassFlowOut} - \dot{q}_{MassFlowIn} = \dot{m}_g c_p (T_g - T_a) \quad \text{Equation 4-37}$$

Specific heat capacity ( $c_p$ ) for both out flowing gas and in flowing air is taken to be 1.0 kJ/kg.K. It is noted that although  $c_p$  increases slightly with gas temperature, the error in assuming constant  $c_p$  is negligible compared with measurement errors associated with measurement of temperature, neutral plane height and wind effects.

#### 4.3.4.2 Mass flow energy transfer through doors A and B

Temperatures were measured at various heights for doors A and B enabling numerical integration of Equation 4-36 to estimate mass flow. The following calculation procedure was applied:

- The observed neutral plane height over time was measured by scaling from video footage.
- For each door the total opening area was divided into 12 vertically spaced areas so that a door thermocouple was located at the centre of each area.
- For each time step the measured temperatures at thermocouples located above the observed neutral plane height were assumed to be the out flowing gas temperatures.
- The mass flow rate and associated energy flow rate for each time step, for each area interval above the neutral plane was calculated applying equations Equation 4-36 and Equation 4-37.
- The total energy flow rate for each time step was calculated by summing energy flow rate for each area interval above the neutral plane.

Observed neutral plane heights for Doors A and B are plotted in Figure 4.16. This shows that the observed neutral plane heights for Doors A and B were reasonably consistent. The neutral plane height at door B is slightly higher than at door A. This is most likely due to the closer proximity of door A to the fitted materials and the

majority of combustion. Another significant cause of variation in the observed neutral plane heights is likely to be wind effects.

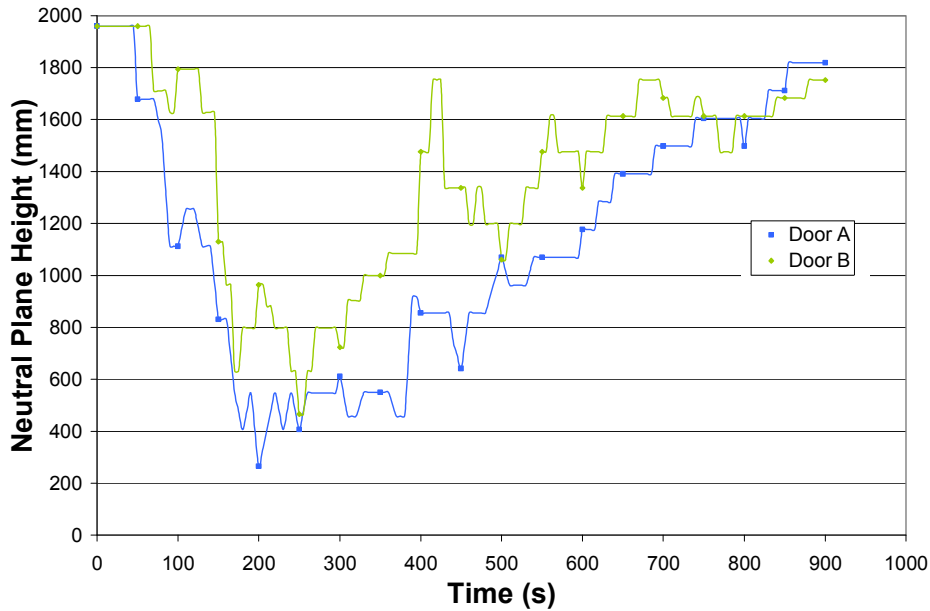


**Figure 4.16. Observed neutral plane heights for doors A and B**

The vertical temperature profiles for doors A and B at 140 s (just prior to flashover) and 350 s (around the time of observed peak flames out doors) are shown in Figure 4.17 and Figure 4.18. These profiles demonstrate that for this experiment the out flowing gas temperatures measured are not well represented by one or two zones of uniform temperature. Instead the out flowing gas temperature steadily increases with height. It is also evident that thermocouple A7 (1.3 m in door A) was faulty. For the flow calculations the temperature at this height was taken to be the average of the temperatures above and below.

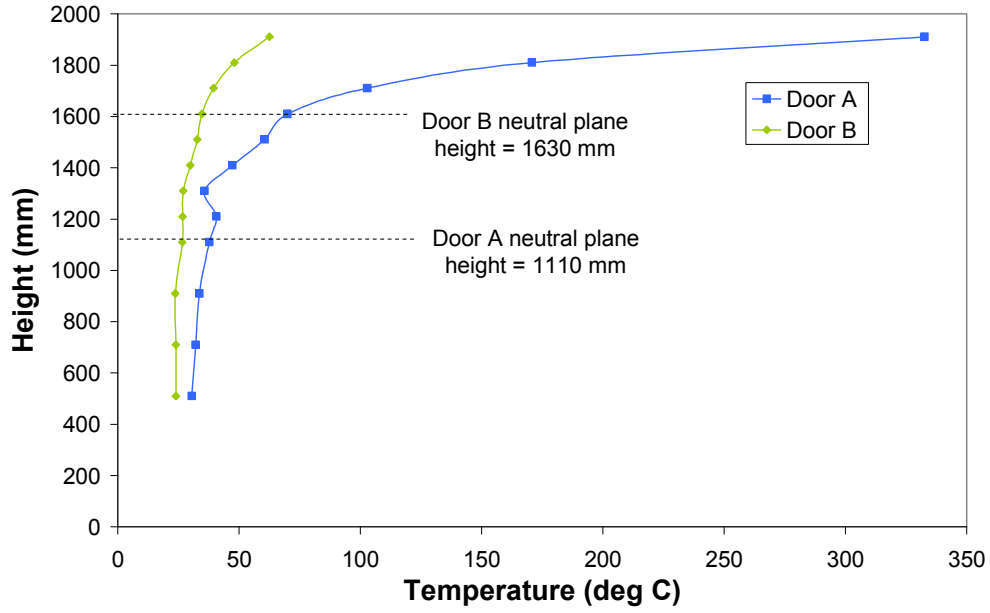


Figure 4.17. Vertical temperature profile for doors A and B at 140 s

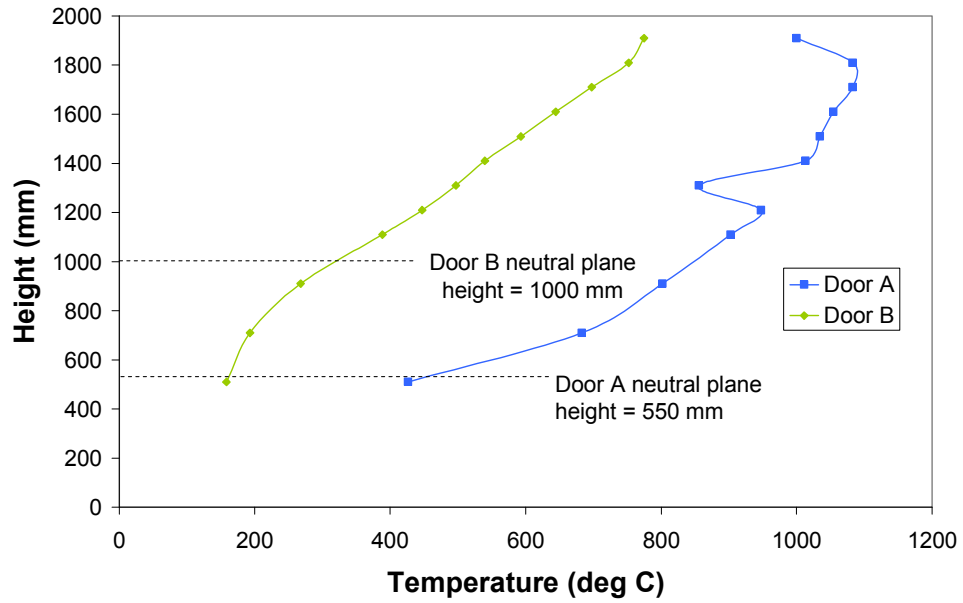


Figure 4.18. Vertical temperature profile for doors A and B at 350 s

The total rate of mass flow energy transfer out doors A and B is shown in Figure 4.19

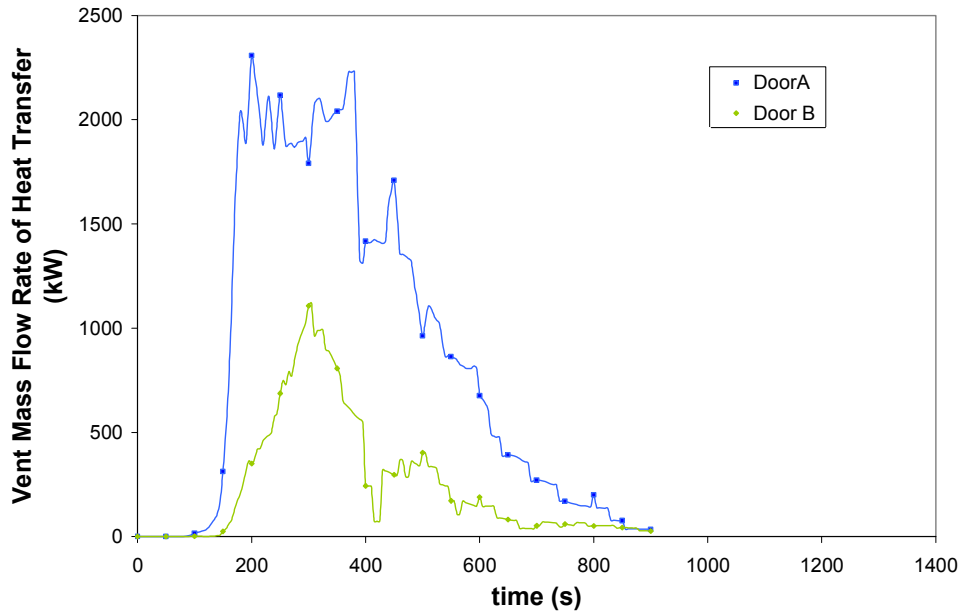


Figure 4.19. Total rate of mass flow energy transfer out Doors A and B

#### 4.3.4.3 Mass flow energy transfer through windows and North East Door.

For most glazed windows temperatures were measured at two or more points, however temperatures were not measured for the three glazed windows furthest from the ignition end of the carriage. The plaster blocking the north east door failed during the experiment resulting in significant mass flow, however there was no temperature measurement at this opening. Due to the lack of temperature measurements the simplifying assumption of uniform temperatures across these openings has been adopted. The following calculation procedure was applied:

- Times of progressive window opening were observed from video footage. It was observed that windows broke incrementally rather than all at once. It was observed that progressive window opening could be expressed as a percentage of the total window and that these openings generally progressed from the top of the window down. Window openings were simplified in terms of 25%, 50% or 100% open from the top. Observed opening times are given in Appendix G.
- From video footage it was observed that the neutral plane for windows was below the opening of the windows for much of the experiment due to inflow of air at the bottoms of doors. It was not possible to directly observe the neutral plane height at each window. Considering the consistency of observed neutral plane heights for doors A and B the following assumptions were made:

- The neutral plane height for all windows north of door A (windows A, B, C and D) and NE door was equal to the neutral plane height for door A.
- The Neutral plane height for all other windows located between doors A and B was equal to the average of the neutral plane heights for doors A and B.
- The temperature of out flowing gas for each window and the NE door is assumed to be uniform across the area of each opening. Where two outside thermocouples were located at the top and bottom pane of a window the uniform temperature is taken to be equal to the average of the two measured temperatures. For other windows and the NE door where temperatures were not measured, the uniform temperature is taken to be the average of the top and mid height thermocouple temperatures from the nearest thermocouple tree.
- Equation 4-36 has been integrated for the case of uniform gas temperature above the neutral plane, where the neutral plane may lay below or above the sill of the opening, as shown in Figure 4.20.

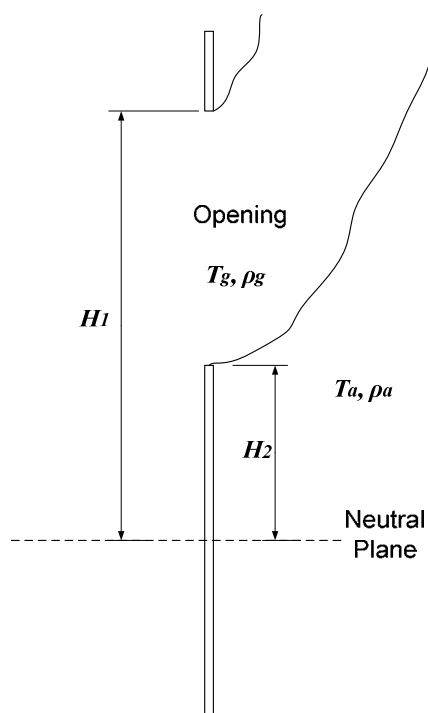


**Figure 4.20.** Case of uniform gas temperature flowing out a window.

Integrating across the area of out flowing gas provides the following expression for total mass flow out the opening:

$$\dot{m}_g = \frac{2}{3} C_d W \rho_g \sqrt{\frac{2h(\rho_a - \rho_g)g}{\rho_g}} (H_1^{3/2} - H_2^{3/2}) \quad \text{Equation 4-38}$$

The total mass flow for each opening, for each time step was calculated applying this expression.

- The total energy flow rate for each opening, for each time step was calculated applying Equation 4-37.

The resulting estimates of vent mass flow HRR for windows and the NE door are shown in Figure 4.21 and Figure 4.22.

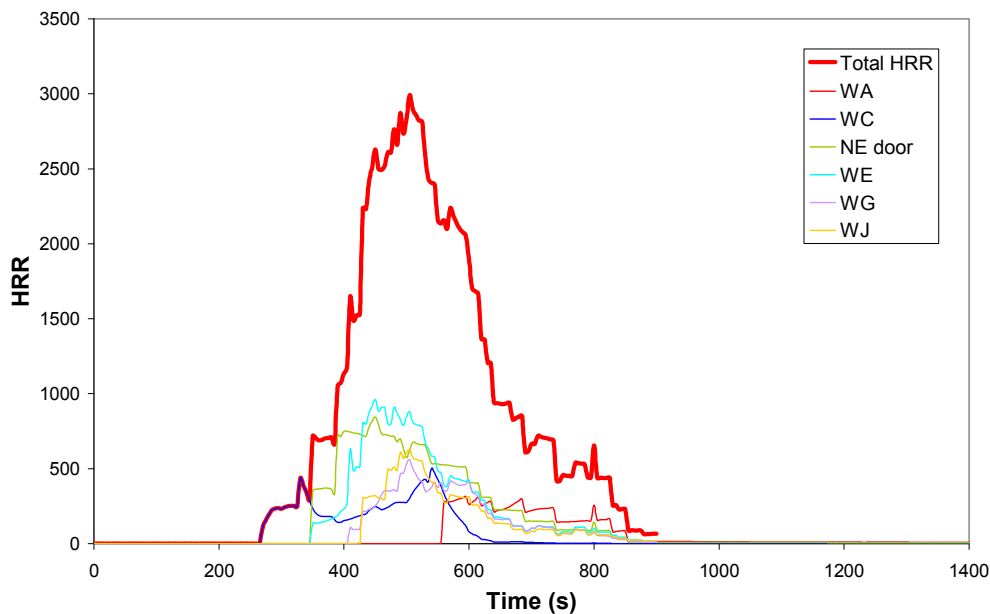


Figure 4.21. Vent mass flow HRR for east windows and NE door

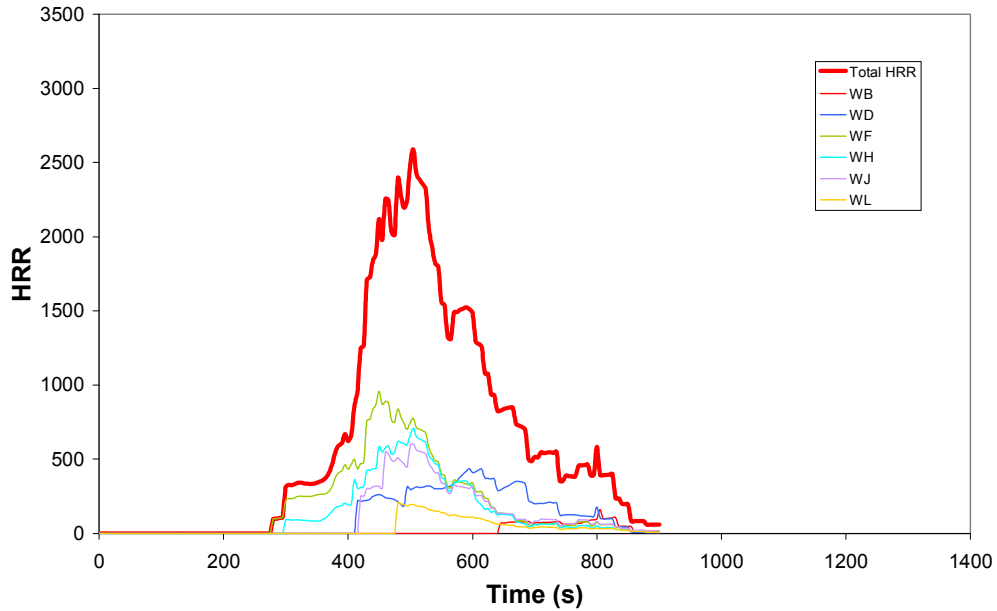


Figure 4.22. Vent mass flow HRR for west windows

#### 4.3.4.4 Total vent mass flow HRR

The estimated HRR curves for vent mass flow through all doors and windows have been summed to provide the total vent mass flow HRR estimate shown in Figure 4.23.

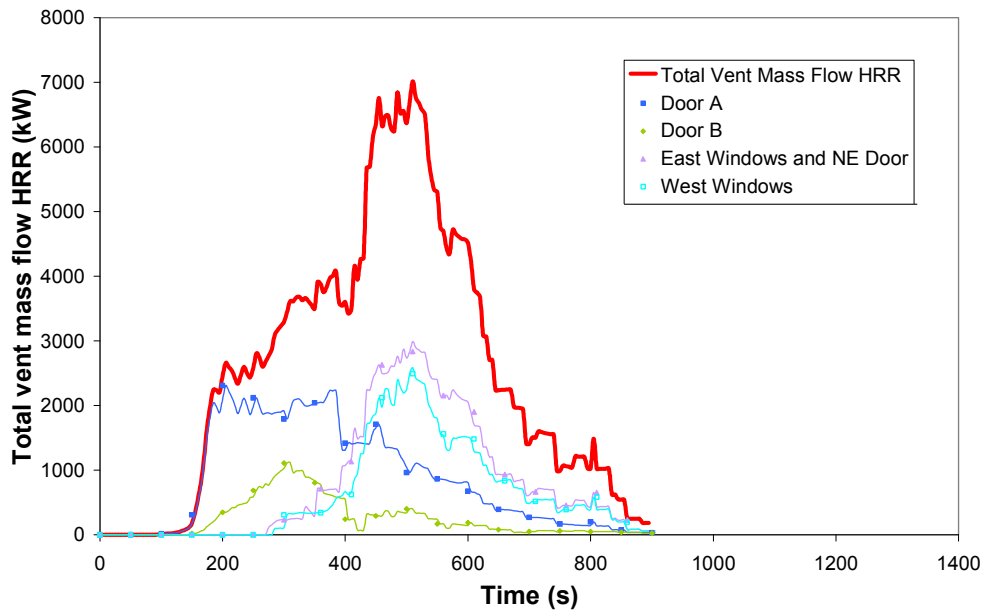


Figure 4.23. Total vent mass flow HRR

Mass flow energy transfer through doors A and B is most significant prior to 400 s. After 400 s glazing failure resulted in mass flow energy transfer becoming more significant through windows.

The main sources of error for this estimate are:

- Wind effects due to a moderate easterly wind.
- Estimation of neutral plane height.
- Temperature measurement and assumed temperature distribution.

### **4.3.5 Exterior Fire Heat Release Rate**

#### **4.3.5.1 Observed exterior fire characteristics**

Exterior combustion was observed to occur in flames extending from open passenger doors A and B and other openings after failure. The peak external HRR was observed to be from flames extending from Doors A and B at around 280-320 s. Failure of window glazing and the plasterboard closing the north east passenger door did not result in significant flames from these openings until after 400 s. At this time the flames out of doors A and B had reduced. Some limited external combustion was also observed to occur through smaller penetrations such as holes for A/C units in the roof. The contribution to the total HRR from flames extending from these small openings was observed to be small and occurring during the decay of the fire and thus will be neglected.

All observed flames were diffusion flames. Flows within the flames were dominated by buoyancy rather than momentum. Although flames issuing from doors A and B exhibited a small horizontal momentum component due to the horizontal flow velocity of unburnt gases and flames through the vents, ultimately these vent flows were driven by buoyancy. The base of flames issuing from doors A and B protruded out from the vent due to the horizontal flow component and the quantity of gas flowing through the vent. It is reasonable to approximate the flame as having a circular or semicircular cross section near the base. Flames issuing from broken windows and the north east passenger door after failure were smaller and they did not protrude away from the vent far in relation to the width of the vent. Therefore it is more reasonable to approximate the cross section near the base of these flames as being closer to a line source.

Flames issuing from the carriage were observed to be turbulent. This turbulence was characterised by billowing or pulsing of the flames with large eddies shedding at the flame edge. This resulted in an intermittent flame zone at the tops of flames where the flame height fluctuated.

The characteristic flame width and mean flame height for all external flames of significance from each opening has been measured by scaling from video footage of the experiment. The measurements are given in Appendix G. Difficulties in obtaining these measurements included:

- Parallax of the video images.
- Fluctuation of flame heights.
- Obscuration of flames by smoke and other flames.
- Wind effects.

Given these difficulties the measured flame dimensions are estimated to be accurate to approximately  $\pm 20\%$ . Mean flame height was defined to be the height that the flame appears half the time. The characteristic flame width was defined as the width of the flame issuing from the vent (usually the width of the vent).

A light gusting easterly wind added to the fluctuation of flame heights. Review of video footage from multiple angles indicates that wind caused the smoke plume to tilt up to  $45^\circ$  from vertical. However due to buoyancy the flames did not tilt as much. Flames fluctuated between being vertical and tilted approximately  $20\text{-}30^\circ$  from vertical. The mean flame height along the tilt axis did not vary significantly with angle of tilt.

#### 4.3.5.2 Flame height correlations

Fire engineers commonly use flame height correlations to predict flame height for a given HRR.<sup>[130]</sup> Here the inverse problem shall be solved, predicting HRR based on observed flame heights.

Due to turbulent behaviour, equations for flame heights derived from first principles are not applied. Instead empirical correlations are applied.

The non-dimensional Froude number ( $Fr$ ) is used to describe the relative magnitude of the effects of momentum and buoyancy in fluid flow:

$$Fr = \frac{u^2}{g \cdot D} \quad \text{Equation 4-39}$$

The numerator of Equation 4-39 is in proportion to momentum, the denominator to gravity forces. A number of experimentally based correlations have been published to relate flame heights to HRR and source diameter. Experimenters have found it convenient to express data in terms of the following form of the non-dimensional square root of Froude number given in terms of HRR:

$$\dot{Q}^* = \frac{\dot{Q}}{\rho_a c_p T_a \sqrt{g} D D^2} \quad \text{Equation 4-40}$$

Correlations for flame height derived from experiments carried out by different investigators are given in Table 4-4 and Figure 4.24.

**Table 4-4 Flame Height Correlations**

Symbol	Fuel, Geometry	$\dot{Q}^*$ Range	Correlation	Reference
Z	Natural gas, 10-50 cm diameter burner	$\dot{Q}^* < 0.15$ $0.15 < \dot{Q}^* < 1$ $1 < \dot{Q}^* < 40$	$L/D = 40 \dot{Q}^{*2}$ $L/D = 3.3 \dot{Q}^{*2/3}$ $L/D = 3.3 \dot{Q}^{*2/5}$	Zukowski <sup>[131]</sup>
C	Natural gas, 45, 60 cm square burner	$0.13 < \dot{Q}^* < 0.28$ $0.28 < \dot{Q}^* < 0.55$	$L/D = 15.1 \dot{Q}^{*2}$ $L/D = 3.2 \dot{Q}^*$	Cox & Chitty <sup>[132]</sup>
T	Wood Cribs, 10-200 cm side	$0.75 < \dot{Q}^* < 8.8$	$L/D = 3.4 \dot{Q}^{*0.61}$	Thomas <sup>[133]</sup>
H	Gas, Liquid, Solid, Literature	$0.12 < \dot{Q}^* < 1.2 \times 10^4$	$L/D = 3.7 \dot{Q}^{*2/5} - 1.02$	Heskestad <sup>[134]</sup>
S	Literature and gas jets	$1 < \dot{Q}^* < 10^4$	$L/D = 4.16 \dot{Q}^{*2/5}$	Steward <sup>[135]</sup>
B	Literature and 0.7-4.6 mm tubes, various gases	$\dot{Q}^* < 1.7$ $1.7 < \dot{Q}^* < 21$ $33 < \dot{Q}^* < 10^3$ ( $20 < \xi_L < 40$ ) $10^3 < \dot{Q}^* < 10^6$ ( $1 < \xi_L < 20$ ) $\dot{Q}^* > 10^6$ ( $\xi_L < 1$ )	$L/D = 1.52 \dot{Q}^{*2}$ $L/D = 3.6 \dot{Q}^{*2/5}$ $\psi = 0.064 \xi_L - 0.58$ $\psi = 0.18 + 0.022 \xi_L$  $L/D < 11(\beta r) \sqrt{\rho_0 / \rho_\infty}$	Becker & Liang <sup>[136]</sup>
K	Various gases, 1-10 mm tubes	( $2 < \xi_L < 11$ )	$\psi = 0.2 + 0.024 \xi_L$	Kalghatgi <sup>[137]</sup>
W	Various gases from small nozzles		$\frac{L - \ell}{D} = 5.3(\beta r) \sqrt{\rho_0 / \rho_\infty}$	Hawthorne et al <sup>[138]</sup>
-	Line source gas burners	(applicable only where longer side (D) at least 3 times shorter side)	$L = 0.035 \left( \frac{\dot{Q}}{D} \right)^{2/3}$	Karlson and Quintierre <sup>[5]</sup>

Note -  $\xi_L$  and  $\psi$  are correlating variables as they are not applied in this thesis they are not defined in detail.

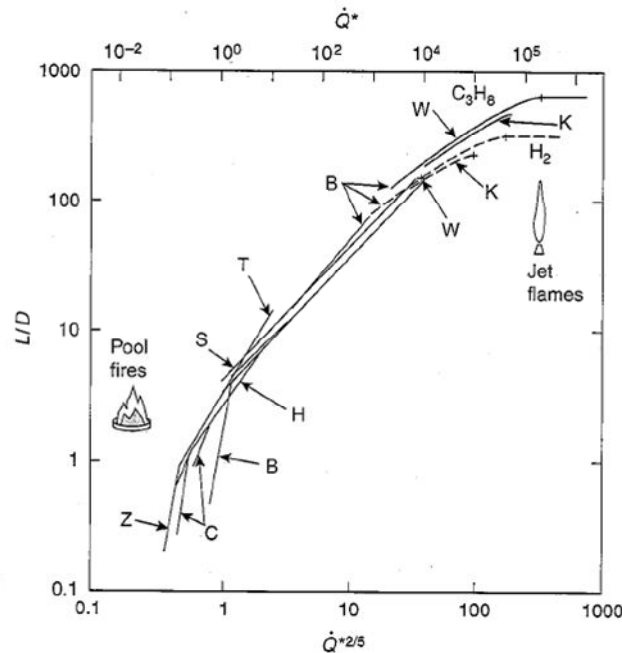


**Figure 4.24. Flame height for the entire Froude number spectrum. Capital letters correspond to studies listed in Table 4-4 (reproduced from McCaffrey<sup>[130]</sup>)**

The left side of the plot in Figure 4.24 represents fires where the diameter is the same order of magnitude as the flame height and the Froude number is low indicating Buoyancy dominated flows. Buoyancy also dominates at intermediate Froude numbers. The right hand side of the plot represents high Froude number, high momentum jet flames.

The correlations relating to high momentum flames are not appropriate for the buoyancy dominated flames observed in the full scale train fire experiment.

The line source fire plume is not appropriate for the flames observed issuing from passenger doors as the base of the flames did not have a large aspect ratio.

Several fire engineering texts recommend the use of the Heskestad correlation for application to buoyancy dominated flames as it gives good results for the pool fires and intermediate fire regimes shown in Figure 4.24.<sup>[5,130]</sup> Therefore the Heskestad flame height correlation shall be applied for the large flames issuing from doors A and B.

For the smaller flames issuing from broken windows and the failed north east passenger door, the flame base is more linear, with the flame width of the order of three times greater than the flame depth. Therefore the line source flame height correlation will be applied for these flames.

#### 4.3.5.3 Estimated exterior fire HRR

The flame heights for doors A and B given in Appendix G are measured from the sill of the door. Unlike pool fires the actual base height of flames issuing from doors or windows is not well defined but changes with the size of flames. Inspection of video footage indicated that the effective base height of flames can be approximated as the average of the soffit height and the neutral plane height. On this basis the actual mean flame height was calculated.

Given that the product of standard values for  $\rho_a c_p T_a g^{1/2} \approx 1000$ , Heskestad's correlation becomes:

$$L = 0.235\dot{Q}^{2/5} - 1.02D \quad \text{Equation 4-41}$$

This can be rewritten as:

$$\dot{Q} = \left( \frac{L + 1.02D}{0.235} \right)^{5/2} \quad \text{Equation 4-42}$$

This was applied to the observed flame dimensions to calculate HRR curves for flames outside door A and Door B, see Figure 4.25.

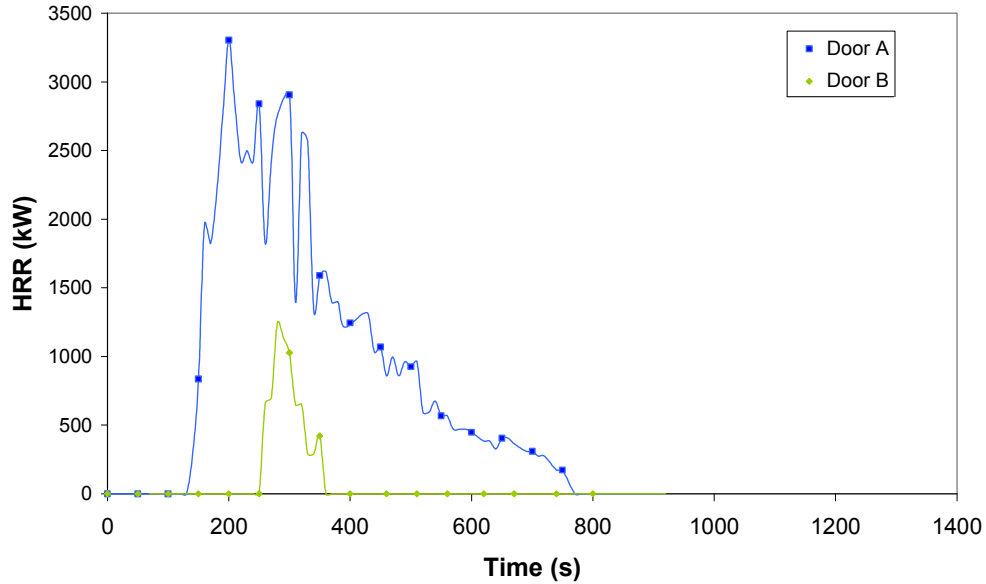


**Figure 4.25. HRR for exterior flames issuing from Door A and Door B vs. time**

Large fluctuations in HRR for door A flames are due to observed fluctuations in flame height that lasted 10 s or more. These fluctuations may have been caused by prolonged gusts and lulls in wind.

It is noted that in applying the Heskestad correlation inaccuracies associated with flame height become exaggerated due to the exponent 5/2. For example the maximum observed flame height of 4.5 m at door A results in a predicted HRR of 3.3 MW. If the flame height is increased by 20% to 5.4 m the predicted HRR is increased by approximately 40% to 4.65 MW.

The line source flame height correlation may be rewritten as:

$$\dot{Q} = D \left( \frac{L}{0.035} \right)^{3/2} \quad \text{Equation 4-43}$$

Observed dimensions for flames issuing from broken windows and the failed north east passenger door are given in Appendix G. The line source has been applied to these exterior flames. For comparison the Heskestad flame height correlation has also been applied. The results are shown in Figure 4.26 to Figure 4.29.

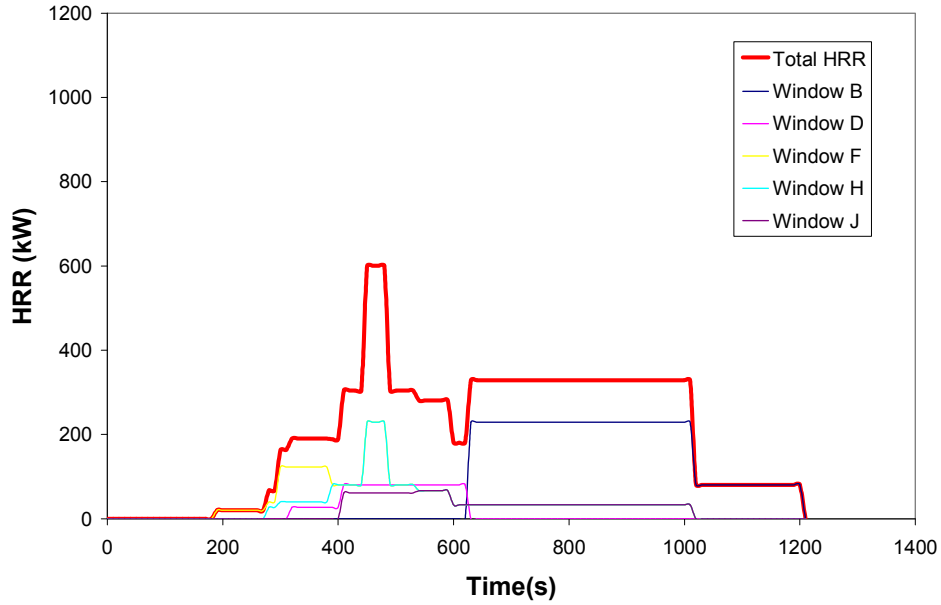


Figure 4.26. HRR for flames issuing from west windows calculated using the line source flame height correlation

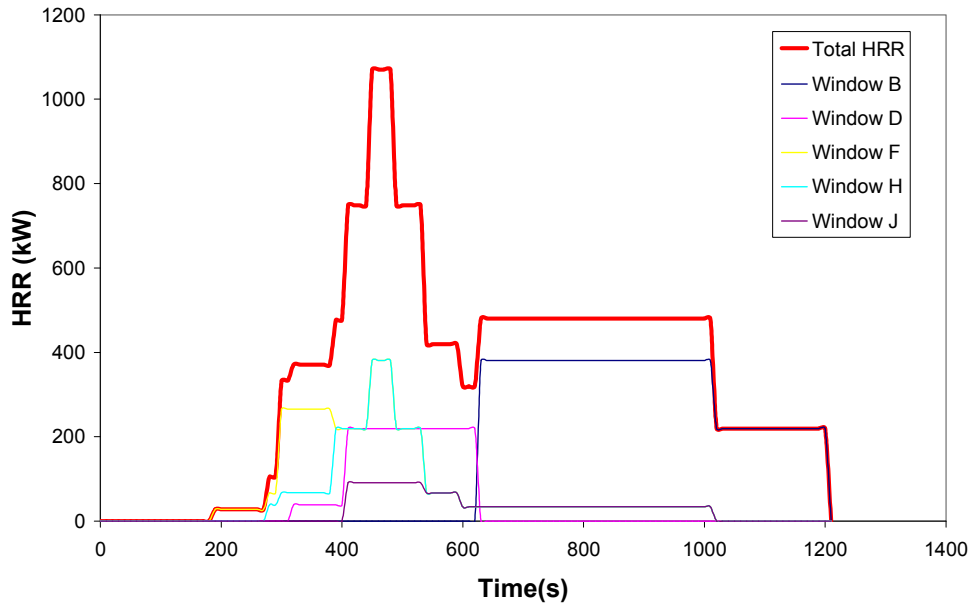
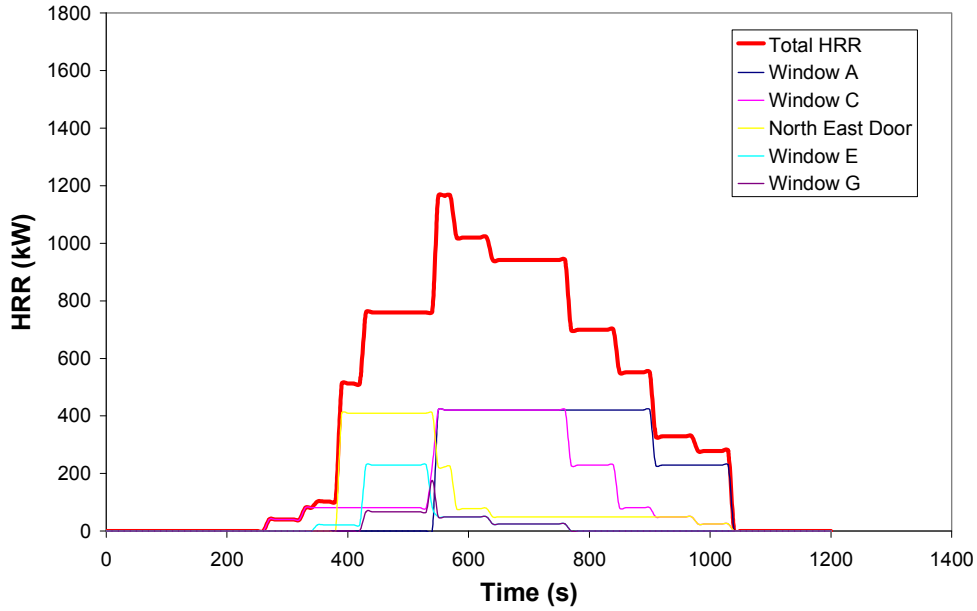
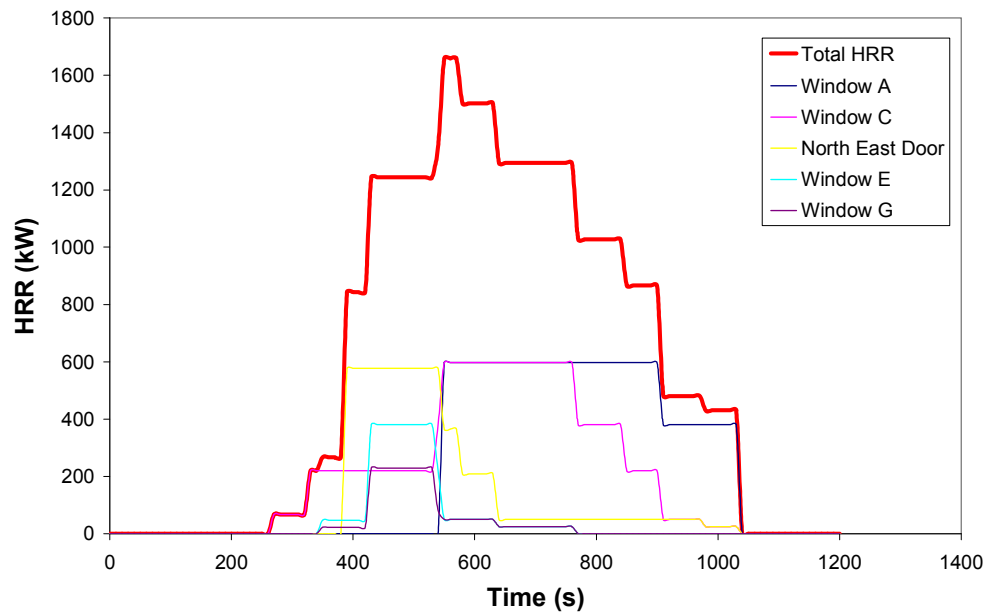


Figure 4.27. HRR for flames issuing from west windows calculated using the Heskestad flame height correlation



**Figure 4.28.** HRR for flames issuing from east windows and failed north east passenger door calculated using the line source flame height correlation



**Figure 4.29.** HRR for flames issuing from east windows and failed north east passenger door calculated using the Heskestad flame height correlation

The Heskestad correlation predicts a larger HRR for a given flame height than the line source correlation because it assumes a broader base of flame. The line source correlation results appear more credible for the smaller, flatter flames issuing from windows and are applied.

All calculated HRR for exterior flames have been summed to give the total shown in Figure 4.30.

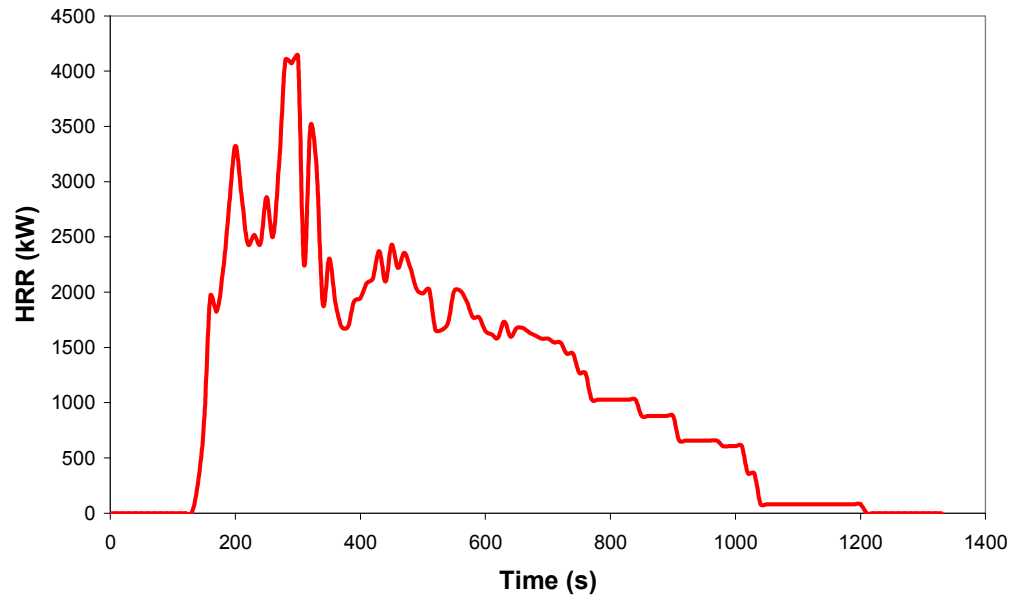
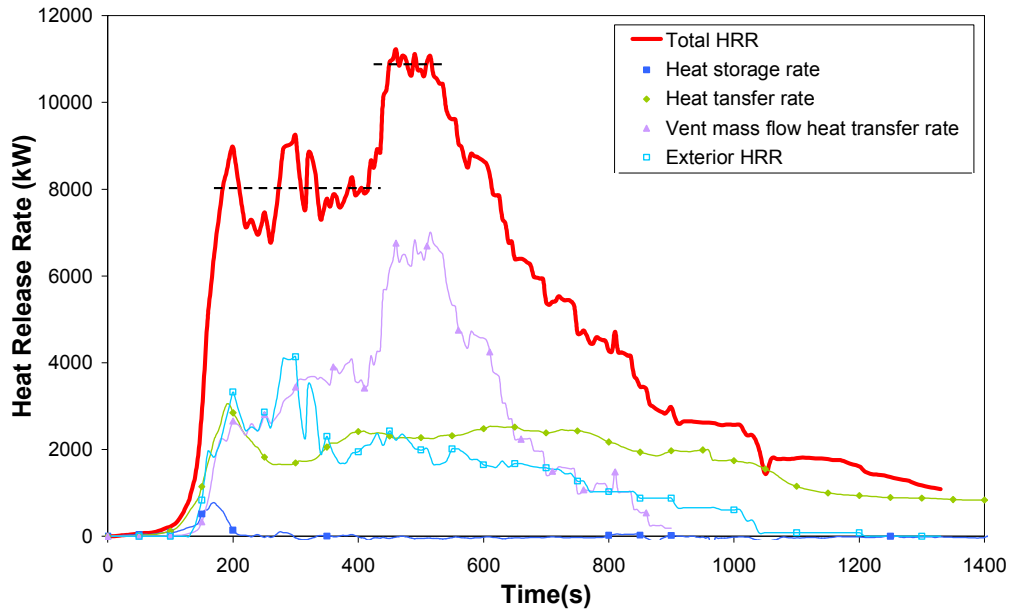


Figure 4.30. Total HRR for all exterior flames

#### 4.3.6 Total Heat Release Rate

Equation 4-5 and Equation 4-7 are applied, summing the individual heat rate components, to estimate the total heat release rate for the large scale experiment shown in Figure 4.31.



**Figure 4.31. Total HRR for full scale experiment estimated from conservation of energy model**

The estimated total HRR maintains an average of 8 MW during the period where windows were intact and significant exterior combustion occurred out of doors A and B. The estimated total HRR then maintained an average of 11 MW for a shorter duration after windows had broken and vent mass flow had increased. During the test it was observed that flames extending out the doors reduced at the time windows began to break and mass flow through openings increased. From this result it is concluded that from 200s to 400 s the HRR was affected by available ventilation with approximately 40% of the total HRR due to combustion exterior to the carriage. From 400 s mass flow through the windows rapidly increased. Increasing ventilation of the carriage enabled more combustion to occur inside the carriage and increased total HRR. During this period approximately 15% of the total HRR was due to combustion exterior to the carriage (mostly flames out windows). From 500 s the fuel began to burn out and the HRR began to decay.

The most significant components of HRR in the conservation of energy model are the vent mass flow heat transfer rate, the exterior HRR and the heat transfer rate through bounding surfaces. The heat storage rate was not a considerable component and was only significant during the early fire growth stage.

Significant sources of error for this estimate have been discussed and may be summarised in the two following groups;

Errors resulting from simplifying assumptions including:

- Material properties and constants such as  $C_d$ .
- One dimensional, steady state heat transfer.
- Accuracy of flame height correlations.
- Assumed temperature distributions.

Errors in measurement including:

- Scaling of flame dimensions, window breakage and neutral plane height from video records.
- Temperature measurements which were affected by damage or displacement during the experiment. Gas temperatures were also influence by radiant heating from flames.
- Wind speed which was not measured and was mostly neglected.

Given the complexity of these errors is not possible to quantify the total uncertainty of this estimate. Recent full-scale tunnel HRR measurements applying oxygen consumption calorimetry typically have uncertainties of the order of 15% with a 95% confidence interval.<sup>[139]</sup>

The estimate of HRR derived from the conservation of energy model is compared to the estimates produced by the Average HRR method and Duggan's method in Figure 4.32.

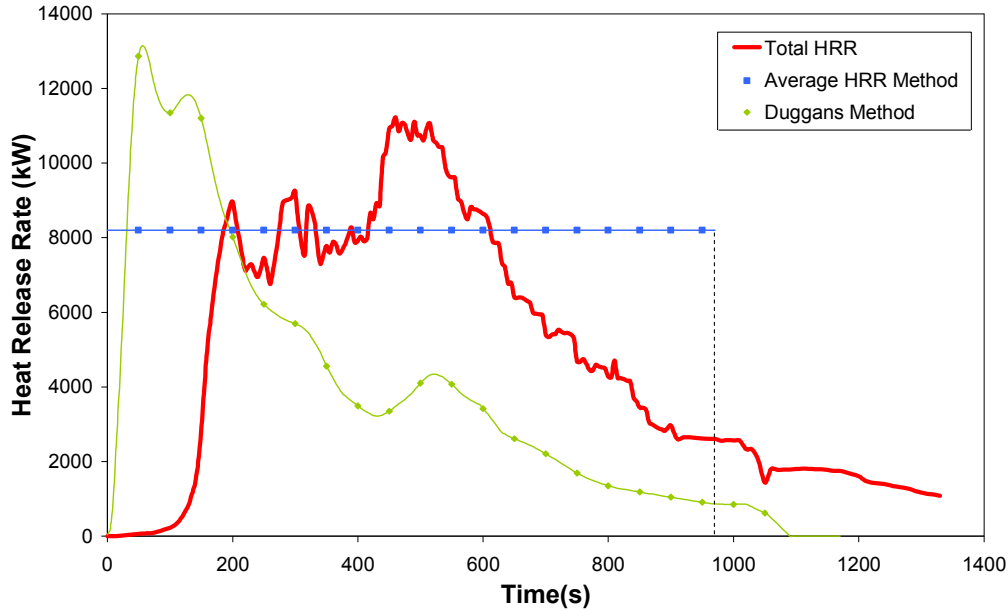


**Figure 4.32. Comparison of HRR estimates for full-scale experiment**

Clearly, the average HRR method estimate does not describe the fire development that was observed and measured. The Average HRR for the conservation of energy model over 970 s is 5.2 MW. The Average HRR method estimate is 8.2 MW. This difference may be due to:

- Incomplete combustion of materials, particularly at floor level where materials such as carpet were observed to be partially shielded by debris.
- Reduced combustion efficiency due to poor ventilation compared with conditions in the cone calorimeter.
- Inaccuracies in estimation of total mass of materials.
- Inaccuracy of the conservation of energy model total HRR estimate

Clearly, the Duggan's method estimate also does not describe the fire development that was observed and measured. This is discussed in Section 4.2.2. As expected Duggan's method over predicts the Peak HRR for the full scale experiment

The ventilation controlled correlation estimates a ventilation controlled HRR of 12 MW prior to significant window breakage. This is greater than the average of 8 MW prior to window breakage estimated by the conservation of energy model and

would require a correction factor of  $\eta = 0.67$ . The ventilation controlled correlation estimates a ventilation controlled HRR of 25 MW after significant window breakage from 400-500s. This is much larger than the average of 11 MW estimated by the conservation of energy model. Considering that  $\eta$  increases for increasing ventilation conditions it is concluded that insufficient fuel was available for the HRR to become restricted by ventilation during this period. It is noted that if more interior material had been fitted the fire duration would increase and HRR after 400 s would have increased and may possibly have become restricted by ventilation. As suitable correction factors are not known, the ventilation controlled correlation does not describe the fire development that was observed and measured as discussed in Section 4.2.4.

Although the existing design fire estimation methods fail to reasonably describe the fire behaviour observed in the experiment the resulting estimate of a peak HRR in the range of 8-13 MW approximately matches with observations and the results of the conservation of energy model. Therefore the existing design fire estimation methods are appropriate for producing an “order of magnitude” estimate of Peak HRR. They are not appropriate for estimating fire growth or decay rates or duration of burning.

## 4.4 ANALYSIS CONCLUSIONS

Based on this analysis the following conclusions have been drawn:

- A conservation of energy model was used to estimate HRR for the full-scale experiment based on experimental measurements and observation. Fully developed HRR was estimated to be 8 MW prior to significant window breakage, with 40% HRR occurring exterior to the carriage. After significant window breakage the fully developed HRR was estimated to be 11 MW with 15% HRR occurring exterior to the carriage.
- The accuracy of conservation of energy model is affected by errors resulting from simplifying assumptions and errors in measurement. However it represents the best available HRR estimate for the full-scale experiment based on experimental measurements given that HRR could not be directly measured.
- The conservation of energy model highlights the significant affect of ventilation on HRR for the full-scale experiment. By estimating the internal and external HRR separately it became apparent that prior to window breakage ventilation into the carriage was restricted resulting in large external flames but also restricted internal HRR which controlled pyrolysis of materials. As ventilation into the carriage increased due to window breakage internal combustion increased resulting in an increase in pyrolysis of materials and total HRR until the fuel began to burn out.
- It is expected the peak HRR would be higher and burn duration would be longer for a fully fitted carriage interior under the same initial ventilation conditions.
- Because the full-scale experiment involved a carriage half fitted with interior materials the conservation of energy model does not represent an appropriate design fire for a fully fitted carriage but does provide a basis for understanding train fire development and evaluating design fire estimation methods.
- Design fire estimation methods including the average HRR method, Duggan's method and the ventilation controlled method were applied to the full-scale experiment. It was found that these methods do not appropriately represent real fire behaviour resulting in poor estimation of rate of fire growth and burn

duration. The methods provided a rough order of magnitude estimate of peak HRR, to within approximately 30% of the peak HRR based on the conservation of energy model for the Full-scale experiment. Duggan's method and the ventilation controlled method both over predicted peak HRR. The average HRR method over predicted average HRR but under predicted peak HRR.

## **CHAPTER 5 FDS MODELLING TO ESTIMATE TRAIN FIRE HRR**

### **5.1 INTRODUCTION TO CFD AND FDS**

Computational fluid dynamics (CFD) is a numerical method for modelling fluid flow and heat transfer that is applied by a wide range of engineering disciplines.<sup>[140]</sup>

CFD models divide the volume to be modelled into a finite grid of sub-volumes. Time dependent and three-dimensional conservation of mass, conservation of energy and conservation of momentum equations known as the Navier-Stokes equations are applied to each sub volume and solved numerically. In addition to the conservation equations, equations for other physical or chemical processes may be solved for each sub volume. A compromise exists between the accuracy of the model and the computational power and time required, as both are heavily dependent on the size of the grid and number of time steps.

Only in recent times has CFD become a practical method for fire modelling and computational power still remains a limiting factor. A small number of CFD programs have been specifically developed to incorporate the physical and chemical processes required for modelling fire.<sup>[5,140]</sup>

Fire Dynamics Simulator (FDS)<sup>[141,142]</sup> developed at the National Institute of Standards and Technology (NIST), is a CFD model that has been widely adopted by fire engineers and researchers due to its specific features for fire simulations and its public domain, open source availability. Smokeview is a post-processing software tool used to visualise simulation data generated by FDS.<sup>[142]</sup> FDS has been specifically designed to simulate the following fire phenomena:

- Low speed transport of heat and combustion products from fire.
- Radiant and convective heat transfer between flame, gas and solid surfaces.
- Pyrolysis and combustion of pyrolates in the fire plume.
- Flame spread and fire growth.
- Sprinkler, heat detector, and smoke detector activation.
- Sprinkler sprays and suppression by water.

Two principal methods of simulating fires using FDS are:

**Prescribed fire size** – A fire size is prescribed, usually as a vent with a specified flow of unmixed gas phase fuel with specified combustion parameters. All other surfaces are specified as non combustible. The combustion and heat release of the fuel as it mixes with air is simulated and the resulting transport of heat and combustion products is simulated. The global HRR is specified by specifying the flow of combustible gas into the system provided that all combustible gas is able to burn.

**Simulated fire growth** – A source fire size is prescribed. Other surfaces are specified as combustible materials with specified thermal and flammability properties. Heat transfer, pyrolysis, flame spread, fire growth and fire decay due to burn out or suppression are modelled to predict the resulting global HRR for the system. The resulting transport of heat and combustion products through the system is modelled.

The “prescribed fire size” method is most often applied by fire engineers to model conditions within a series of enclosures to assess tenability and fire safety systems operation for a well defined design fire. For this type of application the FDS technical reference guide<sup>[141]</sup> provides many examples of experimental validation and states that accuracy varies from being within experimental uncertainty to being about 20% different from experimental results.

The “simulated fire growth” method has been applied by researchers to simulate fire spread and fire growth phenomena and as a tool for forensic reconstructions. It has also been applied to a lesser extent by fire engineers to estimate design fires. There are very few examples of experimental validation of this application. The FDS technical reference guide concludes that simulated fire growth is very sensitive to

material properties input, and physical phenomena of interest may not be simulated due to limitations in the model algorithms or numerical grid.

The following chapter focuses on the application of FDS Version 4 to simulate fire growth for passenger trains. It is noted that FDS Version 5 was released late 2007 with some significant changes. At the time of writing, FDS Version 5 has not been released for a sufficient time for significant application in this field and will not be discussed further.

## **5.2 GOVERNING THEORY AND ASSUMPTIONS FOR FDS**

### **5.2.1 Hydrodynamic Model**

The hydrodynamic model describes the fluid motion and dynamics in the system. Four conservation equations for mass, species, momentum and energy and the equation of state for a compressible multi-component mixture of ideal gases are solved by FDS. These equations are a form of the Navier-Stokes equations. These equations are expressed in their simplest form in the following sections.<sup>[141,143]</sup>

In the following notation, terms in bold are vector quantities. For example  $\mathbf{u}$  is velocity with three components ( $u$ ,  $v$ ,  $w$ ) in the  $x$ ,  $y$  and  $z$  axis. Partial differences in

the three axis are notated by the following vector operator  $\nabla = \left( \frac{\partial}{\partial x}, \frac{\partial}{\partial y}, \frac{\partial}{\partial z} \right)$ .

#### **Conservation of Mass**

Conservation of mass states that matter can be neither created nor destroyed and that the rate of change of mass within a control volume is equal to the rate of mass flow through the control surface. In mathematical notation:

$$\frac{\partial \rho}{\partial t} + \nabla \cdot \rho \mathbf{u} = 0 \quad \text{Equation 5-1}$$

The first term represents the rate of mass change within a control volume and the second term represents mass flow through the control surface.

#### **Conservation of Species**

Conservation of mass is expressed for the mass fractions of individual gaseous species ( $Y_i$ ) as follows:

$$\frac{\partial}{\partial t}(\rho Y_i) + \nabla \cdot \rho Y_i \mathbf{u} = \nabla \cdot \rho D_i \nabla Y_i + \dot{m}_i''' \quad \text{Equation 5-2}$$

The  $\frac{\partial}{\partial t}(\rho Y_i)$  term represents the rate of mass change of species  $Y_i$  within a control volume. The  $\nabla \cdot \rho Y_i \mathbf{u}$  term represents the mass flow of species  $Y_i$  through the control surface due to mass convection. The  $\nabla \cdot \rho D_i \nabla Y_i$  term represents the mass flow of species  $Y_i$  through the control surface due to mass diffusion where  $D_i$  is the diffusion coefficient. Mass production rate of a species within a control volume is represented by  $\dot{m}_i'''$ . Summing Equation 5-2 for all species yields the conservation of mass equation. Therefore the sum of the mass fractions  $\sum Y_i = 1$ , the sum of the production/loss rates  $\sum \dot{m}_i''' = 0$ , and the sum of the diffusion terms  $\sum \nabla \cdot \rho D_i \nabla Y_i = 0$ .

### Conservation of Momentum

Conservation of momentum is derived applying Newton's second law of motion which states that the rate of change of momentum of mass within a control volume and the rate of flux of momentum through the control surface is equal to the sum of all external forces acting on the control volume. In mathematical notation:

$$\frac{\partial}{\partial t}(\rho \mathbf{u}) + \nabla \cdot \rho \mathbf{u} \mathbf{u} = -\nabla P + \rho \mathbf{f} + \nabla \cdot \tau_{ij} \quad \text{Equation 5-3}$$

The  $\frac{\partial}{\partial t}(\rho \mathbf{u})$  term represents the rate of change of momentum of mass within the control volume. The  $\nabla \cdot \rho \mathbf{u} \mathbf{u}$  term represents the flux of momentum through the control surface. The right hand consists of forces acting on the control volume including pressure  $p$ , a viscous stress tensor  $\tau_{ij}$ , and an external force vector  $\mathbf{f}$  (which consists of gravity plus other forces such as drag exerted by liquid droplets. Of these forces, gravity is very important as it represents the influence of buoyancy on the flow.

### Conservation of Energy

Conservation of energy is a statement of the first law of thermodynamics which states that the rate of change of energy within the control volume and the net flux of energy

through the control surface is equal to the net heat added to the control volume plus the net work done by the control volume. In mathematical notation:

$$\frac{\partial}{\partial t}(\rho h) + \nabla \cdot \rho h \mathbf{u} = \left( \frac{\partial P}{\partial t} + \mathbf{u} \cdot \nabla P \right) + \dot{q}''' - \nabla \cdot \mathbf{q} + \Phi \quad \text{Equation 5-4}$$

The terms on the left represent the rate of change of energy within the control volume and the net flux of energy through the control surface. The  $\left( \frac{\partial P}{\partial t} + \mathbf{u} \cdot \nabla P \right)$  term represents the pressure work. The term  $\dot{q}'''$  represents the rate of heat generation by combustion in the control volume. The term  $\nabla \cdot \mathbf{q}$  represents the radiant and conductive heat flux through the control surface and the vector  $\Phi$  represents the rate at which kinetic energy is transferred to thermal energy due to viscosity of the fluid.

#### Equation of State for an Ideal Gas

Pressure, density and temperature are related by Boyle's law as follows:

$$P = \frac{\rho R T}{M} \quad \text{Equation 5-5}$$

The above equations represent a broad variety of fluid flow applications. FDS relies upon simplifying assumptions specific to the application of fire to enable efficient solution of these equations. FDS assumes low mach number (<0.3) flows which eliminates compressibility effects that give rise to acoustic waves. This is reasonable for most fire flows.

Another important simplifying assumption relates to the treatment of turbulence. Fire flows are typically turbulent. Turbulence occurs in flows of high Reynolds numbers and is characterised by rotational flow structures (turbulent eddies) with a wide range of length and time scales occurring within a flow field. The smallest eddies may have a length scale and frequency of the order of  $10^{-6}$  m and 10 kHz.<sup>[5,143]</sup> The three different approaches to modelling turbulence in CFD are schematically represented in Figure 5.1 and are:

- Direct numerical simulation (DNS).
- Large eddy simulation (LES).
- Reynolds-averaged Navier-Stokes (RANS) equations (or  $k$ - $\epsilon$  model).

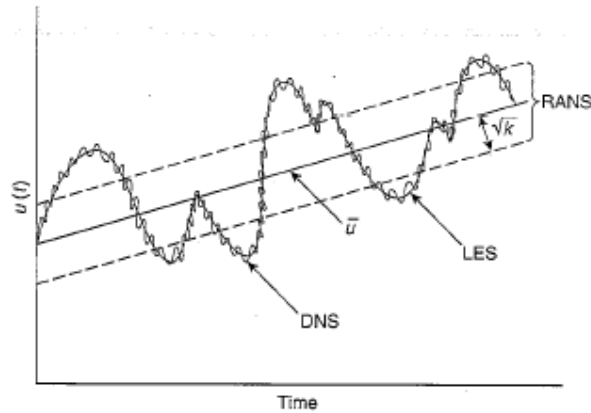


**Figure 5.1 Schematic representation of different treatments for turbulence.**<sup>[140]</sup>

FDS enables either the DNS or LES approaches to be applied. DNS involves direct solution of the Navier-stokes equations to model turbulent eddies at all scales. This requires a numerical grid on the order of 1mm or less and very small time steps. This is only appropriate for research on small-scale combustion and is not appropriate for large enclosure fire models. DNS is not considered further in this thesis.

LES assumes that it is the largest scale eddies that are mainly responsible for transport of momentum and energy in the flow field and that the structure of large eddies is dictated by geometry and flow type. Small eddies primarily have a dissipative effect on the large eddies and are more random in structure. In LES the Navier-Stokes equations are filtered to remove small eddies from the flow field, so that only large scales of fluid motion are solved by the filtered equations. A sub-grid scale (SGS) model is applied to describe the average dissipative effects of small eddies on large-scale fluid motion. There are a number of different SGS models applied in different CFD applications.<sup>[143,144]</sup> FDS applies the Smagorinsky SGS model.<sup>[145]</sup>

The RANS approach solves only for time averaged properties where the effects of turbulence at all length scales are averaged. Only the evolution of mean flow is modelled.<sup>[140]</sup> For fire models this approach does not model plume and ceiling jet entrainment correctly without significant empirical corrections.<sup>[5]</sup> There is no RANS capability in FDS.

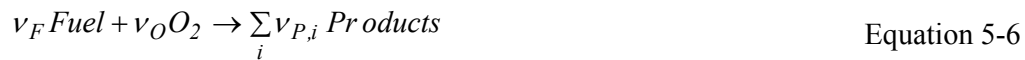
LES improves the simulation of turbulent fire effects compared with RANS and is generally accepted to be an appropriate hydrodynamic model for simulation of large enclosure fire. However there is some debate regarding validity of alternative SGS models.

### 5.2.2 Combustion Model

For both the “prescribed fire size” and “simulated fire growth approach” the fire is not represented as a point or area based heat source as is common in zone models. Instead, to capture the effects of distributed combustion, FDS models combustion of gaseous fuel.

Chemical processes of combustion for fire are extremely complex. The simulation of diffusion of oxygen and fuel and multi-step, rate controlled chemical equilibrium reactions<sup>[146]</sup> requires a fine grid and time step resolution that is impractical for LES models of large fire enclosures. Instead, as a default, FDS adopts a mixture fraction combustion model.<sup>[147]</sup> This is based on the very simplified assumption that combustion occurs at an instantaneous rate when fuel is exposed to oxygen. HRR is therefore calculated from the mixing rates of fuel and oxygen.

FDS defines combustion model parameters via its REAC name list group. The default parameters are set to represent propane. It is assumed that only a single hydrocarbon fuel is being burnt as represented by the following stoichiometric reaction:



Where the quantities  $v_i$  are the stoichiometric coefficient for the overall combustion process that reacts fuel “F” with oxygen “O” to produce a number of products “P”.

The species of interest, fuel and oxygen, at any location in the flow field are represented by a single variable, the mixture fraction  $Z(x,t)$  defined as follows:

$$Z = \frac{sY_F - (Y_O - Y_O^\infty)}{sY_F^I + Y_O^\infty}; \quad s = \frac{v_O M_O}{v_F M_F} \quad \text{Equation 5-7}$$

Where  $Y_O^\infty$  is the un-depleted ambient mass fraction of oxygen,  $Y_F^I$  is the mass fraction of fuel in the fuel stream,  $M_F$  and  $M_O$  are the fuel and oxygen molecular weights respectively. By design mixture fraction varies from  $Z=1$  in a region containing only fuel to  $Z=0$  in a region containing only ambient air, as shown in the state relation diagram for propane.

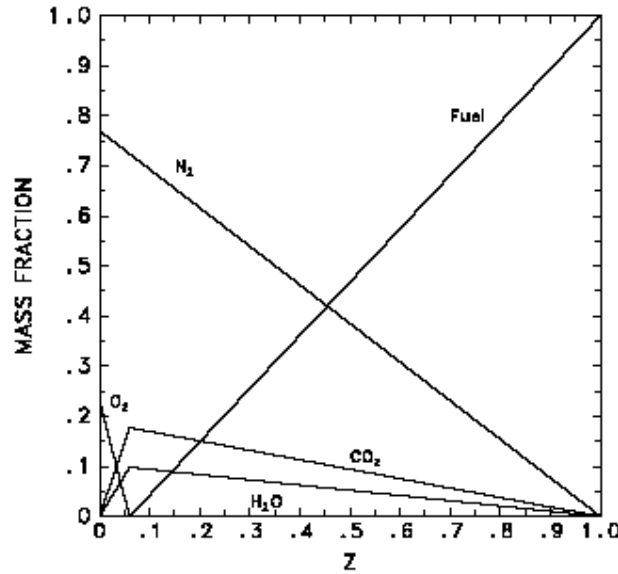


Figure 5.2. State relation diagram for propane.<sup>[141]</sup>

The assumption of instantaneous combustion implies that oxygen and fuel cannot coexist and  $Y_F=Y_O=0$  as shown in Figure 5.2. From Equation 5-7 the flame mixture fraction  $Z_f$  is obtained which defines the flame surface as a flame sheet:

$$Z_f = \frac{Y_O^\infty}{sY_F^I + Y_O^\infty}; \quad s = \frac{\nu_O M_O}{\nu_F M_F} \quad \text{Equation 5-8}$$

The oxygen mass conservation equation (Equation 5-2) is expressed in terms of mixture fraction  $Z$  to determine the mass rate of oxygen consumed at the flame sheet  $Z=Z_f$ . Huggett's relationship for HRR as a function of oxygen consumption<sup>[148]</sup> is applied to determine the local HRR:

$$\dot{q}''' = \Delta H_O \dot{m}''_O \quad \text{Equation 5-9}$$

FDS applies a default energy per unit mass of oxygen consumption of  $\Delta H_O = 13,100$  kJ/kg. As the flame sheet is a surface, the local flame sheet HRR is calculated in terms of local HRRPUA. FDS numerically locates the flame sheet

(where  $Z=Z_f$ ), computes the local HRRPUA and averages this energy over the entire volume of the grid cell cut by the flame sheet. For larger grid sizes this has the affect of reducing the calculated flame temperature.

For coarser grids the mixture fraction combustion model underestimates flame height.<sup>[149]</sup> Consequently HRR is also under predicted. FDS compensates for this by increasing the value of  $Z$  used to define the combustion region for coarse grids, which increases predicted flame height. The different value of mixture fraction used  $Z_{f,eff}$  is:

$$\frac{Z_{f,eff}}{Z_f} = \min\left(1, C \frac{D^*}{\delta x}\right) \quad \text{Equation 5-10}$$

Where  $C$  is an empirical constant,  $\delta x$  is the grid size and  $D^*$  is the characteristic fire diameter defined as:

$$D^* = \left(\frac{\dot{Q}}{\rho_a c_p T_a \sqrt{g}}\right)^{2/5} \quad \text{Equation 5-11}$$

FDS applies this compensation by default however it may be turned off using the `AUTOMATC_Z` input parameter.

For coarse grids the mixture fraction combustion model predicts a disproportionate amount of local HRR at the base of the fire. To compensate for this FDS applies a maximum limit on the local HRRPUA of flame sheet. This limit is based on the HRRPUA determined applying Heskestad's flame height correlation (see Section 4.3.5.2) and assuming a flame sheet that is conical in shape. For finer grids this limit is never reached. Any energy that is clipped off due to this limit is redistributed over the entire flame sheet volume.

The mixture fraction combustion model does not model flame suppression due to low temperatures and dilution of oxygen near the flame surface. To compensate, FDS implements an empirical suppression algorithm that prevents burning when the conditions in the flow field immediately adjacent to the flame sheet fall into a no burn region as described in Figure 5.3.

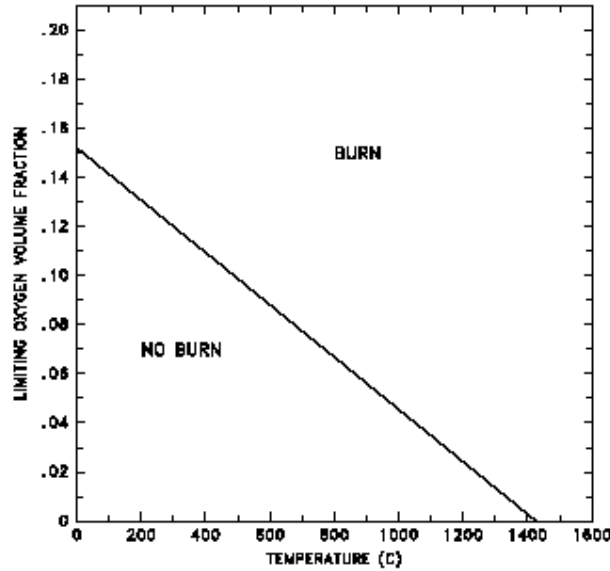


Figure 5.3. Oxygen-temperature phase space for burn and no burn conditions.<sup>[141]</sup>

The user may alter the no burn conditions by changing the parameters `CRITICAL_FLAME_TEMPERATURE` and `X_O2_LL` (limiting oxygen index) which have default values of 1427°C and 0.15 respectively. FDS applies the suppression algorithm by default but it can be turned off using the `SUPPRESSION` input parameter.

The net production of smoke particulate from the fire is simply assumed to be a constant fraction of the fuel mass burnt,  $y_s$  and is defined by the `SOOT_YIELD` input parameter (default = 0.01).

By default the fraction of fuel mass burnt converted into carbon monoxide,  $y_{CO}$ , is linked to soot yield via the following correlation for well ventilated fires:

$$y_{CO} = \frac{12x}{M_f v_f} 0.0014 + 0.37 y_s \quad \text{Equation 5-12}$$

Where  $x$  is the number of carbon atoms in the fuel molecule. Alternatively CO yield may be user defined as a constant fraction of fuel mass burnt using the `CO_YIELD` input parameter.

### 5.2.3 Thermal Radiation Model

FDS applies a finite volume method to solve the radiant transport equation for a non-scattering grey gas to estimate radiant heat flux. For grid cells of the order of a centimetre or larger the flame sheet temperature is underestimated due to temperature averaging across a cell cut by the flame sheet. Due to the  $T^4$  dependence, radiant heat intensity ( $I_b$ ) from the flame sheet is significantly under estimated applying Stefan-boltzmen law for black bodies. Instead, for cells in the flame sheet zone FDS applies an empirical estimate of the local radiant fraction ( $\chi_r$ ) of the chemical HRR per unit volume ( $\dot{q}'''$ ). Elsewhere, there is greater confidence in the computed temperatures and the Stefan-Boltzmann law is applied:

$$\kappa I_b = \begin{cases} \kappa \sigma T^4 / \pi & \text{Outside flame zone} \\ \max(\chi_r \dot{q}''' / 4\pi, \kappa \sigma T^4 / \pi) & \text{Inside flame zone} \end{cases} \quad \text{Equation 5-13}$$

FDS applies a default value for  $\chi_r$  of 0.35 which can be altered via the RADIATIVE\_FRACTION parameter.

For LES models FDS applies convection correlations to compute convective heat fluxes to surfaces. As radiant heat flux is typically orders of magnitude greater than convective heat flux for enclosure fires modelling of convection by FDS is not discussed in detail.

### 5.2.4 Thermal Boundary Conditions

The thermal boundary conditions assumed for an FDS simulation define the heat transfer at bounding surfaces. This significantly affects surface temperatures and fuel pyrolysis. Four types of thermal boundary conditions can be chosen for each different surface material in FDS:

- Fixed Temperature solid surface.
- Fixed heat flux solid surface.
- Adiabatic solid surface.
- Solid surface that heats up due to radiant and convective heat transfer.

The default boundary condition for all solid surfaces is a cold fixed temperature and non-combustible. Fixed heat flux and adiabatic boundary conditions are rarely applied in FDS fire growth simulations and are not discussed any further.

In order to model fire spread on a surface, the surface must be specified to heat up due to heat transfer. Such surfaces may be specified as either:

**Thermally thick** - a temperature gradient exists through the solid and a one-dimensional heat conduction equation for the material temperature  $T_s(x,t)$  is applied across the solid. For a thermally thick solid the following parameters must be prescribed:

- `KS` – Thermal conductivity (W/m-K) (may be ramped as a function of temperature).
- `DENSITY` – (kg/m<sup>3</sup>).
- `C_P` – Specific heat (kJ/kg/K) (may be ramped as a function of temperature).
- `DELTA` – Thickness (m).

**Thermally thin** – The temperature is assumed to be uniform across the thickness of the solid. Either the parameter `C_DELTA_RHO` (the product of specific heat, density and thickness) is prescribed or the three parameters `C_P`, `DELTA` and `DENSITY` are prescribed individually.

Other parameters that affect the simulated behaviour of thermally thick or thermally thin solids are `EMISSIVITY` and `BACKING` which defines the heat transfer at the back of the surface. The `BACKING` default is `VOID` (exposed to ambient air) but may be set to `INSULATED` (no heat loss at back) or `EXPOSED` (exposed to computational domain on both sides of the surface).

### 5.2.5 Pyrolysis Model

Production of gaseous fuel from combustible surfaces can be simulated by FDS in either of two ways:

- Specification of the `HRRPUA` parameter applies a prescribed, constant or ramped, production rate of gaseous fuel per unit area that is independent of thermal feedback to the surface once a specified ignition temperature is achieved; or
- Application of a pyrolysis model where `HEAT_OF_VAPORIZATION` and other parameters are specified and pyrolysis rate is affected by thermal feedback to the surface as described below.

For either of these two approaches the surface will not produce gaseous fuel until the surface has reached a specified ignition temperature which is input as the parameter `TMPIGN`.

Pyrolysis of solid surfaces applying `HEAT_OF_VAPORIZATION` may be modelled either as a thermoplastic or charring fuel.

#### 5.2.5.1 Thermoplastics

For thermoplastics it is assumed that pyrolysis occurs directly at the exposed surface. The solid may be modelled as thermally thick or thermally thin. In both cases surface temperature ( $T_{(0)}$ ) and mass loss rate of fuel ( $\dot{m}''$ ) are calculated based upon solution of the following two equations:

- An energy balance equation summing the rate of radiant and convective heat received, the rate of energy stored in the solid (related to rate to temperature change of solid), the rate of heat conducted through the solid (for thermally thick only) and the rate of energy required to vaporize the fuel (expressed as  $\dot{m}'' \Delta H_v$ ).
- The following Arrhenius expression for pyrolysis rate where  $R$  is the universal gas constant and  $A$  (pre-exponential factor) and  $E$  (activation energy in kJ/kmol) is prescribed so that the material pyrolyzes and burns in the neighbourhood of the prescribed `TMPIGN`.

$$\dot{m}'' = A\rho_s e^{-E/RT} \quad \text{Equation 5-14}$$

Although  $A$  and  $E$  may be directly input they are usually not known for real fuels. Instead the parameter `MASS_FLUX_CRITICAL` (kg/m<sup>2</sup>/s) is usually prescribed which directs FDS to chose  $A$  and  $E$  so that the fuel pyrolyzes at the rate `MASS_FLUX_CRITICAL` (default value is 0.02 kg/m<sup>2</sup>/s) when its surface reaches `TMPIGN`.

### 5.2.5.2 Charring fuels

By default if `HEAT_OF_VAPORIZATION` is specified the material is treated as a thermoplastic. However materials may be specified as charring fuels. Charring is simulated applying a one-dimensional model where pyrolysis is assumed to take place over an infinitesimally small front that leaves an insulating char in its wake as it progresses into the material. The virgin material and char are assumed to be thermally thick. The gaseous fuel produced is assumed to be instantaneously transported to the exposed surface. Governing equations for  $T_{(0)}$  and  $\dot{m}''$  for charring fuels<sup>[150,151]</sup> are :

- An energy balance equation summing the rate of radiant and convective heat received at the surface, the rate of energy stored and rate of energy conducted through both the virgin material and the char, and the rate of energy required to vaporize the fuel and evaporate moisture contained with the material.
- The following Arrhenius expression for pyrolysis rate where  $\rho_{s0}$  and  $\rho_{char}$  are the density of the virgin material and char respectively:

$$\dot{m}'' = A(\rho_{s0} - \rho_{char})e^{-E/RT} \quad \text{Equation 5-15}$$

- Progress of the pyrolysis front into the material is given by the following equation for velocity of the front:

$$v = \frac{\dot{m}''}{\rho_{s0} - \rho_{char}} \quad \text{Equation 5-16}$$

For charring fuels the following parameters must be specified:

- HEAT\_OF\_VAPORIZATION – heat required for vaporization of virgin material at pyrolysis front.
- MOISTURE\_FRACTION – mass fraction of water in virgin material.
- DELTA - Initial thickness of material.
- Density, thermal conductivity and specific heat for both the virgin and char materials (as required for thermally thick model).
- TMPIGN - Ignition temperature.
- Either *A* and *E* or MASS\_FLUX\_CRITICAL.

### 5.2.5.3 Other parameters influencing pyrolysis

The following parameters also affect simulation of pyrolysis:

BURNING\_RATE\_MAX (kg/m<sup>2</sup>/s) imposes an upper limit on the rate of pyrolysis. FDS uses this parameter in recognition that errors due to model assumptions often result in over prediction of heat flux to surfaces, resulting in unreasonable pyrolysis rates.<sup>[141]</sup> The default for BURNING\_RATE\_MAX is 0.1 kg/m<sup>2</sup>/s.

If BURN\_AWAY is set to true then burning material will be removed as the mass contained within the volume of each grid cell is consumed until no material remains. Due to the extra memory required for this calculation BURN\_AWAY is set to false by default resulting in continuous modelling of pyrolysis regardless of the quantity available for consumption.

The mixture fraction combustion model assumes only one gaseous fuel. The heat of combustion of this fuel is implicitly defined by parameters for reaction stoichiometry and the energy release per unit mass of oxygen consumed ( $\Delta H_O$ ). If it is desired to specify a second material that produced volatiles with a different reaction stoichiometry or  $\Delta H_O$  then the HEAT\_OF\_COMBUSTION parameter can be applied. This adjusts the pyrolysis rate of the one gaseous fuel from the given material to compensate for the difference in stoichiometry or  $\Delta H_O$ .

## **5.3 VALIDITY/LIMITATIONS OF HRR PREDICTION BY FDS**

### **5.3.1 Causes of Error for HRR Prediction**

Based on the review of governing theory and assumptions in Section 5.2, the following sources of error for simulation of fire growth and prediction of HRR by FDS have been identified.

#### **5.3.1.1 Grid resolution**

Grid resolution significantly affects the error of simulations of hydrodynamic, heat transfer, pyrolysis and combustion phenomena which, in reality, occur on very small scales. Ideally, sensitivity analysis, where the grid resolution is increased until a grid independent result is achieved, should be performed on simulations. However, in practise grid resolutions are normally limited by computing and time resources which may lead to a large error.

#### **5.3.1.2 Mixture fraction combustion model**

The mixture fraction combustion model is a substantial simplification of the combustion that occurs in real fires. This simplifying model is a source of errors.

The mixture fraction model has been found to be sensitive to grid resolution and for coarser grids will underestimate flame height and HRR. Although FDS attempts to compensate for this by modifying the stoichiometric mixture fraction, this modification is only empirically based on axi-symmetric flames<sup>[149]</sup> and is likely to introduce additional errors for more complex scenarios such as enclosure fires with flame spread along surfaces. One study comparing predicted and measured fire sizes of pool fires in enclosures reveals that this empirical modification may be responsible for some deviations of predicted fire sizes from a grid independent solution.<sup>[152]</sup>

The mixture fraction model assumes stoichiometric combustion. This may introduce errors for simulations of under ventilated fires where non stoichiometric combustion usually occurs.

The mixture fraction model does not allow fuel and oxygen to coexist due to suppression of combustion in low temperature or oxygen conditions. FDS attempts to

compensate applying an empirical model for flame extinction. However this empirical model does not capture the full complexity of flammability limits.

#### 5.3.1.3 Soot and other gas species yields

FDS assumes soot yield and yields of other species is directly proportional to the mass of fuel burnt. In reality, incomplete combustion caused by restricted ventilation results in significant increases in soot yield. This is neglected by FDS. Soot affects emissivity of both flames and hot gas. This is likely to be a source of error affecting predicted heat fluxes, particularly for poorly ventilated fires.

#### 5.3.1.4 Radiant heat flux

Due to the high temperatures of flames and combustion gases, radiant heat is normally the dominant mechanism for heat transfer in fire enclosures. Inaccuracies in predicted heat transfer can be a cause of significant errors in pyrolysis and HRR predictions.

For grid resolutions practical for the resources of most modellers the flame sheet temperature is underestimated due to temperature averaging across a cell cut by the flame sheet. Due to the  $T^4$  dependence, radiant heat intensity from the flame sheet is significantly under estimated applying the Stefan-boltzmen law.

FDS attempts to compensate for this applying an empirical radiant heat fraction of local HRR per unit volume of flame sheet. However this introduces other errors as the radiant heat fraction varies with different fuels and ventilation conditions. Uncertainty in absorption and emission coefficients also introduces errors. The FDS technical reference guide<sup>[141]</sup> states that heat flux is often over estimated due these empirical constants.

#### 5.3.1.5 Material properties

Material properties include combustion reaction parameters and parameters to characterise the materials thermal and pyrolysis behaviour. There is usually very limited, if any, data available for the required material properties. Selection of inputs which poorly represent materials actual properties is potentially the largest source of error for simulated fire growth. The range of material properties that must be input to

FDS and methods of selection or measurement of these properties are summarised in Section 5.4

#### 5.3.1.6 Pyrolysis models

FDS only enables surfaces constructed of single material layers to be modelled. In reality many interior surfaces consist of multiple layers of materials. This is a source of error especially where the different layers may behave significantly differently as they become exposed in a fire.

Prescribing a materials pyrolysis rate (either as a constant or as a curve determined from tests such as the cone calorimeter) and ignition temperature via the parameters `HRRPUA` and `TMPIGN` is the simplest approach. However after the ignition temperature is achieved this approach neglects the affect of thermal feedback (which in reality controls pyrolysis). This results in a similar assumption as for Dugan's method (where `HRRPUA` is multiplied by exposed surface area) except that ignition of the surface is delayed by achievement of ignition temperature. This results in significant error.

While use of the thermoplastic and charring fuel pyrolysis models is theoretically more realistic it introduces errors relating to radiant heat and material property inputs. Many common materials are not well represented by the thermoplastic model. The charring fuel model is very simplistic and does not include behaviour such as cracking or degradation of the char layer. In reality pyrolysis involves multiple stages of transition rather than the simple single step models incorporated in FDS.

#### 5.3.1.7 User competence

A number of significant sources of error, mostly stemming from required simplifying assumptions in FDS, have been identified. The user's competence is critical in both;

- Managing and minimising the errors for a given simulation
- Interpreting results given a knowledge of the errors.

### 5.3.2 Experimental validation of HRR prediction

There is no definitive quantification of the accuracy of FDS available in the literature primarily because accuracy varies depending on the application. There has been no single, consistent, effort to validate all predictive outputs of FDS over the entire possible range of its application against experimental data. Instead there have been many efforts at validating specific predictive outputs for specific applications. Most of the validation work has focused on prediction of fire generated temperatures, smoke and flows given a prescribed fire size. Far less validation work has focussed on simulated fire growth predictions of flame spread and HRR. The following is brief summary of experimental validation related to HRR prediction by FDS

Quintierre and Ma<sup>[149]</sup> studied axi-symmetric fire plumes comparing predicted flame heights and plume centre line temperatures to both empirical correlations and experimental data. Good agreement occurred in the far field plume region except for very coarse grids, but results near the flame region were very grid dependent. This work was instrumental in developing the adjustment to stoichiometric mixture fraction for larger values of  $D^*/\delta x$ . Predicted flame temperature was found to increase with decreasing grid resolution and was over predicted for very fine grids.

At the time of adoption of the current mixture fraction combustion model and radiation model Floyed et al.<sup>[147,153]</sup> compared predictions and experimental results for fires in a medium sized enclosure 1.2m x 1.8m x 1.2 m high. Fires ranged from well ventilated to under ventilated and ranged in size from 90 kW to 440 kW. Predictions matched well for well ventilated tests with temperatures and heat fluxes within 15%; however the performance of FDS degraded for under ventilated fires with over prediction of enclosure temperatures and the size of the upper layer. FDS over predicted the amount of combustion occurring inside the enclosure.

Liang<sup>[154]</sup> compared simulations and experimental temperatures and heat fluxes on a non combustible wall with a propane burner placed against the wall. Temperatures and heat fluxes were within 30% however they were significantly over predicted in the flame (fuel rich) region and under predicted in the upper plume region. Liang also compared simulations to Factory Mutual Research Corporation experiments for flame

spread on 5m and 1.2 m PMMA (polymethyl-methacrylate) vertical walls. Mixed results were obtained with good predictions for the 5 m wall but significant over prediction of flame spread and HRR for the 1.2 m wall. Kwon<sup>[155]</sup> also compared FDS prediction to Factory Mutual Research Corporation experiments of flame spread on a 5m vertical PMMA wall. In this case, the flame spread, HRR and pyrolysis were not well matched. When the `AUTOMATIC_Z` function was turned off the prediction became worse with very early onset of flame spread.

Hostikka et. al.<sup>[156]</sup> compared simulations and experiments for pyrolysis and combustion of wood in cone calorimeter experiments and ISO 9705 experiments. Reasonable predictions for the cone calorimeter were achieved for high imposed heat fluxes of 50 kW/m<sup>2</sup> and 30 kW/m<sup>2</sup>, however poor predictions were achieved for 20 kW/m<sup>2</sup> and 15 kW/m<sup>2</sup> with ignition time predicted too early. Predictions of ISO 9705 were very grid dependent. Predictions did not improve for decreasing grid resolution for the range of resolutions reported.

Moghadam et. al.<sup>[157]</sup> assessed simulations of ISO room pool fire tests and ISO room tests with fire spread on timber linings. For ISO room pool fire tests temperatures were predicted with close agreement applying a prescribed HRR. For the ISO room fire tests with flame spread, onset of flashover and HRR were poorly predicted. There was significant variation of results as grid size and choice of fuel reaction were varied. Predictions did not improve for decreasing grid resolution.

As part of experiments to validate FDS for use in a world trade centre investigation NIST compared simulations and experiments for a fire involving three office workstations in a compartment.<sup>[158]</sup> Pyrolysis of some materials such as desks, partitions and carpet were defined using `HEAT_OF_VAPORIZATION` other materials such as boxes and papers were defined using `HRRPUA`. Peak HRR and temperatures were predicted to within 20% for all tests however there were significant deviations in the timing and trends for HRR and temperature curves. The input parameters had been tuned based on free burns of single work stations prior to simulating the full enclosure experiments.

VTT have conducted a large range of validation assessments. The materials assessed include spruce timber, MDF board, PVC wall carpet, upholstered furniture, electric cables and heptane pool fires. Experiments used for validation include cone calorimeter, SBI (single burning item) test and room corner tests. For all materials the predictions of cone calorimeter results were extremely well matched suggesting that cone calorimeter results had been used as a basis to selection and tuning of input parameters to be used for all other test simulations. For SBI tests and room fire tests on Spruce and MDF the prediction of HRR during fire growth and time to flashover was extremely well matched which is surprising considering other validation work on timber materials, however post flashover HRR was poorly predicted. For wall carpet the SBI and room fire tests results were heavily influenced by the backing insulation specified, results for the room fire test were very poor. For SBI and room fire tests on upholstered furniture the ignition delay and HRR during fire growth was not well matched with ignition and growth predicted too early.

In summary:

- Validation of FDS simulated fire growth is very limited, particularly for enclosures with multiple materials.
- No validation of FDS applied to simulate fire growth on passenger trains has been found in the literature.
- Simulation errors are typically much higher where FDS is applied to simulate fire growth than for applications where HRR is specified.
- Errors appear to increase for under ventilated fires.
- FDS simulated fire growth does appear to qualitatively approximate trends such as fire spread and flashover (with large errors) however this is critically dependent on correct input selection.
- Users should validate simulations with experiments where possible and interpret results carefully given the errors and unknowns.

## 5.4 MEASUREMENT OF MATERIAL PROPERTIES FOR INPUT TO FDS

Input material properties have a dominant affect on predictions of fire growth. Depending on the pyrolysis model applied there are a large number of inputs used to characterise material properties as summarised in Table 5-1.

**Table 5-1 Inputs parameters for material properties**

Parameter	Description	Units
<b>Parameters critical to pyrolysis model</b>		
DELTA	Material thickness	M
DENSITY, CHAR_DENSITY	Density, density of char (may also be specified as a ramped property)	kg/m <sup>3</sup>
C_P, C_P_CHAR	Specific heat, specific heat of char (may also be specified as a ramped property)	kJ/kg.K
C_DELTA_RHO	Product of specific heat, thickness and density may be specified for thermally thin materials in place of individual parameters	kJ/m <sup>2</sup> .K
KS	Thermal conductivity, thermal conductivity of char (may also be specified as a ramped property)	W/m.K
TMPIGN	Ignition temperature	°C
HEAT_OF_VAPORIZATION	Heat of vaporisation	kJ/kg
A	Arrhenius pre-exponential factor	m/s
E	Arrhenius activation energy	kJ/kmol
MASS_FLUX_CRITICAL	Mass flux at TMPIGN (specified in place of A and E)	kg/m <sup>2</sup> .s
MOISTURE_FRACTION	Water content by mass (only specified for charring pyrolysis0)	kg/kg
<b>Parameters affecting behaviour but not critical to pyrolysis model</b>		
BACKING	Back face boundary condition (insulation)	Logic
BURN_AWAY	Remove burnt mass	Logic
BURNING_RATE_MAX	Limit pyrolysis to a maximum burning rate	kg/m <sup>2</sup> .s
HEAT_OF_COMBUSTION	Heat of combustion (adjusts pyrolysis rate to compensate for a difference in stoichiometry etc)	kJ/kg

In many instances users simply adopt material properties either from the database supplied with FDS V4 or from literature for a material deemed similar to the material to be modelled. It is difficult to obtain valid material properties as the database and literature only contain properties for a limited number of materials. The properties for similar materials may be significantly different due to formulation or fire retardants. This can result in significant errors in the simulation. The materials database has been removed from FDS V.5 to encourage users to more carefully select properties.

There is no established process recommended by the developers of FDS to determine material properties based on experimental data.<sup>[159]</sup> The most common approach is to conduct well instrumented cone calorimeter tests and conduct iterative FDS

simulations of the cone calorimeter tests, altering estimates of material properties until a reasonable agreement between simulation and experiment is achieved. Examples of this approach are presented by Jiang<sup>[160]</sup> and Lee.<sup>[161]</sup> Conducting the iterative simulations is a laborious task due to the multiple parameters that can be varied. Some parameters can be eliminated by direct measurement as follows:

- Thickness can be directly measured.
- Density can be calculated from mass and volume measurements.
- Moisture content may be calculated from mass measurements and oven drying.
- Ignition temperature may be measured by measuring surface temperature prior to ignition in cone calorimeter tests. Surface temperature has been measured either applying fine wire thermocouples or infrared pyrometers. Sources of error for thermocouple measurement are radiant heating of the thermocouple tip and poor surface contact. Errors for infrared measurement are unknown emissivity and reflected radiant heat. Measurement of back face and internal temperatures is useful for estimating other thermal properties such as specific heat and thermal conductivity.
- Activation energy and pre-exponential factor may be estimated based on thermo gravimetric analysis (TGA).<sup>[160]</sup>

The remaining parameters are estimated from FDS cone calorimeter simulations where input parameters are iteratively varied to obtain a good match of simulation results to experimental results.

It is suggested that the iterative selection of parameters be conducted in two stages:

- Stage 1. Iterative simulations of the test prior to ignition are compared on the basis of measured surface temperatures (and other temperatures if measured). From this thermal conductivity and heat capacity are estimated.
- Stage 2. Iterative simulations of the test including after ignition are compared on the basis of measured mass flux and HRR curves. From this heat of vaporization, activation energy and pre-exponential factor are estimated.

Lautenberger et. al.<sup>[162]</sup> have developed and applied an automated optimisation technique to determine material parameters. Software is used to automatically re-run FDS cone calorimeter simulations and a genetic algorithm is used to locate a set of input parameters that provide optimal agreement between the model predictions and the experimental data. This eliminates the laborious task of manual iterative simulation, reduces the number of iterations required and generally produces cone calorimeter simulations with good agreement to experimental data.

Chiam<sup>[163]</sup> has applied correlations for determining the required material properties directly from cone calorimeter data.<sup>[164]</sup> Critical radiant heat flux for ignition is determined as a function of time to ignition at different exposed heat fluxes. Ignition temperature is determined as a function of critical radiant heat flux. Thermal inertia ( $k\rho c$ ) is determined as a function of time to ignition at different exposed heat fluxes, critical radiant heat flux and ignition temperature. Heat of vaporization is determined as a function of effective heat of combustion and peak HRR at various exposure heat flux levels. However when properties determined using these procedures were used to simulate the original cone calorimeter experiments very poor agreement was found for both time to ignition and the resulting HRR curve. Subsequently properties determined using these procedures were discarded and properties were calibrated against cone calorimeter results using iterative simulations.

Properties can be significantly influenced by, and are sometimes defined by, the experimental conditions used to measure them. For example ignition temperatures measured in the cone calorimeter are typically much lower than ignition temperatures measured in furnace apparatus.<sup>[165]</sup>

As discussed in Section 5.2, the governing assumptions of FDS do not fully describe the phenomenon of ignition and combustion. Therefore material properties based on calibration of simulations against cone calorimeter tests may not accurately represent the actual properties of the material. No experimental validation has been found in literature determining if properties based on cone calorimeter tests provide optimal agreement for simulation of larger fires with significantly different fire conditions to the conditions of the cone calorimeter.

## 5.5 APPLICATION OF FDS TO PASSENGER TRAIN FIRES

FDS has been applied by fire engineers to model fire growth on passenger trains however often the results are not published for reasons of commercial security. The following examines two examples of application of FDS to predict fire size for passenger train interiors. In the second example, FDS simulations of the full scale passenger train experiment were developed and compared.

### 5.5.1 Simulation of a Singapore metro train fire

Chiam<sup>[163]</sup> has used FDS to simulate fire scenarios on a Singapore metro train. The objective was to predict the peak HRR for tunnel ventilation system design.

#### 5.5.1.1 Singapore metro train geometry and materials

The metro train consisted of single deck carriages connected as 3 car sets. Cars were connected by a flexible bellows connection providing open gangways with no end door fitted, resulting in no barrier to fire spread between cars. Each carriage interior was approximately 23 m long, 3.2 m wide and 2 m high. There were six windows and four passenger doors on either side of each carriage. Each carriage had approximately 50 seats arranged longitudinally backing against the wall on each side of the carriage. The main exposed interior materials are summarised in Table 5-2.

**Table 5-2 Singapore metro train materials**

Component	Material
Seats	Polyester GRP – hard moulded seats with no cushion material
Floor covering	Styrene butadiene – a type of synthetic rubber
Wall and ceiling lining	Aluminium with a thin coat of powder paint
Windows	Laminated safety glass
Gangway bellows	WPE Varmac – a type of elastomer

The fire load is significantly less than typical for Australian passenger trains which usually have more seats with cushioning and more use of GRP for wall and ceiling linings. The above floor fire load was 17900-20700 MJ depending on the particular carriage from the 3-car set. A complete 3-car set stopped inside a tunnel was simulated.

### 5.5.1.2 Fire scenarios

Two alternative ignition sources were modelled:

- An arson ignition source with a constant HRR of 200 kW for a 1800s period.
- A larger ignition source with a constant HRR of 1500 kW for a 1800s period.

The larger ignition source was intended to represent an undercarriage fire that burns through the floor. Several different scenarios for ignition source location and carriage ventilation were simulated but most were not found to result in fire spread or flashover. Window failure was assumed to occur when the modelled temperature on each window exceeded 675 °C. A constant tunnel ventilation rate of 31 m<sup>3</sup>/s (2.2 m/s longitudinal velocity) was assumed for all simulations. The direction of flow was from the rear to the front of the train.

### 5.5.1.3 Simulation approach and parameters

Two different methods of defining rate of fuel pyrolysis were applied in separate simulations and compared. One method was the specification of HRRPUA and the other was specification of heat of vaporization with all combustibles assumed as thermoplastic. Combustion reaction parameters based on average values from literature for polyester GRP were applied instead of the default values for propane. Only seat and floor materials were modelled as combustible. All other materials such as wall and ceiling linings and windows were modelled as non-combustible.

The final simulations of the complete train applied a computational domain 70 m long by 5.5 m wide by 4.4 m high. Some initial simulations of a smaller domain of one carriage were run to conduct grid sensitivity analysis and investigate simulation behaviour applying material properties from literature.

Grid sensitivity analysis was conducted applying grid resolutions of 300, 200 and 150 mm. Simulations with all 3 grid resolutions were found to give consistent prediction of HRR for all scenarios simulated. On this basis a grid resolution of 300 was chosen for final simulations

The total simulation time was 3600 s. The computers used were Intel ® Pentium 4®, 3.2 GHz, 1 GB RAM. Times taken to complete simulations were between 20 to 80 hours each.

#### 5.5.1.4 Material property parameters

Average material properties from literature were used for initial simulations. Materials were initially assumed to be thermally thick.

Cone calorimeter tests were conducted on seat material and flooring material at exposure heat fluxes of 25, 35, 50 and 65 kW/m<sup>2</sup>. Due to limited samples the seat specimens were 100mm x 50 mm. Surface temperature was not measured.

Chiam<sup>[163]</sup> applied correlations for determining the required material properties directly from cone calorimeter results.<sup>[164]</sup> Based on the correlation of time to ignition both the seat and floor materials were treated as thermally thin.

**Table 5-3 Material properties from literature vs. derived from cone calorimeter tests**

Material Property	Seat – polyester GRP		Flooring	
	Average values from literature used for initial simulations	Derived from test data using correlations	Average values from literature used for initial simulations	Derived from test data using correlations
TMPIGN (°C)	346	488	360	419
C_DELTA_RHO (kJ/m <sup>2</sup> K)	n/a	3.341	n/a	8.363
HEAT_OF_COMBUSTION (kJ/kg)	12870	13670	17950	14570
HEAT_OF_VAPORIZATION (kJ/kg)	1390	10300	2700	12320
MASS_FLUX_CRITICAL (kg/m <sup>2</sup> s)	Default	0.0044	default	0.0024
BURNING_RATE_MAX (kg/m <sup>2</sup> s)	0.021	0.0161	0.01	0.0079

However when properties determined using these procedures were used to simulate the original cone calorimeter experiments very poor agreement was found for both time to ignition and the resulting HRR curve.

To improve prediction of cone calorimeter results, iterative simulations of cone calorimeter experiments were used to calibrate a restricted number of material property parameters. For the HRRPUA method  $\rho c \delta$  was calibrated. For the HEAT\_OF\_VAPORIZATION method  $\rho c \delta$  and HEAT\_OF\_VAPORIZATION was calibrated. The values of these parameter required to match simulations to test data was found to vary significantly with exposure heat flux. However the following values were selected

**Table 5-4 Calibrated properties for HRRPUA method**

Material	$\dot{q}_e''$ (kW/m <sup>2</sup> )	Calibrated $\rho c \delta$ (kJ/m <sup>2</sup> K)
Floor covering	25	22.2
Seat – polyester GRP	35	5.4
Seat – polyester GRP	50	3.94

**Table 5-5 Calibrated properties for heat of vaporization method**

Material	Calibrated $\rho c \delta$ (kJ/m <sup>2</sup> K)	$\Delta H_v$ , (kJ/kg)
Floor covering	3700	6250
Seat – polyester GRP	5.4	13.9

The large variance in material properties demonstrates the difficulty selecting appropriate values.

#### 5.5.1.5 Simulation results

Final simulations of the entire 3-car set applying the 200 kW and 1500 kW ignition sources did not predict any significant fire spread except for one scenario applying a 1500 kW ignition source with doors at both ends of the train open. In this case flashover conditions resulting in window failure and fire spread through the entire train was predicted. Chiam concludes that forced airflow through the train due to tunnel ventilation influenced fire spread for this scenario. The lack of fire spread for

other scenarios may be reasonable considering the sparse fuel load and assumption of non-combustible wall and ceiling linings. However in reality it is possible for painted surfaces to ignite and influence flashover. The prediction of peak HRR and time to flashover for this scenario are summarised in Table 5-6.

**Table 5-6. Simulation results for flashover scenario**

<b>Pyrolysis prediction method</b>	<b>Peak HRR</b>	<b>Time to flashover</b>
HRRPUA method	11.8 MW	600s
Thermoplastic model	8.2 MW	900s

Because there is no comparison of the simulated results against full-scale experimental data, it is not possible to determine if the simulation results are realistic. Although there is significant difference in the results of the two pyrolysis prediction methods, they both predict the same general trends of fire behaviour. This example demonstrates the difficulties in selecting appropriate input parameters and how errors and assumptions reduce confidence in accuracy of predictions for fire growth, fully developed fire size and fire duration.

### **5.5.2 WPI Simulations of Full-Scale Train Fire Experiment**

FDS Simulations of the full-scale train fire experiment described in Section 3.5 have been undertaken by fire engineering students at Worcester Polytechnic Institute. The objective was to obtain an estimate of the HRR curve based on development of an FDS simulation that has good agreement with experimental measurement.

The work was conducted in two stages by two separate student groups. In Stage 1<sup>[166]</sup> an initial FDS model of the experiment was developed. Stage 2<sup>[167]</sup> attempted to improve upon perceived flaws in the initial model. The author of this thesis provided students with an experimental report, experimental data including cone calorimeter test results for interior materials (without surface temperature measurement) and guidance regarding the experimental methodology, measurements and observations. Based on this the students developed the models independently.

### 5.5.2.1 Stage 1 – Initial simulation of full-scale experiment

The geometry and interior layout of the experiment was represented in the model with only limited rounding of dimensions to fit the computational grid. A grid resolution of 60 mm was applied. No details of grid sensitivity analysis were reported. The computational domain only extended approximately 400 mm beyond the exterior of the carriage. It is noted that this domain would be insufficient to model the HRR from flames external to the vehicle which extended up to 3.5 m above the vehicle. The mixture fraction combustion model was applied and reaction parameters for polyurethane, taken from literature were applied. Pyrolysis of the GRP, seat cushion and carpet materials was modelled by specification of `HEAT_OF_VAPORIZATION`. Initial material properties were selected from literature and iterative simulations of cone calorimeter experiments for these materials were used to improve selected material properties. For this purpose, PYRO4, a demonstration simulation provided with FDS that models pyrolysis and combustion of a 200 mm x 200 mm sheet of material given an exposed heat flux was used. Results were scaled proportional to 100 mm x 100 mm cone calorimeter sample size. The GRP and seat cushions were modelled as thermoplastic and the carpet was modelled as charring. The input parameters varied were `HEAT_OF_COMBUSTION` and `BURNING_RATE_MAX`. Other properties were maintained as literature values. Resulting cone calorimeter simulations are compared against experimental results in Figure 5.4 to Figure 5.6.

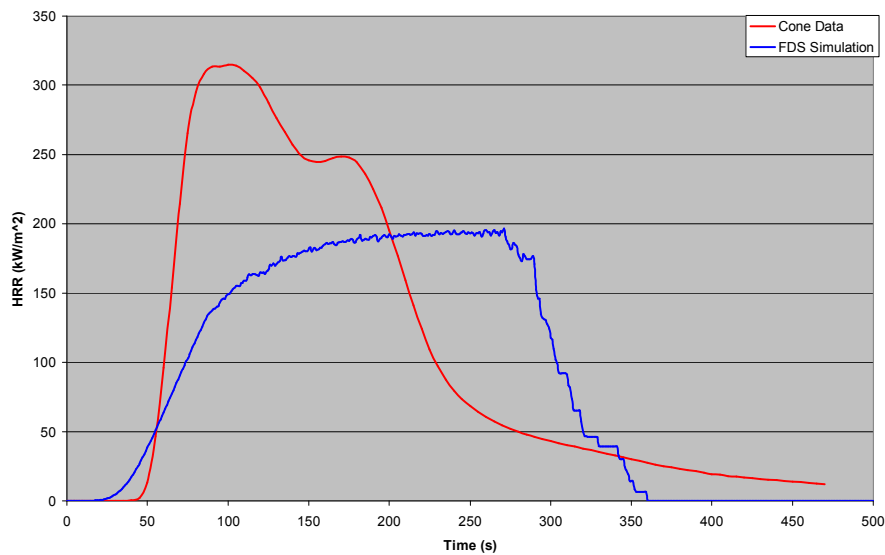


**Figure 5.4. Simulated and experimental cone calorimeter results for GRP at exposed heat flux of 35 kW/m<sup>2</sup>**

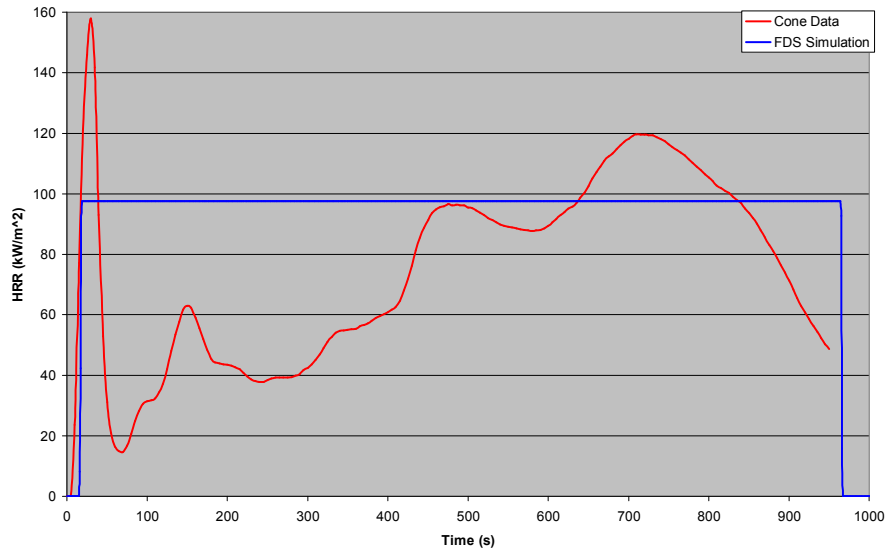


**Figure 5.5. Simulated and experimental cone calorimeter results for seat cushion assembly at exposed heat flux of  $35 \text{ kW/m}^2$**

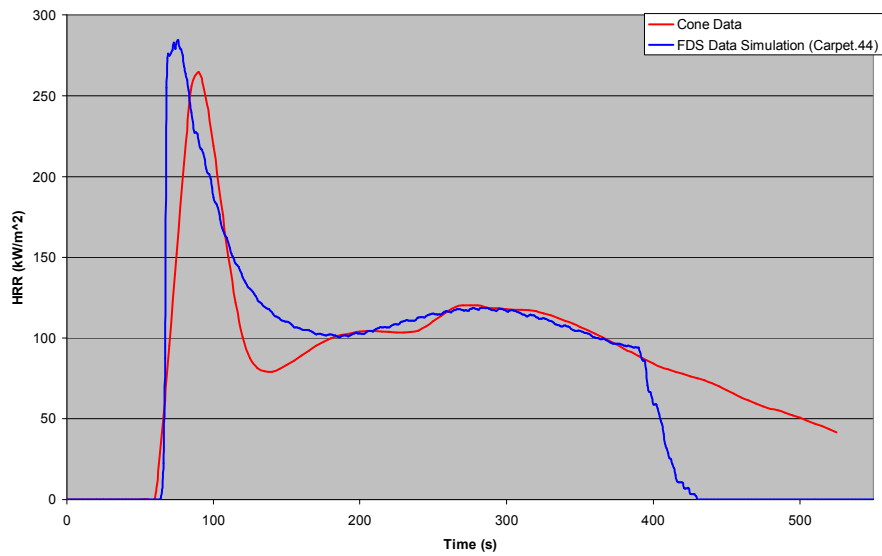


**Figure 5.6. Simulated and experimental cone calorimeter results for carpeted at exposed heat flux of  $35 \text{ kW/m}^2$**

Cone calorimeter simulations and experiments were matched based on total heat released and burn time. Material properties were also tuned based on initial simulations of the full-scale experiment. As a result the simulated trends for instantaneous HRR curves for GRP and seat cushions are poorly matched to experimental results. The carpet was initially modelled as a thermoplastic. Initial simulations of the full-scale experiment resulted in no ignition and flame spread on the carpet. Subsequently the carpet was remodelled as a charring fuel with better

agreement to cone calorimeter results. Steel and glass were modelled as non combustibles. The exposed plywood floor was modelled as charring applying the FDS database properties for spruce. Paper faced plasterboard (used to block openings) was modelled with a prescribed HRRPUA of  $100 \text{ kW/m}^2$ , a TPIGN of  $400 \text{ }^\circ\text{C}$  and a thickness of 13 mm. The reasoning for this is not reported however it is an overestimate of sustained HRR of plasterboard which has a very thin layer of combustible paper facing.

For the 1kg newspaper ignition source the students were provided two sets of fire calorimeter data. One for 1 kg of crumpled paper piled on an open floor with a peak HRR of 180 kW and one for 1 kg crumpled paper piled under a non-combustible seat against a non-combustible wall corner, with a peak HRR of 140 kW more truly representing the conditions of the full-scale experiment. The students applied the 180 kW peak HRR data by inputting it as a vent with a prescribed HRR curve.

Windows in the simulation were specified to open at the observed experimental failure times. The effects of wind were neglected as they were not well characterised in the experiment.

Many preliminary simulations of the full-scale experiment were run with results in poor agreement with the experiment. Initially flashover and ignition and fire spread on the flooring were not predicted. Model inputs were modified to improve agreement of the simulation. The final simulation was run for a total simulation time of 1000s. Only results for the final simulation were reported by the students. Example plots of simulated temperatures compared with experimental temperatures are provided below.

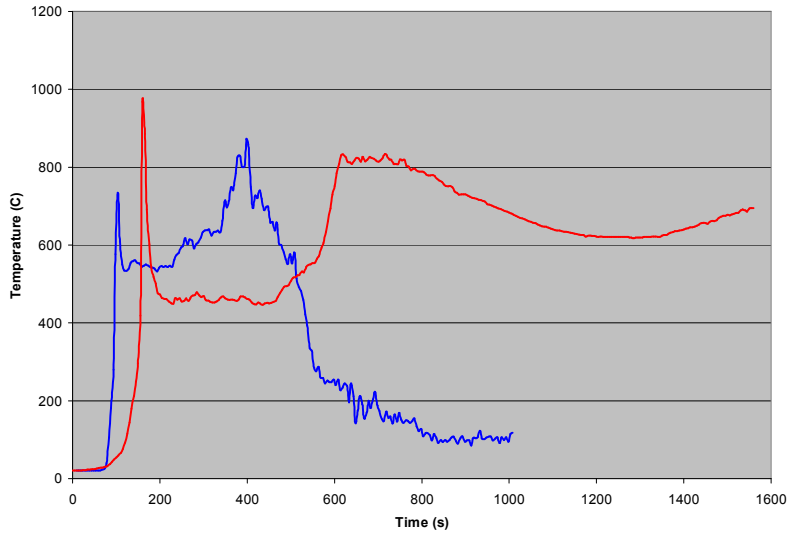


**Figure 5.7.** Comparison of simulated and experimental temperature at thermocouple A2

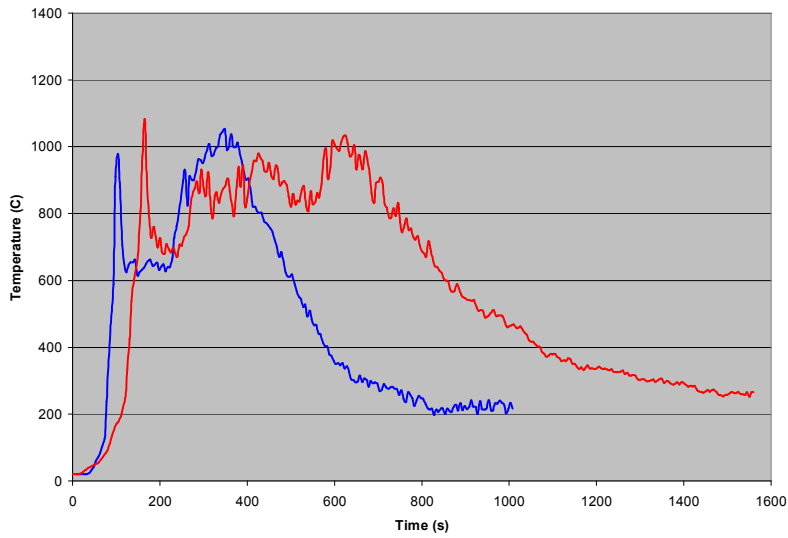


**Figure 5.8.** Comparison of simulated and experimental temperature at thermocouple B3

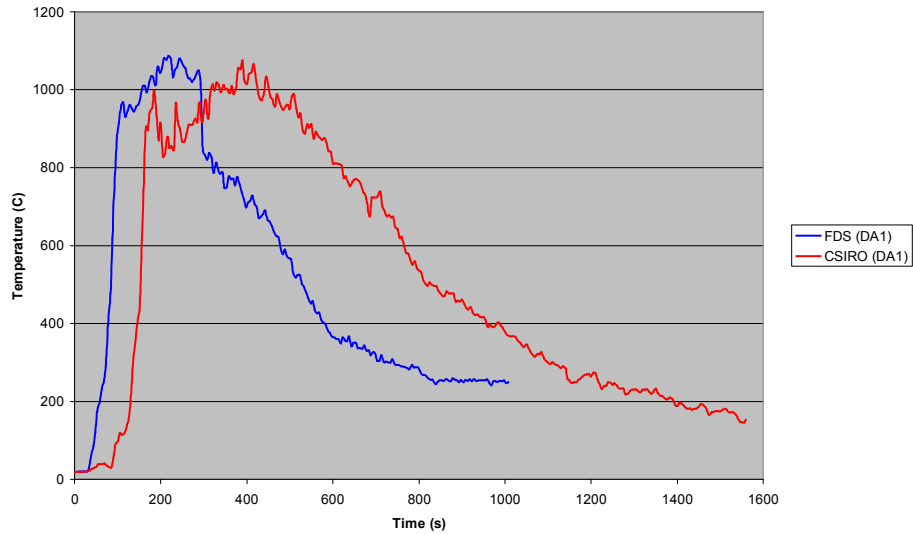


**Figure 5.9.** Comparison of simulated and experimental temperature at top of Door A

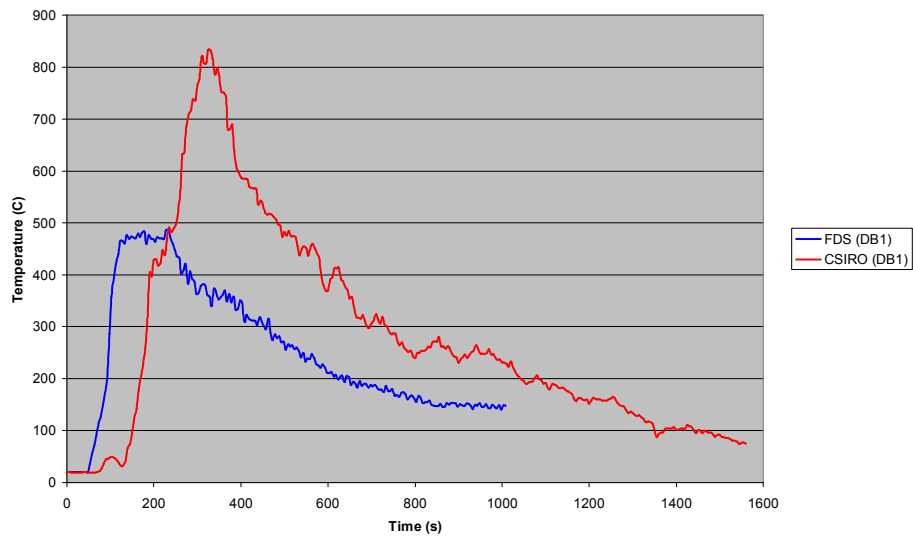


**Figure 5.10.** Comparison of simulated and experimental temperature at top of Door B

As discussed in Section 4.3, temperatures provide a good indication of trends in fire growth and decay. The simulation roughly predicted similar magnitudes and trends of temperature growth and decay. The simulation predicted flashover and fire spread through the entire section of the vehicle fitted with materials as occurred in the experiment

However the simulation deviated from the experiment as it predicted a significantly earlier onset of flashover at 90 s compared 140s as observed in the experiment. Also

the temperatures indicate that the simulated fire burned out and decayed much earlier than observed in the experiment.

The trough in internal carriage temperatures observed after flashover in the experiment due to restricted ventilation and choked combustion inside the carriage prior to significant window failure, was predicted by the simulation. However the timing of this was earlier for the simulation.

The simulation failed to predict flames extending to Door B. The flame sheet in the simulation did not extend far past the middle of the carriage. The model did not simulate external flame plumes or the contribution of these flames to HRR due to the restricted domain.

The resulting HRR curve predicted by the simulation is shown in Figure 5.11. The simulation sustains a relatively steady HRR of 8 MW from 100 – 250 s and then decays. Although openings at times of observed window breakage was input to the FDS model, this FDS simulation failed to predict a second peak in HRR after 400 s due to increased ventilation as predicted in Section 4.3. Instead, the FDS simulation predicts fire decay earlier than was observed.

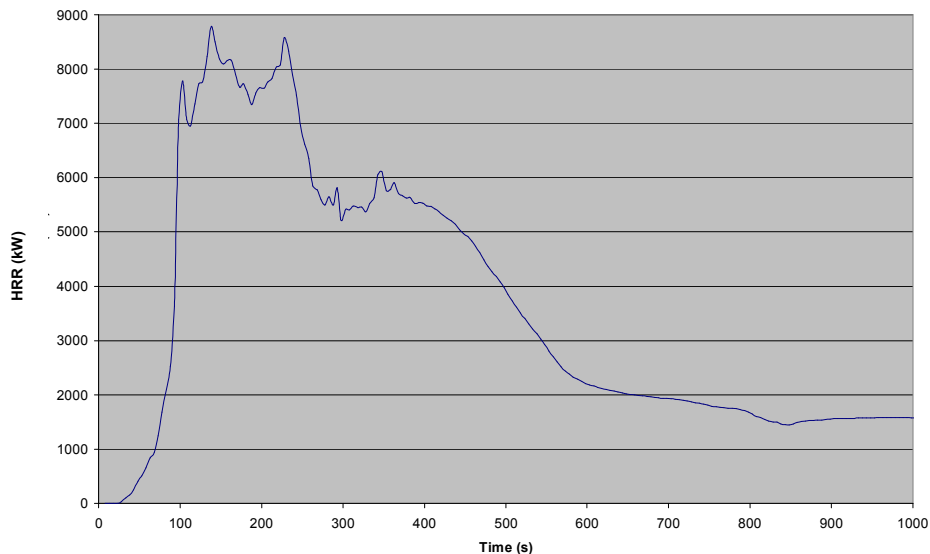


**Figure 5.11. Predicted HRR of experiment from FDS simulation**

Due to the deviation between experimental and simulated temperatures and the errors in HRR prediction by FDS discussed in Section 5.3.1; this should not be considered an accurate estimate of HRR for the full-scale experiment.

#### 5.5.2.2 Stage 2 – Attempted improvements to full-scale experiment simulation

Stage 2 was undertaken by a second group of WPI fire engineering students.

The students identified the following faults with the models from Stage 1:

- Flames from the ignition source reached the ceiling earlier in the simulation than for the experiment.
- Flashover occurred earlier in the simulation than for the experiment.
- The estimated peak HRR was higher than expected.

No justification was reported for the statement that HRR was higher than expected and this statement is likely to be incorrect. Based on experimental observation and comparison to the predicted HRR curve from Section 4.3 the peak HRR and burn duration were likely to have been underestimated by the Stage 1 simulation.

The students conducted further fire calorimeter testing on the 1 kg newspaper ignition source varying both packing density and temperature/humidity conditioning of the paper. It was concluded that a HRR curve with a peak of approximately 140 kW better represented the ignition source located under the seat.

The model was changed to include multiple grids and parallel processing. A grid resolution of 20 mm was used in a 1m<sup>2</sup> floor area in the ignition corner. A 40 mm grid resolution extended for 4 m from the ignition end of the carriage and a grid resolution of 80 mm was applied to the rest of the vehicle. The model domain was not increased.

The geometry of the gap between the seat back and the end wall under which the ignition source was located was more accurately defined. Iterative simulations were conducted varying the ignition source area until the predicted time of ignition source flames reaching the ceiling matched with experimental observation.

Further iterative simulations of cone calorimeter tests for GRP and carpet were conducted to modify material properties and improve agreement with cone calorimeter data. The GRP was modelled as a charring fuel rather than a thermoplastic. The resulting simulations shown in Figure 5.12 and Figure 5.13, agree well with cone calorimeter data. The properties for the seat cushion assembly were not changed although the cone calorimeter data was poorly matched to experimental data.

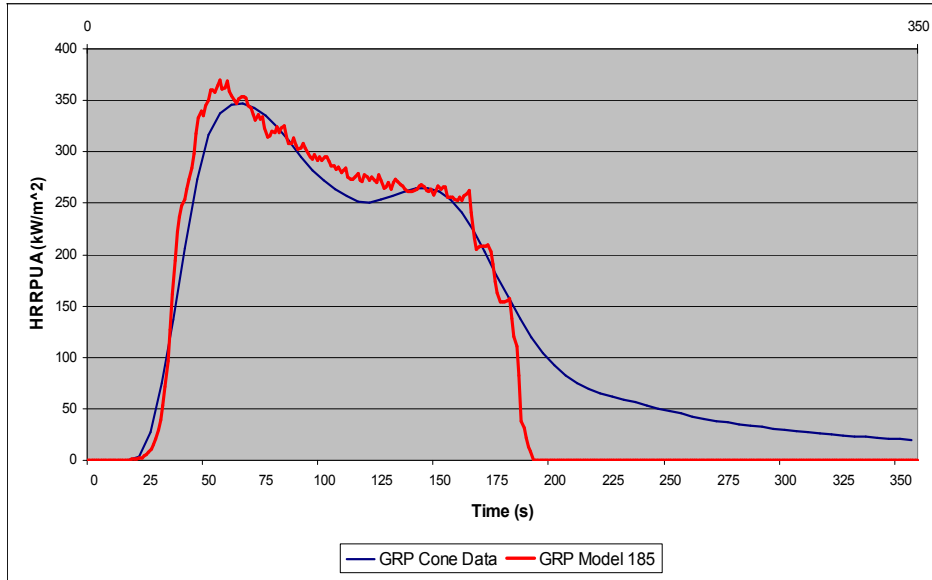


Figure 5.12. Cone calorimeter simulation to select material properties for GRP

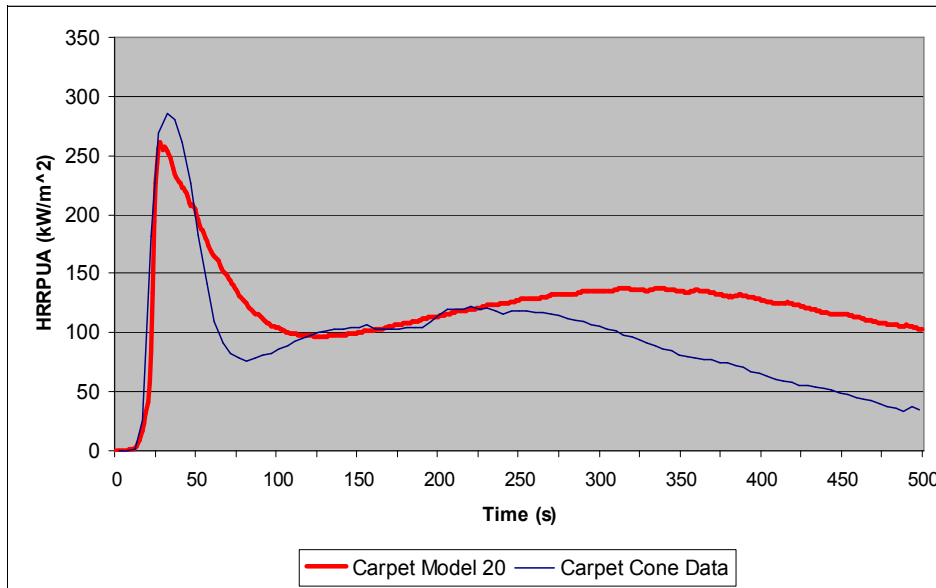


Figure 5.13. Cone calorimeter simulation to select material properties for carpet.

During the process of optimising ignition source and material properties a number of simulations of the full scale experiment were run with run times of 30-100 s. The predicted peak HRR varied from 0-13.3 MW demonstrating that there was large variation in simulated fire behaviour dependent on model inputs. The final simulation was run for a run time of 242 s and attained a peak HRR of 6.1 MW at 119 s. Example plots of simulated temperatures compared with experimental temperatures are provided below

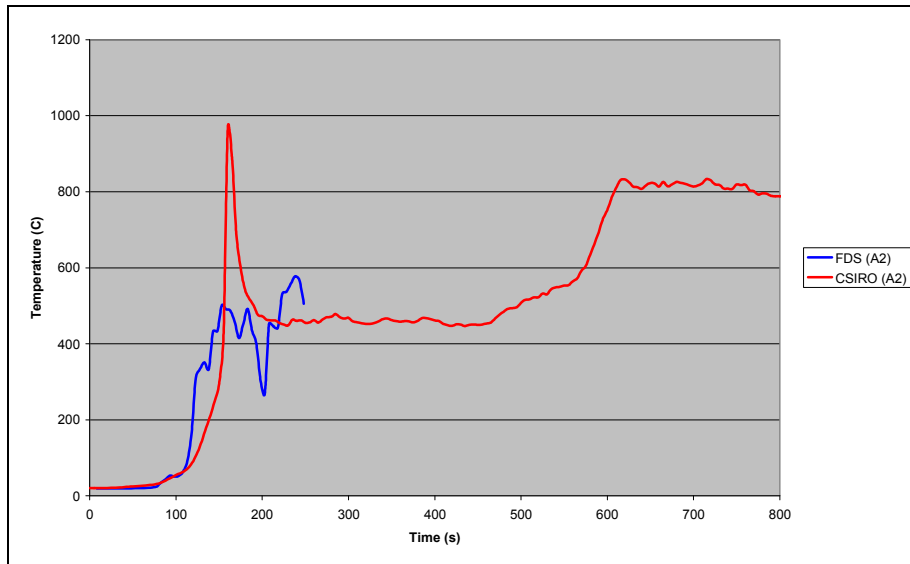


Figure 5.14. Comparison of simulated and experimental temperature at thermocouple A2

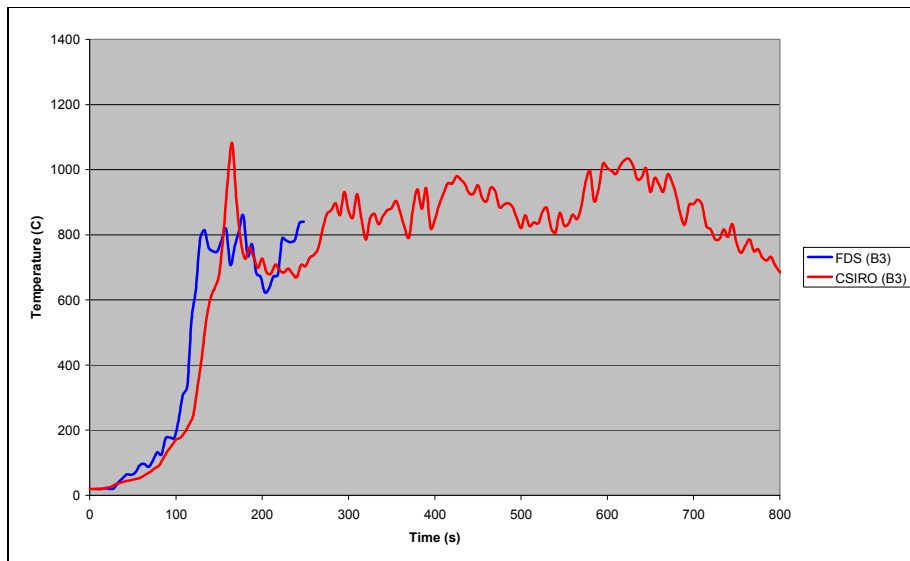


Figure 5.15. Comparison of simulated and experimental temperature at thermocouple B3

Based on simulated temperatures the FDS model successfully predicts flashover and flame spread however the onset of flashover is predicted early at approximately 100 s compared to 140s observed in the experiment. There is no improvement in agreement of simulated and experimental temperatures from the results of the Stage 1 simulation. As the simulation was only run to 242 s the effects of increased ventilation from significant window failure were not simulated and the fire decay and total fire duration were not simulated. The HRR predicted by the stage 2 model is compared to the stage 1 model below.

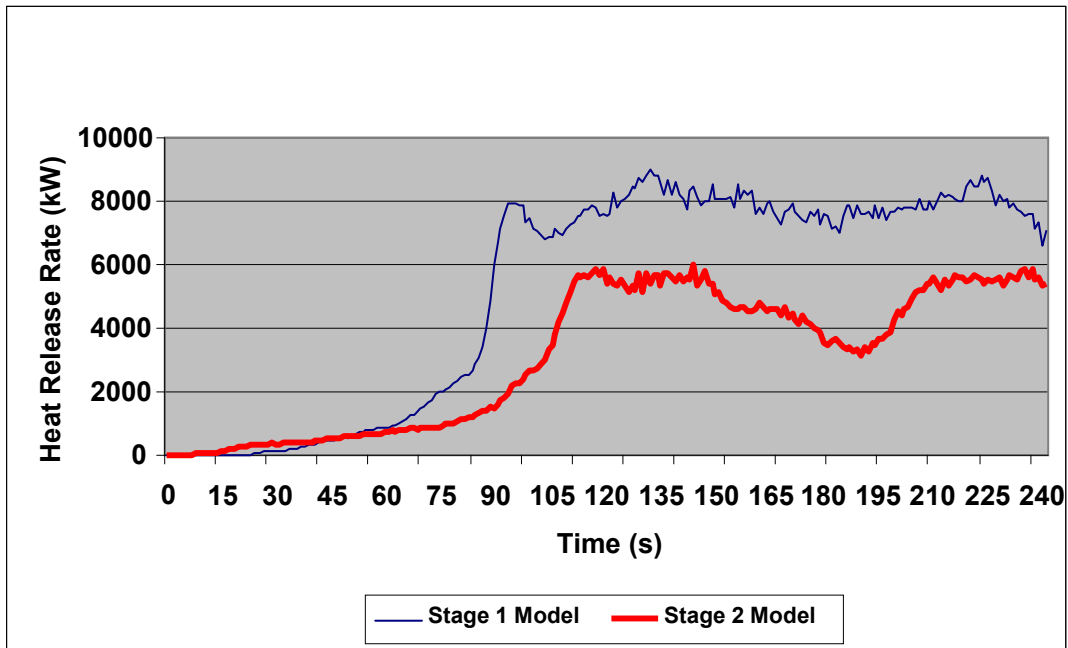


Figure 5.16. HRR predicted by Stage 2 model

The peak HRR of 6.1 MW predicted by the stage 2 model is lower than predicted for the Stage 1 model and most likely too low based on comparison of simulated temperatures, experiment observations the HRR estimated in Section 4.3. Combustion exterior to the vehicle was not simulated due to a restricted domain.

## **5.6 FDS CONCLUSIONS**

Although FDS is one of the most advanced fire models available, several sources of error for application of FDS to estimate HRR have been identified. Errors stem from limitations or simplifying assumptions relating to grid resolution, mixture fraction combustion model, soot and other gas species yields, radiant heat flux, materials properties and pyrolysis models. Application of FDS to assess conditions for tenability within a train given an assumed HRR is reasonable however FDS application to predict HRR for a train fire is not well validated and cannot be relied upon to yield accurate results. Other conclusions are:

- Input of appropriate material properties is likely to be the most significant source of error. There is no well defined method to determine appropriate material properties. Methods which calibrate properties against cone calorimeter test results are time consuming and not well validated.
- The full-scale experiment has been modelled applying FDS. A simulation that accurately predicted the experimental temperatures was not attained, even though simulations were iteratively tuned based on knowledge of the experimental result. This highlights the difficulties of selecting appropriate inputs.
- Arbitrary events such as collapse of linings may have significant affects on fire behaviour but cannot be predicted by FDS.
- General fire growth trends such as flashover, ventilation effects and fuel burn out can be roughly simulated by FDS provided appropriate inputs are selected, However the estimated timing and magnitude of such events cannot be relied upon.
- Further development of FDS may improve confidence of HRR estimation.

## CHAPTER 6 CONCLUSIONS AND FURTHER RESEARCH RECOMMENDATIONS

### 6.1 *Conclusions*

In the current study, a series of fire experiments have been conducted on a 20 year old passenger train carriage. Experiments included a full-scale fully developed carriage fire, large-scale corner ignition experiments and cone calorimeter tests. A conservation of energy model has been used to estimate the HRR for the full-scale experiment based on measurements and observations. Design fire estimation methods have been evaluated against the full-scale experiment. Application of FDS to estimate design fires for passenger trains has been reviewed and evaluated.

The main conclusions and findings from this research are:

- The literature reviewed suggests an ignition source of the order of 100-300 kW peak HRR is typically required for fire spread to occur on passenger train interiors, dependent on materials and design. In this research an ignition source of the range 100-170 kW peak HRR located on a corner seat was required. Ignition sources of this size are credible arson events that may be achieved using newspaper fuel. Combustible panels in a closely spaced vertical arrangement are very susceptible to fire spread from even smaller ignition fires and should be avoided in design.
- Ignition of upper wall and ceiling linings is critical for fire spread beyond the ignition area leading to flashover. Improved fire performance of these materials will reduce the likelihood of flashover.
- Flashover resulting in fire spread to the entire carriage can occur. In this research flashover occurred starting from the ignition area at 140s. Flashover may not spread instantaneously to all locations in the carriage. In this research flashover conditions took 35 s to spread 10 m from the ignition point to the end of the fitted area.
- Time available for driver response and safe evacuation in a train fire that progresses to flashover can be very short. In this research conditions inside the carriage became untenable rapidly after the onset of flashover at 140-150 s

- Fully developed fire size for passenger trains can be significantly affected by ventilation conditions. In this research, prior to window breakage, combustion inside the carriage became partially choked with a significant portion of combustion occurring in exterior flames extending from open doors. This reduced pyrolysis of interior materials and HRR. After significant breakage of windows sufficient fuel was not available to achieve ventilation restricted HRR.
- Window performance affects ventilation and fire size. After significant window breakage occurred, fire behaviour changed with more combustion occurring inside the carriage. This resulted in an increased HRR until materials began to burn out.
- A conservation of energy model was used to estimate HRR for the full-scale experiment based on experimental measurements and observation. Fully developed HRR was estimated to be 8 MW prior to significant window breakage, with 40% HRR occurring exterior to the carriage. After significant window breakage the fully developed HRR was estimated to be 11 MW with 15% HRR occurring exterior to the carriage. It is expected the peak HRR and burn duration would be greater for a fully fitted carriage interior. Due to the limited amount of materials fitted, this result does not represent an appropriate design fire but does provide a basis for understanding train fire development and evaluating design fire estimation methods.
- Design fire estimation methods including the average HRR method, Duggan's method and the ventilation controlled method were applied to the full-scale experiment. It was found that these methods do not appropriately represent real fire behaviour resulting in very poor estimation of rate of fire growth and burn duration. The methods provided a rough order of magnitude estimate of peak HRR, to within approximately 30% of the peak HRR based on the conservation of energy model for the full-scale experiment. Duggan's method and the ventilation controlled method both over predicted peak HRR. The average HRR method over predicted average HRR but under predicted peak HRR.
- Due to simplifying assumptions in the FDS combustion and pyrolysis models and difficulty selecting appropriate input parameters for combustible material

and glazing, FDS does not reliably predict accurate design fires for passenger trains. FDS simulations of fire growth for the full-scale experiment did not reasonably match experimental measurements and observed fire development.

- Through the study, it is demonstrated that no ideal method for estimating design fires for passenger trains exists. However in order to engineer fire safety designs for rail infrastructure, the existing tools for design fire estimation must be applied. It is critical that these tools be applied by competent users giving proper consideration to both the limitation of the models and knowledge of real fire behaviour as demonstrated by this and previous research. Where possible, design fires should be supported by experiments.
- Given the uncertainty of design fire estimation methods it is recommended sensitivity analysis should be undertaken to ensure robustness of the fire safety design to various design fires. However this can result in less cost effective designs.
- Due to cost and difficulty of measurement of HRR in the full-scale it is not practical to conduct full-scale experiments for every variation of passenger train design.

## **6.2 Further Research Recommendations**

Clearly there is a need and wide scope for further research in this field. Future work should consider the following:

- Full-scale HRR measurement of a limited number of different carriage designs and ventilation scenarios would provide fire engineers with better guidance on appropriate design fires and would also provide data required to develop design fire estimation models. Ideally experiments should be well instrumented full-scale carriage fire tests conducted in a purpose built, accurate HRR measurement facility, including a diverse selection of materials and scenarios.
- Given sufficient fuel, it is likely that HRR for most post flashover train fires will be limited by ventilation. It is critical that the research of Bullen and Thomas<sup>[99]</sup> and Ingason<sup>[56,57]</sup> should be furthered to gain a complete

understanding of real ventilation controlled fire behaviour and its deviation from assumptions implicit in the correlation for ventilation controlled HRR discussed in Section 2.4.5. A series of experiments could be undertaken on a model carriage of at least 1:4 scale and compared against limited full scale carriage tests investigating the variation of correction factor  $\eta$  with ventilation conditions and interior materials.

- FDS continues to evolve. Improvement of pyrolysis and combustion models and development of appropriate methods to measure required material properties may increase ability to reasonably model fire growth. This development requires large-scale and full-scale fire tests purposefully designed to provide data required for development and evaluation of FDS improvements.
- Design fires are also required for passenger trains of significantly different designs to the typical single enclosed carriage considered in this research. These include double deck carriages and carriage sets with open, interconnected gangways which effectively result in a single, long multi-carriage enclosure. Further research on the affects of such vehicle designs on fire behaviour needs to be undertaken as existing design fire estimation methods may be even less reliable for such carriage designs.
- Tunnel geometry and ventilation conditions significantly influence HRR for a given fire compared with its occurrence in open air. This influence has been well investigated for pool fires and timber crib fires<sup>[31,33]</sup> but there is little known of the affect for train fires which differ as the burning material is partially enclosed by the carriage body. Research in this area would be valuable.

## REFERENCES

1. Babrauskas, V. and Peacock, R. D. (1992) Heat Release Rate: The Single Most Important Variable in Fire Hazard. *Fire Safety Journal*, 18, 255-272.
2. Hudson, Steve. (2001) *Train fires - Special Topic Report*. Railway Safety - Controller, Safety Strategy & Risk, London
3. England, Paul and Flower, Geoff. (2005) *A Framework For Fire Engineering Design For Passenger Rail Networks*. Fire Safety - Sea Road Rail, Rocarm Pty Ltd, Melbourne
4. FCRC. (1996) *Fire Engineering Guidelines, 1st edition*. Fire Code Reform Centre Limited, Sydney, Australia
5. Karlsson, Bjorn and Quintiere, James G. (2000) *Enclosure Fire Dynamics*. CRC Press LLC, Florida, USA
6. Milke, James A. and Klote, John H. (1998) *Smoke management in large spaces in buildings*. Building Control Commission of Victoria and BHP Ltd, Melbourne, Australia
7. England, J. P., Young, S. A, Hui, M. C., and Kurban, N. (2000) *Guide for the Design of Fire Resistant Barriers and Structures*. Building Control Commission, Warrington Fire Research, Melbourne, Australia
8. Schifiliti, Robert P., Meacham, Brian J., and Custer, Richard L. P. (2002) *Section 4, Chapter 1: Design of Detection Systems*. National Fire Protection Association, Quincy, Massachusetts
9. AFAC. (1997) *Fire Brigade Intervention Model V2.1*. Australasian Fire Authorities Council, Melbourne, Australia
10. McGillivray, Glenn. (2001) *Tunnels - the fire within*. Canadian Consulting Engineer
11. Dowling, P. V. and White, Nathan. (2004) *Fire Sizes in Railway Passenger Saloons*. 6th Asia-Oceania Symposium on Fire Science and Technology, Korean Institute of Fire Science and Engineering, Korea
12. Peacock, Richard D., Bukowski, Richard W., Jones, Walter W., Reneke, Paul A., Babrauskas, Vytenis, and Brown, James E. (1994) *Fire Safety of Passenger Trains: A Review of Current Approaches and New Concepts*. NIST Technical Note 1406, National Institute of Standards and Technology, Gaithersburg, MD
13. Wikipedia, the free encyclopedia. (2005) *List of Rail Accidents*. [http://en.wikipedia.org/wiki/List\\_of\\_rail\\_accidents](http://en.wikipedia.org/wiki/List_of_rail_accidents)
14. Office of Rail Regulation. (*Train Accident At Ladbroke Grove Junction, 5*

*October 1999, Third HSE Interim Report.* Office of Rail Regulation,  
<http://www.rail-reg.gov.uk/server/show/nav.1204>

15. Park, Hyung-ju. (2004) *An investigation into Mysterious Questions arising from the Daegu underground railway arson case through fire simulations and small scale fire tests.* 6th Asia-Oceania Symposium on Fire Science and Technology, Daegu, Korea
16. Sam-Kew Roh, Jun-Ho Hur, Jong Hoon Kim, Woon Hyung Kim, and Kwan Sup Lee. (2004) *Early response system and improvement of fire safety performance in Dae-gu Subway disaster.* 6th Asia-Oceania Symposium on Fire Science and Technology
17. Duck-Hee Lee, Woo-Sung Jung, Cheul-Kyu Lee, Samn-Kyu Roh, Woon-Hung Kim, and JOng-Hoon Kim. (2004) *Fire Safety Characteristics of Interior Materials of Korean Railway Vehicles.* 6th Asia-Oceania Symposium on Fire Science and Technology
18. BBC News. (2005) *India train fire not mob attack.* BBC News,  
[http://news.bbc.co.uk/2/hi/south\\_asia/4180885.stm](http://news.bbc.co.uk/2/hi/south_asia/4180885.stm)
19. Wikipedia. (2005) *2002 Gujarat Violence.*  
[http://en.wikipedia.org/wiki/2002\\_Gujarat\\_violence](http://en.wikipedia.org/wiki/2002_Gujarat_violence)
20. The Hindu National. (2005) *Engineering experts question police theory on Godhra fire.* The Hindu National, India,  
<http://www.hindu.com/2005/01/18/stories/2005011806461100.htm>
21. BBC. (2002) *Minister Resigns Over Egypt Train Fire.* BBC news,  
[http://news.bbc.co.uk/1/hi/world/middle\\_east/1835451.stm](http://news.bbc.co.uk/1/hi/world/middle_east/1835451.stm)
22. BBC News. (2002) *Stove blamed for Egypt train inferno.* BBC News,  
[http://news.bbc.co.uk/1/hi/world/middle\\_east/1830863.stm](http://news.bbc.co.uk/1/hi/world/middle_east/1830863.stm)
23. Answers.com. (2005) *Kaprun Disaster.*  
<http://www.answers.com/topic/kaprun-disaster>
24. BBC News. (2000) *How could it have happened?* BBC News,  
<http://news.bbc.co.uk/1/hi/world/europe/1019665.stm>
25. Hedefalk, J., Wahlstrom, B., and Rohlen, P. (98) *Lessons from the Baku Subway Fire.* International Conference on Safety in Road and Rail Tunnels
26. Pearce, Kenn. (1994) *Australian Railway Disasters.* IPL Books, Smithfield NSW, Australia
27. ABCNews. (2006) *Three arrested over Sydney train fire.* Sydney,  
<http://www.abc.net.au/news/stories/2006/10/23/1770791.htm>
28. Barrett, P. J. and et al. (1976) *Fire in Double Deck Suburban Passenger Carriages.* Public Transport Corporation of NSW, Sydney

29. McArthur, Neville. (2001) *Report on material behaviour in a fire in Queensland Rail vehicle EM162*. Confidential BCE Doc. 01/200, CSIRO Fire Science and Technology Laboratory, Melbourne, Australia
30. Munro, John, Smith, Graham, Dowling, Vince, and White, Nathan. (2002) *Combining design fires and risk assessment to achieve tunnel safety*. Proceedings TMI Fourth International Conference
31. Carvel, R. O., Beard A.N., Jowitt, P. W. and Drysdale, D. D. (2004) The Influence of Tunnel Geometry and Ventilation on the Heat Release Rate of a Fire. *Fire Technology*, 40, pp 5-26.
32. Carvel, R. O., Beard, A. N., Jowitt, P. W., and Drysdale, D. D. (2001) *Variation of heat release rate with forced longitudinal ventilation for vehicle fires in tunnels*. *Fire Safety Journal*, <http://www.sciencedirect.com/science/article/B6V37-439VBJ3-3/2/457389c69145e11ea10bedaa8b2f65ef>
33. Carvel, R. O. , Beard, A. N. and Jowitt, P. W. (2001) A BAYESIAN ESTIMATION OF THE EFFECT OF FORCED VENTILATION ON A POOL FIRE IN A TUNNEL. *Civil Engineering and Environmental Systems*, 18, pp 279-302.
34. Haack, A. ( 2002) *Current safety issues in traffic tunnels*. *Tunnelling and Underground Space Technology*
35. Kirkland, Collin J. (2002) *2002 ITA Open Session: Fire and Life Safety - The fire in the Channel Tunnel*. *Tunnelling and Underground Space Technology*, [www.elsevier.com/locate/tust](http://www.elsevier.com/locate/tust)
36. Department of Infrastructure. (2006) *Fire incident data for Melbourne passenger trains for the years 1993-1999 and 2002-2005 (excel spread sheet)*. DOI, Melbourne, \\Fnsnw1-syd\CMIT-Share1\FireEng\2005 New Projects from 1815\1873M - DOI smoke detector risk\train fires.xls
37. Bennetts, Ian. D, Poh, K. W., and Thomas, I. R. (1998) *Risk Assessment of Construction Over Railway lines at Federation Square*.
38. Bennetts, Ian. D., Moinuddin, K., Weinert, Darryl, and Thomas, I. R. (2004) *Fire Safety Evaluation of Siemens Nexus Train*.
39. Railcorp. ( 2007) *RailCorp safety performance statistics - January to December 2006*. Railcorp, Sydney, [http://www.railcorp.info/our\\_safety\\_performance](http://www.railcorp.info/our_safety_performance)
40. Railcorp. ( 2007) *RailCorp safety performance statistics - 2007*. Railcorp, Sydney, [http://www.railcorp.info/our\\_safety\\_performance](http://www.railcorp.info/our_safety_performance)
41. SRA. (2000) *State Rail Authority fire incident database 1991-2000 hardcopy*. State Rail Authority, Sydney, Melbourne
42. Barnett, Jonathan. (2005) *Events Driving Fire Safety for Sea Road and Rail*. Sea Road Rail Fire Safety Conference, Rocarm Pty Ltd, Melbourne, Australia

43. Takita, Teruo. (1976) *Behaviour of a fire on a running train - Frpm the train fire tests at Karikachi test track - quarterly reports Vol. 17 No. 3*. Railway Technical Research Institute, JNR, Japan
44. Takita, Teruo. (1977) *Research on prevention of train fire*. Rail International
45. Peacock, Richard D. and Braun, Emil. (1984) *Fire Tests of Amtrak Passenger Rail Vehicle Interiors*. US Department of Commerce/National Bureau of Standards, Washington DC
46. Goransson, Ulf and Lundqvist, Annika. (1990) *Fires in buses and trains, fire test methods*. SP Report 1990:45, SP Swedish National Testing and Research Intitute, Fire Technology, Boras, Sweden
47. Haack, Alfred, Casale, Eric, Ingason, Haukur, Malhotra, H. L., and Richter, Ekkehard. (1995) *EUREKA Project EU 499: FIRETUN - Fires in Transport Tunnels - Report on Full-Scale Tests*. Velag und Vertriebsgesellschaft, Dusseldorf, Germany
48. Haack, A. (1998) *Fire Protection in Traffic Tunnels: General Aspects and Results of the EUREKA Project*. Tunneling and Underground Space Technology
49. Ingason, Haukur, Gustavson, Soren, and Dahlberg, Martin. (1994) *Heat Release Rate Measurments in Tunnels, BRANDFORSK project 723-924*. SP, Swedish National Testing and Research Institute, Sweden
50. Briggs, Peter, Le Tallec, Yannick, Sainrat, Alain, Metral, Serge, Messa, Silvio, and Breulet, Herve. (2001) *The Firestarr Research Project on the Reaction to Fire Performance of Products in European Trains*. Interflam
51. FIRESTARR. (2001) *Final Report*. Fire Standardisation Research in Railways Project, France
52. White, N. (2005) *Fire growth on passenger rail interiors*. International Conference Fire Safety- Sea Road Rail, Melbourne, Australia, \\fs1syd-ln\CMIT-FileSharing\FireEng\Tools calcs specs\Papers and info\White 2005a.pdf
53. Peacock, Richard D. and Braun, Emil. (1999) *Fire Safety of Passenger Trains; Phase I: Material Evaluation (Cone Calorimeter)*. NISTIR 6132, National Institute of Standards and Technology, Gaithersburg MD
54. Peacock, Richard D., Reneke, Paul A., Averill, Jason. D, Bukowski, Richard W., and Klote, John H. (2002) *Fire Safety of Passenger Trains; Phase II: Application of Fire Hazard Analysis Techniques*. NISTIR 6525, National Institute of Standards and Technology, Gaithersburg MD
55. Peacock, Richard D., Averill, Jason. D, Madrzykowski, Daniel, Stroup, David W., Reneke, Paul A., and Bukowski, Richard W. (2004) *Fire Safety of Passenger Trains; Phase III: Evaluation of Fire Hazard Analysis Using Full-*

- Scale Passenger Rail Car Tests*. NISTIR 6563, National Institute of Standards and Technology, Gaithersburg, MD
56. Ingason, Haukur. (2005) *Model scale railcar fire tests*. SP REPORT 2005:49, SP Swedish National Testing and Research Institute, Boras, Sweden.
  57. Ingason, H. (2007) Model scale railcar fire tests. *Fire Safety Journal*, 42, pp 271-282.
  58. Weinert, Darryl and Bennetts, Ian. D. (2002) *Transient Fire Loads on Suburban Melbourne Trains*.
  59. ISO. (2002) *ISO 5660-1: Reaction-to-fire tests - Heat release, smoke production and mass loss rate - Part 1: Heat release rate (cone calorimeter method)*. International Organization for Standardization, Geneva, Switzerland
  60. ISO. (1994) *ISO 5659-2 Plastics - Smoke generation - Part 2: Determination of optical density by a single chamber test*. International Organisation for Standardization, Geneva Switzerland
  61. ISO. (2006) *ISO 5658-2:2006 : Reaction to fire tests - Spread of flame - Part 2: Lateral spread on building and transport products in vertical configuration*. International Organisation for Standardization, Geneva Switzerland
  62. Anon. ( *NFX70-100*).
  63. ISO. (2002) *ISO 9239-1 Reaction to fire tests for floorings - Part 1: Determination of the burning behaviour using a radiant heat source*. International Organisation for Standardization, Geneva, Switzerland
  64. NORDTEST. ( 1987) *NT FIRE 032 Upholstered Furniture: Burning Behaviour - Full Scale Test*. NORDTEST, Finland
  65. ASTM. (2002) *ASTM E 162 - 02a Standard Test Method for Surface Flammability of Materials Using a Radiant Heat Energy Source*. ASTM International, West Conshohocken, PA, USA
  66. ASTM. (2005) *ASTM D 3675 - 05 Standard Test Method for Surface Flammability of Flexible Cellular Materials Using a Radiant Heat Energy Source*. ASTM International, West Conshohocken, PA, USA
  67. ASTM. (2006) *ASTM E 648 - 06a Standard Test Method for Critical Radiant Flux of Floor-Covering Systems Using a Radiant Heat Energy Source*. ASTM International, West Conshohocken, PA, USA
  68. FAA. (1997) *14 CFR, Part 25, Subpart 25.853, Compartment Interiors, Sections (a)-(d); Subpart 25.855, Cargo or Baggage Compartments; and Appendix F to Part 25*. National Archives and Records Administration, Washington, DC
  69. ASTM. (2005) *ASTM E 662 - 05 Standard Test Method for Specific Optical Density of Smoke Generated by Solid Materials*. ASTM International, West

Conshohocken, PA, USA

70. Sato, Shigemasa and Osaki, Takashi. (1993) *Study on Fire Protection Measures for Railcars*. Japanese Railway Engineering
71. Braun, Emil. (1975) *A Fire Hazard Evaluation of the Interior of WMATA Metrorail Cars*. NBSIR 76-971, Centre for Fire Research, National Bureau of Standards, Washington DC, USA
72. Dowling, Vince. P. (2004) *The need for a national approach to fire safety in passenger trains*. Lloyds List DCN conference, Rail Safety, 2004
73. Standards Australia. (1995) *AS 4292 Part 1: Railway safety management - General and interstate requirements*. Standards Australia, Sydney, Australia
74. Standards Australia. (1997) *AS 4292 Part 3: Railway safety management - Rolling stock*. Standards Australia, Sydney, Melbourne
75. Railways of Australia. (1992) *ROA Manual of engineering standards and practices*. Railways of Australia
76. Australian Building Codes Board. (2007) *Building Code of Australia 2007 - Volume 1*. Australian Building Codes Board, Canberra
77. EDI Rail - Bombardier Transportation. (2002) *Specification for fire risk assessment, material fire testing and fire performance for Perth Urban Rail Development EMU*. 224ESPE0014, EDI Rail - Bombardier Transportation, Maryborough, Queensland
78. NFPA. (2003) *NFPA 130 Standard for Fixed Guideway Transit and Passenger Rail Systems 2003 Edition*. National Fire Protection Association, 1 Batterymarch Park, Quincy, MA, USA
79. FRA. (2002) *Passenger Rail Car and Locomotive Fire Safety*. FRA Regulation 49 CFR, Part 238, Federal Railroad Administration, USA
80. National Railroad Passenger Corporation. (1991) *Specification for Flammability, Smoke Emission and Toxicity*. AMTRACK Specification No. 352, National Railroad Passenger Corporation, USA
81. State of California. (1991) *Technical Bulletin 133 - Flammability Test Procedure for Seating Furniture for use in Public Occupancies*. State of California, Dept. of Consumer Affairs, Bureau of Home Furnishings and Thermal Insulation, North Highlands, California
82. ASTM. (2001) *ASTM E 2061 - 01 Guide for Fire Hazard Assessment of Rail Transportation Vehicles*. ASTM International, West Conshohocken, PA, USA
83. BSI. (1999) *BS 6853:1999 Code of practice for fire precautions in the design and construction of passenger carrying trains*. British Standards Institute, London

84. DIN. (2003) *DIN 5510 Parts 1-8 Preventative fire protection in railway vehicles: Levels of protection, fire preventative measures and certification*. Deutsches Institut Fur Normung e.V., Germany
85. UIC. (1991) *UIC code 564-2 : Regulations relating to fire protection and fire fighting measures in passenger carrying railway vehicles or assimilated vehicles used on international services*. International Union of Railways, Paris, France
86. National Fire Protection Association. (1999) *NFPA 72 National Fire Alarm Code*. National Fire Protection Association, Quincy, MA
87. Drysdale, Dougal. (1998) *An Introduction to Fire Dynamics*. John Wiley & Sons Ltd., Chichester, West Sussex, England
88. Walton, William D. and Thomas, Phillip H. (2002) *Section 3, Chapter 6: Estimating Temperatures in Compartment Fires*. National Fire Protection Association, Quincy, Massachusetts, U.S.A.
89. Babrauskas, Vytenis. (1980) *Estimating Room Flashover Potential*. Fire Technology
90. Thomas, Phillip H. (1981) *Testing Products and Materials for Their Contribution to Flashover in Rooms*. Fire and Materials
91. McCaffrey, B. J., Quintierre, James G, and Harkleroad, M. F. (1981) *Estimating Room Fire Temperatures and the Likelihood of Flashover Using Fire Test Data Correlations*. Fire Technology
92. Chow, W. K. (2001) *Flashover for Bus Fires From Empirical Equations*. Journal of Fire Sciences
93. Kennedy, William D., Ray, Richard E., and Guinan, James W. (98) *A short history of train fire heat release calculations*. Annual ASHRAE Meeting
94. Duggan, Gary. J. (97) *Usage of ISO 5660 Data in UK Railway Standards and Fire Safety Cases*. Fire Hazards, Testing, Materials and Products, Rapra Technology Limited, Shawbury, UK
95. Dowling, Vince P. and Delichatsios, Micheal A. (2000) *Material Flammability in Train Saloons*. New Railway Systems, London
96. Kawagoe, Kunio. (1958) *Fire behaviour in rooms*. Report No. 27, Building Research Institute, Tokyo
97. Rockett, J. A. (1976) Fire Induced Gas Flow in an Enclosure. *Combustion Science and Technology*, 12, 165-175.
98. Thomas, Phillip H. and Heselden, A. J. M. (1972) *Fully Developed Fires in Single Compartments*. Fire Research Note No. 923, Fire Research Station, Borehamwood, England

99. Bullen, M. L. and Thomas, P. H. (1979) *Compartment Fires with Non-cellulosic Fuels*. 17th Symposium (International) on Combustion, The Combustion Institute, Pittsburgh, U.S.
100. Bowditch, P. A., Sargeant, A. J., Leonard, J. E., and Macindoe, L. (2006) *Window and Glazing Exposure to Laboratory-Simulated Bushfires*. CMIT Doc 2006-205, Bushfire CRC, Melbourne, Australia
101. Harada, K., Enomoto, A., Uede, K., and Wakamatsu, T. (2000) *An experimental study on glass cracking and fallout by radiant heat exposure*. *Fire Safety Science – Proc. 6th Int. Symp*, International Association for Fire Safety Science, London, UK
102. Mowrer, F. W. (1998) *Window Breakage Induced by Exterior Fires*. NIST-GCR-98-751, National Institute of Standards and Technology, Gaithersburg, MD, USA.
103. Babrauskas, V. (2005) *Glass Breakages in Fires*. <http://www.doctorfire.com/glass.html>
104. Strege, S., Lattimer, B. Y., Beyler, C., and . (2003) *Fire Induced Failure of Polycarbonate Windows in Railcars*. *Fire and Materials*
105. Walton, W. D. (2002) Chapter 7 - Zone Computer Fire Models for Enclosure. In *The SFPE Handbook of Fire Protection Engineering*, National Fire Protection Association, Quincy, Massachusetts, USA.
106. Peacock, Richard D., Forney, Glenn P., Reneke, Paul A., and Jones, Walter W. (2005) *CFAST - Consolidated Model of Fire Growth and Smoke Transport (version 6) - Technical Reference Guide*. NIST Special Publication 1029, Building and Fire Research Laboratory, National Institute of Standards and Technology, Gaithersburg, MD
107. Wade, Colleen A. (2003) *BRANZFIRE Technical Reference Guide*. Study Report No. 92., Building Research Association of New Zealand, Porirua City, New Zealand
108. Babrauskas, Vytenis. (1979) *COMPF2 - A Program for Calculating Post Flashover Fire Temperatures*. NBS TN 991, National Bureau of Standards, Washington, DC
109. Lattimer, Brian and Beyler, Craig. (2005) *Heat Release Rates of Fully-Developed Fires in Railcars*. *Fire Safety Science - Proceedings of the 8th International Symposium, IAFSS, Beijing, China*
110. Thematic network on fire in tunnels (FIT). (2001-2004) *Technical Report - Part 1: Design Fire Scenarios*. European Commission under the 5th Framework Program, Brussels, Belgium
111. PIARC. (1999) *Fire and smoke control in road tunnels*. 05.05B-1999, World Road Association, France

112. NFPA. (2001) *NFPA 502 - Standard for road tunnels, bridges and other limited access highways*. National Fire Protection Association, Quincy, MA, USA
113. NFPA. (2008) *NFPA 502 - Standard for road tunnels, bridges and other limited access highways*. National Fire Protection Association, Quincy, MA, USA
114. Ingason, Haukur. (2006) *Design fires in tunnels*. Safe & Reliable Tunnels. Innovative European Achievements. Second International Symposium
115. Ingason, H. (1995) Design fires in tunnels. In *Conference Proceedings of Asiaflam 95, 15-16 March, 1995*, Hong Kong, pp. pp. 77-86.
116. Bentley, R. E. (1998) *Handbook of Temperature Measurement - Volume 3 - Theory and Practice of Thermoelectric Thermometry*. Springer-Verlag Singapore Pty Ltd, Lindfield, NSW, Australia.
117. Janssens, M. (2006) Chapter 2: Fundamental measurement techniques. In *Flammability testing of materials used in construction, transport and mining*, Edited by Apte, V. B. Woodhead Publishing, Cambridge, England, pp. 22-62.
118. McCaffery, B. and Heskestad, G. (1976) A Robust Bidirectional Low-Velocity Probe for Flame and Fire Application. *Combustion and Flame*, 26, 125-127.
119. Purser, D. A. (2002) Section 2, Chapter 6: Toxicity assessment of combustion products. In *SFPE Handbook of fire protection engineering*, National Fire Protection Association, Quincy, Massachusetts.
120. Buchanan, A. H. (2001) *Fire Engineering Design Guide*. Centre for Advanced Engineering, University of Canterbury, New Zealand
121. Babrauskas, V. (1992) Chapter 8: Related Quantities (a) Heat of Combustion and Potential Heat. In *Heat Release in Fires*, Elsevier Science Ltd, Essex, England.
122. Babrauskas, V. (2002) Section 3, Chapter 1: Burning Rates. In *The SFPE Handbook of Fire Protection Engineering*, National Fire Protection Association, Quincy, Massachusetts.
123. Incropera, Frank P. and De Witt, David P. (1990) *Fundamentals of heat and mass transfer*. John Wiley & Sons, USA
124. White, N, Barnett, J, and Bennetts, I. (2005) *Fully developed passenger train fire experiment*. International Conference Fire Safety- Sea Road Rail, \\fs1syd-ln\CMIT-FileSharing\FireEng\Tools calcs specs\Papers and info\White 2005b.pdf
125. McArthur, N. A., Webb, A. K., and Bradbury, G. P. (1998) *Wood Crib Experiments in a Medium-Scale Enclosure - Sponsored by Fire Code Reform Centre under direction of Dr Ian Thomas*. BCE Doc 98/179, CSIRO,

## Melbourne

126. SFPE (2002) SFPE Handbook of Fire Protection Engineering. In National Fire Protection Association, Quincy, MA, USA.
127. Eastop, T. D. and McConkey, A. (1997) In *Applied thermodynamics for engineering technologists*, Addison Wesley Longman Limited, Essex, UK.
128. SFPE (2007) Engineering guide to fire exposures to structural elements. In Society of Fire Protection Engineers, Quincy, MA, USA.
129. Emmons, H. W. (2002) Section 2, Chapter 5: Vent Flows. In *The SFPE Handbook of Fire Protection Engineering*, National Fire Protection Association, Quincy, Massachusetts.
130. McCaffrey, B. (2002) Section 2, Chapter 1: Flame Height. In *The SFPE Handbook for Fire Protection Engineering*, National Fire Protection Association, Quincy, Massachusetts.
131. Zukoski, E. (1995) Properties of fire plumes. In *Combustion Fundamentals of Fire*, Academic Press, London.
132. Cox, G. and Chitty, R. (1985) Some source-dependent effects of unbounded fires. *Combustion and Flame*, Volume 60.
133. Thomas, P. H. (63) *The Size of Flames from Natural Fires*. Ninth Symposium (International) on Combustion, The Combustion Institute
134. Heskestad, G. (1983) Luminous Heights of Turbulent Diffusion Flames. *Fire Safety Journal*, Volume 5.
135. Steward, F. R. (1970) Prediction of the height of turbulent buoyant diffusion flames. *Combustion Science and Technology*, Volume 2.
136. Becker, H. A. and Liang, D. (1978) Visible length of vertical free turbulent diffusion flames. *Combustion and Flame*, Vol. 32, pp. 115-137.
137. Kalghatgi, G. T. (1984) Lift-Off Heights and Visible Lengths of Vertical Turbulent Diffusion Flames in Still Air. *Combustion Science and Technology*, Vol. 41.
138. Hawthorne, W. R., Weddell, D. S., and Hottel, H. C. (49) *Third Symposium on Combustion, Flame and Explosion Phenomena*. Third Symposium on Combustion, Flame and Explosion Phenomena, Williams and Wilkins, Baltimore
139. Ingason, H. and Lonnermark, A. (2005) Heat Release Rates from Heavy Goods Vehicle Trailers in Tunnels. *Fire Safety Journal*, Volume 40, pp 646-668.
140. Cox, G. and Kumar, S. (2002) Chapter 8 - Modelling Enclosure Fires using CFD. In *The SFPE Handbook of Fire Protection Engineering*, National Fire

Protection Association, Quincy, Massachusetts.

141. McGrattan, Kevin B. (2006) *Fire Dynamics Simulator (Version 4) Technical Reference Guide*. NIST Special Publication 1018, National Institute of Standards and Technology, Washington
142. McGrattan, Kevin B. and Forney, Glenn P. (2006) *Fire Dynamics Simulator (Version 4) User's Guide*. NIST Special Publication 1019, National Institute of Standards and Technology, Washington
143. Abbott, M. B. and Basco, D. R. (1990) *Computational Fluid Dynamics An Introduction for Engineers*. Longman Scientific & Technical, UK
144. Brandt, Tellervo T. (2006) *Study of Large Eddy Simulation and Smagorinsky Model using Explicit Filtering*. 36th AIAA Fluid Dynamics Conference and Exhibit, American Institute of Aeronautics and Astronautics Inc
145. Smagorinsky, J. (1964) *General Circulation Experiments with the Primitive Equations. I. The Basic Experiment*. The Monthly Weather Review
146. Friedman, R. (2002) Section one - Chapter 6 - Chemical Equilibrium. In *The SFPE Handbook of Fire Protection Engineering*, National Fire Protection Association, Quincy, Massachusetts.
147. Floyd, Jason E., McGrattan, Kevin B., Hostikka, Simo, and Baum, Howard R. (2003) *CFD Fire Simulation Using Mixture Fraction Combustion and Finite Volume Radiative Heat Transfer*. Journal of Fire Protection Engineering
148. Huggett, C. (1980) *Estimation of the Rate of Heat Release by Means of Oxygen Consumption*. Journal of Fire and Flammability
149. Ma, T and Quintierre, James G . (2003) *Numerical Simulaiton of Axi-Symmetric Fire Plumes: Accuracy and Limitations*. Fire Safety Journal
150. Atreya, A. (1883) *Ignition and Fire Spread on Horizontal Surfaces of Wood*. NBS GCR 83-449, National Bureau of Standards, Gaithersburg, Maryland
151. Ritchie, S. J., Steckler, K. D., Hamins, Anthony, Cleary, T. G., Yang, J. C., and Kashiwagi, T. (97) *The effect of sample size on the heat release rate of charring materials*. Fire Safety Science - Proceedings of the 5th International Symposium, International Association for Fire Safety Science
152. Moinuddin, Khalid A. M. and Thomas, Ian R. (2007) *Factors affectinng grid independent results for compartment fire modeling*. 16th Australian Fluid Mechanics Conference
153. Floyd, Jason E., Wieczorek, C., and Vandsburger, U. (2001) *Simulations of the Virginia Tech Fire Research Laboratory Using Large Eddy Simulation with Mixture Fraction Chemistry and Finite Volume Radiative Heat Transfer*. Proceedings of the Ninth International Interflam Conference, Interscience Communications, London

154. Liang, Ming. (2002) *Evaluation Studies of the Flame Spread and Burning Rate Predictions by the Fire Dynamics Simulator : Masters thesis*. University of Maryland, US
155. Kwon, Jae-Wook. (2006) *Evaluation of FDS V.4: upward flame spread - Masters Thesis*. Worcester Polytechnic Institute, US
156. Hostikka, Simo and McGrattan, Kevin B. (2001) *Large Eddy Simulations of Wood Combustion*. Proceedings of the Ninth International Interflam Conference, Interscience Communications Ltd, London
157. Moghaddam, A. Z., Moinuddin, Khalid, Thomas, Ian. R., Bennetts, Ian. D., and Culton, Micheal. (2004) *Fire Behaviour Studies of Combustible Wall Linings Applying Fire Dynamics Simulator*. 15th Australian Fluid Mechanics Conference
158. Hamins, Anthony, Maranghides, Alexander, McGrattan, Kevin B., Ohlemiller, Thomas J., and Anleitner, Robert L. (2005) *Federal Building and Fire Safety Investigation of the World Trade Centre Disaster: Experiments and Modelilng of Multiple Workstations Burning in a Compartment*. NIST NCSTAR 1-5E, National Institute of Standards and Technology, Washington U.S.
159. McGrattan, Kevin. (2007) *FDS Road Map - The FDS/Smokeview Research Plan*. [http://code.google.com/p/fds-smv/wiki/FDS\\_Road\\_Map](http://code.google.com/p/fds-smv/wiki/FDS_Road_Map)
160. Jiang, Yun. (2006) *Decomposition, ignition and flame spread on furnishing materials - A thesis submitted in fulfilment of the requirement for the degree of Doctor of Philosophy*. Centre for Environment Safety and Risk Engineering, Victoria University, Melbourne, Australia
161. Lee, Seung Han. (2006) *Material property estimation method using a thermoplastic pyrolysis model - Masters Degree thesis*. Worcester Polytechnic Institute, Worcester, Massachusetts, U.S.
162. Lautenberger, C., Rein, G. and Fernandez-Pello, C. (2006) The application of a genetic algorithm to estimate material properties for fire modelling from bench-scale fire test data. *Fire Safety Journal*, pp 204-214.
163. Chiam, Boon Hui. (2005) *Numerical simulation of a metro train fire - Masters Degree Thesis*. Fire Engineering Research Report 05/1, University of Canterbury, Christchurch, New Zealand
164. Janssens, M L, Kimble, J, and Murphy, D. (2003) *Computer tools to determine material properties for fire growth modelling from cone calorimeter data*. Fire and Materials 2003, 8th International Conference, Interscience Communications Limited
165. Babrauskas, V. (2003) *The Ignition Handbook*. Fire Science Publishers, Issaquah, WA.
166. Barden, Tara, Brown, Jason, and Hetrick, Todd. (2005) *Train Fire Modeling in Fire Dynamics Simulator -WPI undergraduate project report*. Project

Number: JRB-2402, Worcester Polytechnic Institute, Worcester, US

167. Gamache, Jason, Goldberg, Daniel, Montplaisir, Eric, and Wong, William. (2006) *Train Fire Modeling with FDS-WPI undergraduate project report*. Project Number: JRB-25CS, Worcester Polytechnic Institute, Worcester, US
168. ASTM. (2006) *ASTM C 1166 - 06 Standard Test Method for Flame Propagation of Dense and Cellular Elastomeric Gaskets and Accessories*. ASTM International, West Conshohocken, PA, USA
169. Peacock, Richard D., Bukowski, Richard W., Jones, Walter W., Reneke, Paul A., Babrauskas, Vytenis, and Brown, James E. (1994) *Fire Safety of Passenger Trains: A Review of Current Approaches and of New Concepts*. NIST Technical Note 1406, National Institute of Standards and Technology, Building and Fire Research Laboratory, Gaithersburg, MD 20899
170. NFPA. (2001) *NFPA 258 Recommended Practice for Determining Smoke Generation of Solid Materials*. National Fire Protection Association, Quincy, MA, USA
171. Ostman, Brigit A-L. (1992) *Smoke and Soot*. Elsevier Science Publishers Ltd, New York, USA
172. Hirschler, Marcelo M. (1993) *Carbon Monoxide and Human Lethality: Fire and Non-Fire Studies*. Elsevier Science Publishers Ltd, Essex, England
173. AFNOR. (1986) *NF X 70-100 Fire tests - Analysis of pyrolysis and combustion gases, Tube furnace method*. l'association francaise de normalisation (AFNOR), France
174. BSI. (1989) *BS 476: Part 6 - Fire test on building materials and structures Part 6: Method of test for fire propagation for products*. British Standards Institution, London, UK.
175. BSI. (1997) *BS 476 Part 7 - Fire tests on building materials and structures Part 7 - Method of test to determine the classification of the surface spread of flame of products*. British Standards Institute, London, UK
176. ISO. (2002) *ISO 9239-2 Reaction to fire tests for floorings - Part 2: Determination of flame spread at a heat flux level of 25 kW/m<sup>2</sup>*. International Organization for Standardization, Geneva, Switzerland
177. McArthur, Neville A., Bradbury, G. P., Bowditch, P. A., and Leonard, J. A. (1998) *Comparative Assessment of the Performance of Various Fire Tests for Floor Coverings*. BCE Doc. 98/131, CSIRO Building Construction and Engineering, Highett, Australia
178. ASTM. (2005) *ASTM E 119 - 05a Standard Test Methods for Fire Tests of Building Construction and Materials*. ASTM International, West Conshohocken, PA, USA
179. BSI. (1987) *BS 476: Part 20: Fire tests on buildings materials and structures*

*Part 20 - Method for determination of the fire resistance of elements of construction (general principals).* British Standards Institute, London, UK

180. BSI. (1987) *BS 476: Part 22 - Fire tests on building materials and structures Part 22 - Methods for determination of the fire resistance of non-load bearing elements of construction.* British Standards Institute, London, UK
181. Thornton, W. (1917) The Relation of Oxygen to the Heat of Combustion of Organic Compounds. *Philosophical Magazine and J. of Science* , 33.
182. Parker, W. J. (1984) Calculation of the Heat Release Rate by Oxygen Consumption for Various Applications. *Journal of Fire Sciences*, 2, 380-395.
183. Babrauskas, V. (1992) Chapter 4: The Cone Calorimeter. In *Heat Release in Fires*, Elsevier Science Ltd, Essex, England.
184. Standards Australia. (1998) *AS/NZS 3837 Method of test for smoke and heat release rates for materials and products using an oxygen consumption calorimeter.* Sydney, Australia
185. ASTM. (2004) *ASTM E 1354 - 04a Standard Test Method for Heat and Visible Smoke Release Rates for Materials and Products Using an Oxygen Consumption Calorimeter.* ASTM International, West Conshohocken, PA, USA
186. Babrauskas, V. (1992) Chapter 2: From Bunsen Burner to Heat Release Rate Calorimeter Heat Release in Fires. In *Heat Release in Fires*, Elsevier Science Publishers Ltd, Essex, England.
187. ISO. (1996) *ISO 4589-2 Plastics - Determination of burning behaviour by oxygen index - Part 2: Ambient temperature test.* International Organization for Standardization, Geneva, Switzerland
188. SFPE (2002) Appendix C: Physical and combustion properties. In *SFPE Handbook of Fire Protection Engineering*, National Fire Protection Association, Quincy, MA, USA.

## APPENDIX A - Standard Test Methods

Standard test methods applied to passenger train interior materials for the purposes of regulation and experimental work are summarised and critiqued as follows. Only test methods referred to in other sections of this literature review are summarised. It is beyond the scope of this research to summarise all other test methods such as the German DIN tests. All test methods are small-scale unless otherwise described.

### A.1 Small Flame Tests

#### FAR 25.853 (a)

This U.S. test method was developed by the Federal Aviation Administration (FAA) to assess seat upholstery, mattress ticking and covers and curtains<sup>[68]</sup>. A 50mm wide, 305 mm long specimen is held vertically. A 39mm long flame is applied to the lower edge of the specimen either for 12 seconds or 60 seconds (determined by end use of the material). The test records flame time, burn length and flaming time of dripping material.

#### ASTM C 542 and ASTM C 1166

ASTM C 542 is applied for elastomers. The test consists of a 460 mm long specimen suspended vertically over a Bunsen burner flame for 15 min inside a controlled ventilation combustion chamber. ASTM C 1166<sup>[68]</sup> is a similar test method applied for dense and cellular elastomeric gaskets and accessories. The Bunsen burner flame is applied for 15 min for dense materials and 5 min for cellular materials. The length of material left after exposure to the flame is intended to provide a measure of the flame propagation.

#### NF P 92504

This French test method<sup>[69]</sup> is applied if there has been significant dripping or melting in the NF P 92501 and NF P 92503 test methods. A specimen is supported horizontally and exposed to a Bunsen burner flame at one end. The time to burn a set distance along the specimen is the criterion for classification.

#### Discussion of small flame tests

Small flame tests have been used and misused to test the flammability of materials since the 1930's.<sup>[53]</sup> During the 1950's and 60s there was an increased reliance on small flame tests but in recent years this reliance has decreased as new test methods that produce more useful measurements have been introduced. Small flame tests have originated from a need to perform quick and cheap screening tests (such as holding a match to a material to see if it burns) Some methods have become overly complex given these origins. These methods assess the ease of ignition and the ability to sustain flaming under set laboratory conditions but do not provide useful data that can be used to predict fire behaviour for real fire scenarios. They can only be used for screening. Dripping of materials can unseat and extinguish flaming in these tests producing a good test result however in real fire scenarios the material may be orientated or restrained so that it either forms a molten pool or drips onto other combustible materials which may increase hazard of flame spread.

## A.2 Smoke Tests

### NFPA 258, ASTM E 662 and ISO 5659-2 smoke density chamber tests

NFPA 258<sup>[170]</sup> and ASTM E 662<sup>[69]</sup> are identical US test methods which measure smoke density that is contained within a chamber that is approximately 0.5m<sup>3</sup>. This type of smoke measurement is cumulative as smoke density is contained and can only increase. Smoke density is measured as the decrease in light transmission due to the smoke produced from a vertically mounted solid specimen exposed to a heat source. The optical light path is vertical from the base to the top of the chamber. Specimens are typically exposed to a radiant heat flux of 25 or 35 kW/m<sup>2</sup> and a small burner flame system can be applied to simulate flaming combustion. The fraction of light transmission ( $T_L$ ) is used to compute the specific optical density,  $D_s$ , defined as

$$D_s = \frac{V}{AL} \log_{10}(100/T_L)$$

Where      V = chamber volume  
               L = light beam path length  
               A = surface area of the specimen

$D_s$  is a dimensionless quantity. The maximum specific optical density and optical density at 1.5 and 4 minutes is recorded. Optical density can be related to visibility through smoke. ISO 5659-2<sup>[60]</sup> is a similar smoke density chamber test with the main difference being the specimen is mounted horizontally under a conically shaped radiator and the specimen is tested either at an irradiance of 25 kW/m<sup>2</sup> in the presence or absence of a pilot flame or at an irradiance of 50 kW/m<sup>2</sup> in the absence of a pilot flame.

### BS 6853 Annex D smoke test

Annex D of BS 6853<sup>[83]</sup> specifies a cumulative smoke test conducted in a 3m cube test chamber applying a horizontal optical light path at a height of 2.15 m. A fan is used to mix the smoke in the test chamber. Depending on the type of specimen tested either 1 L of alcohol or 0.5 kg of charcoal is used as the fire source. The fire sources are applied to large specimens such as complete seats, or 1m × 0.5m panel sections. Optical density is measured during a 20 min test duration.

### Discussion of smoke tests

An issue with all small-scale smoke test methods is that they all represent a particular ventilation condition, being either well ventilated, dynamic, flow through systems such as the cone calorimeter or contained (no ventilation), cumulative systems. Real fires may vary from being well ventilated to poorly ventilated. Ventilation effects not only the dilution of smoke but also the completeness of combustion and hence the density of smoke produced per mass burnt. Ostmen<sup>[171]</sup> suggests that early stages of certain full-scale fire scenarios can be predicted from small-scale tests however post-flashover smoke production cannot be resolved yet. Smoke and toxic gas production are a critical factor in fire fatalities.<sup>[172]</sup> However it is not clear that requirements for materials based on small-scale smoke and toxic gas tests is an effective method of improving life safety. In post flashover fires most combustible materials produce large quantities of smoke and toxic gases. As smoke and toxic gas production is related to HRR a more effective strategy for life safety is likely to be careful selection of materials so as to minimise the likelihood of a large HRR fire occurring.

### **A.3 Toxicity Tests**

#### **NF X 70-100 toxicity test**

In this French test method<sup>[173]</sup> a 1 g sample is placed in a tube furnace which is heated to 600 °C for all materials except electrical wiring which for which it is heated to 800 °C. Combustion and pyrolysis gases are pumped from the tube furnace during the 20 minute test duration and the total yield of CO, CO<sub>2</sub>, HCl, HF, HBr, HCN, SO<sub>2</sub> and NO<sub>x</sub> is measured.

#### **BS 6853 Annex B.2 toxicity test**

BS 6853 utilises two different tests for assessing toxicity depending on the type and use of material. For minor materials, textiles and cables the NF X 70-100 test method is used. Surfaces, seat trim, seat shells are tested according to Annex B.2 of BS6853. In this test method a horizontal specimen is exposed to a radiant heat flux of 25 kW/m<sup>2</sup> using the ISO 5659-2 smoke test apparatus, with concentrations of CO, CO<sub>2</sub>, HCl, HF, HBr, HCN, SO<sub>2</sub> and NO<sub>x</sub> being measured. BS 6853 requires the results to be expressed as area-based yields, i.e. grams of gas produced per square metre of material exposed. These yields are compared against reference yields and the final test result is expressed in terms of a weighted ratio (R value).

#### **Discussion of toxicity tests**

Most toxicity tests represent a well ventilated pyrolysis condition. In real fire scenarios toxic gas usually threatens life safety when the quantity of gas produced is high at near or post flashover conditions. For these conditions the fire is usually not well ventilated and CO is usually the primary toxic gas. Toxicity tests do not represent near or post flashover fires and do not provide adequate data to predict toxic gas production in such a fire scenario

### **A.4 Flame Spread Tests**

#### **ASTM E 162 and D 3675 flame spread tests.**

These two test methods<sup>[65,66]</sup> measure surface flame spread and heat evolution behaviour when a material is exposed to an external radiant heat flux. The test methods are functionally identical. The minor difference is that ASTM E 162 is intended for general materials and ASTM D 3675 is intended for flexible cellular foam materials that have a tendency to shrink and fall out of the holder and thus a more secure specimen holder is required. An inclined specimen (152x457 mm) is placed in front of a vertical radiant panel (305 x 457 mm) such that ignition is forced near its upper edge with a pilot and flame spread progresses downward. An exhaust stack containing thermocouples is mounted above the radiant panel and specimen. The mean stack temperature rise per unit rate of heat input is obtained prior to testing using a calibration burner. A flame spread factor  $F_s$  is calculated as a function of time vs. distance of spread. A heat evolution factor  $Q$  is calculated as a function of stack temperature measurements. A radiant panel index  $I_s$  is then calculated as the product of  $F_s$  and  $Q$ .

#### **BS 476 Part 6 fire propagation test**

This British test method<sup>[174]</sup> is primarily intended for internal wall and ceiling linings. A 225 mm square specimen is mounted vertically in a small chamber. The chamber is heated using electrical elements and a gas burner tube is applied to the bottom of the

specimen. The result expressed as a fire propagation index is calculated based on flue gas temperatures.

#### **BS 476 Part 7 lateral flame spread test**

This British test method<sup>[175]</sup> is intended primarily for wall and ceiling linings. A rectangular specimen 885 × 270 mm is mounted perpendicular to a large 850 mm square gas fired radiant panel. The radiant heat flux along the specimen decreases from 30 kW/m<sup>2</sup> at the near end to 5 kW/m<sup>2</sup> at the far end. A pilot burner is applied to the near end. Materials are classified from class 1 to Class 4 dependent on the extent of lateral flame spread.

#### **NF P 92501 and NF P 92503 radiant panel tests**

NF P 92501 and NF P 92503 are similar French test methods.<sup>[169]</sup> NF P 92501 is for rigid materials, a specimen is mounted at 45° and an electric radiator provides a heat flux of 30 kW/m<sup>2</sup> at one end of the specimen. Pilot flames are applied to ignite the specimen. Time to ignition, maximum flame length and temperatures are observed and results are stated in terms of a flammability index, a spread index and an index for maximum flame length. NF P 92503 is similar but is for flexible materials and the specimen is mounted differently at 30°

#### **ISO 9239, ASTM E 648 and NFPA 253 flooring critical radiant heat flux**

ISO 9239-1,<sup>[63]</sup> ASTM E 648<sup>[67]</sup> and NFPA 253 are functionally identical test methods. A 1 m long flooring specimen is mounted horizontally beneath a radiant heat panel inclined at 30° at one end. The radiant heat flux gradient varies along the 1m length from 11 kW/m<sup>2</sup> to 1 kW/m<sup>2</sup>. The specimen is ignited using a pilot at the high heat flux end and the distance at which the specimen extinguishes itself determines the critical radiant heat flux (CRF) required to support flame propagation. ISO 9239-2<sup>[176]</sup> is similar except that the heat flux varies from 25 kW/m<sup>2</sup> to 2 kW/m<sup>2</sup> along the 1m long specimen.

#### **NF P 92506 radiant panel test for flooring**

NF P 92506 is a French test method for flooring.<sup>[169]</sup> A 400 × 95 mm specimen is mounted perpendicular to a vertical radiant panel run at temperature of 850 °C. The specimen is mounted with the long edge horizontal and the short edge vertical. A pilot is applied to the end closest to the radiant panel. Length of lateral flame spread is observed.

#### **Discussion of flame spread tests**

None of these methods measure HRR by oxygen consumption calorimetry (see next section) however some attempt to measure HRR by measuring stack gas temperatures and flows. As the apparatus is not adiabatic and the ratio of convective heat to radiative heat varies for different materials errors exist in the measurement of heat evolution by exhaust temperature. These methods commonly express results in terms of indexes such as a radiant panel index or flame spread index. The use of an index does not provide useful engineering properties that could be used to predict real fire scenario behaviour. This makes these methods only useful for comparative testing and ranking of materials. The orientation of a material is likely to have a critical effect on its flame spread properties. Some test methods use an inappropriate orientation for the type of material considered, ie NF P 92506 test carpet in a vertical orientation. Testing of plastic materials in a vertical orientation which melt and flow and are intended for

use in a horizontal prone or supine orientation (such as carpet) can produce results which do not match with real performance.<sup>[177]</sup>

Floors are not usually the material first ignited but rather ignite due to exposure from a developing fire on other interior materials. Flooring radiant panel test methods are more appropriate as these test the flooring in the correct orientation exposing it to a heat flux range representing a realistic fire exposure.<sup>[177]</sup> Although the critical radiant heat flux required to support flame propagation as determined by the test is expressed in engineering units it is not a useful fundamental flammability property that can be used to predict behaviour in real fire scenarios. Flooring radiant panel test methods only produce data that enables ranking of material performance.

## **A.5 Fire Resistance Tests**

### **AS 1530.4, ASTM E 119 and BS 476:Parts 20 and 22 fire resistance tests**

AS 1530.4, ASTM E 119<sup>[178]</sup> and BS 476:Parts 20 and 22<sup>[179,180]</sup> are all similar test methods. Different types of structural and barrier assemblies are tested in a variety of different furnaces. The furnace temperature is increased over time according to the following standard time-temperature curve

$$T(K) = 345 \log_{10}(8t + 1) + 293$$

For load bearing assemblies a load is applied. The results are stated in terms of time to failure according to 3 criteria relating to integrity, insulation and load bearing capacity.

### **Discussion of fire resistance tests**

Due to the slow temperature rise of the exposure, fire resistance tests have been identified to poorly represent fast growing fires such as hydrocarbon pool fires or fast flashover fires. A different time-temperature curve called the “Hydrocarbon” curve has been introduced to address this. However many conventional furnaces are not capable of achieving the hydrocarbon curve. Although it may not precisely represent a real fire scenario, fire resistance tests are appropriate for ensuring suitable fire resistance of critical fire barriers in trains (such as floors) for the period required for safe egress if a suitable factor of safety is incorporated to allow for faster growing fires.

## **A.6 Heat Release Rate Tests**

### **Principal of oxygen consumption calorimetry**

Early attempts at measuring HRR of fires involved relating HRR to measurements of temperature increases in flues or insulated box systems. Some attempts also involved relating HRR to specimen mass loss rate. The principal of oxygen consumption calorimetry is a more practical and accurate method to measure the rate of heat release from fire. In 1917, Thornton<sup>[181]</sup> demonstrated that a wide range of organic liquids and gases released a roughly constant net amount of heat per unit mass of oxygen consumed for complete combustion. Huggett<sup>[148]</sup> demonstrated that this also applied for organic solids and that the average value for this constant is 13.1 MJ/kg of O<sub>2</sub>. This is accurate for a wide range of materials, with a few exceptions, to within ± 5%.

Since the 1970's this principal has been used to measure heat release of fires. The apparatus required for this includes a collection hood and exhaust duct to capture combustion gases with gas flow rate and oxygen concentration measurements taken from the exhaust duct. Parker<sup>[182]</sup> provides equations to calculate HRR by O<sub>2</sub> consumption for various applications. This technique is the principal method of HRR measurement used by fire laboratories around the world, both in small-scale and large-scale.

#### **ISO 5660, AS/NZS 3837 and ASTM E 1354 Cone calorimeter tests**

The cone calorimeter<sup>[183]</sup> is a small-scale oxygen consumption calorimeter. Specimens, 100 mm square are supported horizontally on a load cell and exposed to a set external radiant heat flux in ambient air conditions. The radiant heat source is a conically shaped radiator that can be set to impose any heat flux in the range 0-100 kW/m<sup>2</sup> on the specimen surface. Ignition is promoted using a spark igniter. Combustion gases are extracted in an exhaust duct where instrumentation measures exhaust gas flow, temperature, O<sub>2</sub>, CO and CO<sub>2</sub> concentrations and smoke optical density. From these measurements quantities such as heat release rate and smoke production can be calculated. Time to ignition is determined by observation. The cone calorimeter apparatus and procedure are described in ISO 5660,<sup>[59]</sup> AS/NZS 3837<sup>[184]</sup> and ASTM E 1354.<sup>[185]</sup>

#### **OSU Calorimeter**

The Ohio State University (OSU) calorimeter was first developed in 1972.<sup>[186]</sup> This apparatus consisted of a square insulated combustion chamber with an air inlet at the bottom and an exhaust flue at the top. A 150×150 mm specimen is mounted vertically in front of a vertical electric radiant panel. HRR is determined by measuring exhaust gas temperatures. A calibration curve is determined by operating a gas burner in the apparatus at a series of outputs. Some attempts were made to modify the OSU calorimeter to apply oxygen consumption calorimetry however the cone calorimeter has become much more widely applied.

#### **ISO 9705 room test**

ISO 9705 is a large scale oxygen consumption calorimetry test primarily intended for wall and ceiling linings. Wall and ceiling linings are mounted in a 2.4 m wide × 2.4 m high × 3.6 m long burn room with one doorway leading to a 3m square smoke collection hood. A gas sand burner is applied to one corner of the room with an output of 100 kW for 10 min and 300 kW for a further 10 min. HRR and smoke optical density are measured at the exhaust duct drawing combustion products from the smoke collection hood. The test method does not specify pass fail criteria however other regulations often use time to flashover as criteria. The hood and burn room are often used for non-standard experiments with HRR measurement.

#### **Furniture calorimeter tests**

There are many standard test methods such as BS 5852 which apply various ignition sources to complete seat specimens without measuring HRR. Ignition sources include a range of timber cribs and crumpled newspaper etc. NT FIRE 032<sup>[64]</sup> applies timber cribs to complete seats whilst measuring mass loss by mounting the seat on a load platform. HRR is measured by conducting the test under the ISO 9705 hood. California Technical Bulletin 133<sup>[81]</sup> is another furniture calorimeter test where HRR may be measured. In this case the seat is tested inside a burn room and either newspaper or a gas burner in the form of a 250 × 250 mm square ring with a series of

downward facing holes. A propane flow rate of 13 L/min (17 kW) for a period of 80 seconds is applied to the surface of the seat and is designed to simulate ignition with crumpled sheets of newspaper.

### **Discussion of heat release rate test methods**

The cone calorimeter attempts to measure fundamental flammability properties of materials that are required to predict material behaviour in real fires. Much research has been focused on predicting real fire behaviour based on cone calorimeter results, however the ability to make such predictions remains very limited. Some reasons for this are;

- the cone calorimeter method measures properties under set conditions which affect the properties attempting to be measured,
- the cone calorimeter does not directly measure all fundamental properties that may be required such as heat of volatilisation, heat capacity and thermal conductivity, and
- the theoretical link between fundamental properties and real fire behaviour is complex and not well developed.

The cone calorimeter is a very complex apparatus requiring more maintenance and calibration than other small-scale fire apparatus. Erroneous data can easily be generated if the operator does not have a high level of competency.

The ISO 9705 room test allows mock ups of train interior materials to be tested in large-scale. The size and ventilation of the burn room strongly influence the onset of flashover. Thus, for train materials, ISO 9705, apparatus is only appropriate for investigating the pre flashover fire development. Furniture calorimeter tests allow investigation of the ignitability and HRR of single seats. This allows effects of seat geometry which can be significant to be observed. However improved data for real fire scenarios is likely to be obtained by testing seats in combination with other materials.

## **A.7 Other Test Methods**

### **AS 1530.3 early fire hazard test**

AS 1530.3, known as the early fire hazard was originally intended for testing flammability of wall linings. A specimen 450 × 600 mm is mounted vertically opposite a vertical gas fired radiant panel. The specimen is advanced towards the radiant panel at a prescribed rate. A pilot flame is applied to the specimen surface to ignite pyrolysis gases. A radiometer measures radiant heat produced by ignition of the specimen. Smoke is collected in a hood and rises through a vertical duct where optical density is recorded. These measurements are used to express performance in terms of an Ignitability Index, Spread of Flame Index, Heat Evolved Index and Smoke Developed Index. These index results are not directly related to fundamental flammability properties or real fire performance. This test has been applied to floor and ceiling linings but has been demonstrated as inappropriate for these materials

### **Oxygen Index Test**

ISO 4589-2 defines the oxygen index test.<sup>[187]</sup> A small specimen, typically 150 mm long, is supported vertically in a mixture of oxygen and nitrogen flowing upwards through a glass cylinder. The upper end of the specimen is ignited applying a small

pilot flame and the period and length of specimen burnt is observed. This is repeated for various oxygen concentrations so as to determine the minimum oxygen concentration that will support combustion. This concentration in percentage by volume is expressed as the oxygen index (OI). NF T 51071, NF G 07128 and ASTM D2863<sup>[169]</sup> are similar oxygen index tests. This test method is intended for quality control and cannot be used to predict fire behaviour under actual fire conditions. Results are sensitive to specimen thickness and ignition procedures.

**NF P 92505 test for dripping**

This French test method<sup>[169]</sup> is applied if there has been significant dripping or melting in the NF P 92501 and NF P 92503 test methods. A specimen is supported horizontally with a 500 W radial heater above the specimen. Drippings are collected on cotton wool 300 mm below. The material is categorised based on the quantity of dripping and ignition of the cotton wool. This test method cannot be directly related to behaviour under actual fire conditions

## **APPENDIX B – FIRE SAFETY STANDARD MATERIAL REQUIRMENTS**

**Table B.1 Summary small-scale material flammability and smoke test requirements for NFPA 130 and FRA regulations**

Category	Function of Material	Flammability / Resistance Requirements		Smoke Requirements	
		Test Method	Performance Criteria	Test Method	Performance Criteria
Cushions, mattresses	All	ASTM D 3675	$I_s \leq 25$	ASTM E 662	$D_s (1.5) \leq 100$ $D_s (4.0) \leq 175$
Fabrics	All	14 CFR 25, Appendix F, Part I (vertical test)	Flame time $\leq 10$ s Burn length $\leq 6$ in.	ASTM E 662	$D_s (4.0) \leq 200$
Interior vehicle components	Seat and mattress frames, wall and ceiling lining and panels, seat and toilet shrouds, trays and other tables, partitions, shelves, opaque windscreens, and combustible signage	ASTM E 162	$I_s \leq 35$	ASTM E 662	$D_s (1.5) \leq 100$ $D_s (4.0) \leq 200$
	Flexible cellular foams used in seat, mattress and armrest	ASTM D 3675	$I_s \leq 25$	ASTM E 662	$D_s (1.5) \leq 100$ $D_s (4.0) \leq 175$
	Thermal and acoustical insulation	ASTM E 162	$I_s \leq 25$	ASTM E 662	$D_s (4.0) \leq 100$
	HVAC ducting	ASTM E 162	$I_s \leq 25$ <sup>1</sup>	ASTM E 662	$D_s (4.0) \leq 100$
	Floor covering	ASTM E 648	$CRF \geq 5$ kW/m <sup>2</sup>	ASTM E 662	$D_s (1.5) \leq 100$ $D_s (4.0) \leq 200$
	Light diffusers, windows and transparent plastic windscreens	ASTM E 162	$I_s \leq 100$	ASTM E 662	$D_s (1.5) \leq 100$ $D_s (4.0) \leq 200$
Elastomers	Window gaskets, door nosings, inter-car diaphragms, and roof mats	ASTM C 1166	Average flame propagation $< 4$ in.	ASTM E 662	$D_s (1.5) \leq 100$ $D_s (4.0) \leq 200$
Exterior vehicle components	End caps, roof housings, articulation bellows, exterior shells and component boxes and covers	ASTM E 162	$I_s \leq 35$	ASTM E 662	$D_s (1.5) \leq 100$ $D_s (4.0) \leq 175$
Wire and cable	All	UL 1581, CSA C22.2, UL 1685, NFPA 262, ANSI/UL 1666,	Pass <sup>2</sup>	ASTM E 662 NFPA 262, UL 1685	Pass <sup>2</sup>
	Control and low voltage	ICEA S-19 / NEMA WC3, UL 44, UL 83	Pass <sup>2</sup>		
	Fire alarm cable			IEC 60331-11	Pass <sup>2</sup>
Structural components	Flooring and other barriers to fire spread			ASTM E 119	Fire resistance $> 15$ minutes

Note<sup>1</sup> – Tabulated requirements are for NFPA 130, for FRA Requirements  $I_s \leq 35$ .

Note<sup>2</sup> – Any one or a combination of the tabulated test methods may be used, criteria are too complex to summarise in table.

**Table B. 2 Summary of BS 6853 material requirements**

Function of Material	Flammability requirements					Smoke and toxicity requirements				
	Test method	parameter	Vehicle category			Test method	parameter	Vehicle category		
			Ia	Ib	II			Ia	Ib	II
Interior horizontal supine surface (floor)	BS 476-7 Or BS ISO 9239-1	Surface Spread of flame (worst permissible class)	Class 2	Class 2	Class 2	BS 6853 Annex D flooring tests	A <sub>0</sub> (max.)	220	350	nc
		Critical radiant heat flux at extinguishment (max.)	7.5 kW/m <sup>2</sup>	7.5 kW/m <sup>2</sup>	7.5 kW/m <sup>2</sup>	BS 6853 Annex B	R (max.)	5.0	8.0	18
Interior vertical surfaces (walls)	BS 476-6	i <sub>1</sub> (max.)	6	6	nc	BS 6853 Annex D panel test	A <sub>0</sub> (ON)	2.6	4.2	9.4
		I(max.)	12	12	nc	BS 6853 Annex B	A <sub>0</sub> (OFF)	3.9	6.3	14.0
Interior horizontal prone surface (ceiling)	BS 476-7	Surface spread of flame (worst permissible class)	Class 1	Class 1	Class 1	BS 6853 Annex B	R (max.)	1.0	1.6	3.6
		i <sub>1</sub> (max.)	6	6	nc	BS 6853 Annex D panel test	A <sub>0</sub> (ON)	2.6	4.2	9.4
Interior horizontal prone surface (ceiling)	BS 476-6	I(max.)	12	12	nc	BS 6853 Annex D panel test	A <sub>0</sub> (OFF)	3.9	6.3	14.0
		Surface spread of flame (worst permissible class)	Class 1 0 mm <sup>a</sup>	Class 1	Class 1	BS 6853 Annex B	R (max.)	1.0	1.6	3.6
Exterior horizontal supine surface	BS 476-7 Or BS ISO 9239-1	Surface Spread of flame (worst permissible class)	Class 2	Class 2	Class 2	BS 6853 Annex D flooring tests	A <sub>0</sub> (max.)	370	590	nc
		Critical radiant heat flux at extinguishment (max.)	7.5 kW/m <sup>2</sup>	7.5 kW/m <sup>2</sup>	7.5 kW/m <sup>2</sup>	BS 6853 Annex B	R (max.)	8.5	13.5	18
Exterior vertical surface	BS 476-7	Surface Spread of flame (worst permissible class)	Class 1	Class 1	Class 2	BS 6853 Annex D panel test	A <sub>0</sub> (ON)	4.4	7.0	nc
						BS 6853 Annex B	A <sub>0</sub> (OFF)	6.6	10.5	nc
Exterior horizontal prone surface (under floor)	BS 476-7	Surface Spread of flame (worst permissible class)	Class 1 0 mm <sup>a</sup>	Class 1	Class 1	BS 6853 Annex D panel test	R (max.)	1.7	2.7	nc
						BS 6853 Annex B	A <sub>0</sub> (ON)	4.4	7.0	nc
						A <sub>0</sub> (OFF)	6.6	10.5	nc	
						R (max.)	1.7	2.7	nc	

**Table B.3 Summary of BS 6853 material requirements (continued)**

Function of Material	Flammability requirements					Smoke and toxicity requirements				
	Test method	parameter	Vehicle category			Test method	parameter	Vehicle category		
			Ia	Ib	II			Ia	Ib	II
Interior minor use materials 100-500g	BS EN ISO 4589-3:1996 Annex A  Or BS ISO 4589-2	Flammability temperature (FT) (min.)	300°C	300°C	250°	BS 6853 Annex D small-scale test	A <sub>0</sub> (max.)	0.017	0.027	0.061
		Oxygen Index (min.)	34% (V/V)	34% (V/V)	28% (V/V)		BS 6853 Annex B	R (max.)	1.0	1.6
Exterior minor use materials 100-500g	BS EN ISO 4589-3:1996 Annex A  Or BS ISO 4589-2	Flammability temperature (FT) (min.)	300°C	300°C	250°	BS 6853 Annex D small-scale test	A <sub>0</sub> (max.)	0.029	0.046	nc
		Oxygen Index (min.)	34% (V/V)	34% (V/V)	28% (V/V)		BS 6853 Annex B	R (max.)	1.7	2.7
Seat trim back	BS 476-6	i <sub>1</sub> (max.)	6	6	nc	BS 6853 Annex D seating test	A <sub>0</sub> (max)	8.7	14.0	nc
		I(max.)	12	12	nc		BS 6853 Annex B	R (max.)	2.0	3.2
Seat trim back	BS 476-7	Surface spread of flame (worst permissible class)	Class 1	Class 1	Class 1	BS 6853 Annex D seating test		A <sub>0</sub> (max)	8.7	14.0
		Surface spread of flame (worst permissible class)	Class 1	Class 1	Class 1		BS 6853 Annex B	R (max.)	3.5	5.6
Seat shell (back & base)	BS 476-6	i <sub>1</sub> (max.)	6	6	nc	BS 6853 Annex D seating test	A <sub>0</sub> (ON)	2.6	4.2	9.4
		I(max.)	12	12	nc		A <sub>0</sub> (OFF)	3.9	6.3	14.0
	BS 476-7	Surface spread of flame (worst permissible class)	Class 1	Class 1	Class 1	BS 6853 Annex B	R (max.)	1.0	1.6	3.6

Note nc = no criterion  
a = no spread of flame

## APPENDIX C – IGNITION SOURCES

All ignition sources applied in the full-scale experiments and additional large-scale experiments conducted are described in Table C 1. Most ignition sources were characterised in terms of HRR and burn duration using an ISO 9705 fire calorimeter. Ignition sources were either burnt on the open floor or in different positions on a mock up wall corner and seat constructed of non combustible plasterboard so as to simulate the ventilation and re radiation conditions of a real scenario without involving combustibles. In all cases either duplicate or triplicate tests were performed. The median HRR curves for the characterised ignition sources are shown in Figure C.

1

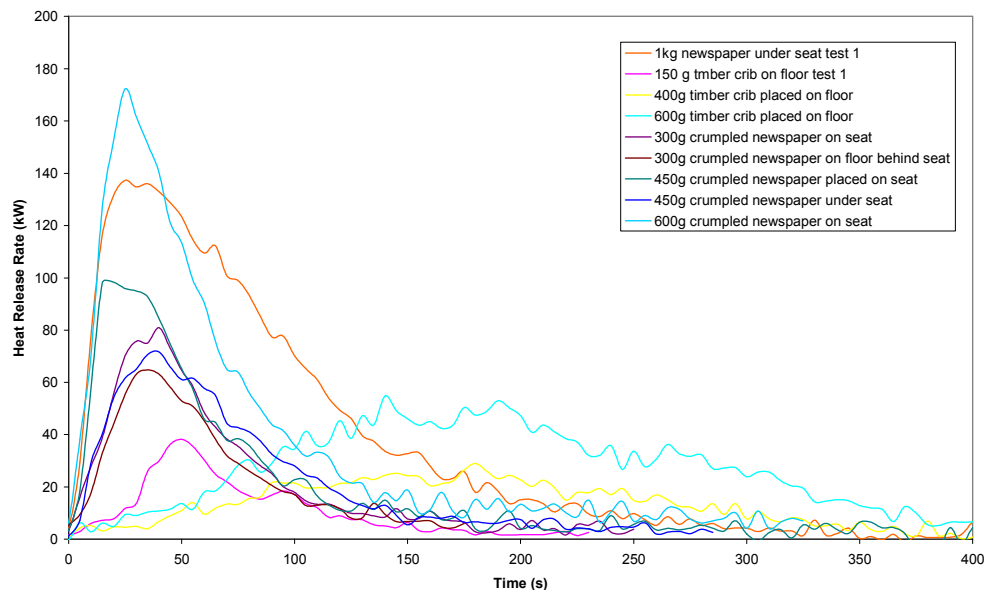


**Figure C. 1 Median HRR curves for ignition sources**

It is noted that crumpled newspaper provides a relatively high peak HRR with short burn duration for mass of material used. The 400g and 600g timber cribs with 6mm thick sticks provide lower peak HRR with longer burn durations for the mass of material used. The 150 g timber crib with 3.5 mm thick sticks burns more rapidly in a similar manner as for crumpled newspaper. Placing the crumpled newspaper ignition sources in a non combustible corner beneath a non combustible seat significantly reduces the peak HRR due to restricted ventilation. The newspaper ignition sources exhibited significantly more variability than timber crib ignition sources.

**Table C 1 Ignition source descriptions and characterisation**

Ignition source	General Description	Arrangement with non-combustible surfaces for characterisation test	Properties measured with non-combustible corner and seat		
			Ave. peak HRR (kW)	Ave. time to peak HRR (s)	Burn duration (s)
match	Redhead Handypack kitchen match	No Characterisation test	-	-	-
Gas torch with pre-mixed flame	Bernz-o-matic TS 2000 head on 400 g propane bottle. Flame length 100 mm with 15 mm blue cone.	No Characterisation test	-	-	-
BS 5852(3) Source 1	Stainless steel tube 200 mm long, 6.5 mm ID. Butane flame 44 l/min, applied for 20s.	No Characterisation test	-	-	-
BS 5852(3) Source 2	Stainless steel tube 200 mm long, 6.5 mm ID. Butane flame 157 l/min, applied for 20 s.	No Characterisation test	-	-	-
150 g timber crib	CSIRO crib. Cross piles of Pinus radiata sticks of density $500 \pm 50$ kg/m <sup>3</sup> conditioned for at least 7 days at $23 \pm 2^\circ\text{C}$ and $50 \pm 5$ % RH. Stick length is $200 \pm 1$ mm, stick width is $3.5 \pm 0.2$ mm, the number of sticks per layer is 7 and the total crib mass is 150 g.	Crib placed on open floor area	38	50	145
300 g timber crib	CSIRO crib. Cross piles of Pinus radiata sticks of density $500 \pm 50$ kg/m <sup>3</sup> conditioned for at least 7 days at $23 \pm 2^\circ\text{C}$ and $50 \pm 5$ % RH. Stick length is $200 \pm 1$ mm, stick width is $5.0 \pm 0.2$ mm, the number of sticks per layer is 10 and the total crib mass is 300 g.	Crib placed on open floor area	40	98	260
400 g timber crib	CSIRO crib. Cross piles of Pinus radiata sticks of density $500 \pm 50$ kg/m <sup>3</sup> conditioned for at least 7 days at $23 \pm 2^\circ\text{C}$ and $50 \pm 5$ % RH. Stick length is $200 \pm 1$ mm, stick width is $6.0 \pm 0.2$ mm, the number of sticks per layer is 11 and the total crib mass is 400 g.	Crib placed on open floor area	26	135	377

Table C.1. *Continued*

Ignition source	General Description	Arrangement with non-combustible surfaces for characterisation test	Properties measured with non-combustible corner and seat		
			Ave. peak HRR (kW)	Ave. time to peak HRR (s)	Burn duration (s)
600 g timber crib	CSIRO crib. Cross piles of <i>Pinus radiata</i> sticks of density $500 \pm 50 \text{ kg/m}^3$ conditioned for at least 7 days at $23 \pm 2^\circ\text{C}$ and $50 \pm 5\%$ RH. Stick length is $200 \pm 1 \text{ mm}$ , stick width is $6.0 \pm 0.2 \text{ mm}$ , the number of sticks per layer is 11 and the total crib mass is 600 g.	Crib placed on open floor area	50	155	387
300 g newspaper	300 g of individual tabloid sized newspaper sheets loosely crumpled into approximately 70 mm diameter balls and stacked against bounding surfaces.	300 g crumpled newspaper piled on seat against wall	90	30	165
		300 g crumpled newspaper piled on floor in corner behind GRP seat shell	62	33	172
450 g newspaper	450 g of individual tabloid sized newspaper sheets loosely crumpled into approximately 70 mm diameter balls and stacked against bounding surfaces.	450 g crumpled newspaper piled on seat against wall	105	22	155
		450 g crumpled newspaper piled on floor in corner behind steel seat shell	74	33	192
600g newspaper	600 g of individual tabloid sized newspaper sheets loosely crumpled into approximately 70 mm diameter balls and stacked against bounding surfaces.	600 g crumpled newspaper piled on seat against wall	167	25	160
1 kg newspaper	1 kg of individual tabloid sized newspaper sheets loosely crumpled into approximately 70 mm diameter balls and stacked against bounding surfaces.	1 kg of crumpled newspaper piled on floor in north-west corner behind the seat shell	136	33	260

Table C.1. *Continued*

Ignition source	General Description	Arrangement with non-combustible surfaces for characterisation test	Properties measured with non-combustible corner and seat		
			Ave. peak HRR (kW)	Ave. time to peak HRR (s)	Burn duration (s)
525 g cardboard box and newspaper	Queensland Railway source comprising a cardboard box (220 x 280 x 190 mm high) nominally weighing 235 g, filled with 290 g of A2 newspaper sheets crumpled individually into balls.	No Characterisation test	-	-	-
500 mL kero	500 mL kerosene poured onto slashed seat	No characterisation test as properties such as HRR and burn duration depend on absorption and spread on material surface	n/a	n/a	n/a
1000 ml of kerosene	About 500 ml of kerosene was poured into the foam under the slash in the seat cushion. About 400 mm was poured into the slash on the back cushion. The remainder was poured on the upper surface of the seat cushion	No characterisation test as properties such as HRR and burn duration depend on absorption and spread on material surface	n/a	n/a	n/a

## **APPENDIX D – FULL-SCALE EXPERIMENTAL DRAWINGS**

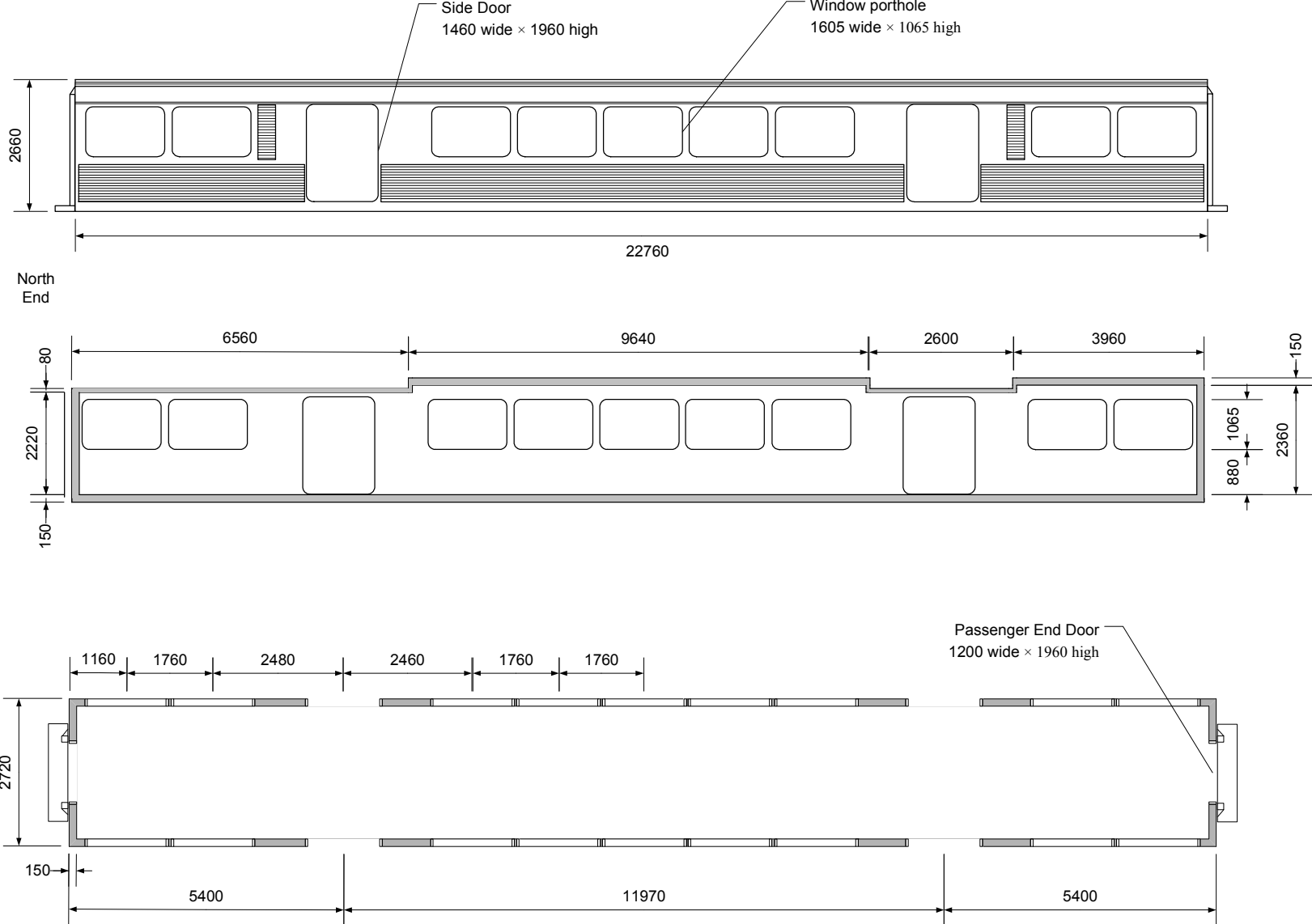
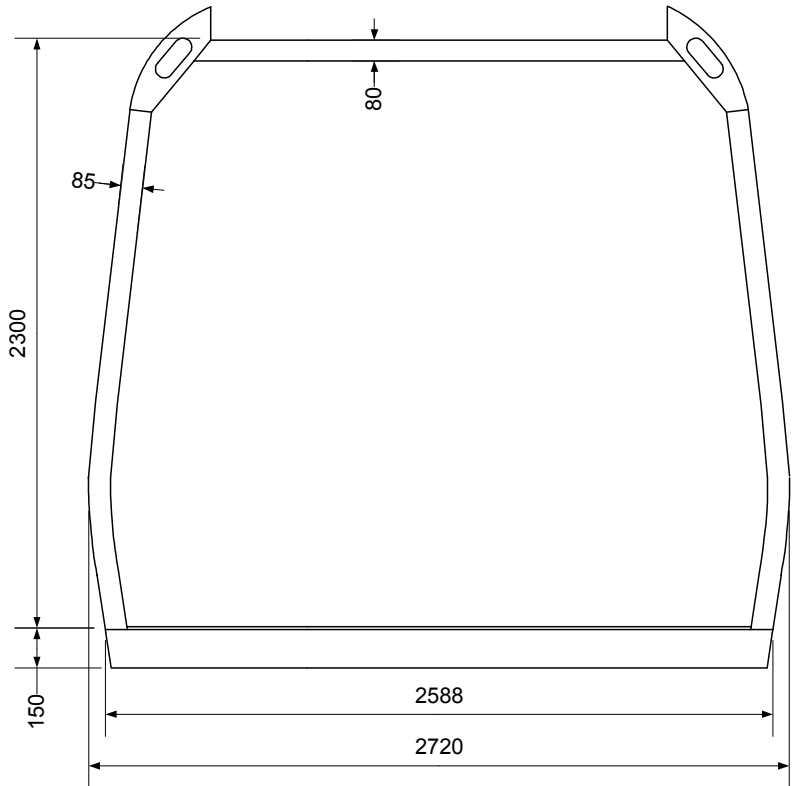
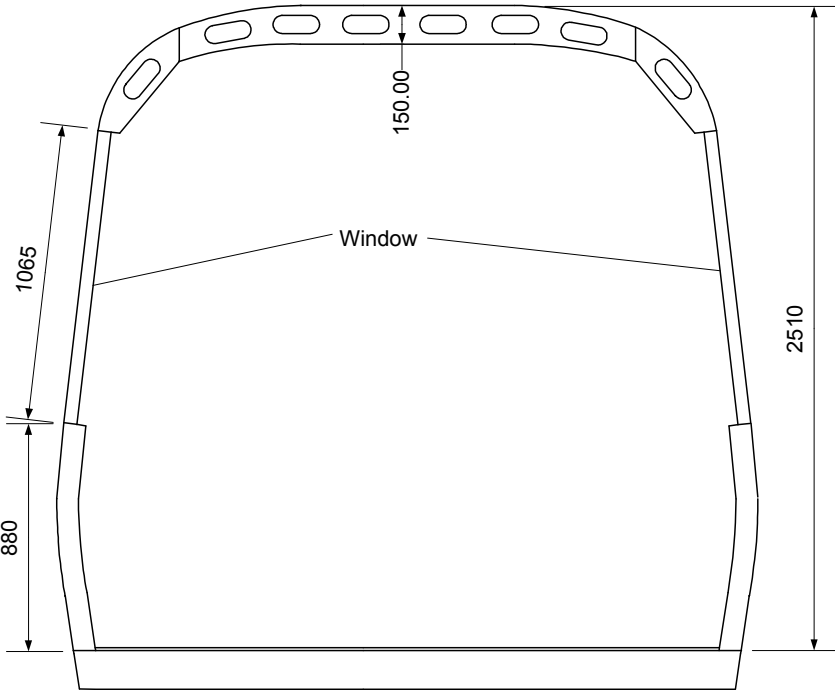


Figure D. 1 Carriage dimensions – side elevation and plan



Typical Section Through Vestibule Area



Typical Section Through Saloon Area

Figure D. 2 Carriage dimensions – cross sections

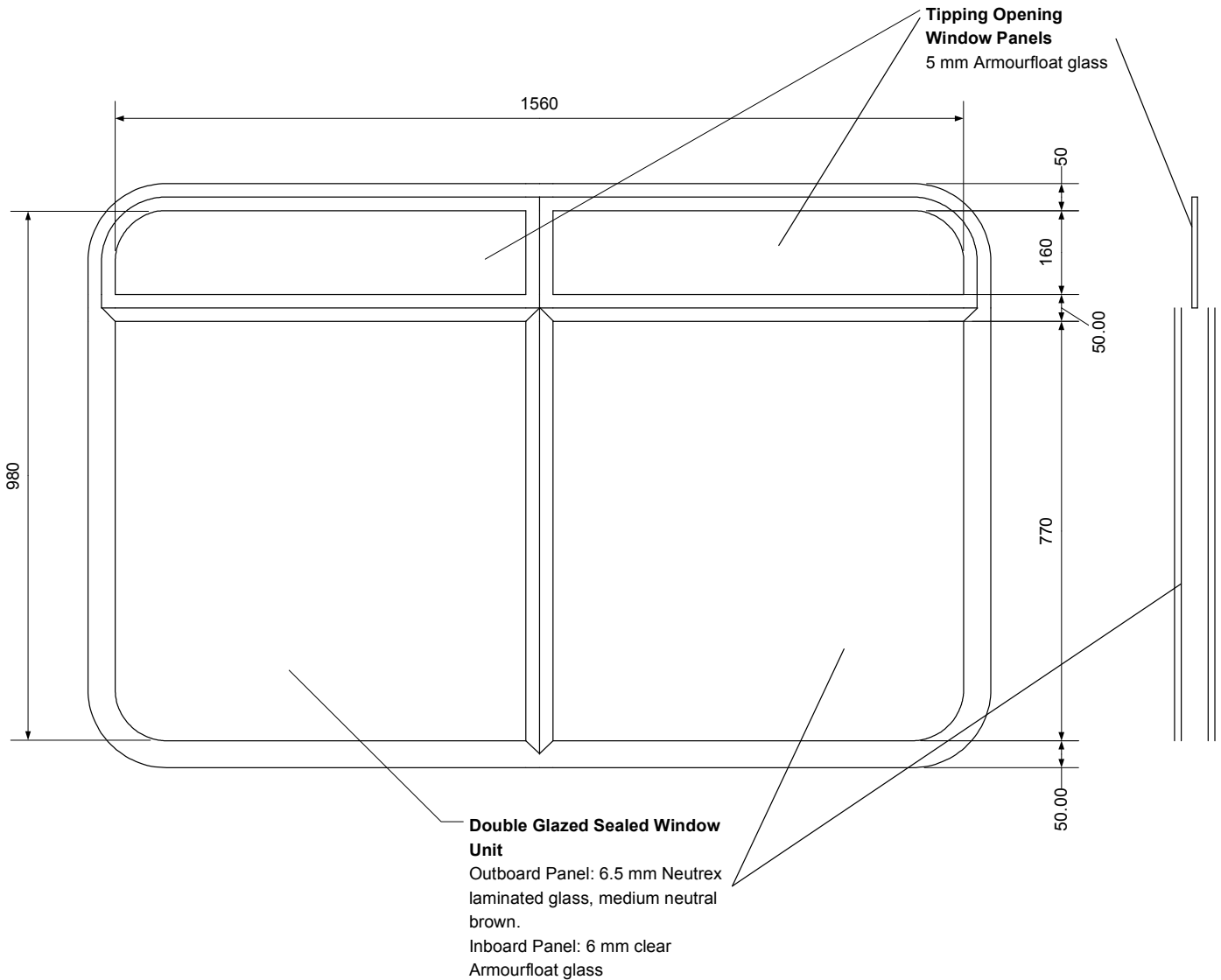


**Figure D. 3 Window unit dimensions**

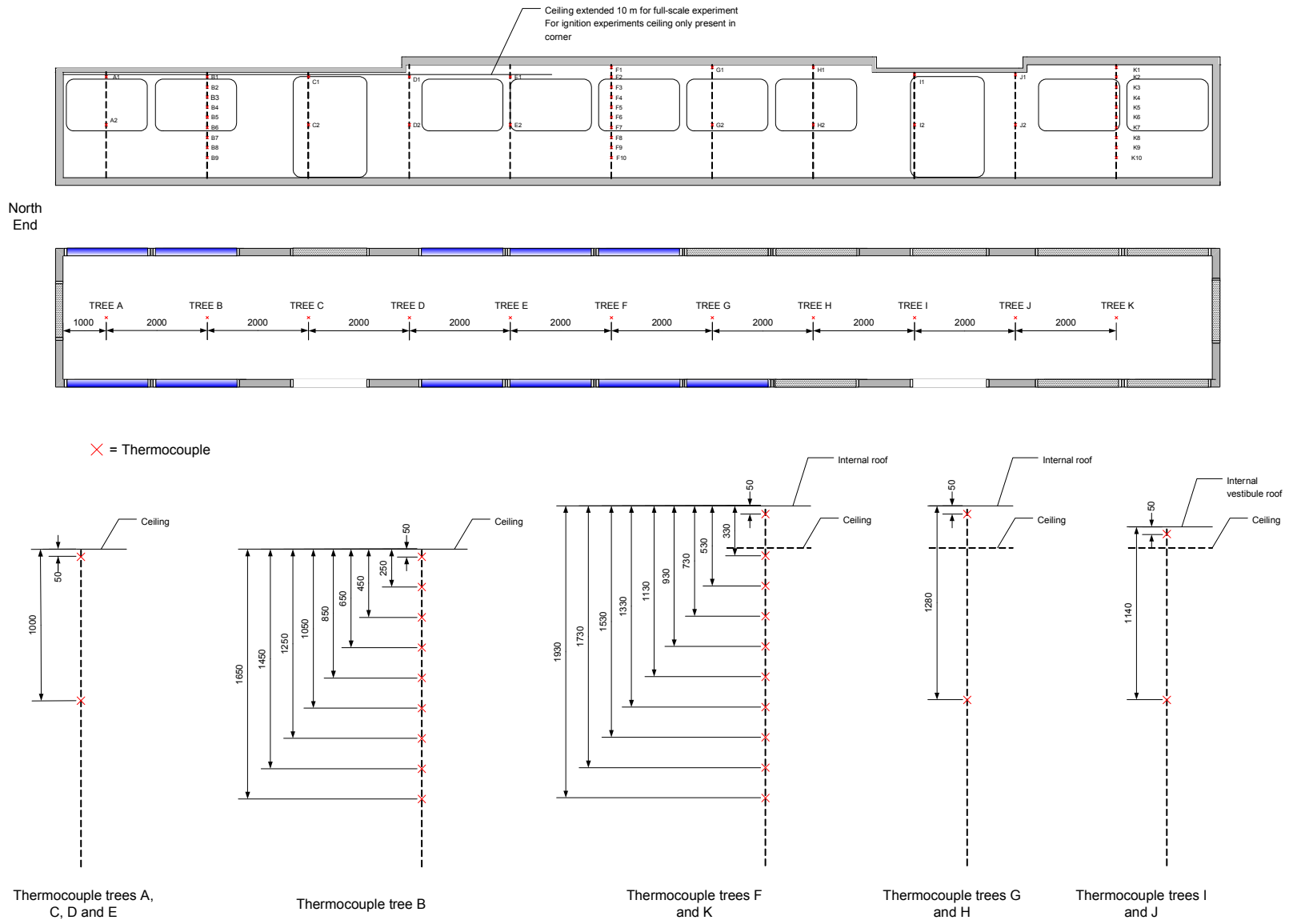
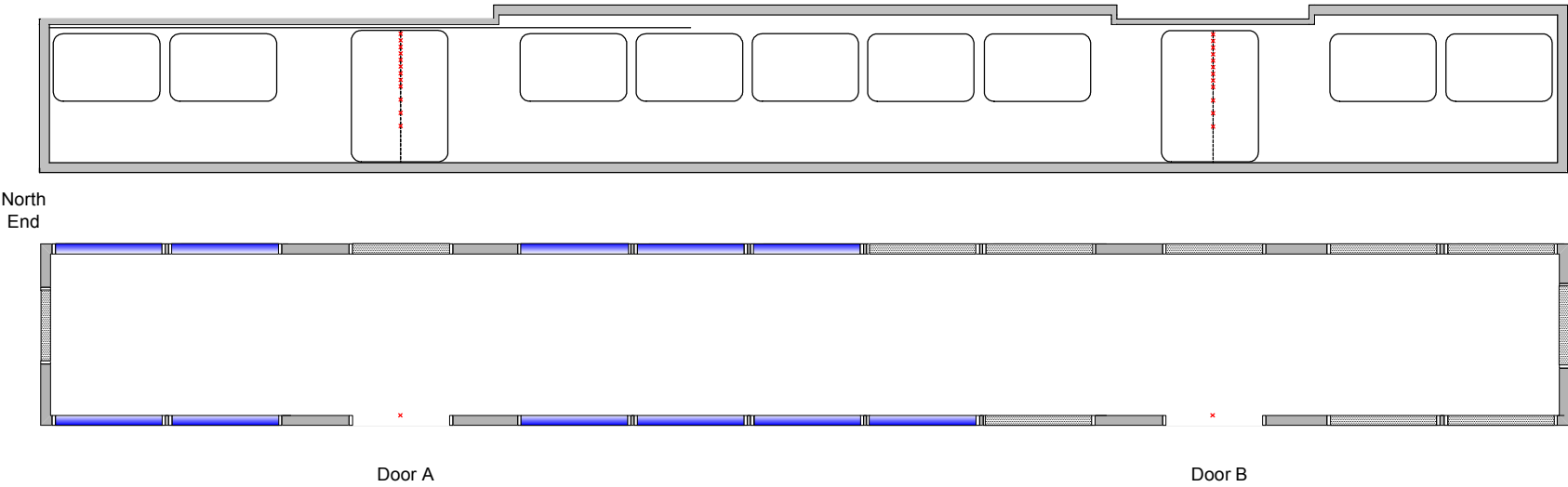
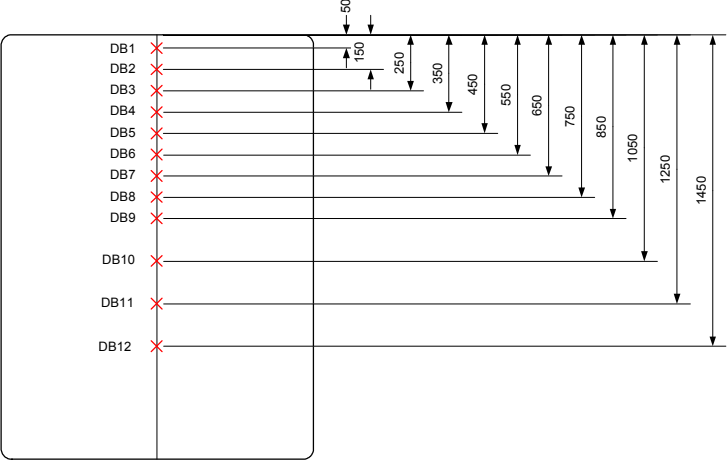
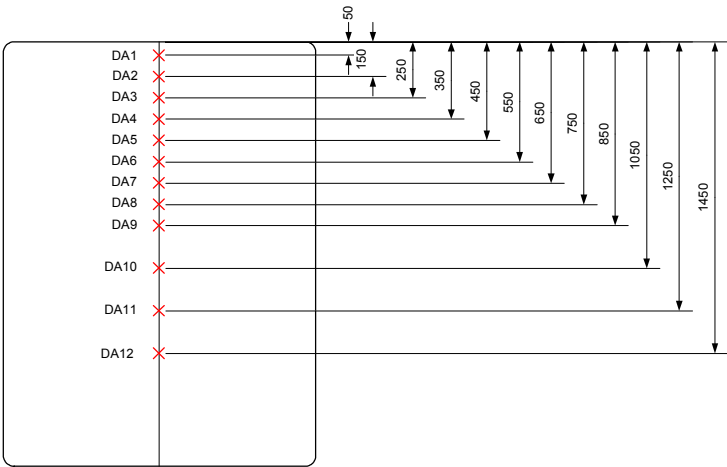


Figure D.4 Instrumentation – centre thermocouple trees for full-scale experiment



× = Thermocouple



**Figure D.5 Instrumentation – door thermocouples for full-scale experiment**

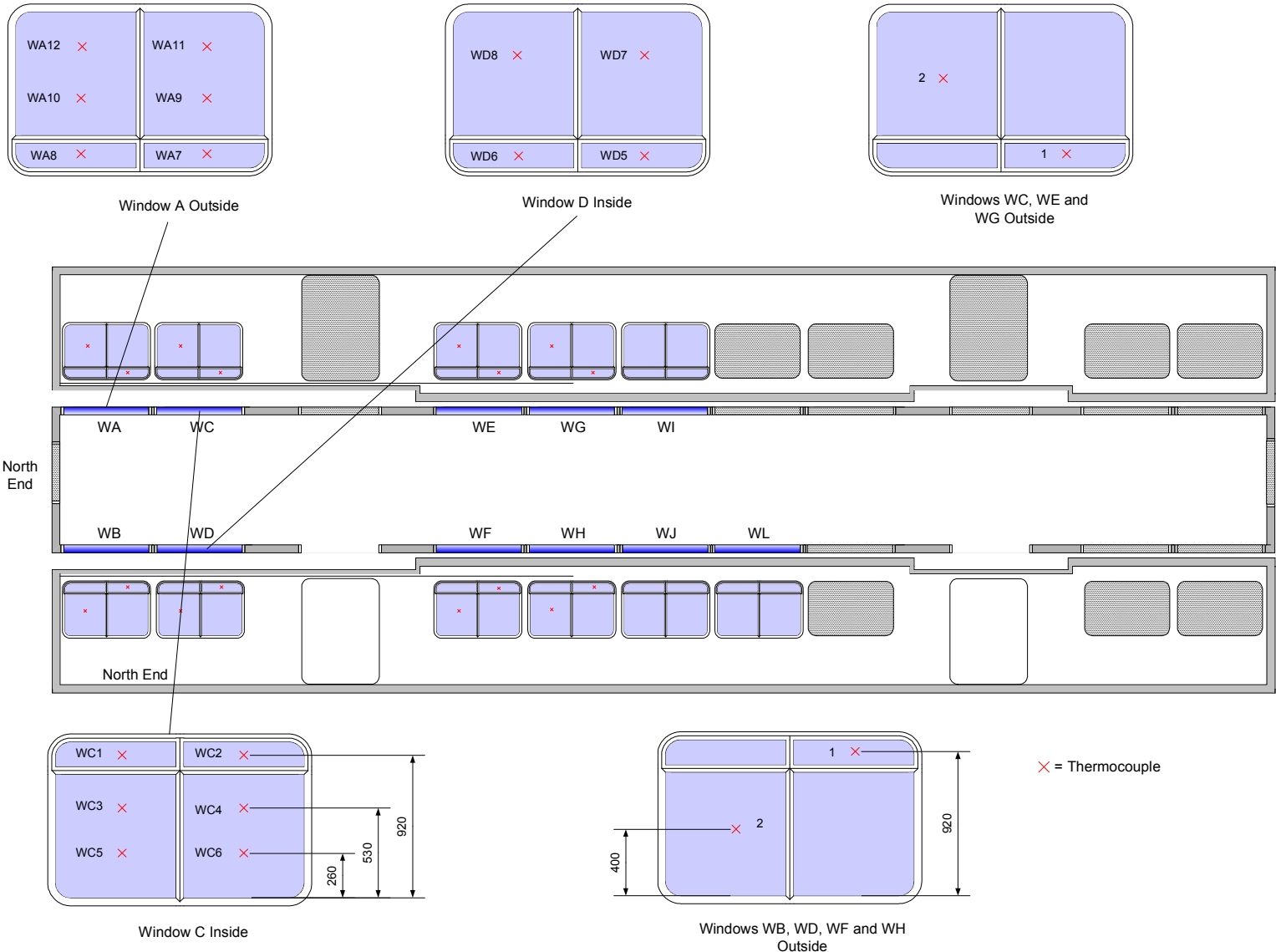


**Figure D.6 Instrumentation – window thermocouples for full-scale experiment**

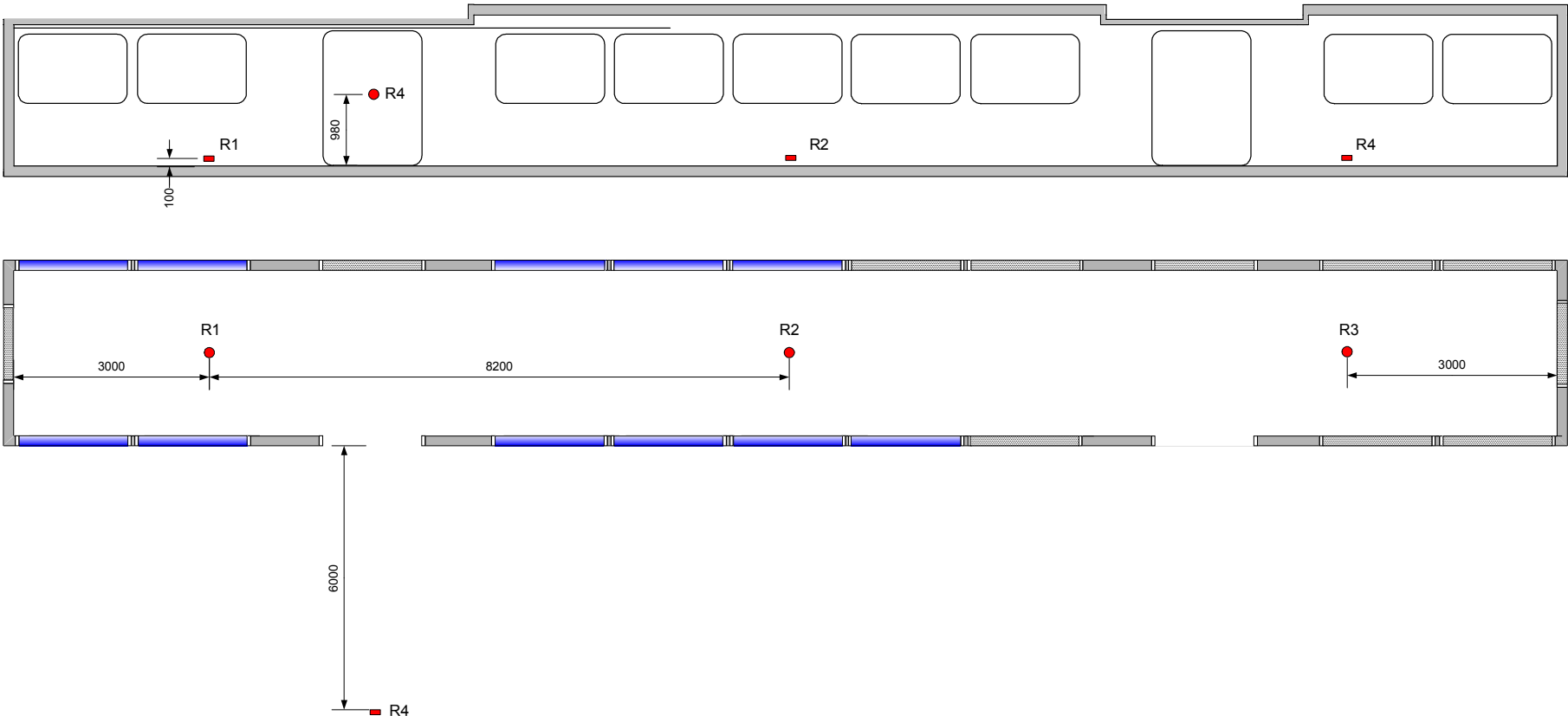


Figure D. 7 Instrumentation – heat flux meter positions for full-scale experiment

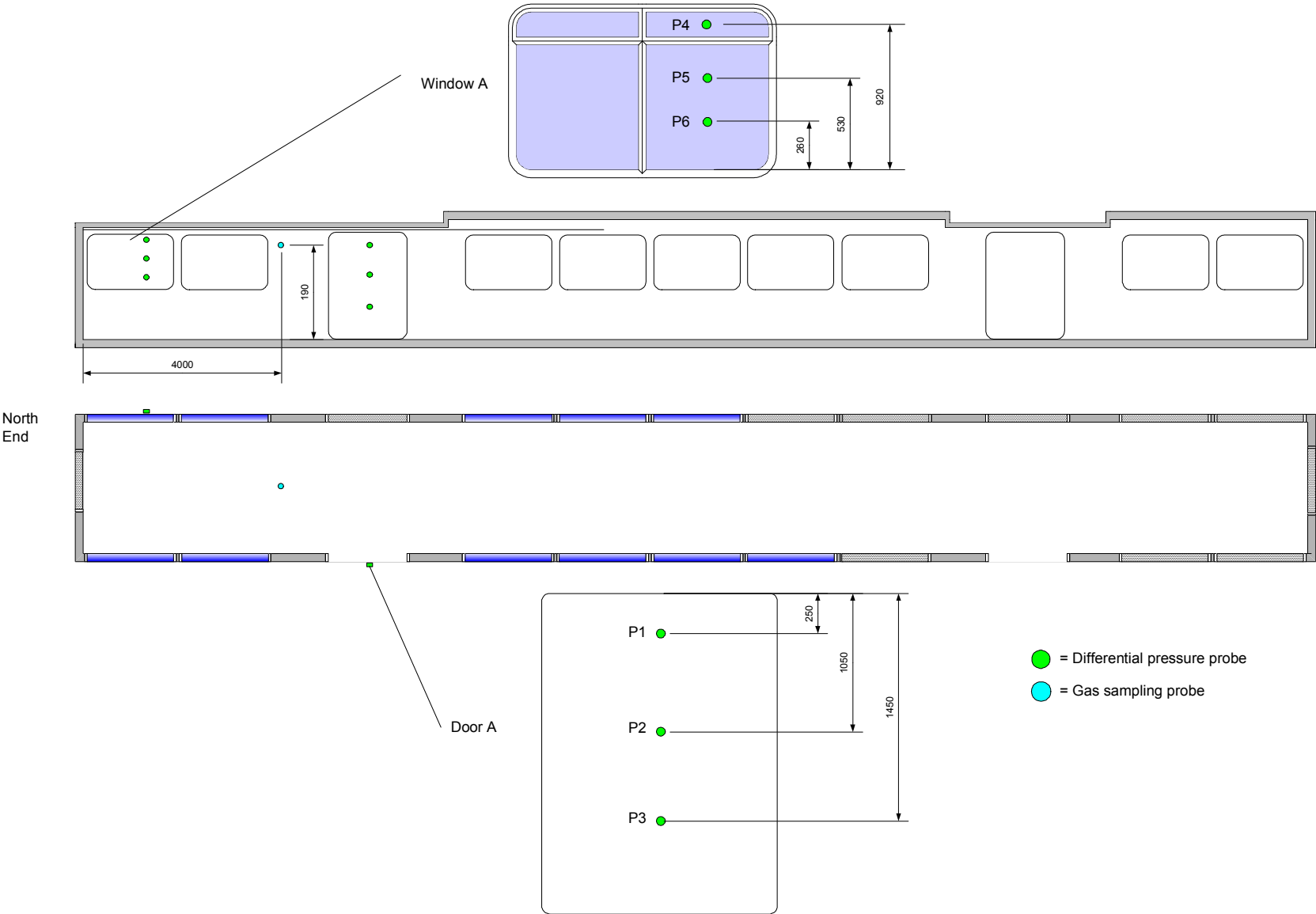


Figure D. 8 Differential pressure probe and gas sampling probes for ignition and full-scale experiments

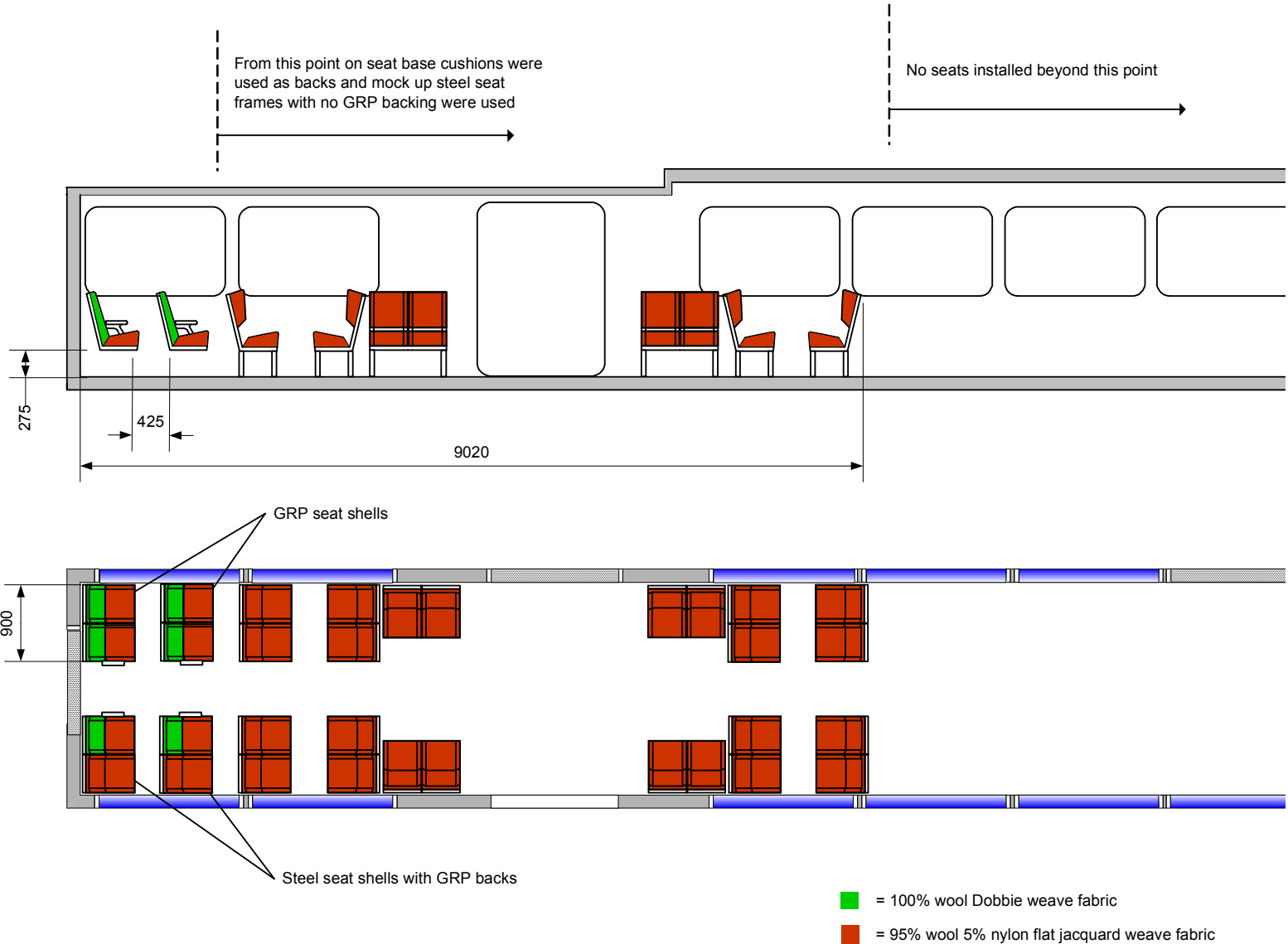


Figure D. 9 Seat arrangements for full-scale experiment

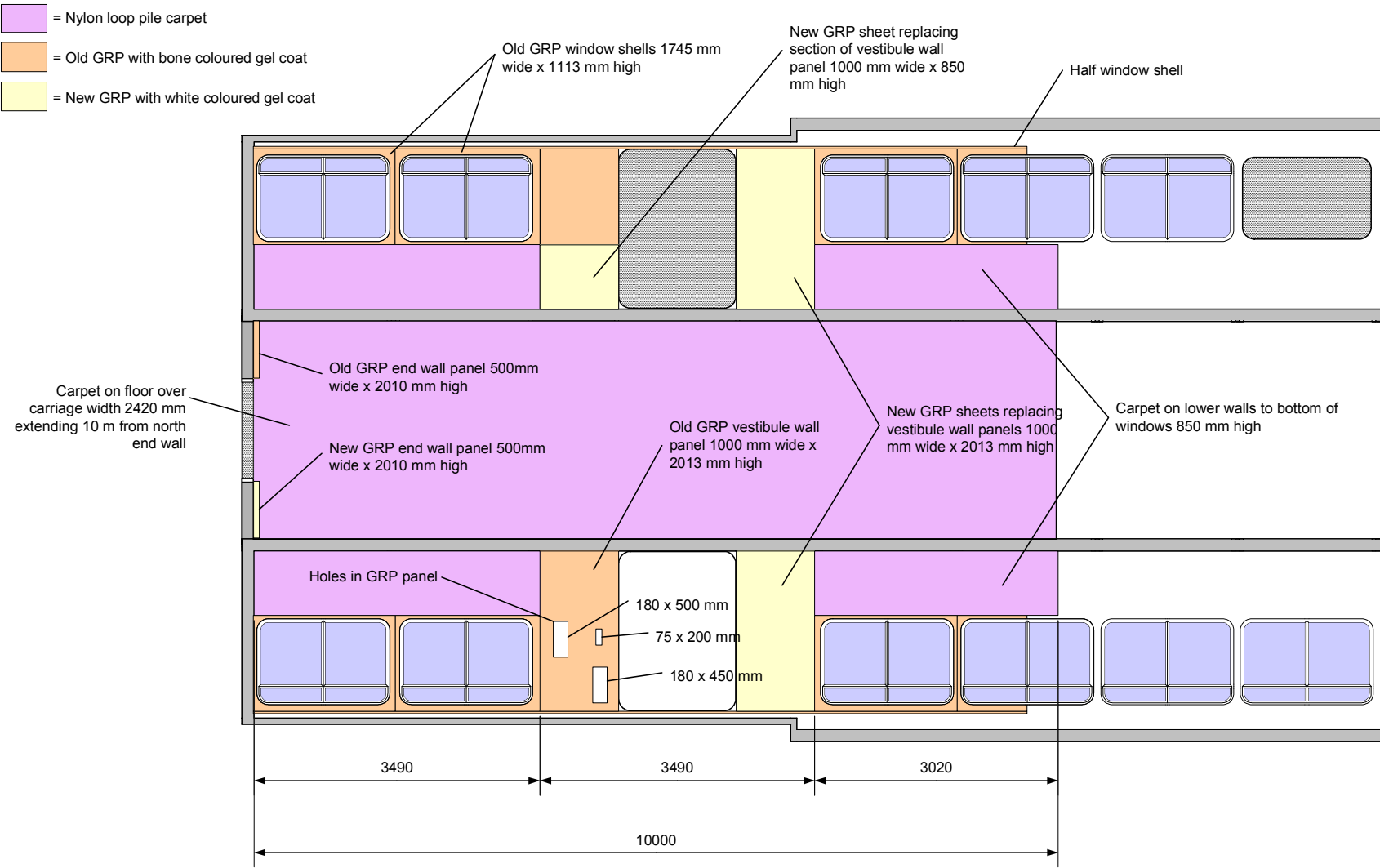
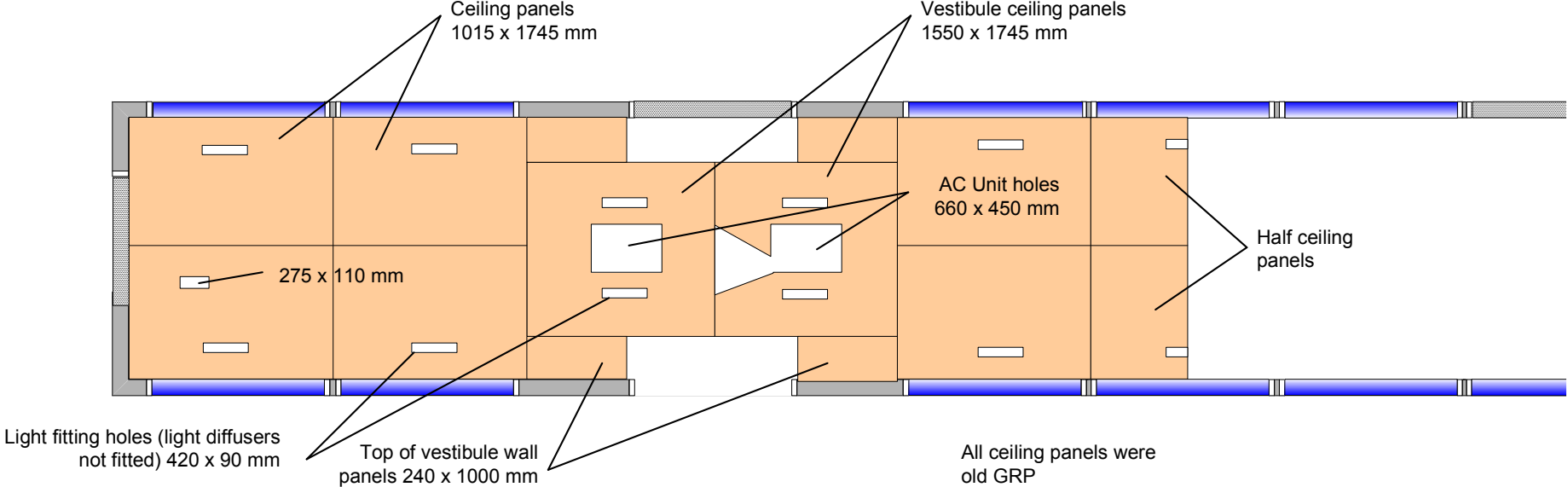


Figure D. 10 Floor and wall lining arrangements for full-scale experiment



**Figure D. 11 Ceiling lining arrangements for full-scale experiment**

## APPENDIX E – FULL-SCALE EXPERIMENT PHOTOGRAPHS



**Figure E. 1** Empty carriage viewed from south-east



**Figure E. 2** Empty carriage viewed from north-west



**Figure E. 3** Empty carriage viewed from south



**Figure E. 4** Interior empty carriage viewed from south end



**Figure E. 5** Jack stand



**Figure E. 6** Carriage interior prior to full-scale experiment



**Figure E. 7** Carriage exterior prior to full-scale experiment



**Figure E. 8** Full-scale experiment – carriage interior at 30 s



**Figure E. 9** Full-scale experiment – carriage exterior at 30 s



**Figure E. 10** Full-scale experiment – carriage interior viewed from south end at 34 s



**Figure E. 11** Full-scale experiment at 50 s



**Figure E. 12** Full-scale experiment at 60 s



**Figure E. 13** Full-scale experiment at 90 s



**Figure E. 14** Full-scale experiment at 120 s



**Figure E. 15** Full-scale experiment at 140 s



**Figure E. 16** Full-scale experiment at 155 s



**Figure E. 17** Full-scale experiment at 180 s



**Figure E. 18** Full-scale experiment at 185 s



**Figure E. 19** Full-scale experiment at 190 s



**Figure E. 20.** Full-scale experiment at 240 s



**Figure E. 21** Full-scale experiment at 240s



**Figure E. 22** Full-scale experiment at 270 s



**Figure E. 23** Full-scale experiment at 300 s



**Figure E. 24** Full-scale experiment at 360 s



**Figure E. 25** Full-scale experiment at 380 s



**Figure E. 26** Full-scale experiment – plasterboard failing at north-east door at 390 s



**Figure E. 27** Full-scale experiment at 420 s



**Figure E. 28** Full-scale experiment at 480 s



**Figure E. 29** Full-scale experiment at 540 s



**Figure E. 30** Full-scale experiment at 600 s



**Figure E. 31** Full-scale experiment at 660 s



**Figure E. 32** Full-scale experiment at 720 s



**Figure E. 33** Full-scale experiment at 780 s



**Figure E. 34** Full-scale experiment at 840 s



**Figure E. 35** Full-scale experiment at 900 s.



**Figure E. 36** Full-scale experiment – damage to external east side



**Figure E. 37** Full-scale experiment – damage to external north end



**Figure E. 38** Full-scale experiment – damage to external west side



**Figure E. 39** Full-scale experiment – internal damage viewed from door B



**Figure E. 40.** Full-scale experiment – internal damage viewed 10 m from north end



**Figure E. 41** Full-scale experiment – insulation burnt from cables



**Figure E. 42** Full-scale experiment – damage to seats, floors and lower walls

# APPENDIX F – FULL-SCALE EXPERIMENT RESULT GRAPHS

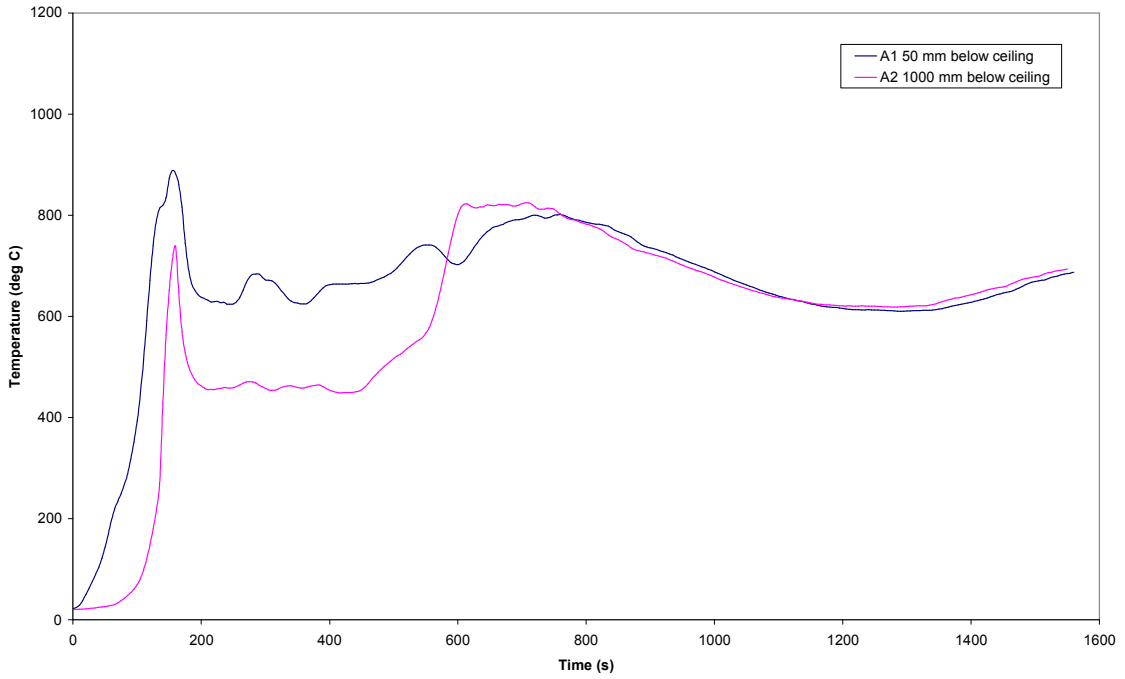


Figure F. 1 Full-scale experiment – Thermocouple Tree A

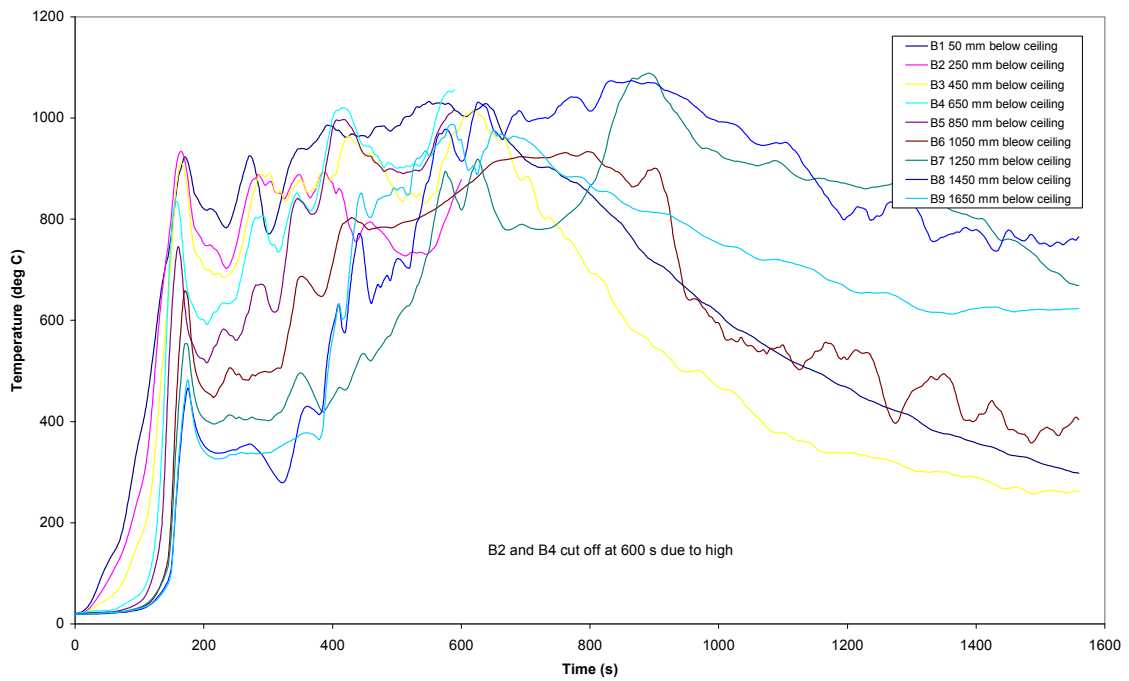


Figure F. 2 Full-scale experiment – Thermocouple Tree B

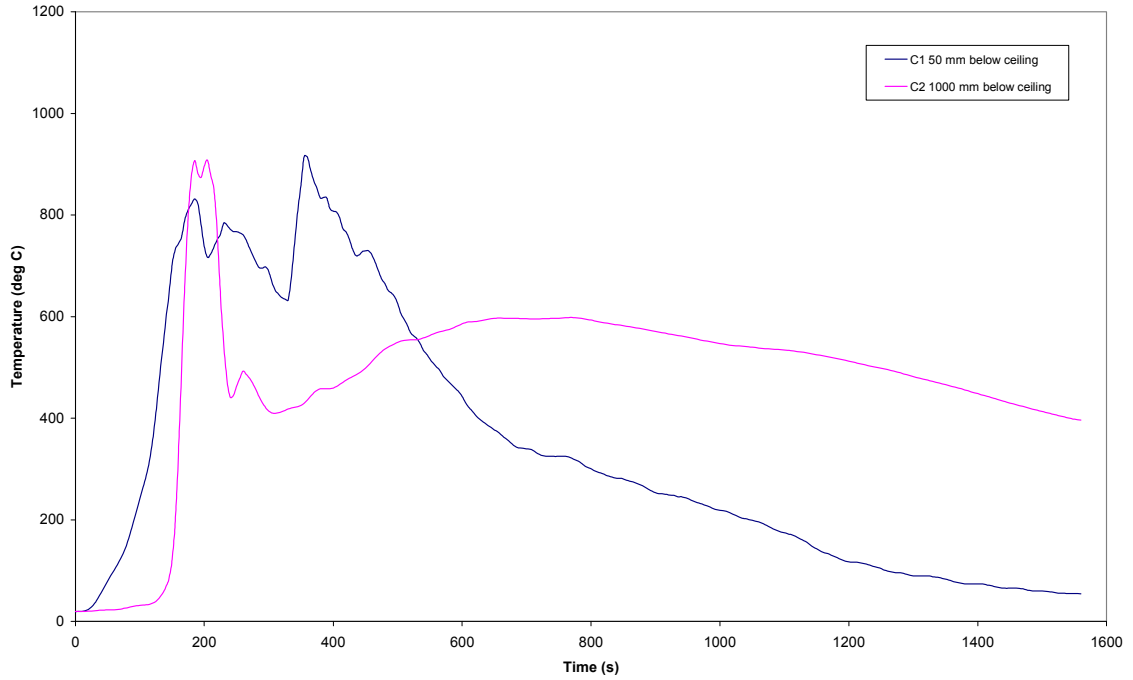


Figure F. 3 Full-scale experiment – Thermocouple Tree C

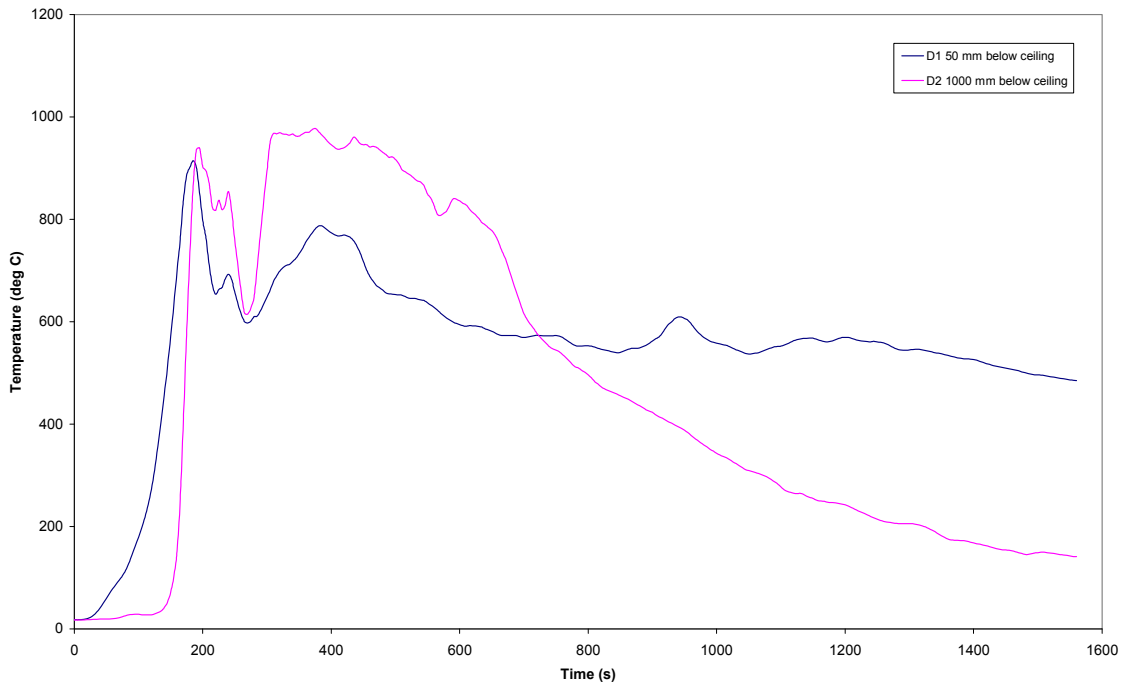


Figure F. 4 Full-scale experiment – Thermocouple Tree D

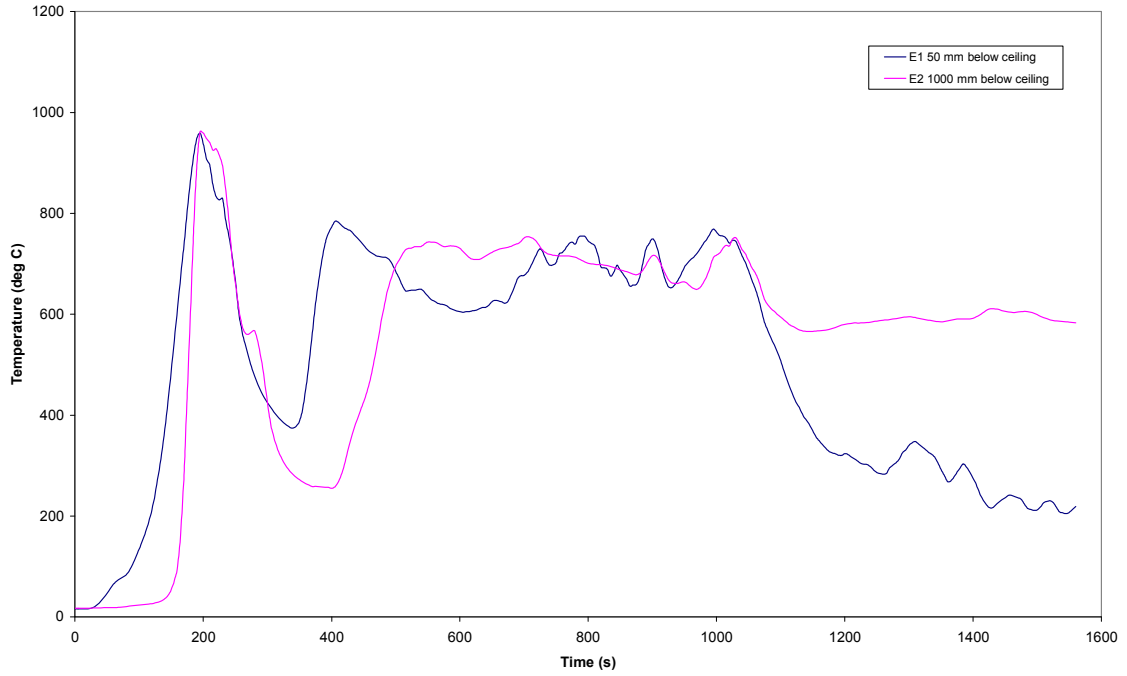


Figure F. 5 Full-scale experiment – Thermocouple Tree E

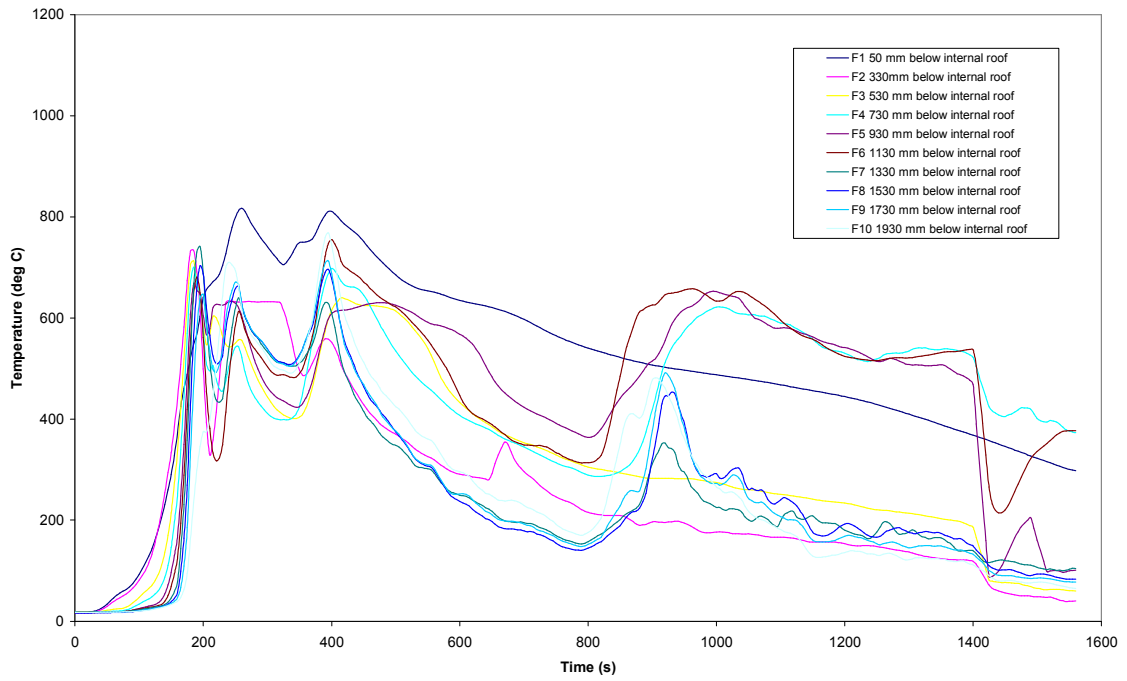


Figure F. 6 Full-scale experiment – Thermocouple Tree F

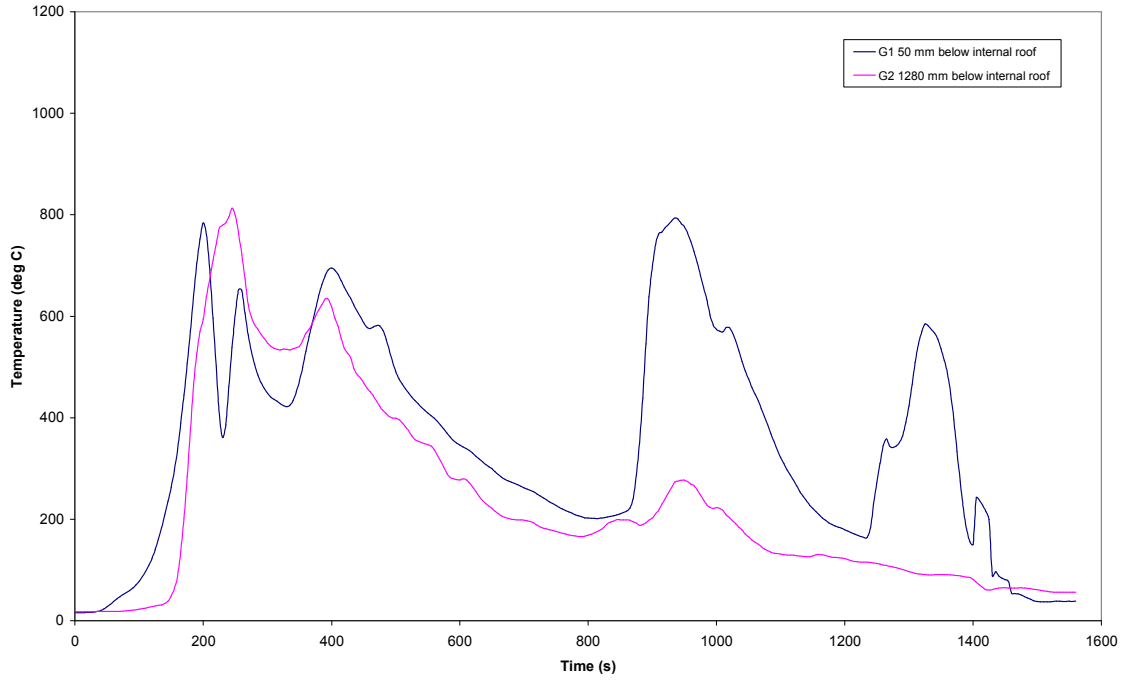


Figure F. 7 Full-scale experiment – Thermocouple Tree G

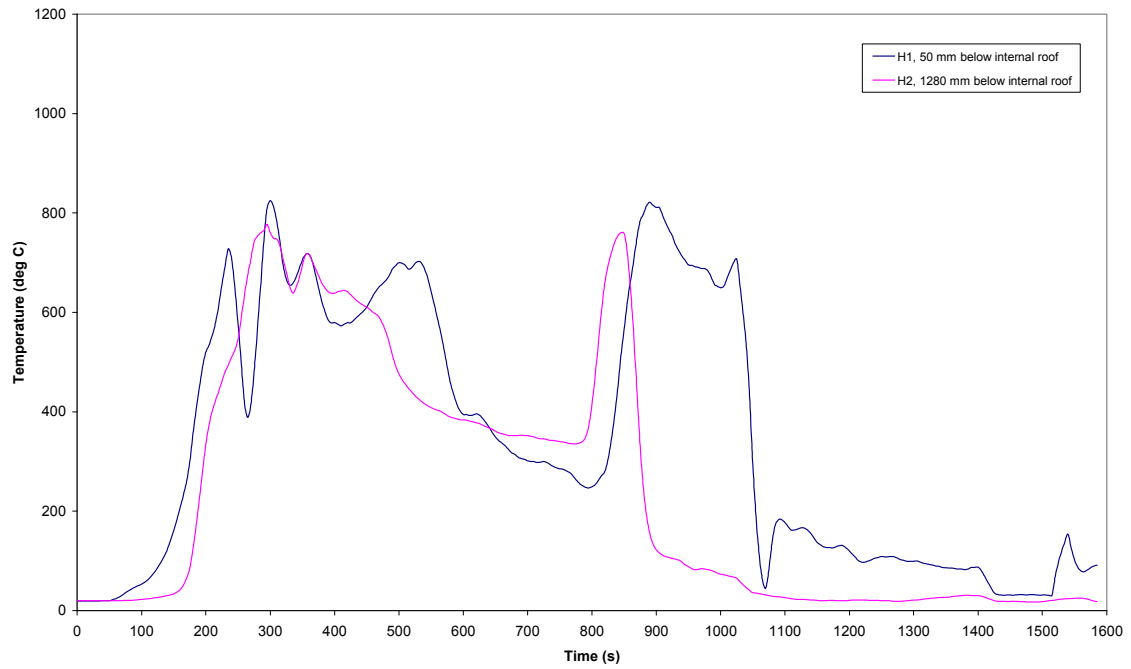


Figure F. 8 Full-scale experiment – Thermocouple Tree H

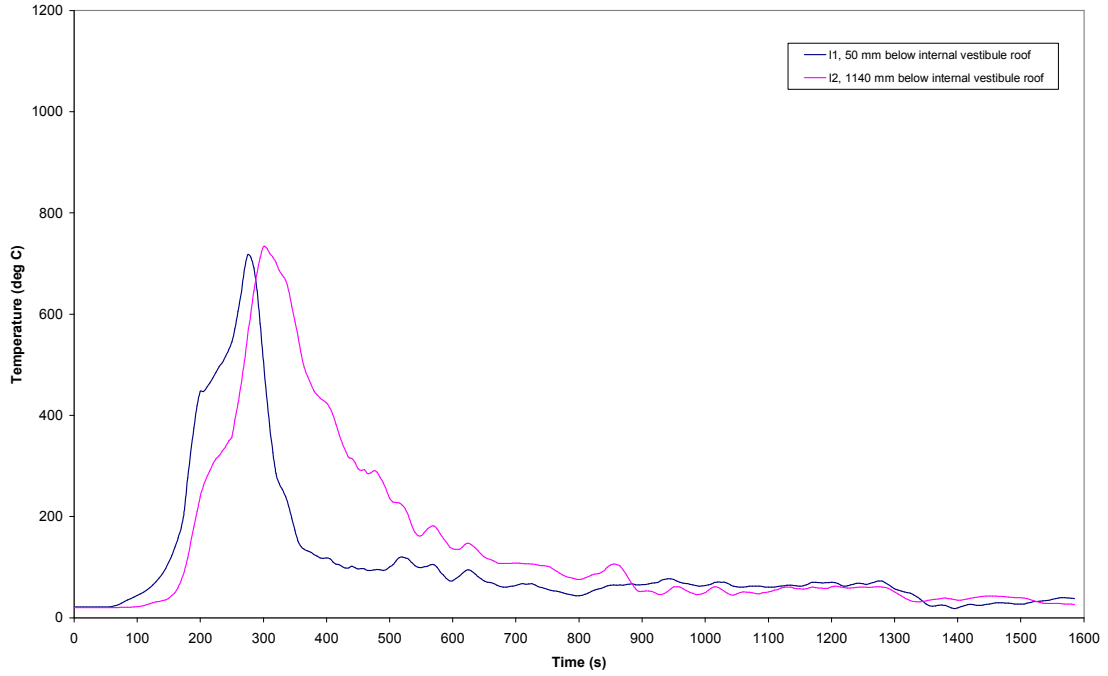


Figure F. 9 Full-scale experiment – Thermocouple Tree I

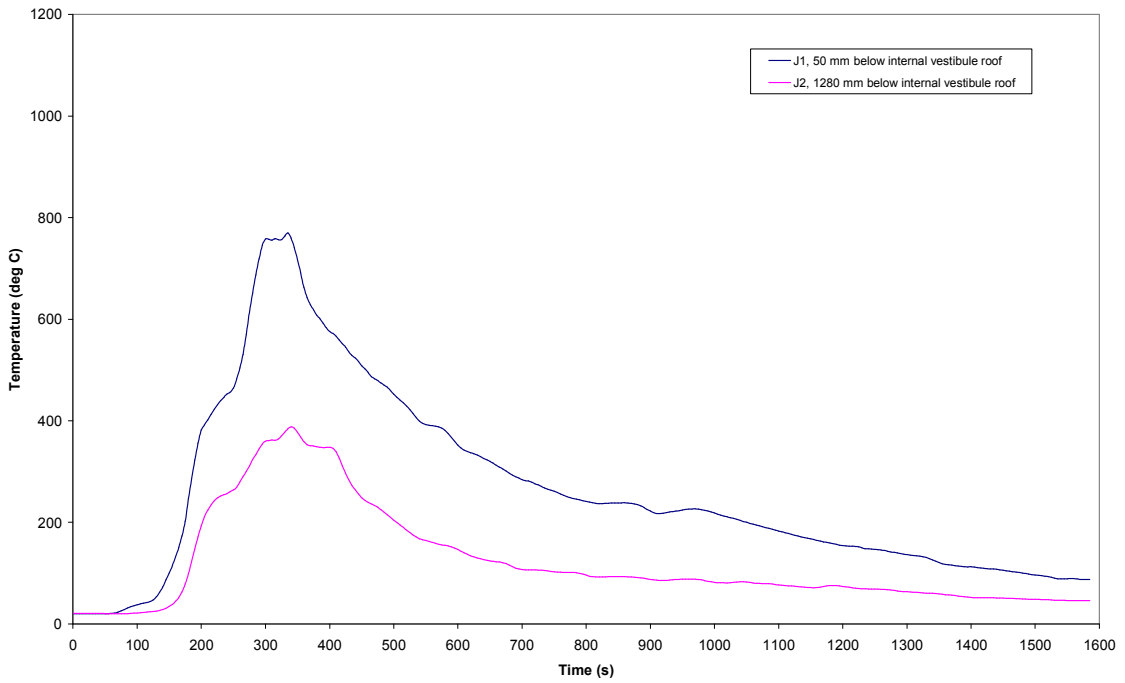


Figure F. 10 Full-scale experiment – Thermocouple Tree J

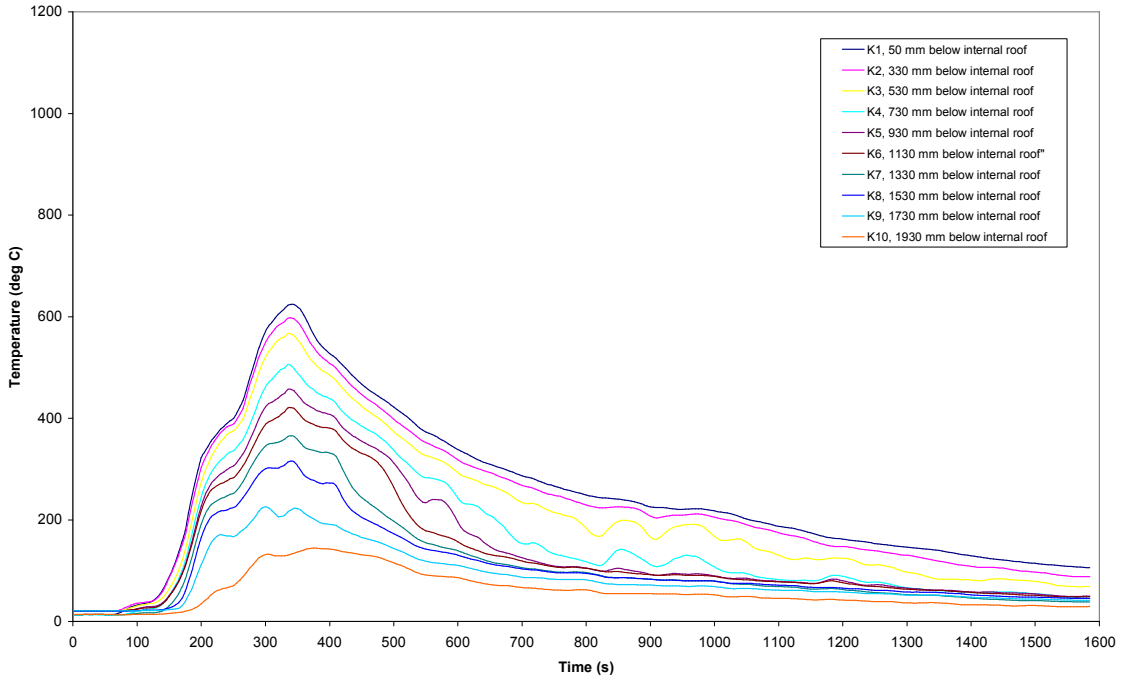


Figure F. 11 Full-scale experiment – Thermocouple Tree K

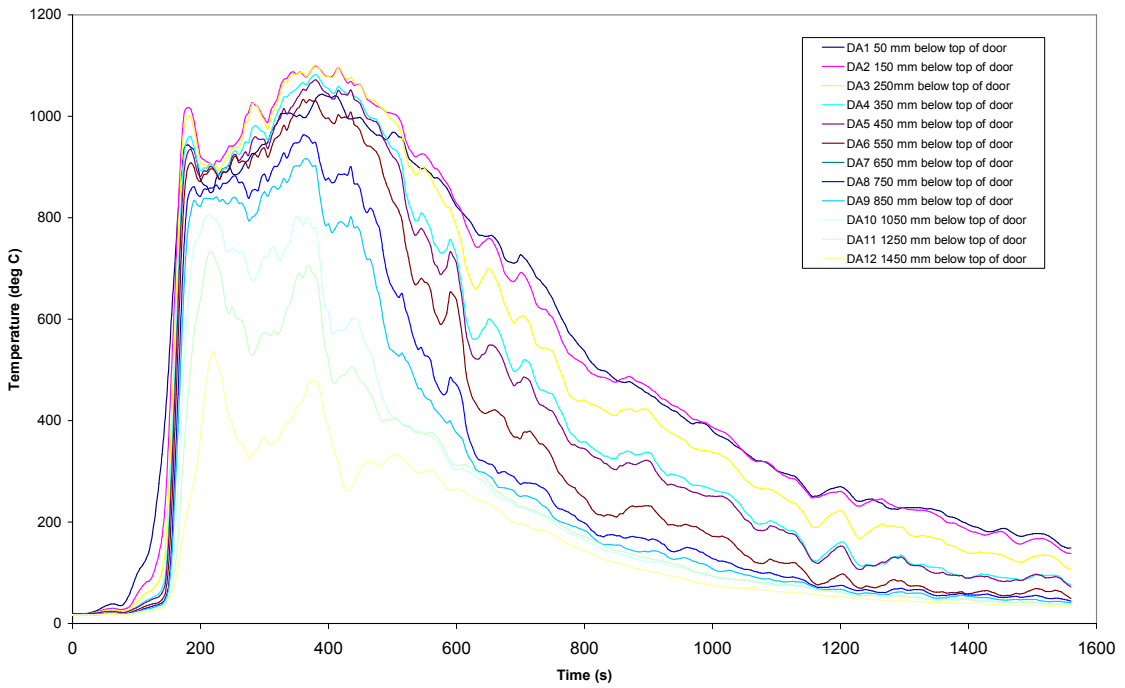


Figure F. 12 Full-scale experiment – thermocouple tree Door A

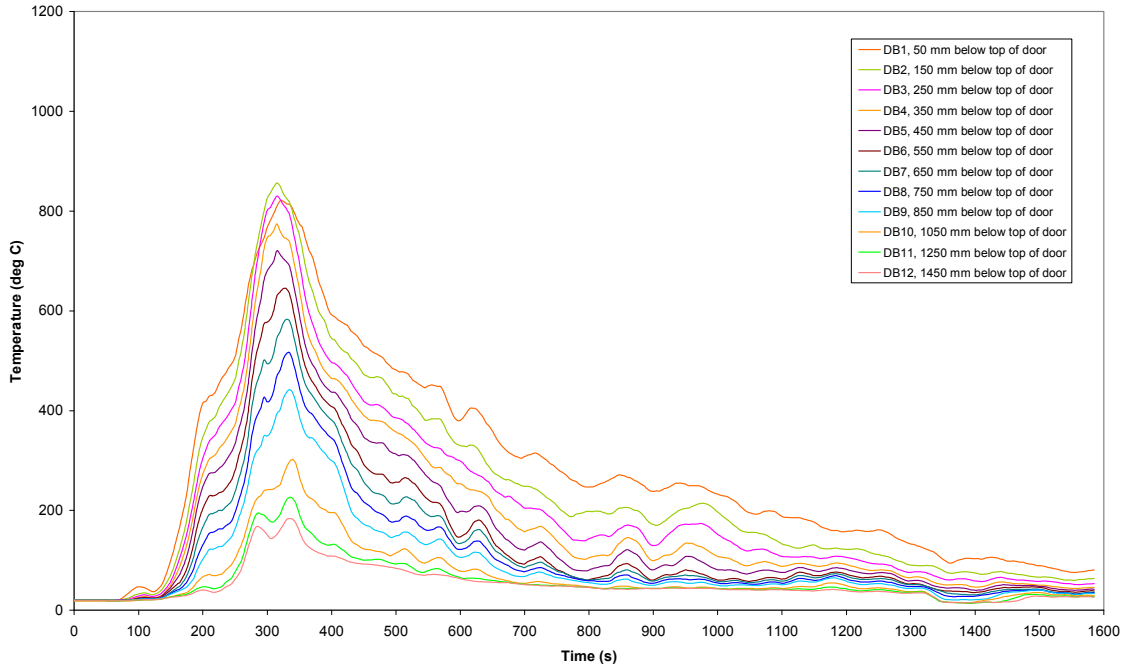


Figure F. 13 Full-scale experiment – thermocouple tree Door B

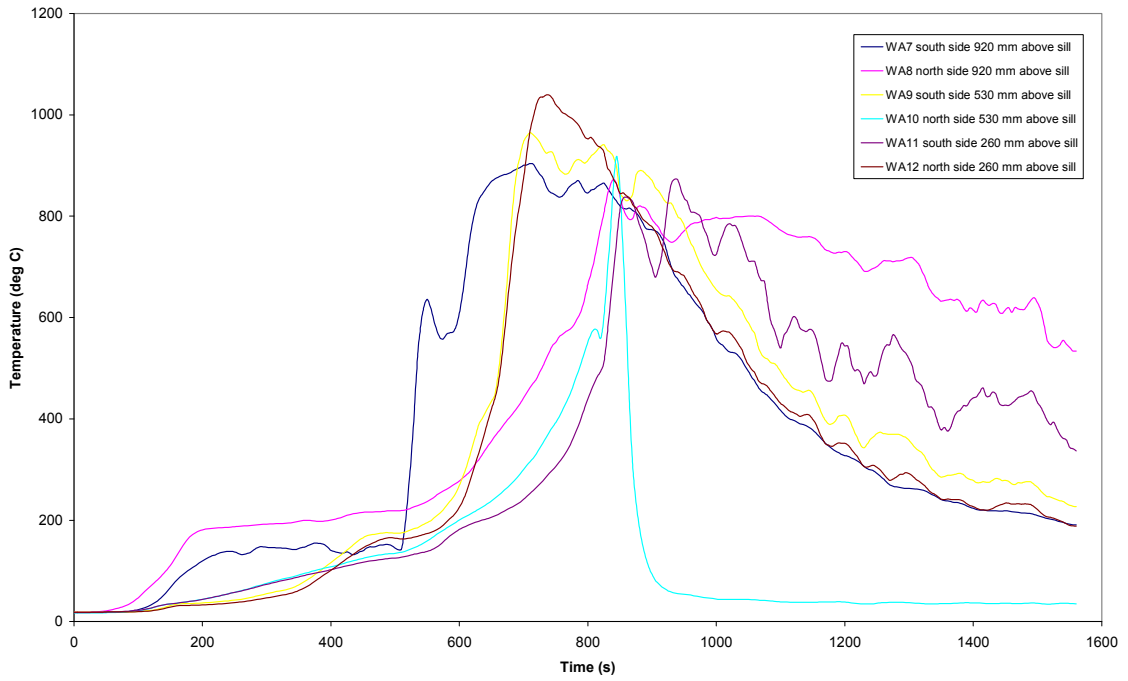


Figure F. 14 Full-scale experiment – thermocouples outside Window A

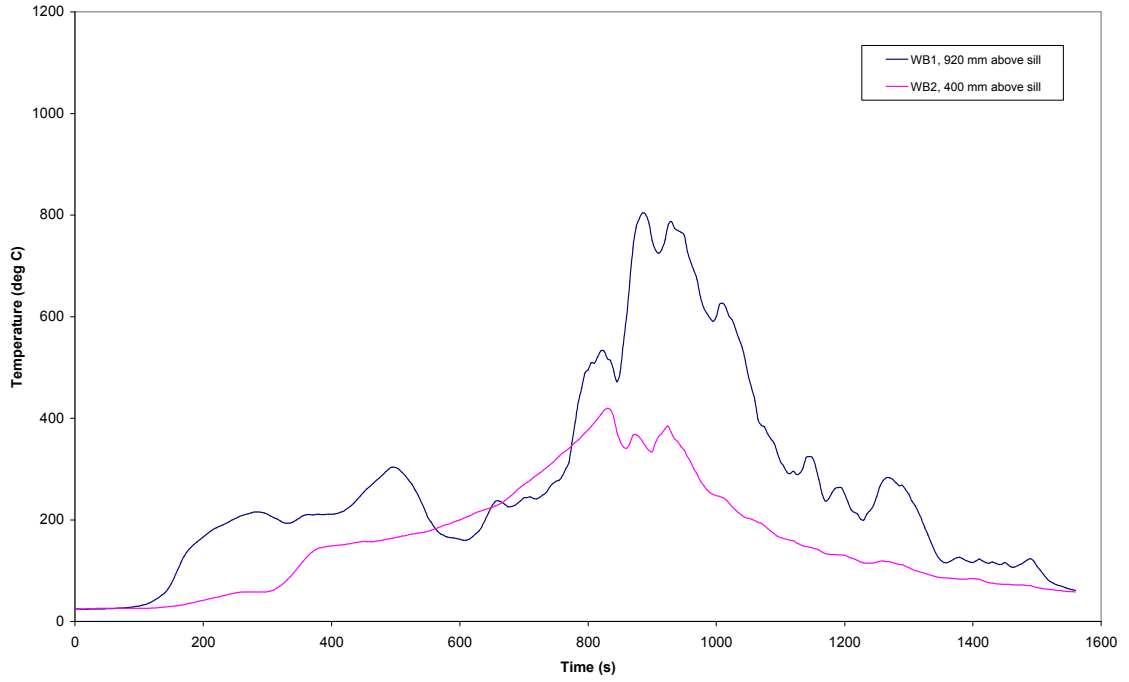


Figure F. 15 Full-scale experiment – thermocouples outside Window B

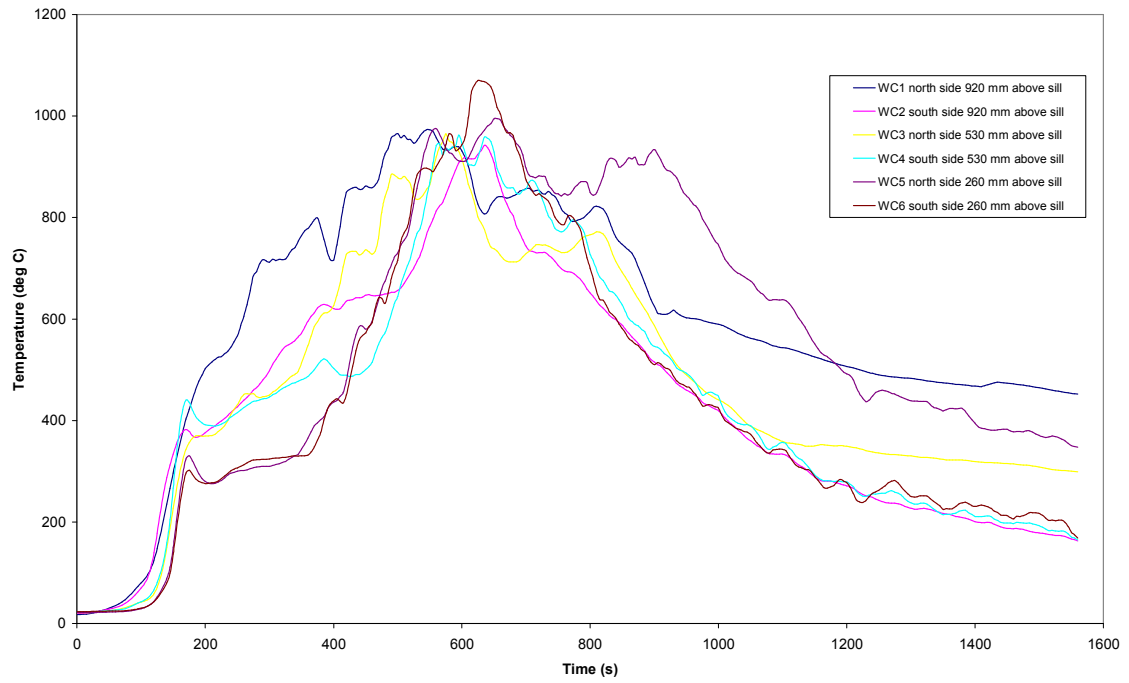


Figure F. 16 Full-scale experiment – thermocouples inside Window C

Appendix F – Full-Scale Experiment Result Graphs

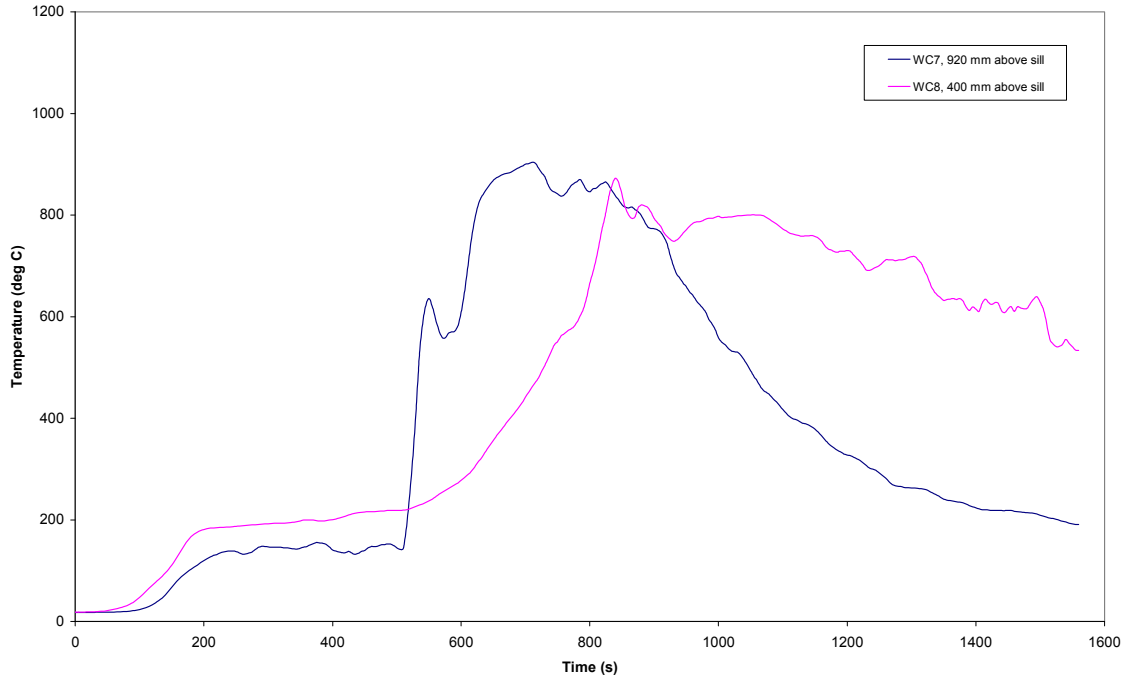


Figure F. 17 Full-scale experiment – thermocouples outside Window C

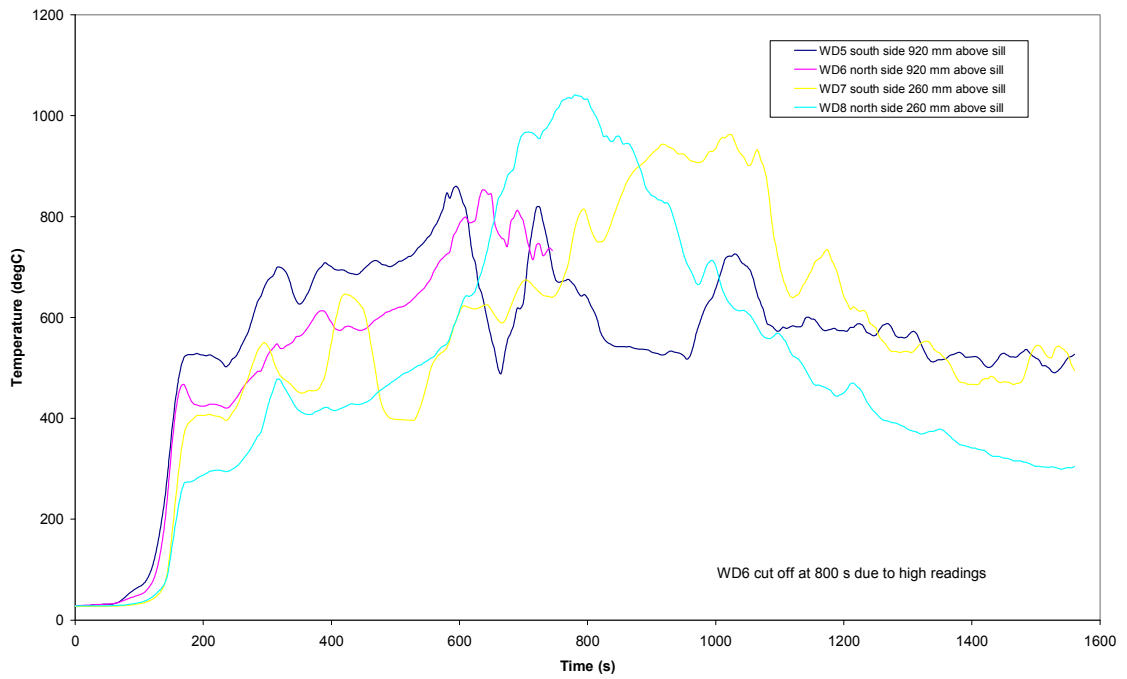


Figure F. 18 Full-scale experiment – thermocouples inside Window D

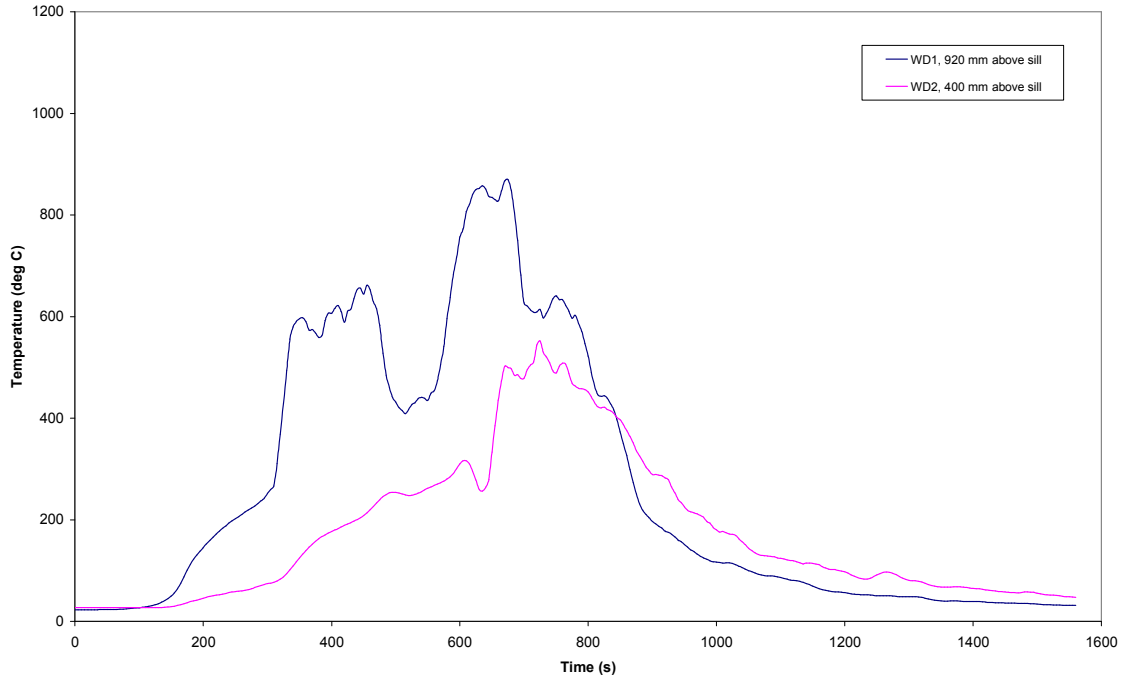


Figure F. 19 Full-scale experiment – thermocouples outside Window D

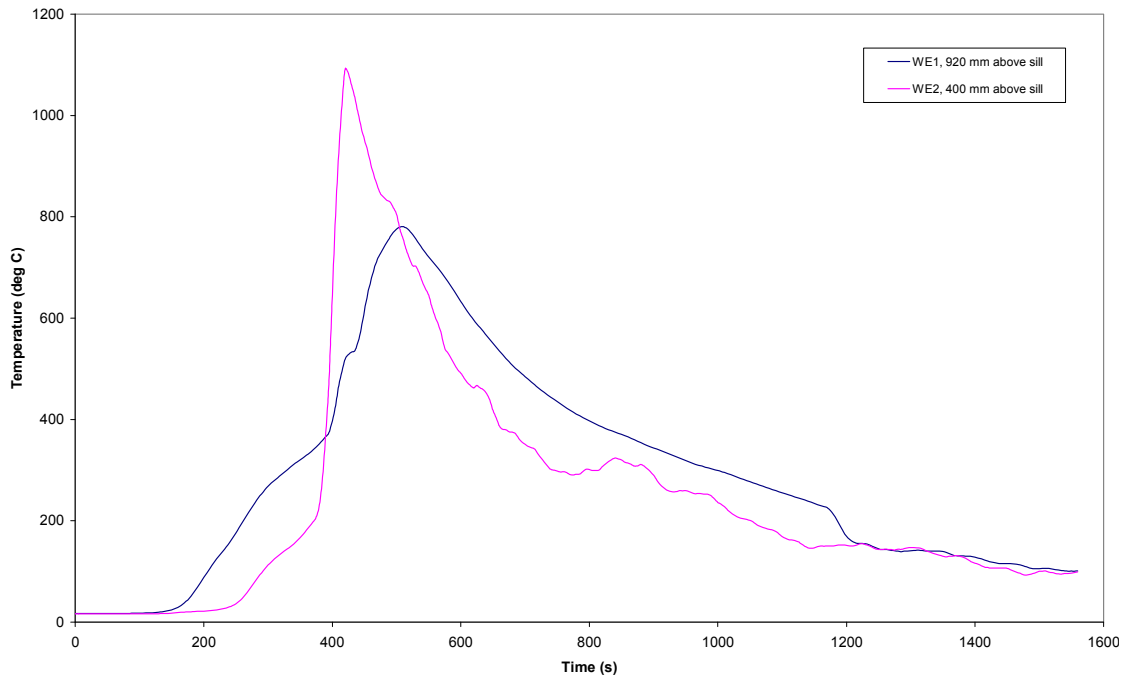


Figure F. 20 Full-scale experiment – thermocouples outside Window E

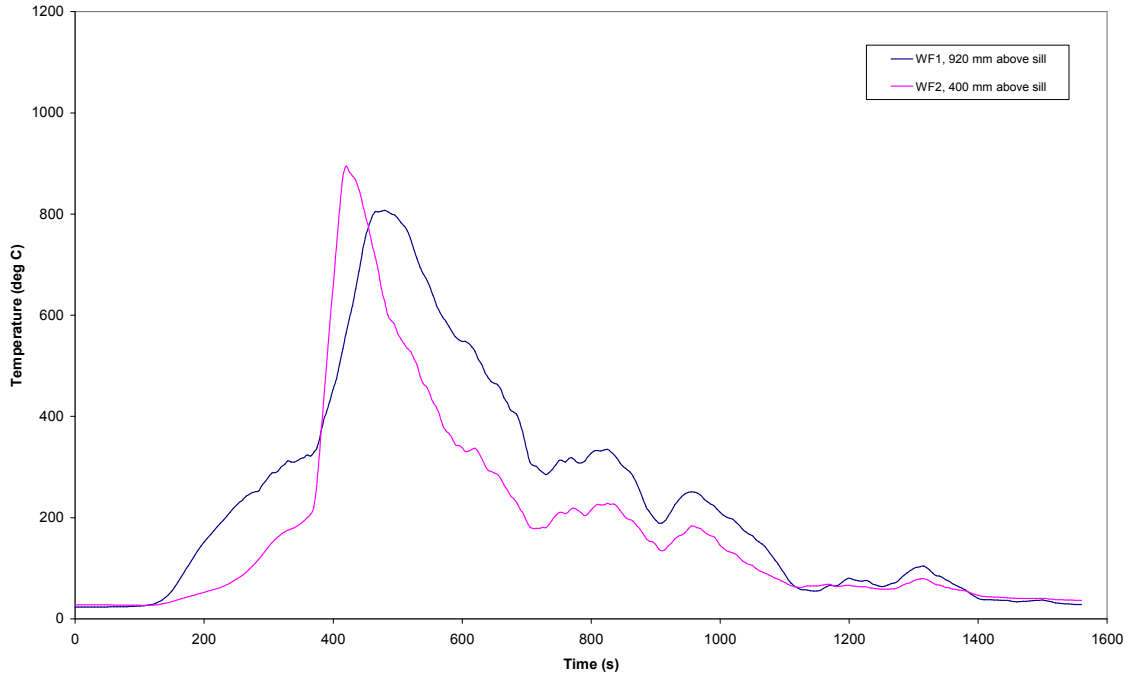


Figure F. 21 Full-scale experiment – thermocouples outside Window F

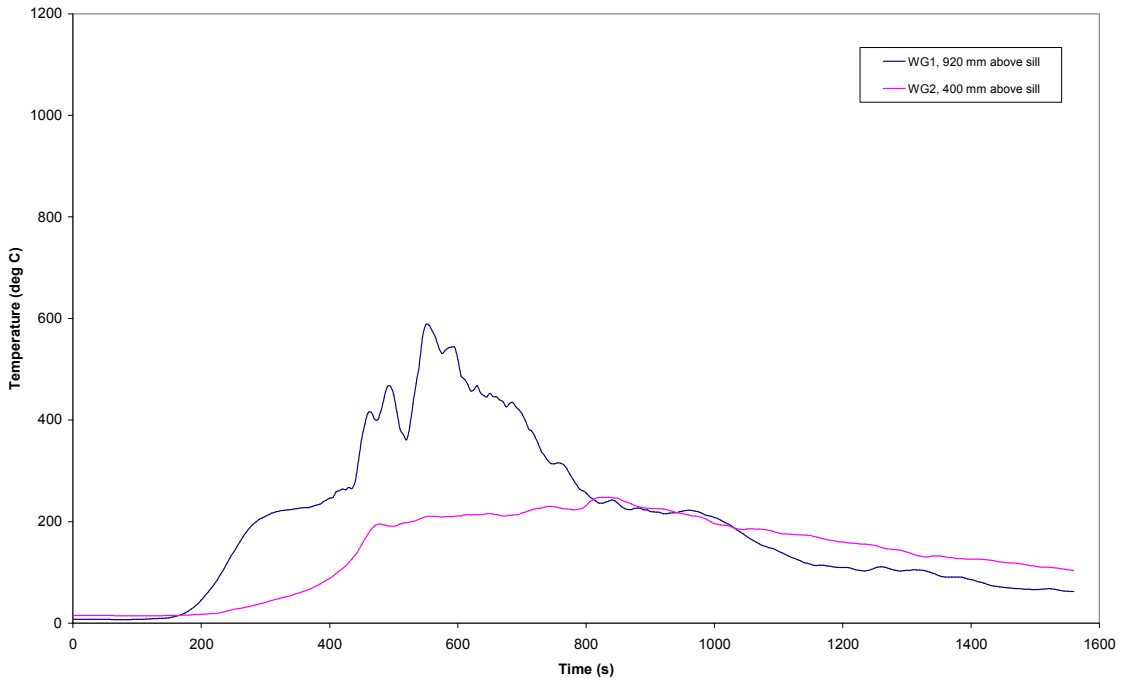
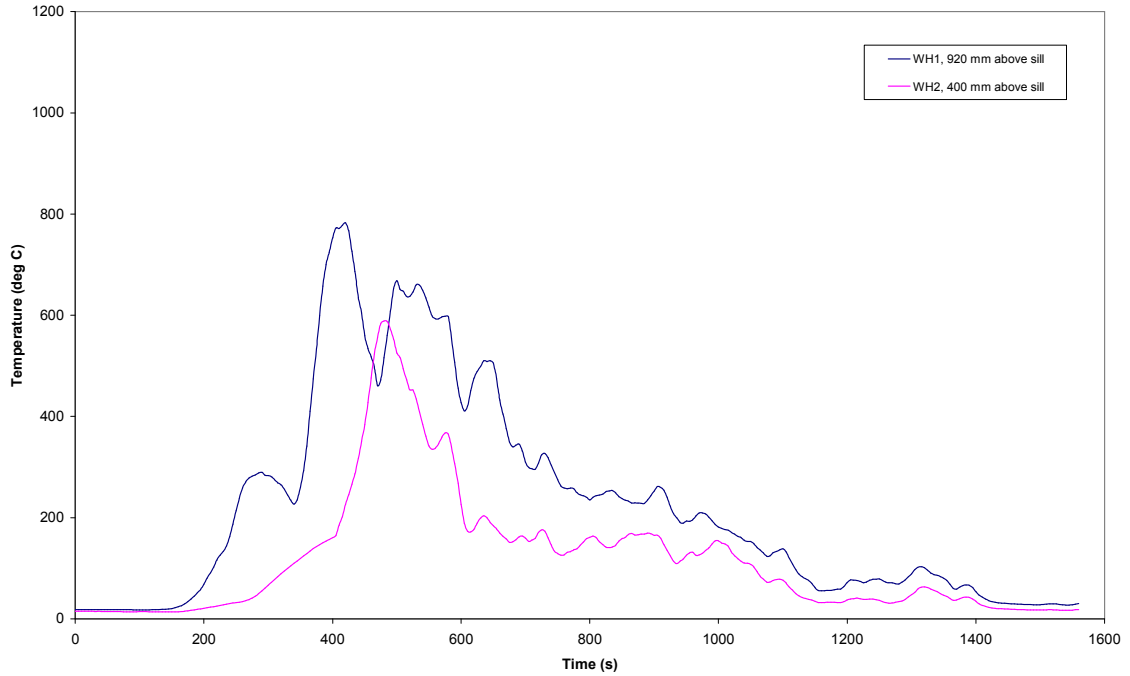
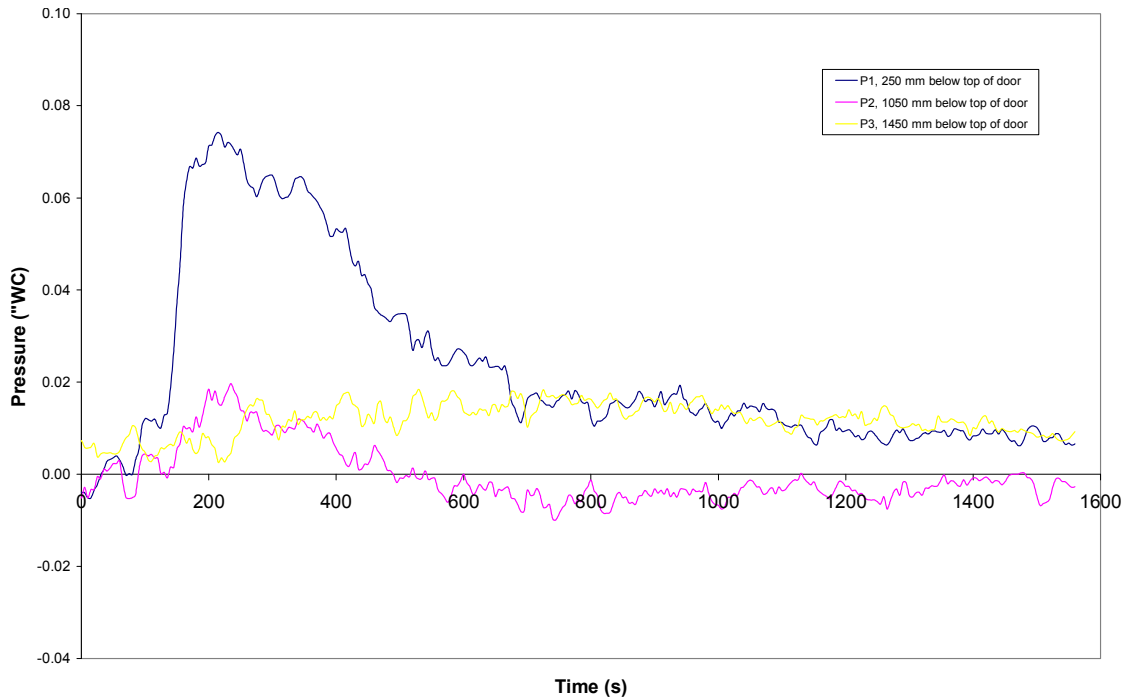


Figure F. 22 Full-scale experiment – thermocouples outside Window G



**Figure F. 23 Full-scale experiment – thermocouples outside Window H**



**Figure F. 24 Full-scale experiment – door flow probes**

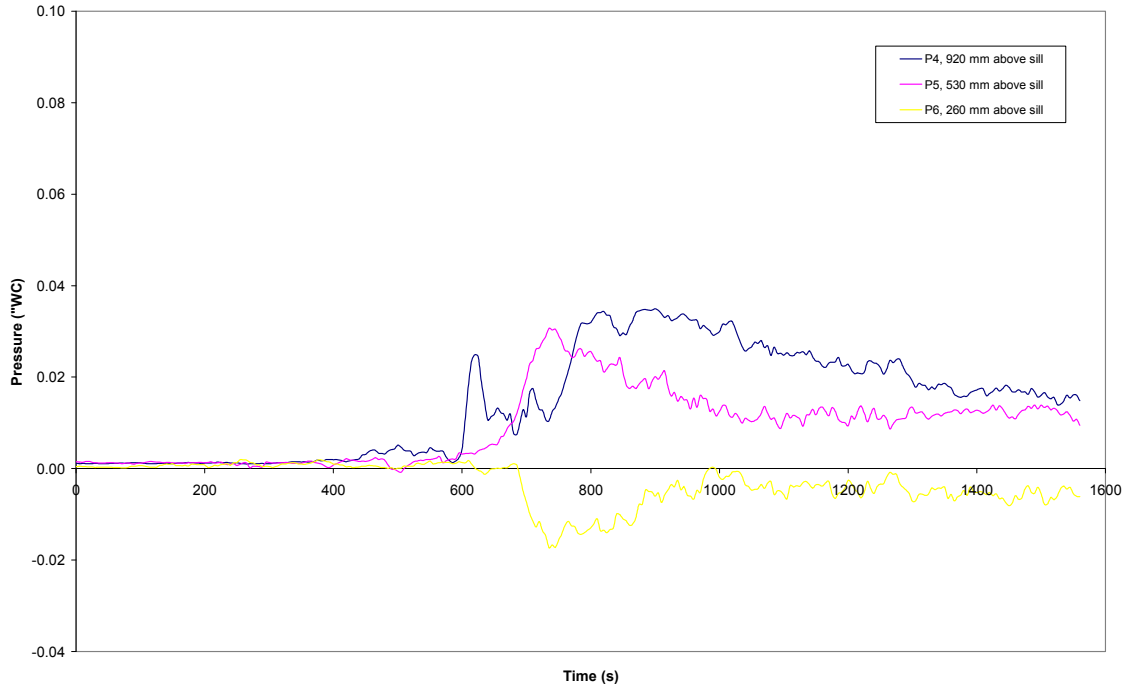


**Figure F. 25 Full-scale experiment – window flow probes**

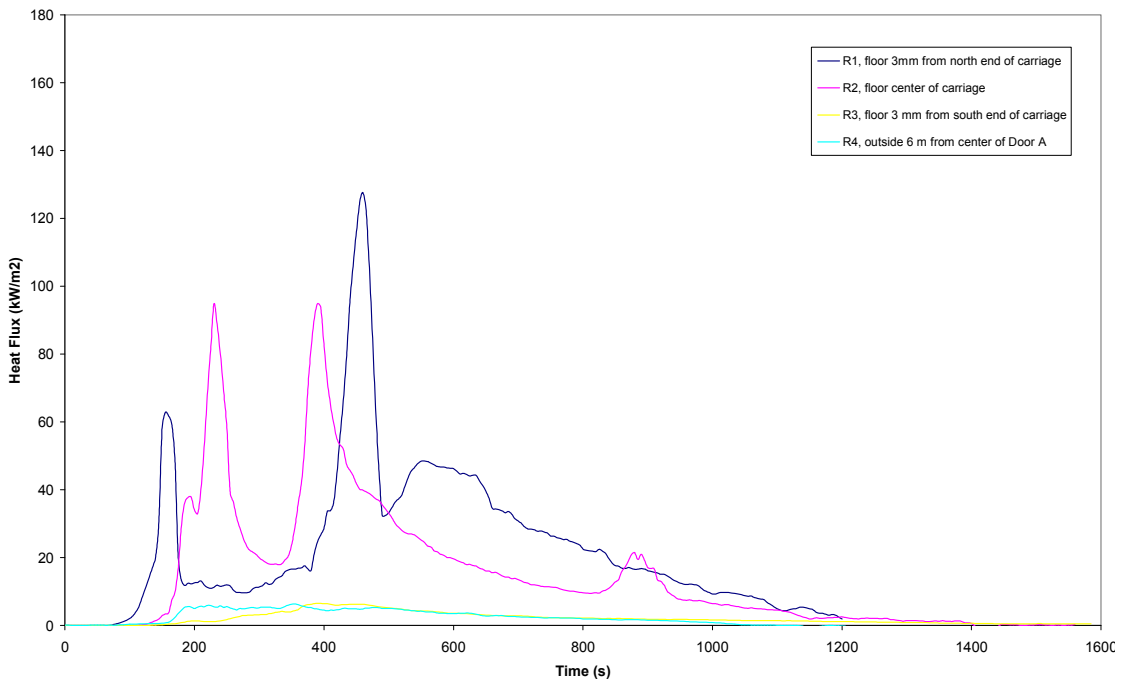


**Figure F. 26 Full-scale experiment – heat flux meters**

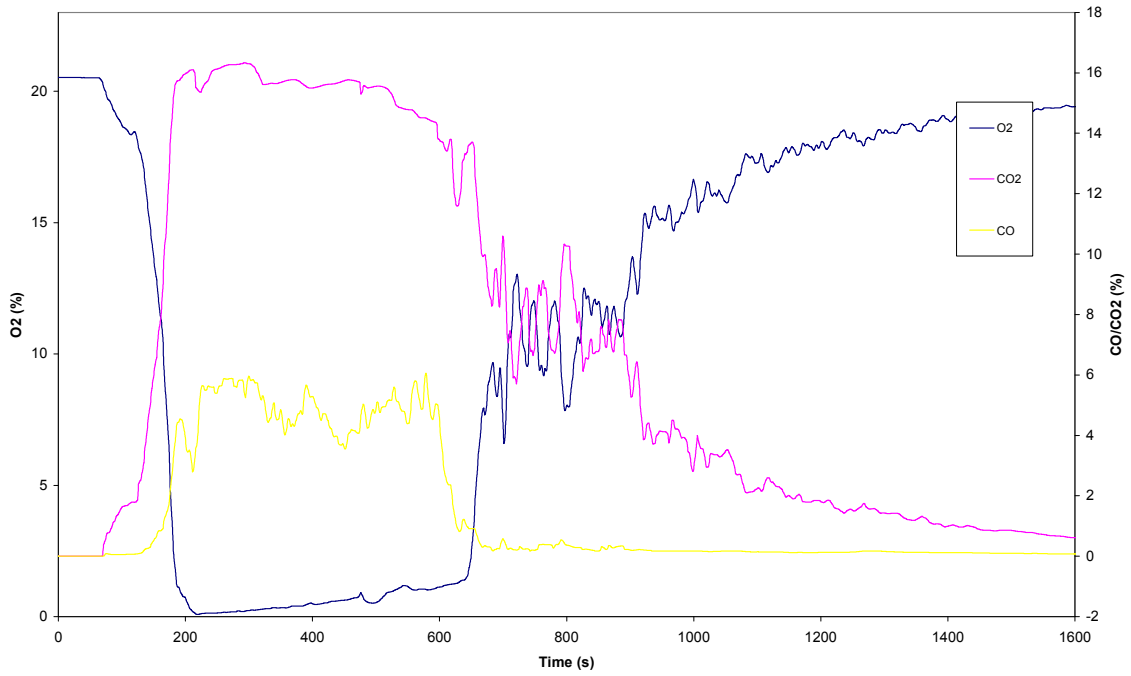


Figure F. 27 Full-scale experiment – gas concentrations

## APPENDIX G – FULL-SCALE EXPERIMENT MEASUREMENTS SCALED FROM VIDEO FOOTAGE

Table G.1 Observed neutral plane height vs time for Door A and B

Time (s)	Door A (mm)	Door B (mm)	Time <i>continued</i> (s)	Door A (mm)	Door B (mm)
0	1960	1960	500	1070	1060
50	1680	1960	510	960	1200
70	1680	1710	530	960	1340
80	1540	1710	540	1070	1340
90	1110	1630	550	1070	1480
100	1110	1790	560	1070	1610
110	1250	1790	570	1070	1480
130	1110	1630	600	1180	1340
150	830	1130	620	1280	1480
160	830	960	630	1280	1610
170	550	630	640	1390	1610
180	410	800	670	1390	1750
190	550	800	690	1500	1750
200	270	960	700	1500	1680
210	410	880	710	1500	1610
220	550	800	740	1600	1680
230	410	800	750	1600	1610
240	550	630	770	1600	1480
250	410	470	780	1600	1610
260	550	630	800	1500	1610
270	550	800	820	1600	1610
300	610	720	840	1710	1680
310	460	900	860	1820	1680
330	550	1180	880	1820	1750
340	610	1180	920	1930	1750
360	550	1090	0	0	0
370	460	1090	0	0	0
390	920	1090	0	0	0
400	920	1480	0	0	0
420	860	1750	0	0	0
430	860	1340	0	0	0
440	750	1340	0	0	0
450	640	1340	0	0	0
460	860	1200	0	0	0
470	860	1340	0	0	0
480	860	1200	0	0	0
490	960	1200	0	0	0

Note:

- All heights are scaled from the door sill to the neutral plane
- Heights were scaled from video at 10 second intervals however for brevity heights are only tabulated where there is a change in observed height. Heights for all 10 s intervals prior to a tabulated value should be taken to be equal to the previous tabulated value.

**Table G. 2 Failure times for East window glazing and plaster blocking North East door.**

Time (s)	Fraction of window area open					
	WA	WC	NE door	WE	WG	WJ
0	0	0	0	0	0	0
270	0	0.25	0	0	0	0
350	0	0.5	0.25	0.25	0	0
390	0	0.5	0.75	0.25	0	0
410	0	0.5	0.75	1	0.25	0
430	0	0.5	0.75	1	0.5	0.25
470	0	0.5	0.75	1	0.5	0.5
490	0	0.5	1	1	1	1
540	0	1	1	1	1	1
560	1	1	1	1	1	1

**Table G. 3 Failure times for West windows**

Time (s)	Fraction of window area open					
	WB	WD	WF	WH	WJ	WL
0	0	0	0	0	0	0
280	0	0	0.25	0	0	0
300	0	0	0.5	0.25	0	0
410	0	0	0.5	0.5	0	0
415	0	0.25	0.5	0.5	0	0
420	0	0.25	0.75	0.5	0.25	0
450	0	0.25	1	0.75	0.25	0
455	0	0.25	1	0.75	0.25	0
460	0	0.25	1	1	0.5	0
480	0	0.25	1	1	0.5	0.25
495	0	0.5	1	1	0.5	0.25
500	0	0.5	1	1	0.75	0.25
640	0.25	1	1	1	0.75	0.25
775	0.5	1	1	1	0.75	0.25
835	1	1	1	1	0.75	0.25

Note for **Error! Reference source not found.** and **Error! Reference source not found.**:

- Window glazing and plaster was generally observed to fail progressively opening from the top of the opening downwards
- Due to the difficulty of observing and scaling window openings these openings have simply been grouped into 25%, 50% and 100% open.
- Opening fractions were scaled from video at regular intervals however for brevity fractions are only tabulated where there is a change in observed opening. Opening fractions for intermediate times should be taken to be equal to the last tabulated value

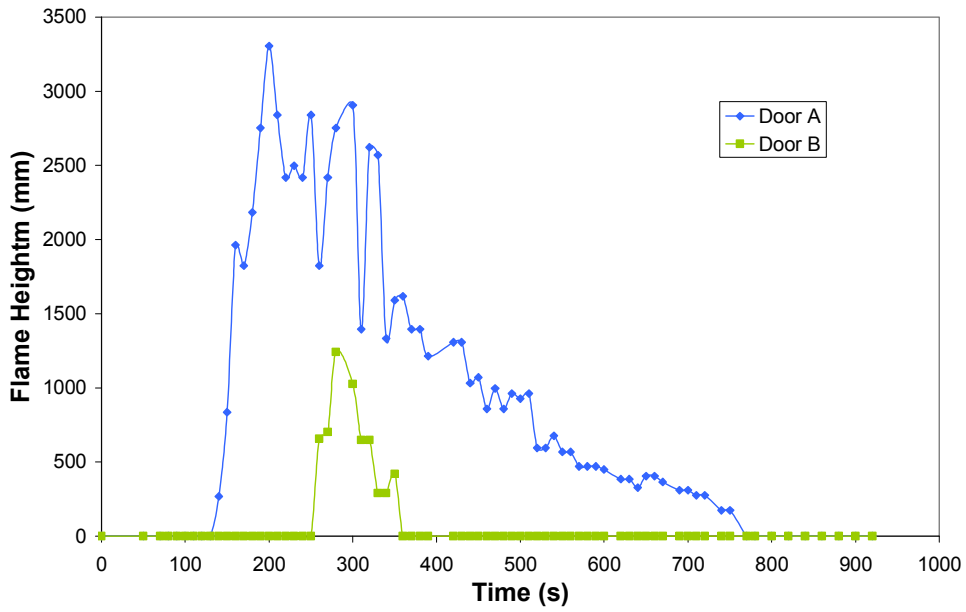


**Figure G.1. Heights of flames from Doors A and B scaled from video**

Note: The effective base of the flames extending from Doors A and B is taken to be the average of the neutral plane height and door soffit height.

**Table G. 4. Observed flame dimensions for flames extending from east windows and North East door vs time**

Time (s)	Window A		Window C		North East Door		Window E		Window G		Window I		
	Width (mm)	Height (mm)	width (mm)	height (mm)	width (mm)	height (mm)	width (mm)	height (mm)	width (mm)	height (mm)	width (mm)	height (mm)	
0	0	0	0	0	0	0	0	0	0	0	0	0	
270	0	0	750	500	0	0	0	0	0	0	0	0	
330	0	0	1500	500	0	0	0	0	0	0	0	0	
350	0	0	1500	500	0	0	750	330	0	0	0	0	
390	0	0	1500	500	1460	1500	750	330	0	0	0	0	
430	0	0	1500	500	1460	1500	1500	1000	750	500	0	0	
540	0	0	1500	1000	1460	1500	1500	500	1500	330	0	0	
550	1500	1500	1500	1500	1460	1000	E+G approx 100 kW					0	0
580	1500	1500	1500	1500	1460	500	E+G approx 100 kW					0	0
640	1500	1500	1500	1500	North east door + E+G approx 100 kW						0	0	
770	1500	1500	1500	1000	North east door + E+G approx 50 kW						0	0	
850	1500	1500	1500	500	North east door + E+G approx 50 kW						0	0	
910	1500	1000	North east door + C + E+G approx 100 kW						0	0			
980	1500	1000	North east door + C + E+G approx 50 kW						0	0			
1030	1500	1000	North east door + C + E+G approx 50 kW						0	0			

Note: Flame dimensions were scaled from video at regular intervals however for brevity dimensions are only tabulated where there is a change in observed dimensions. Dimensions for intermediate times should be taken to be equal to the last tabulated value

**Table G. 5. Observed flame dimensions for flames extending from west windows**

Time (s)	Window B		Window D		Window F		Window H		Window J		Window L	
	width (mm)	height (mm)	width (mm)	height (mm)	width (mm)	height (mm)	width (mm)	height (mm)	width (mm)	height (mm)	width (mm)	height (mm)
0	0	0	0	0	0	0	0	0	0	0	0	0
190	0	0	0	0	375	500	0	0	0	0	0	0
270	0	0	0	0	375	500	0	0	0	0	0	0
280	0	0	0	0	750	500	500	500	0	0	0	0
300	0	0	0	0	1500	660	750	500	0	0	0	0
320	0	0	500	500	1500	660	750	500	0	0	0	0
390	0	0	500	500	1500	500	1500	500	0	0	0	0
410	0	0	1500	500	1500	500	1500	500	750	660	0	0
450	0	0	1500	500	1500	1000	1500	1000	750	660	0	0
490	0	0	1500	500	1500	500	1500	500	750	660	0	0
540	0	0	1500	500	F + H + J estimated to total 200 kW						0	0
600	0	0	1500	500	F + H + J estimated to total 100 kW						0	0
630	1500	1000	0	0	F + H + J estimated to total 100 kW						0	0
1020	1500	500	0	0	0	0	0	0	0	0	0	0
1210	0	0	0	0	0	0	0	0	0	0	0	0

Note: Flame dimensions were scaled from video at regular intervals however for brevity dimensions are only tabulated where there is a change in observed dimensions. Dimensions for intermediate times should be taken to be equal to the last tabulated value

## APPENDIX H – CONE CALORIMETER RESULT GRAPHS

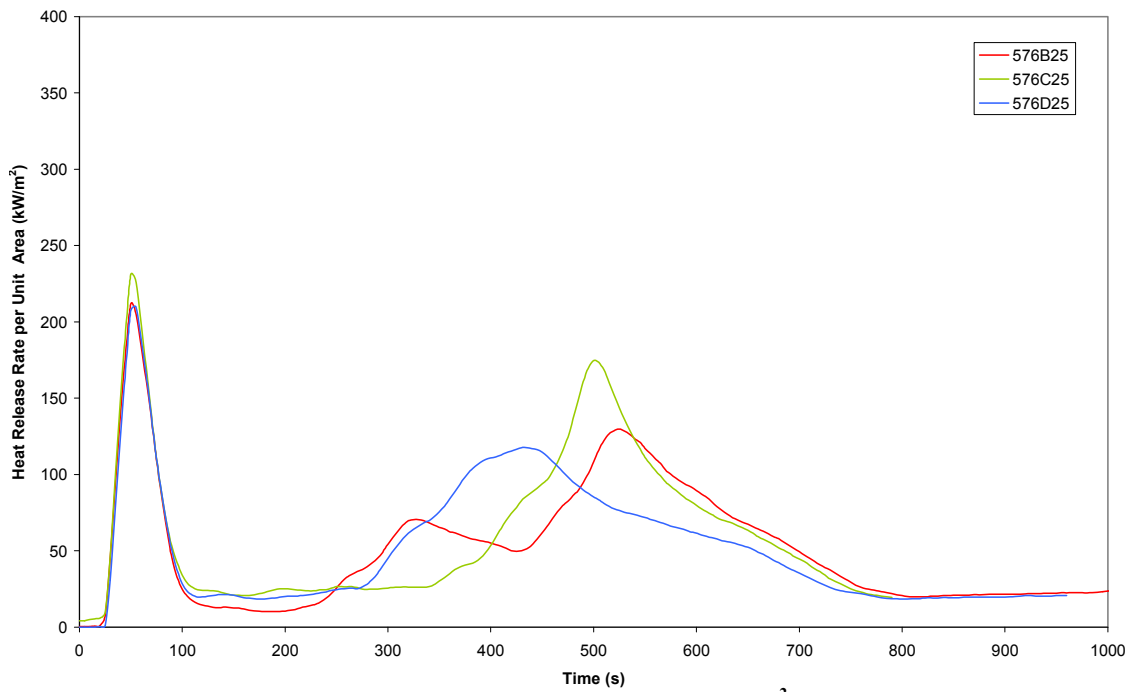


Figure H. 1 HRR per unit area for carpet at 25 kW/m<sup>2</sup> irradiance

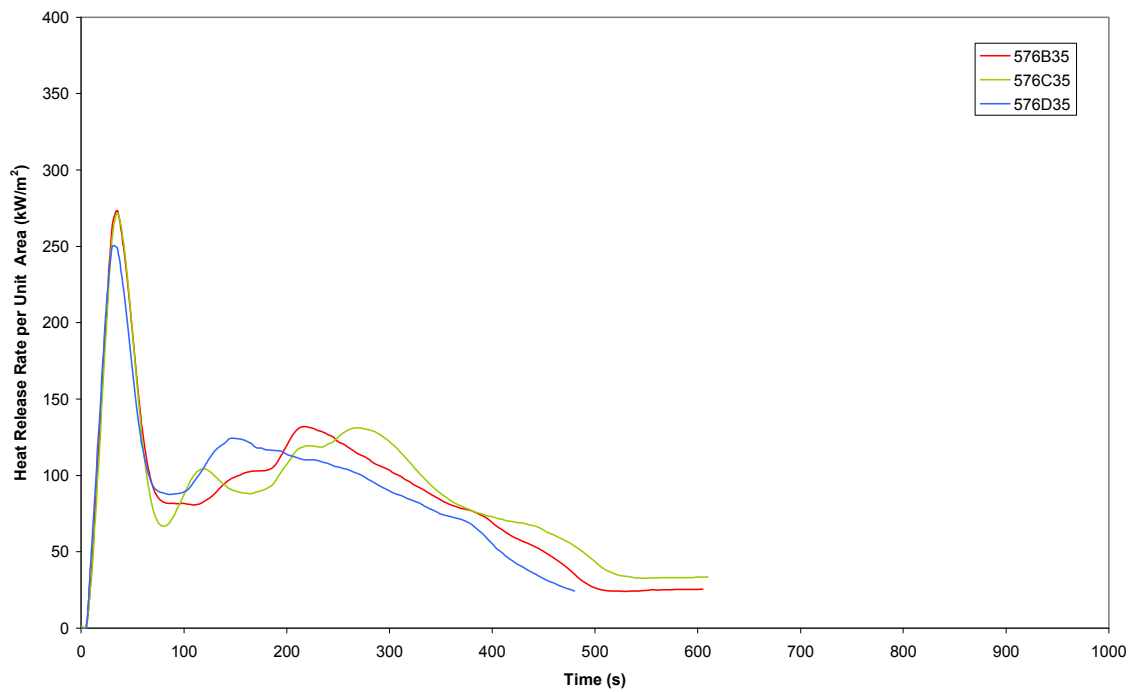


Figure H. 2 HRR per unit area for carpet at 35 kW/m<sup>2</sup> irradiance

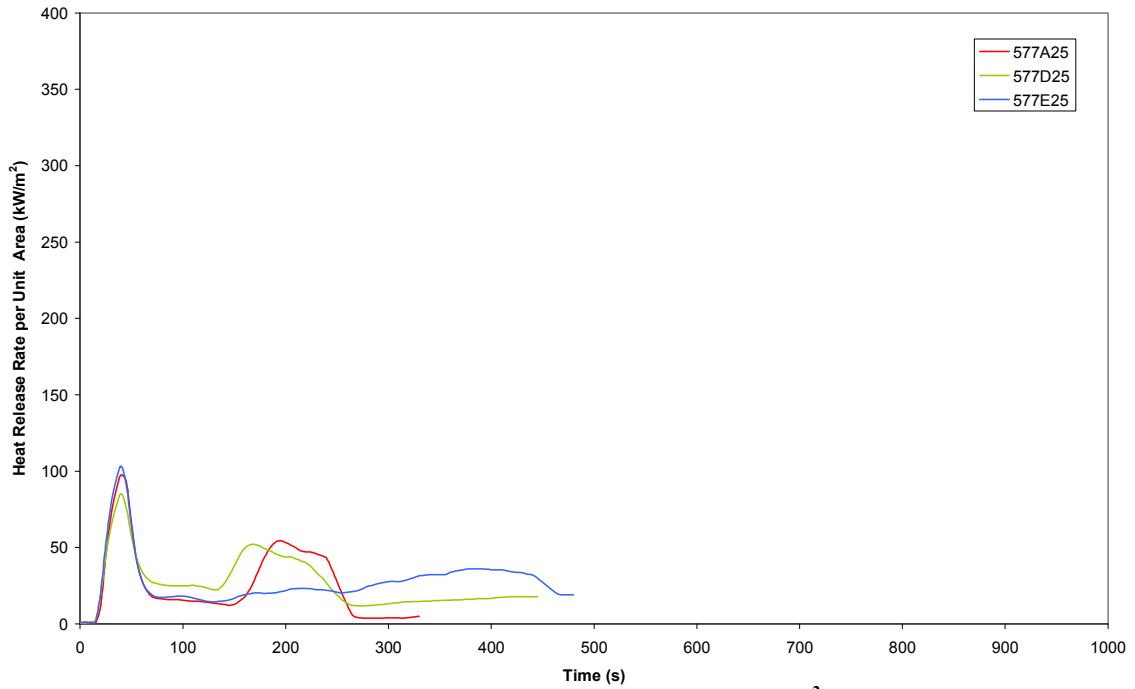


Figure H. 3 HRR per unit area for seat cushions at 25 kW/m<sup>2</sup> irradiance

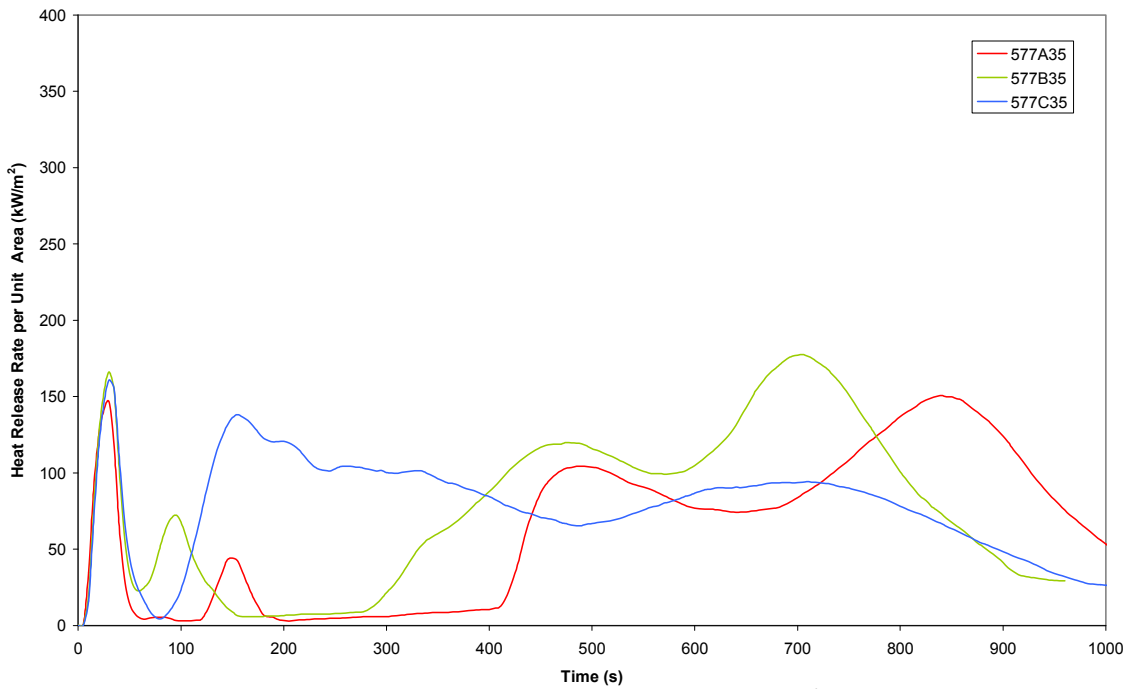
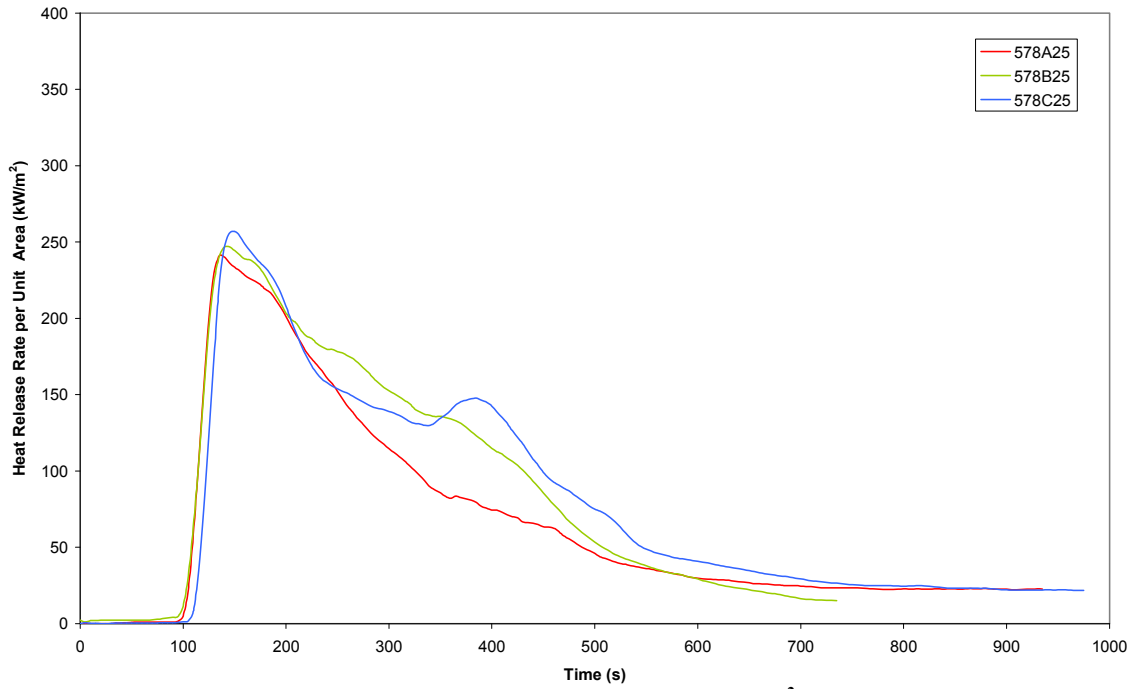
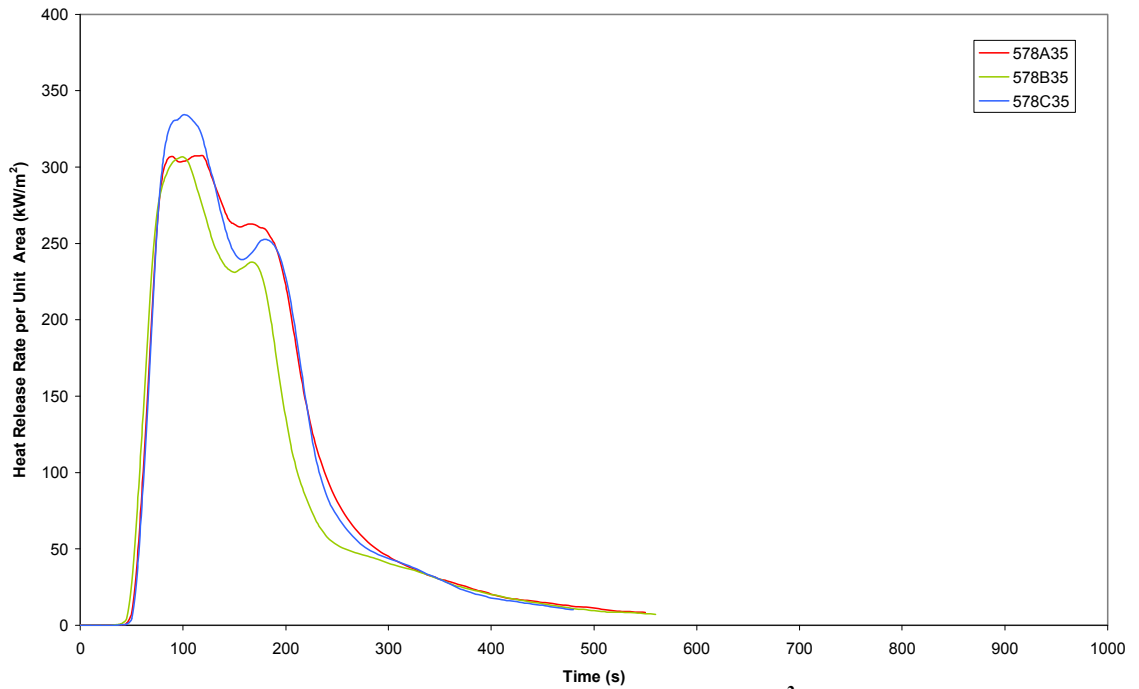


Figure H. 4 HRR per unit area for seat cushions at 35 kW/m<sup>2</sup> irradiance



**Figure H. 5 HRR per unit area for old GRP at 25 kW/m<sup>2</sup> irradiance**



**Figure H. 6 HRR per unit area for old GRP at 35 kW/m<sup>2</sup> irradiance**

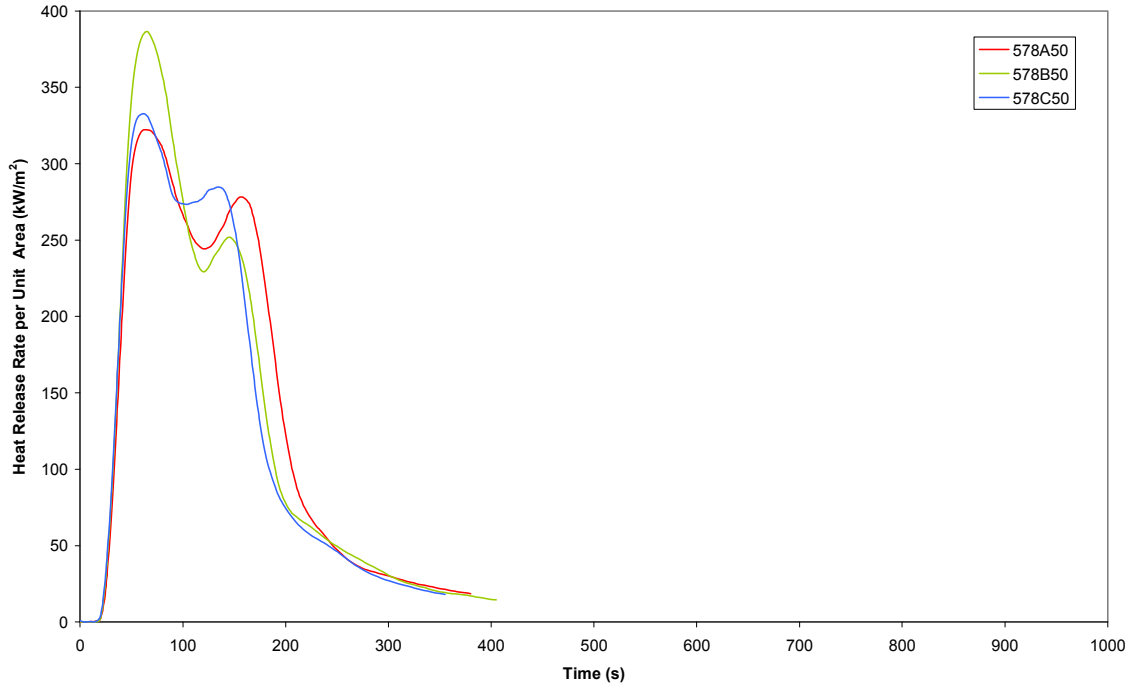


**Figure H. 7 HRR per unit area for old GRP at 50 kW/m<sup>2</sup> irradiance**

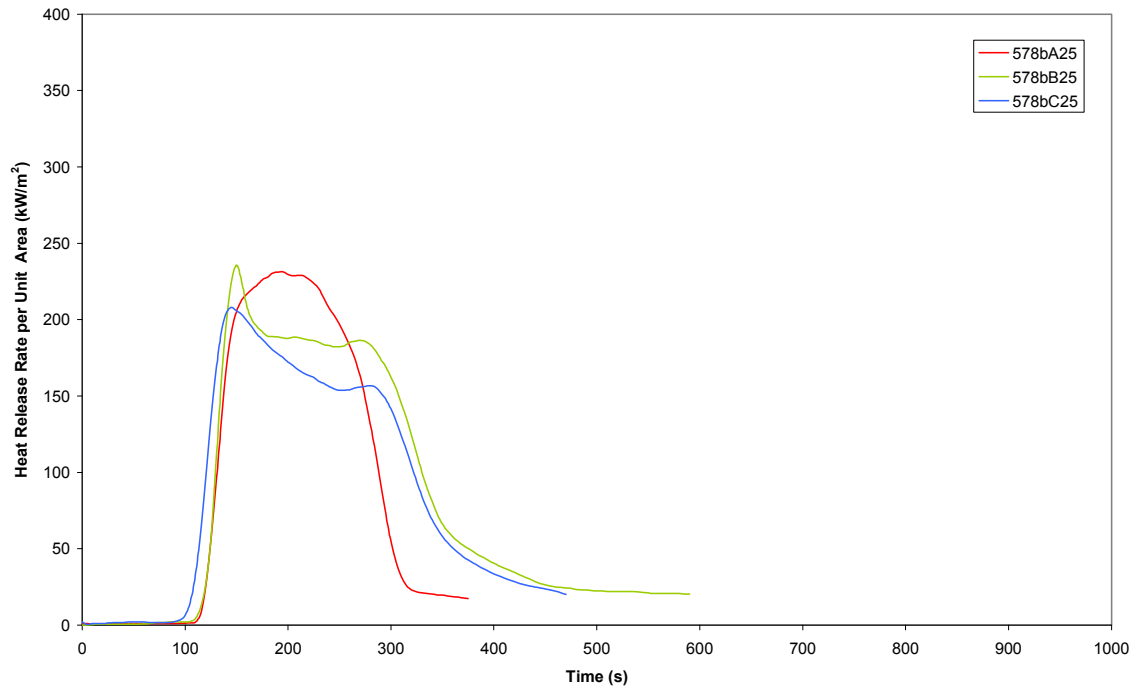


**Figure H. 8 HRR per unit area for new GRP at 25 kW/m<sup>2</sup> irradiance**

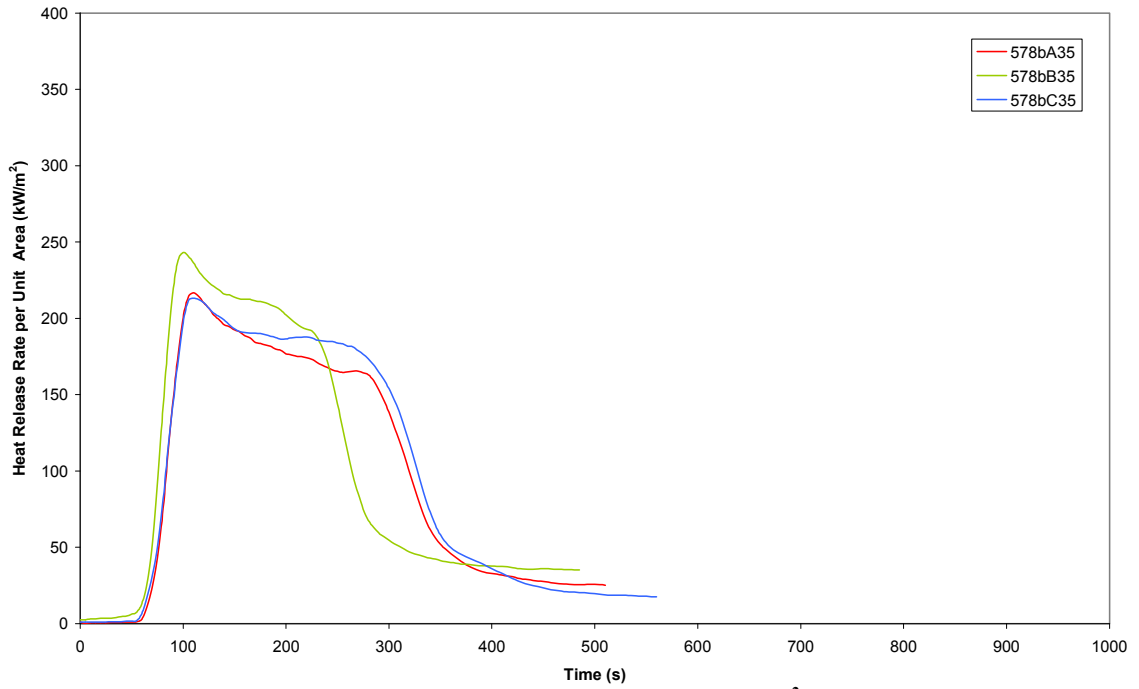


**Figure H. 9 HRR per unit area for new GRP at 35 kW/m<sup>2</sup> irradiance**

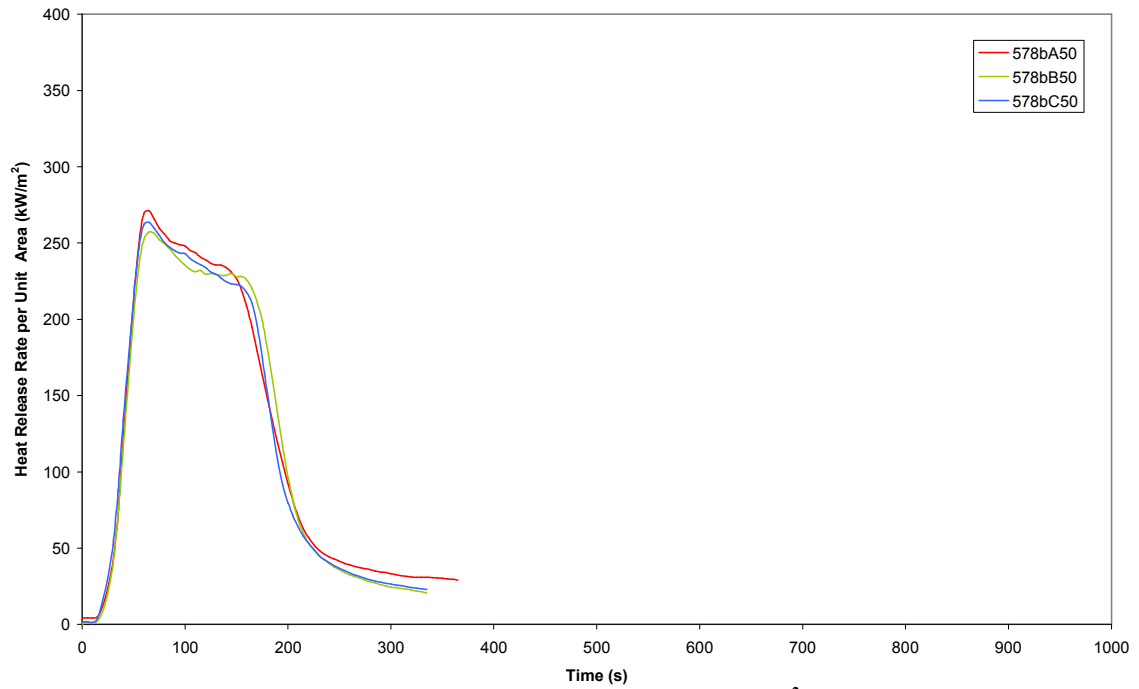


**Figure H. 10 HRR per unit area for new GRP at 50 kW/m<sup>2</sup> irradiance**

## APPENDIX I – MEASUREMENT OF EFFECTIVE HEAT OF COMBUSTION

The gross heat of combustion ( $\Delta H_c$ ) is defined as the heat of combustion for a complete combustion reaction where the oxidant is gaseous oxygen, the primary products are liquid H<sub>2</sub>O, gaseous CO<sub>2</sub>, and gaseous N<sub>2</sub>, there is no CO or unburnt hydrocarbons and the reaction takes place at 25 °C and atmospheric pressure.  $\Delta H_c$  is normally measured in an oxygen bomb calorimeter. This consists of a known mass of fuel being burned in a pure oxygen atmosphere in a constant volume combustion chamber that is submerged in a water bath. The heat released is calculated from the temperature increase of the water bath.

The net heat of combustion ( $\Delta H_{net}$ ) is the heat of combustion determined under the same conditions as the gross heat of combustion except that H<sub>2</sub>O is not liquefied but remains a gas. This is more relevant to combustion in fires as H<sub>2</sub>O is produced as a gas in fires. The net heat of combustion is equal to the gross heat of combustion minus the latent heat of the quantity of water produced at 25 °C. There is no direct method of measuring net heat of combustion.

Gross and net heats of combustion represent idealised, complete combustion. Effective Heat of Combustion ( $\Delta H_{eff}$ ) is the heat of combustion measured under real fire conditions where CO, Hydrocarbons and other products of incomplete combustion are produced.  $\Delta H_{eff}$  is always less than the net heat of combustion.  $\Delta H_{eff}$  is measured in tests, such as the cone calorimeter, where heat release rate and mass loss rate are simultaneously measured using time resolved instruments.

$\Delta H_{eff}$  is the most appropriate heat of combustion to be applied to fuel load calculations as it implicitly includes the combustion efficiency that would have to be considered if applying net heat of combustion. However it is important to note that  $\Delta H_{eff}$  is affected by fire environment conditions such as oxygen concentration. Although conditions may be more oxygen rich in the cone calorimeter than for a fully developed train fire it is common for fire engineers to apply  $\Delta H_{eff}$  determined from cone calorimeter tests to large fully developed fires.  $\Delta H_{eff}$  determined from cone calorimeter tests for the

major interior materials fitted in the full scale experiment have been used in this calculation.

$\Delta H_{eff}$  is obtained in cone calorimeter tests as a time varying quantity that is significantly affected by physical and chemical changes at the fuel surface such as charring or burning through different material layers of a composite material. For the purpose of calculating fuel loads the average  $\Delta H_{eff}$  of material is more appropriate than an instantaneous  $\Delta H_{eff}$  as it better represents the heat that may be released by the material in a fire averaged over its complete burning. The average  $\Delta H_{eff}$  has been calculated as:

$$\begin{aligned} \text{Average } \Delta H_{eff} &= \frac{\text{Total heat released (MJ)}}{\text{Total mass loss during burning (kg)}} \\ &= \frac{\int_{\text{initial}}^{\text{final}} \dot{Q}}{m_{\text{initial}} - m_{\text{final}}} \end{aligned} \quad \text{Equation I.1}$$

The initial values for the totals were taken at the time when  $\text{HRRPUA} \geq 50 \text{ kW/m}^2$ . At this time the materials had properly ignited and the entire surface of the material was involved in combustion. This eliminates mass lost due to pyrolysis prior to ignition. The final values for the totals were at the time when mass lost per unit area over a 1 minute period was less than  $150 \text{ g/m}^2$ . This is the criteria used in AS 3837 to identify the end of test and corresponds well to the time at which all flaming combustion of the specimen has ceased.

The behaviour of different material layers for carpet and seat cushions was found to have a significant effect on the burn rate in the cone calorimeter tests. For both materials the resulting HRRPUA curves display two distinct peaks. The initial peak occurs when the exposed layer of material burns and second peak occurs when the second layer of material is exposed and burns some time later. For the case of carpet the nylon ignites readily producing the first peak however the jute backing takes longer to become significantly involved in combustion. For the case of the seat cushions the wool lining ignites producing the first peak but as it burns it produces a protective char layer preventing significant involvement of the polyurethane foam

beneath until the char breaks down after continued heating and the foam becomes involved. In these cases the burn rate of the materials would reduce to point where mass lost per unit area over a 1 minute period was less than  $150 \text{ g/m}^2$ . In some cases all flaming ceased. However with continued irradiance the second layer of materials ignited and the burn rate increased again as shown in Figure I. 1. For these materials the final point for calculation of total heat released and total mass loss was taken to be the final time that mass loss per unit area over a 1 min period dropped below  $150 \text{ g/m}^2$ .

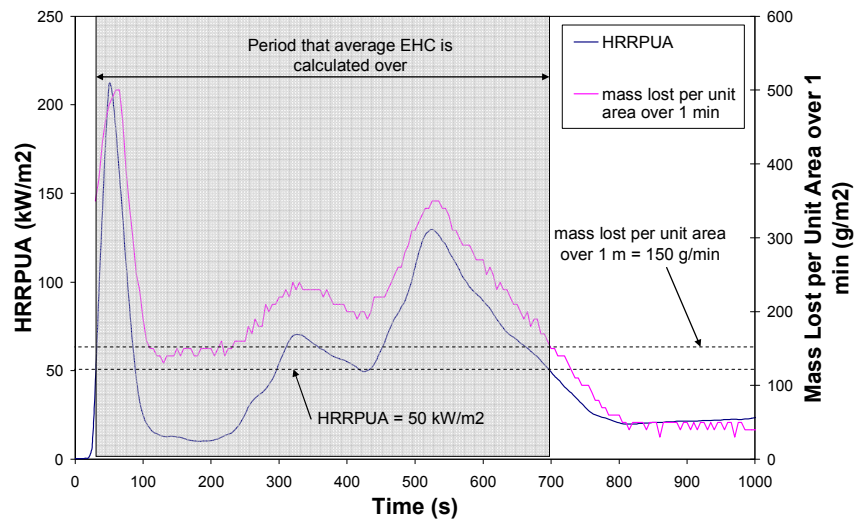


**Figure I. 1** Calculation of  $\Delta H_{eff}$  for carpet at  $25 \text{ kW/m}^2$  irradiance

Seat cushions were tested as a composite of layers, 45 mm total thickness. Seat foam and lining was not tested individually due to limited specimens. It is considered that testing these materials as a composite rather than individually better represents actual burning behaviour in the full-scale test.

The  $\Delta H_{eff}$  calculated for all major interior materials tested in the cone calorimeter are summarised in Table I. 1.

**Table I. 1** Average  $\Delta H_{eff}$  calculated from cone calorimeter tests

Material	Irradiance (kW/m <sup>2</sup> )	Specimen	Total heat released (MJ)	Total mass lost (kg)	Average $\Delta H_{eff}$ (MJ/kg)	Average	Standard Deviation
Carpet	25	576B25	443	0.0271	16.4	16.4	0.45
		576C25	462	0.0273	16.9		
		576D25	428	0.0267	16.0		
	35	576B35	477	0.0282	16.9	16.7	0.72
		576C35	495	0.0286	17.3		
		576D35	449	0.0282	15.9		
Seat cushion	25	577A25	75	0.0082	9.2	10.54	1.67
		577D25	99	0.0098	10.1		
		577E25	118	0.0095	12.4		
	35	577A35	543	0.037	14.7	15.62	0.88
		577B35	603	0.0383	15.7		
		577C35	622	0.0379	16.4		
GRP old	25	578A25	435	0.0278	15.7	16.1	0.45
		578B25	523	0.0325	16.1		
		578C25	543	0.0328	16.6		
	35	578A35	410	0.0234	17.5	17.4	0.09
		578B35	345	0.0199	17.4		
		578C35	401	0.023	17.4		
	50	578A50	407	0.025	16.3	16.7	0.42
		578B50	404	0.0236	17.1		
		578C50	377	0.0227	16.6		
GRP new	25	578aB25	341	0.0224	15.2	15.3	0.49
		578aC25	318	0.0215	14.8		
		578aD25	356	0.0226	15.8		
	35	578aA35	384	0.0266	14.4	14.6	0.28
		578aB35	350	0.0235	14.9		
		578aC35	410	0.0284	14.4		
	50	578aA50	319	0.023	14.6	14.4	0.27
		578aB50	325	0.023	14.1		
		578aC50	325	0.0222	14.4		

For seat cushions the measure  $\Delta H_{eff}$  is significantly higher at the higher irradiance. This is because the higher irradiance level promotes more complete involvement of the second layer materials. The variance of  $\Delta H_{eff}$  with heat flux for all other materials tested is not as significant. For this reason the average of the three  $\Delta H_{eff}$  measured at the highest irradiance tested for each material shall be used for the calculation of average HRR.

The two most significant sources of error for this measurement of  $\Delta H_{eff}$  are the error associated with the principal of oxygen consumption calorimetry and instrument

accuracy. The principal of oxygen consumption calorimetry calculates HRR assuming that all materials in all physical states release 13.1 MJ of heat energy per kilogram of oxygen consumed. This is considered to be accurate with very few exceptions to about  $\pm 5\%$  for organic materials, polymers and many hydrocarbons.<sup>[148]</sup> The combined accuracy of cone calorimeter instruments for measurement of gas flow rate, gas concentration and mass loss is approximately  $\pm 5\%$ .<sup>[184]</sup> The Cone calorimeter is calibrated using a combined C-factor that is calculated by burning a measured mass of either methane or, for these tests, methanol of a known heat of combustion.

No values of  $\Delta H_{eff}$  for these materials were readily available from literature. However values for gross heat of combustion are readily available. Combustion efficiency is the ratio of  $\Delta H_{eff}$  and gross heat of combustion:

$$\chi = \frac{\Delta H_{eff}}{\Delta H_c} \quad \text{Equation I.2}$$

Fuels that produce sooty flames have a combustion efficiency typically around 60 to 70%.<sup>[5]</sup> The following range of  $\Delta H_{eff}$  has been calculated from literature,<sup>[188]</sup> see Table I. 2.

**Table I. 2**      **Estimated effective heats of combustion based on  $\Delta H_c$  from literature**

Material	Representative of	$\Delta H_c$	$\Delta H_{eff}$
Nylon 6	Carpet pile	30.1-31.7	18.0-22.2
Wool	Seat lining	20.7-26.6	12.4-18.6
Polyurethane foam, FR	Seat foam	24.0-25.0	14.4-17.5
Epoxy	Resin in GRP	32.8-33.5	19.6-23.5

Measured values of  $\Delta H_{eff}$  for carpet and GRP are less than expected from literature. Possible reasons for this in the case of carpet may be poor combustion of the jute backing reducing the average  $\Delta H_{eff}$ . For all materials the presence of fire retardant is likely to result in less efficient combustion and reduced  $\Delta H_{eff}$  (the gel coat and epoxy

resin of both the old and new GRP are known to be fire retarded). The measured values of  $\Delta H_{eff}$  are therefore considered reasonable

The average  $\Delta H_{eff}$  measured at the highest irradiance tested for each material has been used to calculate the fuel load. Total heat flux measurements from the full-scale experiment indicate that most materials received heat fluxes in excess of 100 kW/m<sup>2</sup> post flashover which significantly exceeds the irradiance levels tested in the cone. Materials were only tested in the cone calorimeter at irradiances of 25,35 and 50 kW/m<sup>2</sup> as required for Duggan's method. These are the irradiance levels most commonly used for assessment of materials. No tests were conducted at higher irradiance level due to the limited number of specimens. HRR is significantly affected by heat flux received, however  $\Delta H_{eff}$  is relatively independent of heat flux received for most homogeneous materials. The exception is for composite materials such as seats where heat flux influences the complete burning of different materials within the specimen and hence  $\Delta H_{eff}$ .